



HAL
open science

Embankment as a carbon sink: a study on carbon sequestration pathways and mechanisms in topsoil and exposed subsoil

Lorenzo Matteo Walter Rossi

► **To cite this version:**

Lorenzo Matteo Walter Rossi. Embankment as a carbon sink: a study on carbon sequestration pathways and mechanisms in topsoil and exposed subsoil. Ecology, environment. Université de Montpellier; Università degli studi di Cassino e del Lazio meridionale (Cassino, Italie), 2019. English. NNT: 2019MONTG083 . tel-02611049

HAL Id: tel-02611049

<https://theses.hal.science/tel-02611049v1>

Submitted on 18 May 2020

HAL is a multi-disciplinary open access archive for the deposit and dissemination of scientific research documents, whether they are published or not. The documents may come from teaching and research institutions in France or abroad, or from public or private research centers.

L'archive ouverte pluridisciplinaire **HAL**, est destinée au dépôt et à la diffusion de documents scientifiques de niveau recherche, publiés ou non, émanant des établissements d'enseignement et de recherche français ou étrangers, des laboratoires publics ou privés.

THÈSE POUR OBTENIR LE GRADE DE DOCTEUR DE L'UNIVERSITÉ DE MONTPELLIER

En Ecologie Fonctionnelle (Univ. Montpellier) / Méthodes, modèles et technologies pour
l'ingénierie (UNICAS)

École doctorale GAIA

Unité de recherche UMR AMAP

Embankment as a carbon sink: a study on carbon sequestration pathways and mechanisms in topsoil and exposed subsoil

Présentée par Lorenzo MW Rossi

Le 09 Décembre 2019

Sous la direction de Alexia Stokes
et Giacomo Russo

Devant le jury composé de

[Dr Alexia STOKES, DR, HDR, INRA Montpellier]

[Dr Giacomo RUSSO, Associate Prof., UNICAS Cassino]

[Dr Catherine PICON-COCHARD, DR, HDR, INRA Clermont-Ferrand]

[Dr Isabelle BASILE-DOELSCH, DR, HDR, INRA-CEREGE Aix-en-Provence]

[Dr Wilma POLINI, Associate Prof., UNICAS Cassino]

[Dr Sandra LUQUE, DR, HDR, IRSTEA Montpellier]

[Dr Mark BAKKER, IR, HDR, Bordeaux Sciences Agro]

[Dr Paul HALLETT, Full Prof., Univ. Aberdeen]

[Dr Zhun MAO, CR, INRA Montpellier]

[Dr Tiphaine CHEVALLIER, CR, HDR, IRD Montpellier]

[Directeur de thèse]

[Directeur de thèse]

[Rapporteur]

[Rapporteur]

[Examineur]

[Examineur]

[Examineur]

[Examineur]

[Invitée]

[Invitée]

ACKNOWLEDGEMENTS

My gratitude to the reviewers and the members of the jury for taking the time and effort to evaluate this thesis work.

A Ph.D. thesis is the result of choral work, and many people should be thanked. I hope I don't forget anyone, and I ask them to forgive me if that happens.

My heartfelt thanks to Alexia Stokes, my French supervisor. My e-mail as a master student fascinated by her work started this research path more than four years ago; her capacity to never undermine ideas, but support and direct them, made it possible. Thanks for the incredible effort put in this thesis, the scientific directions and insights, accompanied by the not obvious possibility to independently develop my research. And thanks for the infinite patience and kindness.

A sincere thanks to Zhun Mao, my co-supervisor in France. His relentless passion, effort and tremendous capacity made this work not only possible, but 'shiny'. Thanks for reminding me what Science is when I almost forgot.

Grazie di cuore to Giacomo Russo, my Italian supervisor. Our exchanges allowed me to explore my work under a different point of view, challenging me scientifically and helping me grow professionally. His kindness, availability and friendliness, together with the passion and effort that he put in his work, reminded me once again the value of my country. Thanks to Enza Vitale and Sebastiana dal Vecchio for the warm welcome, scientific insights, and the technical assistance in UNICAS.

I have carried out the bulk of my work in AMAP, Montpellier, and I would like to thank Thierry Fourcaud for welcoming me in a warm and stimulating environment. Thanks to Luis Merino-Martin for the priceless scientific collaboration and friendship. Thanks to Nathalie Hodebert and Noemie Caoquil for the help and directions in French bureaucracy, I would have been lost without it. Thanks to Francois Pailler, Stephane Fourtier and Merlin Ramel for the help and collaboration. Many thanks to Awaz Mohamed and Jérôme Nespoulous for guiding me through the Ph.D. life. Thanks to Jing Ma, Christina Orieschnig and Ngô Ha My for their assistance and hard work. Thanks to Sarina Fourcaud-Stokes for the technical help and friendship. Thanks to M. Ika for the unconditional support during the long nights of thesis redaction.

Thanks to Rémi Cardinael, Delphine Derrien, and Caroline Plain for assisting me greatly during all the steps of the thesis project. This collaboration has been truly fundamental to improve the quality of the work and an absolute delight under any point of view.

In CEFE, Montpellier, many thanks to Catherine Roumet, Florian Fort, Nathalie Fromin, Ammar Shihan, Maria Del Rey-Granado, and David Deguledre for their precious collaboration, insights and availability. Thanks to technicians at the PEACE platform Nicholas Barthes, Raphaëlle Leclerc and Bruno Buatuois, for the help and assistance in the analysis.

Thanks to Jaques Roy, Alex Milcu, Sébastien Devidal and Clément Piel. The collaboration with Ecotron Montpellier was a personal success and an incredible opportunity.

I would like to thank all the people involved in the TERRE project, the Professors, the fellow students and the administrators. In particular Alessandro Tarantino and Katharine Houston. It has been a wonderful journey and an incredible chance; talking about plants in such a different and multidisciplinary environment have been truly enlightening.

Finally, I wish to thank my family and friends. I am a very lucky person so there are too many to name individually. A Ph.D. can be a challenging task, and has up and downs like many other things in life. They are the one that, with their love and support, weave a safety net under you that makes even the most difficult jumps feasible and less frightening. A special mention goes to Miriam and Luca, for their astonishing patience and support during the last year. With the most Italian twist, I dedicate this work to my mother Alessandra Zanelli Quarantini.

“Se l’organizzazione del carbonio non si svolgesse quotidianamente attorno a noi, [...], dovunque affiori il verde di una foglia, le spetterebbe di pieno diritto il nome di miracolo.”

Primo Levi, ‘La tavola periodica’ , Einaudi, 1975, pp. 261

“If the elaboration of carbon were not a common daily occurrence, [...], wherever the green of a leaf appears, it would by full right deserve to be called a miracle.”

Primo Levi, ‘The periodic table’ , Einaudi, 1975, pp. 261

FUNDINGS

The work described in this publication was supported by the European Commission H2020 Framework Programme through the grant to the budget of the Marie Skłodowska-Curie European Training Networks (ETN) project TERRE, Contract **H2020-MSCA-ITN-2015-675762**.

DISCLAIMER

This document reflects only the authors' views and not those of the European Community. This work may rely on data from sources external to the TERRE project Consortium. Members of the Consortium do not accept liability for loss or damage suffered by any third party as a result of errors or inaccuracies in such data. The information in this document is provided "as is" and no guarantee or warranty is given that the information is fit for any particular purpose. The user thereof uses the information at its sole risk and neither the European Community nor any member of the TERRE Consortium is liable for any use that may be made of the information.

Résumé

La séquestration du carbone (C) fait l'objet d'une attention scientifique et politique croissante dans le cadre de la réduction des gaz à effet de serre. Cependant, les sols géotechniques ont été négligés en raison de leur potentiel de séquestration du carbone, et l'attention mondiale étant concentrée sur les sols agricoles et naturels. Dans le présent projet de thèse, nous visons à évaluer le potentiel des talus géotechniques comme puits de carbone et, par l'étude des espèces végétales et des sols présentant des caractéristiques contrastées, à mettre en lumière les mécanismes de séquestration du carbone organique et les rôles des différents acteurs impliqués. Nous visons non seulement à quantifier le C gagné et perdu dans le sol, mais aussi son origine (nouveau C frais et ancien C préexistant) et comment il est réparti dans différents pools de C qui montrent une stabilité du C différente (qualité du C stocké). Tout d'abord, nous avons évalué la séquestration du carbone dans différents pools de carbone sous un sol semé de 12 espèces herbacées différentes dans une expérience de 10 mois. En évaluant les différentes caractéristiques des racines, nous nous sommes concentrés sur leurs corrélations avec le stockage du C dans différents bassins de C du sol. Nous avons montré que les espèces dont les caractéristiques racinaires sont associées à une production élevée de C labile entraînent une augmentation plus élevée de C dans le pool stable de SILT+CLAY (<20µm). Les espèces dont les traits racinaires sont associés à un faible apport de C récalcitrant favorisent plutôt l'accumulation dans la fraction POM instable. Ensuite, grâce à une expérience de marquage isotopique stable de 183 jours (CO₂ constamment enrichi en ¹³C), nous avons pu étudier la dynamique du C dans différents pools de C sous deux espèces (*Lolium perenne* and *Medicago sativa*) sur deux sols (terre végétale, profondeur 0-30 cm et sol remonté, profondeur 110-140 cm) aux caractéristiques opposées. Nous avons mis en évidence le grand intérêt de faire le pont entre l'origine du C et les pools de C lors de l'étude des destins du C du sol, ce qui permet de dévoiler des processus que les méthodes plus traditionnelles cachent. Le nouveau C et l'ancien C présentaient une covariation synergique, avec des pertes plus faibles de l'ancien C associées à de nouvelles entrées de C plus élevées. Une part plus importante de nouveau C utilisé par les communautés microbiennes comme substrat peut expliquer ce comportement synergique. La théorie d'une plus grande quantité de nouveau C minéralisé par les communautés microbiennes a également été validée par l'étude de "priming effect" et de la respiration du sol, qui a montré que la concentration de C provenant par les plantes dans le CO₂ inhalé par le sol était plus élevée lorsque l'apport de C par les plantes était élevé, au contraire augmentant la concentration de C provenant par la minéralisation de l'anciennes C lorsque les input de C par les plants étaient faibles, c.-à-d. en sous sol. Nous avons observé de nouveaux apports significatifs de C d'origine végétale dans la fraction SILT+CLAY (<20µm, très stable). Ces résultats viennent étayer le rôle des communautés microbiennes dans la consommation et le transfert de C dans cette fraction fine protégée sous forme de nécromasse et d'exopolysaccharides, comme le confirment les fortes corrélations positives constatées entre l'activité microbienne et l'augmentation de C dans la fraction SILT+CLAY. L'effet de l'espèce s'est produit principalement sur les intrants de nouveaux C, mais il a été maîtrisé par l'effet du sol, avec un stockage de C plus faible dans un sol de faible qualité (faible activité et biomasse d'azote et microbienne). En général, les conditions microbiologiques ont été le principal moteur de la nouvelle accumulation de C et de l'ancienne perte de C et ont aidé à expliquer pourquoi aucun effet de la saturation en C du sol - une théorie centrale dans des études récentes sur la séquestration de C - n'a été trouvé dans le carbone protégé. Cette compréhension fondamentale des interactions plantes-sol nous aide à mieux optimiser la gestion des sols et de la végétation pour la revégétalisation des talus des routes.

Abstract

Carbon (C) sequestration is receiving increasing scientific and political attention in a framework of greenhouse gasses mitigation. However, geotechnical soils have been neglected for their C sequestration potential, with the global attention focusing on agricultural and natural soils. In the present thesis project, we aim to assess the potential of geotechnical embankments as C sink, and, through the study of plant species and soils showing contrasting features, shed light on C sequestration mechanisms and the role of the different actors involved. We aim not only to quantify the C gained and lost in soil, but even its origin (fresh new C input or old preexistent C) and how it is partitioned in different C pools characterized by different C stability (quality of stored C). First, we evaluated the C storage in different pools under soil sowed with 12 different herbaceous species in a 10 months experiment. Assessing different root traits we focused on their correlations with C storage in different soil C pools. We showed how traits linked to high labile C are linked to a higher C increase in the stable SILT+CLAY pool (<20 μ m). Root traits related to a low input of recalcitrant carbon, instead, favor accumulation in the unstable POM fraction. We designed a 183 days stable isotope labelling experiment (CO₂ constantly enriched with ¹³C) and we were able to study the C dynamics in different C pools under two species (*Lolium perenne* and *Medicago sativa*) sowed on two soil (topsoil, 0-30cm depth and subsoil brought to the surface, 110-140 cm depth) showing contrasting characteristics. We evidenced the importance of bridging C origin and C pools when studying soil C fates, allowing unveiling processes those more traditional methods would hide. New C and old C showed synergetic covariation, with lower old C losses associated to higher new C inputs. A higher share of new C utilized by microbial communities as substrate can explain this synergetic behavior. The theory of a higher amount of new C mineralized by microbial communities was also validated with the study of priming effect and soil respiration, that showed higher plant derived C in respired CO₂ when plant C input was high, while increasing old C mineralization when plant C input was low, i.e. in subsoil. We observed significant plant derived new C input in the SILT+CLAY fraction (<20 μ m, highly stable). These results are supporting evidences for the role of microbial communities in consuming and transferring C in this protected fine fraction in form of necromass and exopolysaccharides, as confirmed by the strong positive correlations found between microbial activity and C increase in SILT+CLAY fraction. The species effect mainly occurred on new C input, but it was overpowered by the soil effect, with lower C storage in low quality soil (low nitrogen and microbial biomass and activity). In general, microbiological conditions were the main driver for new C accumulation and old C loss, and helped to explain why no effect of soil C saturation – a central theory in recent studies on C sequestration - was found in the protected carbon. Such fundamental understanding of plant-soil interactions helps us to better optimize soil and vegetation management for road embankment revegetation

2.1.	<i>INTRODUCTION</i>	38
2.2.	<i>MATERIALS AND METHODS</i>	40
2.2.1.	Experimental setup.....	40
2.2.2.	Analysis of carbon content in different soil fractions	42
2.2.3.	Measurement of root elongation rate (RER) and root length production (RLP).....	43
2.2.4.	Analysis of root traits.....	45
2.2.5.	Statistical analysis.....	46
2.3.	<i>RESULTS</i>	46
2.3.1.	Root elongation rate (RER) and root length production (RLP).....	47
2.3.2.	Root biomass, diameter and chemical composition	48
2.3.3.	Soil substrate induced respiration (SIR)	49
2.3.4.	Relationships between soil carbon accumulation (ΔC), root growth dynamics, root traits, and substrate induced respiration (SIR).....	49
2.4.	<i>DISCUSSION</i>	50
2.4.1.	Hypothesis 1: Root elongation rate and root length production are expected to favour carbon accumulation in the C_{SILT} and $C_{SILT+CLAY}$ fractions	51
2.4.2.	Hypothesis 2: more recalcitrant root traits are expected to favour the unprotected coarse POM fraction.....	52
2.4.3.	Hypothesis 3: Fabaceae and Poaceae strongly differ in their influence on accumulation of C into different soil fractions.....	53
2.5.	<i>CONCLUSION</i>	54
	<i>REFERENCES</i>	56
	<i>FIGURES AND TABLES</i>	63
	<i>Supplementary Materials</i>	73
	Chapter III: The fates of fresh new carbon and old soil carbon differ in topsoil and newly exposed subsoil and are explained by root, microbial, and soil particle size	89
3.1.	<i>INTRODUCTION</i>	91
3.1.1.	General context in soil organic carbon sequestration on embankments: can subsoil brought to the surface be used as a C sink?.....	91
3.1.2.	New and old carbon in soil	92
3.1.3.	Soil organic carbon quality: carbon pools are associated to different soil granular fractions	92
3.1.4.	New old carbon distribution in different soil pools: drivers and mechanisms	93
3.1.5.	Research hypothesis.....	95
3.2.	<i>MATERIALS AND METHODS</i>	96
3.2.1.	Soil and plant preparation, experimental design and set-up.....	96
3.2.2.	Soil fractionation and assessment of soil carbon and $\delta^{13}C$	98

3.2.3.	Estimation of new and old carbon in soil fractions	100
3.2.4.	Microbial global metabolic activity (GAM) and Shannon metabolic diversity index (H).....	101
3.2.5.	Microbial DNA concentration as proxy for microbial biomass.....	102
3.2.6.	Percentage of fine fraction in soil, soil nitrogen and aggregate stability.....	103
3.2.7.	Root traits.....	104
3.2.8.	Statistical analysis.....	106
3.3.	<i>RESULTS</i>	106
3.3.1.	Changes in total soil carbon	106
3.3.2.	Changes in soil carbon in different soil C pools associated to soil fractions.....	107
3.3.3.	Changes in carbon quality	108
3.3.4.	Root, soil and microbial characteristics.....	108
3.3.5.	Relationship between changes in new C and old C and soil, microorganism and root variables	110
3.4.	<i>DISCUSSION</i>	111
3.4.1.	Importance of differentiating soil carbon origin and pools (Hypothesis 1)	112
3.4.2.	Generally a strong synergy exists between new and old carbon (Hypothesis 2).....	113
3.4.3.	Root traits influence new carbon gain and old carbon changes, and are strongly mediated by soil variables (Hypothesis 3).....	115
3.4.4.	Microbiological activity can explain the disparity in new C and old C changes between topsoil and subsoil.....	117
3.4.5.	Practical applications.....	118
3.5.	<i>CONCLUSIONS</i>	118
	<i>REFERENCES</i>	121
	<i>FIGURES AND TABLES</i>	128
	<i>SUPPLEMENTARY MATERIALS</i>	137
	Chapter IV: Soil quality drives the priming effect and plant species refine it.....	146
4.1.	<i>INTRODUCTION</i>	147
4.2.	<i>METHODOLOGY</i>	150
4.2.1.	Experimental setup.....	150
4.2.2.	Air sampling.....	151
4.2.3.	Soil and biomass sampling.....	154
4.2.4.	Statistical analysis.....	156
4.3.	<i>RESULTS</i>	158
4.3.1.	Soil characteristics and changes in carbon content	158
4.3.2.	Priming effect	158
4.3.3.	Evolution of ¹³ C abundance in respired CO ₂ (A ¹³ C) over 6 months	159
4.3.4.	Evolution of ratio of CO ₂ derived from fresh plant new C input (f _{Plant}).....	160

4.3.5.	Correlations between OldC loss, NewC input, priming and A ¹³ C	160
4.4.	<i>DISCUSSION</i>	161
4.4.1.	Subsoil and topsoil revegetation: identifying the substrate preference of microbial communities.....	161
4.4.2.	The impact of plants on the two soil types: competition for nitrogen	163
4.4.3.	The priming effect and its implication in practice.....	164
4.5.	<i>CONCLUSIONS</i>	165
	<i>REFERENCES</i>	166
	<i>FIGURES AND TABLES</i>	170
	<i>SUPPLEMENTARY MATERIALS</i>	176
	Chapter V: General discussion	179
5.1.	<i>Carbon quality matters: coarse particle pool versus fine particle pool.....</i>	180
5.2.	<i>Carbon origin matters: new carbon versus old carbon.....</i>	180
5.3.	<i>Microbial community matters: priming and entombing</i>	182
5.4.	<i>Root traits matter: N₂ fixing species (Fabaceae) vsnon N₂ fixing species (Poaceae)</i>	184
5.5.	<i>Soil matters: a major factor in carbon-cycle regulation, but due to indirect effects</i>	185
5.6.	<i>Ecological engineering toward a carbon sequestration goal</i>	187
5.7.	<i>What research remains to be performed?</i>	188
	<i>REFERENCES</i>	191
	<i>FIGURES AND TABLES</i>	194
	Annex I: Perspectives: the influence of vegetation on soil microstructure and its implications on soil carbon sequestration: a geotechnical approach	197
	Résumé exhaustif: Objectifs, résultats, conclusions générales	217

CHAPTER I: General introduction

1 1.1.CONTEXT

2 Soil holds the second largest terrestrial carbon (C) pool (1500 to 2400 GtC to a depth of one meter,
3 IPCC 2014; Adams et al. 1990; Anderson 1992; Eswaran et al. 1993; Batjes 1996) with possibly another
4 900Gt at a depth of 1-2 m (Batjes 1996, Jobbagy et al. 2000), after the lithosphere but in front of
5 vegetation (350 to 550 GtC, mainly in forests) and atmosphere (829 GtC, IPCC 2014). Soil shares the
6 common interface with all the other spheres and thus plays a key role in driving the global C cycle. How
7 to prevent C loss from soil and how to sequester more C into soils has become one of the most
8 important scientific and political quests in global change biology (Sauerbeck 2001; Lal 2004). The
9 European Union is actively involved in this issue, and the topsoil soil organic C content is an official
10 indicator for the EU sustainable Development Goals (EU-SDG, 2018), leading to the funding and
11 supervision of several programs focused on soil conservation and soil C increase. Some examples,
12 among others, that involve assessment of soil organic carbon and potential sequestration, showing the
13 interest and importance of this topic, are the CIRCASA project (<https://www.circasa-project.eu/>),
14 LANDMARK project (<http://landmark2020.eu/>), iSQAPER project (<http://www.isqaper-project.eu/>),
15 and LUCAS project (<https://esdac.jrc.ec.europa.eu/projects/lucas>), all funded in the framework of
16 Horizon2020. The FAO is also involved in numerous projects focusing on soil health, that among other
17 things underline the importance of soil C increase for climate change mitigation, like GSOCmap
18 (<http://54.229.242.119/GSOCmap/>) or the Intergovernmental Technical Panel on Soils (ITPS)
19 (<http://www.fao.org/global-soil-partnership/intergovernmental-technical-panel-soils/en/>). Similarly,
20 on a national basis, different projects have been developed focusing on the potential of soil C storage
21 for climate change mitigation. One of the most striking examples is the 4p1000 initiative
22 (<https://www.4p1000.org/>), launched by France on 1 December 2015 at the COP 21, stating that
23 increasing by 4 % the soil C stock in agricultural soils would completely remove the excess of CO₂ in
24 the atmosphere produce by anthropic actions. However, studies on strategies of C sequestration in
25 soils are mainly limited to “green systems” (e.g. forests, grasslands, plantations, croplands, wetland
26 etc.), where the soils are considered to be or potentially to be, a C sink. We argue that, in an irrevocable

27 era of industrialization and urbanization, soil in “grey systems” connected with geotechnical
28 infrastructure industry must be taken into consideration for soil C sequestration. There are two main
29 reasons for that: i) the high environmental impact of geotechnical industry, in particular on CO₂
30 emissions, that needs to be mitigated, and ii) the drastic increase of geotechnical infrastructures, in
31 particular road and railroads, which means that soils connected to geotechnical infrastructures can no
32 longer be ignored for their potential ecosystem services, among which is soil C sequestration.

33

34 *1.1.1. Impact of geotechnical structures on greenhouse gasses emissions and TERRE* 35 *project*

36 It is well known how construction activities and practices commonly related to geotechnical
37 engineering have a high environmental impact, negatively influencing climate change, soil sealing,
38 erosion, deforestation, desertification, ozone depletion and general air/water/soil pollution (Kibert
39 2008; Misra and Basu, 2011). Regarding the impact of these practices on CO₂ emissions, numbers can
40 vary according to different sources, but there is general agreement that construction and
41 infrastructure have a high impact on global greenhouse gas emissions. Global CO₂ emissions from
42 construction work are attested in a range of 25-40% of the total CO₂ emissions (Dixit et al. 2010,
43 O’Riordan et al. 2011). It is well established among researchers, policy makers and practitioners how
44 a switch towards sustainable geotechnical solutions is not only desirable but absolutely vital to face
45 the challenges of climate change mitigation, and to move toward a sustainable future (Dejong et al.,
46 2011; Misra and Basu, 2011; Gallipoli and Mendes, 2017). In this optic, the current thesis is financed
47 by the Marie Skłodowska-Curie Innovative Training Networks (ITN-ETN) TERRE ([http://www.terre-](http://www.terre-etn.com/)
48 [etn.com/](http://www.terre-etn.com/)): Training Engineers and Researchers to Rethink geotechnical Engineering for a low carbon
49 future. The aim of the TERRE project is to develop new geo-technologies to address the challenge of
50 a low carbon impact European construction industry. In the TERRE action, multiple interdisciplinary
51 projects have been developed under a wide umbrella of practices: optimization of energy requirement
52 for construction, role of plants to increase soil stability via root reinforcement and hydraulic suction,

53 new low C impact materials for construction, etc. The present thesis project aims to investigate the
54 role of geotechnical embankments as C sinks.

55

56 *1.1.2. Road and railroad development*

57 In the last decades, highways and railroad systems have dramatically increased their surface. Especially
58 in developing and emerging countries, major investments have been made to increase and expand the
59 infrastructure systems, since connections among countries and cities are one of the fundamental
60 aspects of economic growth. Globally, the railroad system increased its length by 100000km in the last
61 year (<https://data.worldbank.org/topic/infrastructure>). The Chinese public roads passed from 3.5 to
62 4.8 million km in the last 10 years (<http://statista.com>). In India, in the last 4 years, the length of the
63 highways increased by 60000km, and other 200000km of highways are expected to be finished by 2022
64 (<https://www.ibef.org/industry/roads-india.aspx>). Another striking example of the massive future
65 infrastructure development is the China's 'Belt and Road' initiative, planning to connect via a complex
66 system of roads and maritime route, Asia, Africa and Europe. Together with the development of the
67 Trans-African Highway, consisting of 60000km of highways started in 1971 by United Nations Economic
68 Commission for Africa and not yet completed, we have a picture of the dramatic increase of the global
69 infrastructure system. This overview clearly shows how the soils connected with geotechnical work, in
70 particular with the construction of road and railroad infrastructures (hereafter 'geotechnical soils'), are
71 increasingly important and any potential benefits and ecosystem services need to be explored. Road
72 and railroad embankments play a pivotal role in the interactions between environment and
73 infrastructure, and a correct design could increase the ecosystem services they can provide.

74

75 *1.1.3. Development of sustainable geotechnical practices*

76 Efforts to increase the sustainability of geotechnical structures have already been made. Practices
77 included the use of alternative ecofriendly materials, use of bio-engineering on slopes, reuse and
78 restauration of older structures, underground energy storage, and use of geothermal energy (Misra

79 and Basu, 2011). However, all these practices are based on the reduction of CO₂ emissions. Such a
80 framework relies on a passive role of geotechnical structures (new technologies to reduce CO₂
81 emission), but ignoring the potential active role that geotechnical soil can have in reducing
82 atmospheric CO₂ concentration via soil organic C sequestration.

83

84 *1.1.4. Geotechnical embankments: a new hotspot for soil carbon sequestration?*

85 Geotechnical soils present some unique features that could potentially make them achieve efficient
86 soil carbon sequestration. The main general feature is that geotechnical soils do not present specific
87 constraints regarding their use. The objective of agricultural soils is the production of food and goods
88 for direct consumption or to be placed on the market. Therefore, agricultural soils have an “economical
89 constraint”, and the objective of stakeholders, even in a framework of sustainability, is to increase or
90 maintain production without depleting soils. In a natural ecosystem, it is possible to talk about an
91 ‘ecological constraint’, in the sense that it is not possible to modify the environment to increase soil C
92 storage without disturbing the ecological balance and networks of the systems, affecting the health of
93 the system itself and, ultimately, the ecosystem services that it provides to the community.

94 Geotechnical soils, instead, are heavily anthropized soils, where the ecological balance has already
95 been disturbed. Moreover, soils are frequently moved from other areas or dug and brought to the
96 surface, changing the soil composition, microbiology, fertility and, ultimately, their ecological value.
97 Vegetation planted on geotechnical soils, especially on embankments, is not used for agricultural
98 production. Re-vegetation is therefore artificially implanted, and there are few ecological or economic
99 constraints. These soils and the plants used for revegetation can be chosen and planned to promote
100 regulating, supporting and cultural ecosystem services, including embankment stability maintenance,
101 erosion control, noise dissipation, traffic air pollution isolation, biodiversity conservation and
102 aesthetical effect against driver fatigue. Among these ecosystem services, in particular, we argue that,
103 contrary to agricultural and natural systems, geotechnical soils can be actively designed for CO₂
104 sequestration. Dejong et al. (2011) advocated the possibility of using geotechnical soils to efficiently

105 store C by i) selecting plants that efficiently fix and move C into soil, ii) study different microbial
106 communities that influence soil C cycle and the potential of inoculation, iii) selection of different soils
107 with higher potential for organomineral interaction and C protection, and iv) using soil improvers (like
108 recycled concrete and furnace slag) to increase C sequestration. However, no specific studies have
109 been implemented to really investigate the C sequestration potential of geotechnical soils and how to
110 maximize it. Therefore, in this thesis I aim to start investigating the potential for designing efficient C
111 sequestering embankments, starting with the main issue of soil and plant selection.

112

113 *1.1.5. Embankment design*

114 When designing an embankment, the structure is based on a core of clay soil compacted according to
115 a Proctor compaction test, to achieve maximum dry density (Standard Australia, 2003). This compacted
116 soil core is usually covered with a 30-50 cm layer of uncompacted soil for revegetation (Fig. 1). The
117 construction and design of the embankment is outside the scope of this research, where only the soil
118 layer used for revegetation is considered for potential soil C storage. This soil layer is usually stripped
119 topsoil (\cong 30cm) collected in the area and conserved, while the clay core is usually subsoil excavated,
120 mixed and, if needed, adjusted with additional soils or soil improvers to achieve the optimal density
121 level to support the structure. However, often the layer of topsoil is collected and transported to the
122 construction site from other fertile areas, with a high impact on CO₂ emissions (for the transport) and
123 on environment (for the ecological value of fertile topsoil). We argue that, to improve the sustainability
124 of the embankments, instead of using valuable topsoil for revegetation, mineral subsoil (> 1m depth)
125 collected in the area can be prepared and used for revegetation. Compared to stripped topsoil, subsoil
126 embankments are more economically interesting, but usually demand higher constraints in plant
127 selection due to their less favorable growing conditions (although recent soil inoculation techniques
128 can improve this). Herbaceous plants are essential materials for embankment revegetation.
129 Herbaceous plants usually demand low maintenance cost and intensity, with one or two cuts per year

130 to maintain vegetation vigor. The choice of soil (organic topsoil *versus* mineral subsoil) and vegetation
131 will deeply influence the potential for C sequestration.

132 However, to effectively enhance C sequestration in geotechnical soils, a better understanding of the
133 mechanisms behind the plant-soil C-cycle is necessary. There is a need to understand the influence of
134 different plants on soil C sequestration and their relationships with soil and microbiological
135 communities, to allow the design of the best practices for soil C sequestration, in geotechnical and
136 non-geotechnical soils.

137

138 *1.1.6. Plants: the primary source of carbon input in soil*

139 Plants act as conduits to transport C from atmosphere to soil (Fig. 2). Plants regulate the uptake and
140 fixation of CO₂ in different organic forms via photosynthesis, using water and atmospheric CO₂ as 'raw
141 materials' and light as an energy source (Chan, 2008). Plants also regulate the input of C in soil via two
142 main processes: 1) plant biomass from roots and shoots in the form of litter, forming soil particulate
143 organic matter (POM) and 2) root exudates and other labile C compounds released by roots during
144 plant growth (Hungate et al. 1997; Lal, 2004) (Fig. 2).

145 With regard to C input, the first process strongly influencing the C-cycle is C input in forms of residues
146 derived from vegetation. The selection of plants can considerably influence the C input in soil in terms
147 of quantity (biomass production) and quality. Biomass production and related amount of C input is not
148 the only driver for soil organic C accumulation. It has now been observed that the litter quality,
149 especially regarding the C:N ratio of plant tissues, will strongly influence the decomposability of POM
150 and its residence time in the soil (Castellano et al. 2015). C from exudates also represents a major
151 amount of C that plants transfer from the atmosphere to soil (Balesdent and Balabane, 1996).
152 Estimates vary from more conservative values, such as 5 - 33% of daily photoassimilates (De Deyn et
153 al. 2008), to 40-60% (Högberg et al. 2001; Clemmensen et al. 2013; Keiluweit et al. 2015;) to up to 80%
154 of photosynthetically assimilated C moved in 10 days via exudates in soil (Reid and Mexal, 1977). The

155 input from exudates has traditionally been seen as the 'labile C input' that is consumed and respired
156 quickly in the soil system. However, recent studies showed how C protected via organomineral
157 complexation on minerals and in aggregates mainly derive from plant exudates or microbiological
158 exudates and exopolysaccharides, that in turn originate from plant labile C input consumption and
159 complexation (Lorenz and Lal 2005; Six et al. 2006; Cotrufo et al., 2013; Vidal et al., 2018).

160 In a recent review, Poirier *et al.*, (2018) has argued that the root traits that most influence C
161 stabilization are those related to chemical composition, root exudation and the presence of symbionts
162 (mycorrhizas and dinitrogen (N₂) -fixing *Rhizobium*), whereas the role of morphological traits is not yet
163 clear. More specifically, root traits increasing recalcitrance promote short-term C stabilization by
164 slowing decomposition rates, but traits that reduce recalcitrance contribute to long-term C
165 stabilization via the reaction of microbial products with mineral surfaces. Although several studies have
166 analyzed the link between plant functional traits, microbial activity and C accumulation (Chapin 2003;
167 Lavorel *et al.*, 2007; De Deyn *et al.*, 2008; Poirier et al. 2018), as yet, no study has focused on how root
168 growth and specific traits can alter the accumulation and potential persistence of different soil C pools,
169 that are linked to the physical structure of soil itself (see Cardinael et al., 2015; Fujisaki *et al.* 2018).

170 C entering the soil can face two main fates: be consumed by microorganisms and leave the soil pool
171 via microbiological respiration, or be stored in the soil for different periods of time, often after being
172 processed by microorganisms.

173

174 *1.1.7. Microbiological communities: the carbon pump in different soil fractions*

175 Microbiological communities can be identified as a further main actor for the C storage in soil (Fig. 2).

176 Soil organic C consumption by microorganisms will mainly depend by their substrate use efficiency,
177 meaning the proportion of the C used by microorganisms for biomass growth or enzyme production
178 (part of the C stock in soil) and the C respired or mineralized (Lekkerkerk et al., 1990). The balance
179 between these two fluxes, accumulation in biomass and/or via microbial exudation and loss via

180 respiration, will depend on different factors related to substrate quality, (C:N ratio, molecular
181 complexity, molecular weight and solubility) and the efficiency of different microbiological
182 communities to degrade organic C in soil (Lekkerkerk et al., 1990, Cotrufo et al, 2013) which can vary
183 by microbiological abundance, composition and partition between bacterial and fungal communities
184 (Six et al., 2006). Microorganisms are also mainly responsible for C transformation in soil, consuming
185 C input of plants in form of exudates or root debris, and 'pumping' it into the soil structures and in
186 contact with mineral surfaces, in the form of microbial exudates and exopolysaccharides (Cotrufo et
187 al., 2013; Vidal et al.; 2018). This active role of microbes have been formalized by the conceptual
188 framework of 'microbial C pump' by Liang et al. (2017). However, this framework does not consider
189 the destination of microbial derived C in different soil C pools. When in symbiosis with plants, the C
190 substrates that are assimilated by microorganisms at the root apex are utilized rapidly for respiration
191 and growth, or lost as microbial exudates or exopolysaccharides that are used as a substrate for
192 subsequent microbial communities. Certain microbial species, such as *Rhizobium*, present in nodules
193 of N₂-fixing species, produce large amounts of exopolysaccharides (Downie, 2010) that can also be
194 adsorbed onto fine silt and clay particles (Fehrmann and Weaver, 1978).

195

196 *1.1.8. Soil: responsible for carbon protection*

197 Finally, the last main actor to consider in the determination of the fate of soil organic C is the soil itself
198 (Fig. 2). The residence time of C is controlled by the protection mechanisms that contribute to stabilize
199 it (Luo et al. 2004; Jastrow et al. 2005). C in soil can be divided into three main pools: an unprotected
200 C pool, referring to the labile particulate organic matter (POM) in the soil, a biochemically protected
201 pool (BPC) (Fig. 3), when C is moved in soil in recalcitrant forms and is difficult for microorganisms to
202 consume it, and a physically protected pool (PPC), when C is protected inside aggregates or absorbed
203 on clay/silt particles and cannot easily be consumed by microorganisms (Fig. 3). The POM and BPC pool
204 fate depends on the nature of the organic matter and the microbiological communities, as discussed
205 previously. The PPC is considered to be the most stable C pool, and therefore the most important for

206 soil C storage (Rumpel et al. 2012). Regarding the PPC, it is particularly worthwhile to explore the
207 linkage between PPC and labile C from plants, i.e. C from exudates. Exudates were usually considered
208 to be immediately consumed by microorganisms and to play a marginal role in C sequestration (van
209 Veen et al. 1991; Van Geijn et al. 1993; Hungate et al. 1997). This assumption is now questioned by
210 more recent studies that state that labile soil C compounds are just partially consumed, and dissolved
211 labile organic C can be protected by soil absorption inside aggregates or on clay and silt (see review by
212 Kalbitz and Kaiser, 2008). Moreover, it has been demonstrated that microbiological exudates and
213 exopolysaccharides are the main precursor of organomineral protected C (Cotrufo et al., 2013; Vidal
214 et al., 2018). To understand the fate of C and increase the PPC, the two main mechanisms of C
215 protection need to be investigated.

216

217 *1.1.9. Soil structure and carbon physical protection in aggregates*

218 Aggregate protection of C is due to the C physical protection from microorganisms by occlusion of C in
219 the smaller pores, limiting the gas and nutrient diffusion and, therefore, microbiological activity, and
220 separating enzymes from substrates on mineral and humic surfaces (O'Brien and Jastrow, 2013).
221 Aggregates are formed by binding of soil particles by fine roots and fungal hyphae (Tisdall and Oades
222 1982) and cementation by microbiological and plants exudates, like glycoproteins, polysaccharides,
223 and mucilage, directly influencing the stability of aggregates (Tisdall and Oades 1982; Caesar-Tonthat
224 2002; Nichols and Wright 2005). The formation of aggregates is different in regards to their size. Abiotic
225 factor, such as ligand exchange and polyvalent cation bridging promoted by drying-rewetting cycles
226 (Bronick and Lal, 2005; Keil and Mayer, 2014), are known to form stable microaggregates.
227 Microaggregates are then complexed in small macroaggregates thanks to the biotic action and
228 cementation from microbes that produce extracellular polymeric substances acting as glues to connect
229 soil aggregates (Blankinship et al., 2016). Fine roots and hyphae of fungi further complex aggregates in
230 bigger structures thanks to their enmeshing action (Tisdall and Oades, 1982; Blankinship et al., 2016).
231 The silt and clay particles are connected with the formation of microaggregates, while sand particles

232 are mostly associated with macro- aggregates (Blagodatskaya and Kuzyakov, 2008). The stability of
233 aggregates is an important factor influencing C protection since it will directly influence the
234 aggregation and disaggregation processes in soils. However, aggregation is a dynamic process, with
235 aggregates continuously forming and being destroyed by natural cycles and animal or anthropogenic
236 disturbance (Eyles et al. 2015). Aggregate size is another important characteristic influencing C
237 protection: Jastrow (2006) states that C turnover is higher in macroaggregates (>212 μm) compared to
238 microaggregates (53-212 μm), implying that microaggregates have a higher C protection potential.

239

240 *1.1.10. Organomineral interactions with fine silt and clay minerals and soil carbon* 241 *saturation*

242 The other main mechanism for C protection is organomineral interactions with cations in soil that
243 decrease the soil C lability (Eyles et al., 2015; O'Brien and Jastrow, 2013). This process can happen
244 inside aggregates or in loose soil and relies on chemical sorption on mineral surfaces, polyvalent cation
245 bridging and layered chemical binding on mineral surface, of microbiological products primarily
246 adsorbed on minerals and covered by exudates (Cotrufo et al., 2015; Kleber et al. 2007; O'Brien and
247 Jastrow, 2013). The soil potential for organomineral interactions relies on the amount of fine elements
248 in the soil (especially clay particles), cations of different reactive elements, in particular Fe and Al
249 (Swanston et al. 2009), and, particularly interesting for this study, C saturation level of the soil. The
250 concept of soil C saturation has been highlighted after some studies reported no increase of soil organic
251 C in soils even after further increase of C input (e.g. Campbell et al. 1991, Solberg et al. 1997, Gill et al.
252 2002). To explain this behavior of soil, Six et al. (2002) introduced the concept of 'soil C saturation',
253 where it was suggested that the different C pools have different saturation points after which they
254 cannot effectively store C anymore. The capacity of these pools to store C depends on their nature.
255 For example, the physically protected C pool relies on the surface area of particles, meaning that after
256 the available areas are occupied by adsorbed C and further C input will not be associated anymore and
257 therefore not protected (Six et al. 2002). This concept was further elaborated by Stewart et al. (2007),

258 who stated that the soil C pool can be saturated with respect to the C inputs and that a linear model
259 cannot efficiently describe the input-storage behavior of a soil (Fig. 4). In this respect, Stewart et al
260 (2007) conclude that a soil poor in C, can store C more efficiently than a soil rich in organic C and,
261 therefore, closer to its C saturation threshold (Fig. 4), depending on the content of clay/silt of the soils,
262 the aggregation capacity, and their adsorption capacity. Several studies suggested that subsoil might
263 protect C more efficiently in fine soil fractions due to lower C saturation that increase the possibility
264 for organomineral interactions (Rasse et al., 2005; Lorenz and Lal 2005; Thomas et al. 2007; Horrocks
265 et al. 2010; Rumpel et al., 2012). However, to our knowledge, no studies focused on the potential of
266 subsoil revegetation and the influence on the C-cycle and organomineral interactions.

267

268 *1.1.11. Soil carbon pools associated to different soil fractions*

269 When analyzing C content in soil, it is difficult to assess the different pools of C present in the soil and
270 their protection (biological protection determined by recalcitrance or physical protection from
271 aggregate occlusion or organomineral interactions). A method commonly used to assess C protection
272 in soil is to fractionate the soil and analyze the C in each fraction (Fig. 5). These soil C pools rely on
273 different protection mechanisms, and the degree of stability increases with decreasing fraction size.
274 These pools are defined as: i) coarse particulate organic matter (coarse POM, soil fraction > 200 μ m)
275 (Fig. 5a), that is free in the soil at different levels of degradation ii) fine POM (soil fraction 50-200 μ m)
276 (Fig. 5b), that comprises organic C occluded in soil aggregates. These two pools are mostly derived
277 from the decomposition of roots and shoots (Kögel-Knabner, 2002) and their C protection from
278 microbial consumption relies mainly on the recalcitrance of their lignocellulose C structures (Six *et al.*,
279 2002). Finally, iii) C protected in the coarse silt (20-50 μ m) (Fig. 5c) and iv) in fine silt+clay pools (<20 μ m)
280 (Fig. 5d). C protected in these pools is mostly derived from labile rhizospheric and microbial
281 compounds (Cotrufo *et al.*, 2013, Vidal *et al.*, 2018). C in these pools is highly degraded via
282 decomposition and mineralized by microbial metabolism, and it is protected from microbial

283 consumption via occlusion in microaggregates and through organo-mineral complexation with clay
284 particles and metals.

285

286 *1.1.12. Short – term changes in soil organic carbon mineralization due to vegetation: the*
287 *priming effect*

288 Although the positive effect of revegetating soils in terms of C input and soil C accumulation potential
289 is well established, the influence of plants on the C-cycle can also have negative impacts on soil C
290 sequestration. As already mentioned, the potential of a soil system in respect to C sequestration is
291 determined by the balance between input of photosynthetically absorbed C in soil and output of CO₂
292 via soil heterotrophic respiration (Smith et al., 2000; De Deyn et al., 2008). The soil heterotrophic
293 respiration is determined mainly by microbial communities and their activity, and their consumption
294 of C in soil (Jones *et al.*, 2009; Kuzyakov and Larionova, 2006). One of the effect of plant C input is to
295 influence the microbial communities structure and activity and the consequent consumption of pre-
296 existent soil C, that is commonly known as ‘priming effect’ (Broadbent and Nakashima, 1974; Sørensen,
297 1974; Wu et al., 1993; Kuzyakov et al., 2000). The priming effect is defined as strong short – term
298 changes in C mineralization due to vegetation (Kuzyakov et al., 2000). We talk about ‘positive priming
299 effect’ when the input of labile C increases the activity of microbial communities and the mineralization
300 of pre-existent C in soil (Fontaine et al., 2003). The positive priming effect has an adverse effect on soil
301 C storage. However, if microbial communities in soil switch from consuming pre-existent C to
302 mineralizing fresh C input, the mineralization of soil C will decrease (Kuzyakov et al., 2000). In this case
303 we talk about a ‘negative priming effect’, beneficial to C storage in soil. The magnitude of the priming
304 effect and its direction (positive or negative) results from a complicated series of interactions between
305 soil, plants and microbial communities (Cheng and Kuzyakov, 2005). The first mechanism is known as
306 the ‘competition hypothesis’ (Jackson et al., 1989; Schimel et al., 1989; Kaye and Hart, 1997; Hodge et
307 al., 2000; Cheng and Kuzyakov, 2005) and postulates that competition for mineral N will determine the
308 direction of priming. If the soil is poor in N, then the priming effect is negative due to competition

309 between plants and microbes. In the long run, plants have a higher efficiency for N mining, and they
310 will reduce the nutrient sources for microbial communities, decreasing their C consumption (Cheng
311 and Kuzyakov, 2005). Instead, when mineral nutrients are not limiting and there is no competition
312 between plants and microbes, rhizodeposition will increase microbial activity resulting in increased soil
313 C consumption and a positive priming effect (Cheng and Kuzyakov, 2005). These mechanisms hold
314 when microbial communities need to mine C for nutrients and energy, and are usually observed in
315 studies involving poor soils (pine forests and dry grasslands) (Ehrenfeld et al., 1997; Schimel et al.,
316 1989; Cheng and Kuzyakov, 2005).

317 When mineral nutrients are not limiting and the input of labile C is high, the priming effect might be
318 controlled by the preference of microbes for labile root derived C compared to nutrient rich soil C
319 (Cheng and Kuzyakov, 2005). If no nutrient limitation is present, microbes will prefer labile derived C
320 as an abundant and ready available source of energy (Cheng, 1999; Cheng and Kuzyakov, 2005). In this
321 case, a switch of substrate utilized will decrease the C consumption and result in a negative priming
322 effect, favouring soil C storage (Cheng and Kuzyakov, 2005, De Graaf et al. 2010). These effects are
323 regulated by microbial metabolism (Cheng and Coleman, 1990). Increased microbial biomass is linked
324 with positive priming, while negative priming is usually correlated to decreased microbial biomass
325 (Cheng and Coleman, 1990; Reid and Goss, 1982; 1983; Sallih and Bottner, 1988). However, De Graaaf
326 et al. (2010) showed how different levels of labile C input can influence microbial dynamics and
327 consequent priming effect. Low input of labile C ($\cong 0.7 \text{ mgC g}^{-1} \text{ soil}$) will increase microbial activity and
328 soil C mining, resulting in a positive priming effect. Instead, high labile C input ($> 7.2 \text{ mgC g}^{-1}$) increases
329 microbial biomass but induce microbes to switch preference of substrate consumption, from old C
330 present in the soil to the fresh C inputted from plants substrate utilization switch, decreasing old C
331 consumption compared to unvegetated soil and resulting in a negative priming effect (De Graaf et al.,
332 2010).

333

334 *1.1.13. Possible impacts of revegetating geotechnical soils on the priming effect*
335 In geotechnical works, soils are often heavily managed and revegetated. Environmental conditions are
336 perturbed and it is not uncommon that subsoil is excavated, brought to the surface and revegetated.
337 Subsoils have a high C stability given by i) low microbial biomass (Taylor et al. 2002; Andersen and
338 Domsche 1989; Ekklund et al. 2001) and activity (Fang and Moncrieff 2005), ii) oxygen limitation
339 (Rumpel and Kögel-Knabner, 2010), iii) energy limitation due to reduced labile C inputs (Fontaine et al.
340 2007) and iv) spatial heterogeneity of organic C in subsoil and consequent separation from microbes
341 (Von Lützow et al. 2006; Holden and Fierer 2005). Fontaine et al. (2007) showed how a supply of fresh
342 C in deep soil can decrease the stability of pre-existent old C and increase positive priming. However,
343 to our knowledge, no in vivo experiment has been implemented on this topic, and, more importantly,
344 no studies are available on the effects of excavating and revegetating subsoil on the priming effect.
345 Excavating, crushing, mixing, and revegetating soil will have a major impact on the factors determining
346 the stability of C in subsoil, and possibly a high priming effect.

347

348 **1.2. GENERAL KNOWLEDGE GAPS**

349 As stated above, soil embankments represent an interesting structure for C sequestration due to two
350 features: 1) plants can be chosen to vegetate the embankments, and therefore the C input in the
351 system, and 2) soil can be managed and chosen to optimize C sequestration. Embankments are
352 constituted of a core of compacted soil, usually excavated from a depth of >1m and with a high
353 percentage of clay, and they can be covered by a layer of stripped topsoil to be revegetated. The choice
354 of revegetating organic topsoil (down to 30 cm depth) stripped and used to cover the embankment,
355 or directly on an uncompacted surface layer of mineral subsoil (>1 m depth), will deeply influence the
356 soil C storage potential of the geotechnical structure. However, no studies have been developed in
357 depth on the effects of revegetating subsoil brought to the surface on C storage, and their potential as
358 C sink. There is a need of comparing C storage potential of different plants and soils to design the most

359 efficient C storage system in geotechnical soils, a potential that have been hypothesized before but
360 never addressed (Dejong et al., 2011).

361 The study of two soils showing diverse characteristics (fertility, microbial communities, C saturation
362 levels), and the use of plant species that have contrasting root traits connected with higher
363 recalcitrance or lability, allows to tackle fundamental knowledge gaps regarding the actors and
364 mechanisms driving C sequestration in soil. The next paragraphs give an overview of the knowledge
365 gaps addressed in each chapter of the thesis.

366

367 *1.2.1. Plant carbon input: influence of root traits and carbon accumulation in different* 368 *soil C pools*

369 Rhizosphere is considered as the main pathway for C to enter the soil, however few studies have
370 tackled the relationships between root traits and C storage. The studies that have indeed explored the
371 effect of the root economics spectrum on C storage (e.g. De Deyn et al., 2008; Bardgett et al., 2014;
372 Poirer et al., 2018; Henneron et al., 2019) considered the C storage in bulk soil, without exploring the
373 effect of root traits on C quality, i.e. the accumulation of C in different pools. Moreover, among the
374 different explored root traits, the root elongation rate has never been studied in relationship to C
375 storage. We state that root economics spectrum is lacking an important trait, since changes in root
376 elongation rate affect the production and the spatial distribution of root exudates, the main precursor
377 of C stored in SILT+CLAY pool (Cotrufo et al., 2013; Holz *et al.*, 2018).

378 *1.2.2. Subsoil brought to the surface: effect on C fluxes and actors involved in C-cycle*

379 Soil C stock within a defined time frame is the balance between input and transformation of newly
380 photosynthesized C from plants to soil (new C) and losses of existing soil organic C (old C) (Kuzyakov
381 and Domansky, 2000; Fontaine et al., 2004). Moreover, the balance between new C and old C is far
382 from being the whole story, as increasing studies have highlighted the equal importance of quality of
383 soil C, as C stored in different C pools (Cardinael et al., 2015). To our best knowledge, no study has ever
384 bridged the link between C pools and the fates of new C and old C. Besides the exploration of the fates

385 of soil new C and old C, as well as their associations with C pool, another significant knowledge gap
386 comes to the predictability of the fates of soil new C and old C using plant and soil features. More
387 specifically, no studies investigated the effect of root traits, microbial communities and soil
388 characteristics (with an eye of attention to the C saturation theory) on new input and old c changes in
389 different C pools.

390

391 *1.2.3. Subsoil brought to the surface: what is the effect of revegetation on the priming* 392 *effect*

393 Revegetating subsoil could have a high impact on pre-existent old C stability and the priming effect. C
394 in subsoil is highly stable, and perturbation of the environmental conditions could deeply influence the
395 stability and protection of this pool. Studies on priming of subsoil have been conducted (Fierer et al.,
396 2003; Fontaine et al., 2007; Wang et al. 2014), however no studies investigated the effect of bringing
397 subsoil to the surface. Understanding the priming effect at soil fraction level may also bring us new
398 insight on the vulnerability of soil C pools to fresh C input.

399

400 **1.3. STRUCTURE OF THE THESIS: OBJECTIVES AND HYPOTHESES**

401 Figure 6 shows the different research questions tackled in the research and discussed in each chapter,
402 plus their link with the main factors and processes discussed in each chapter. In this theses I and the
403 research team collaborating in this project aim to tackle the following general objectives:

- 404 i - Understanding the effect of plant and soil features on soil C sequestration in terms of quantity
405 and quality (fundamental objective)
- 406 ii - Identifying possible plant and soil practices that can be implemented to increase soil C storage
407 in embankments and, possibly, in grey soils from geotechnical work (applied objective)

408 The above two objectives regarding the fundamental mechanisms of C-cycle will be tackled in every
409 chapter of the thesis.

410

411 *1.3.1. Chapter II: Pathway to persistence: plant root traits alter C accumulation in*
412 *different soil carbon pools through microbial mediation*

413 i - Objective 1: Understand what are the relationships between root traits and C accumulation in
414 different soil C pools for 12 different herbaceous species commonly used in embankment
415 revegetation (Fig. 7).

416 Hypothesis 1: We hypothesize that traits related to labile C input (root elongation rate, hemicellulose
417 content, root biomass) promote C accumulation in the protected coarse silt and fine silt + clay C pools,
418 since these traits are expected to favor rhizodeposition and microbial activity, whereas root traits
419 related to recalcitrance (high lignin and cellulose content, high C:N ratio) promote C accumulation in
420 the unprotected coarse POM pool.

421 ii - Objective 2: What is the effect of species selection on the C sequestration in different soil C pools
422 Hypothesis. 2: We hypothesize that N₂-fixing species favor C accumulation in the protected fine
423 silt+clay pools since they have traits more related to labile C input, while non N₂-fixing species will favor
424 C accumulation in the POM fraction.

425

426 *1.3.2. Chapter III: The fates of fresh new carbon and old soil carbon differ in topsoil and*
427 *newly exposed subsoil and are explained by root, microbial, and soil particle size*

428 i - Objective 1: Quantify the fluxes of new C and old C in different soil pools;

429 Hypothesis 1: We hypothesize that soil particle size fractions associated C pools can regulate the fates
430 of old C and new C in the C sequestration process;

431 ii - Objective 2: Examine the pattern of covariation between new C input and changes of old C in
432 different C pools

433 Hypothesis 2: The fate of new C and old C will show independent patterns

434 iii - Objective 3: Investigate if the different actors involved in C storage, and the influence that plant
435 and soil have on them, can explain the patterns of new C and old C fluxes in different soil C pools

436 Hypothesis 3: We hypothesize that plant traits related to chemical composition and recalcitrance will
437 be driving POM accumulation in new C and consumption in old C, while traits related with high C input
438 will drive storage in protected fractions via microbiological consumption and deposition. We expect
439 aggregate stability to be positively correlated with new C and old C accumulation in fine POM and
440 coarse silt fractions due to physical protection of aggregates. We expect that soil N content positively
441 correlates with new C input. Fine fraction in soil is believed to be positively correlated with the new C
442 storage in fine silt+clay fraction due to organomineral interactions, and new C storage in fine silt+clay
443 is expected higher in subsoil than in topsoil due to lower soil C saturation levels. Finally we expect
444 microbial activity, diversity and abundance to be strongly linked with the amount of new C deposited
445 in the protected coarse silt and silt+clay fractions, and with the consumption and transformation of
446 old C in the unprotected coarse POM and fine POM fractions due to mineralization from microbial
447 communities.

448

449 *1.3.3. Chapter IV: Soil quality drives the priming effect and plant species refine it*

450 i - Objective 1: Quantify the changes in C and the input of new C in soil to determine the losses of
451 old C in revegetated topsoil and subsoil brought to the surface (Fig. 8) and the priming effect of
452 revegetating with N₂-fixing (*Medicago sativa*) and a non N₂-fixing species (*Lolium perenne*) species
453 (Fig. 9).

454 Hypothesis 1: Our hypothesis is that topsoil will have higher losses of old C due to higher microbial
455 biomass and activity. However, due to the higher protection of old C in subsoil and the changes in
456 environmental conditions given by revegetation, we hypothesize that subsoil will have higher old C
457 losses compared to bare soil, meaning a higher positive priming effect compared to topsoil.

458 ii - Objective 2: Quantify the priming effect in different C pools related to granulometric soil
459 fractions.

460 Hypothesis 2: Given the higher protection of C in the finer soil fraction (silt and silt +clay fractions) we
461 hypothesis that the priming will occur in the unprotected particulate organic matter fractions (POM
462 and finePOM).

463 iii - Objective 3: Study the evolution over time of the sources of respired C in the system
464 (represented by the abundance of ^{13}C) and its correlations with old C losses, new C input and
465 priming.

466 Hypothesis 3: We hypothesize that the source of respiration in the system will switch more towards
467 labelled plant inputs over time, along with plant development. We believe new C input to be positively
468 correlated with the abundance of ^{13}C in respired CO_2 (A^{13}C). However, we expect different behaviours
469 in the two soils regarding the old C losses. In topsoil we suggest that A^{13}C will be negatively correlated
470 with old C losses, due to switch in microbiological substrate preference, while in subsoil A^{13}C will be
471 positively correlated with old C losses, due to increased microbial activity. In the same way, priming
472 will be negatively correlated to A^{13}C in topsoil, while being positively correlated in subsoil.

473

474 *1.3.4. Chapter V: general discussion, guidelines and prospective for carbon storage in* 475 *geotechnical embankments*

476 In Chapter V I intend to delineate a more comprehensive view on the effect of soil and plant selection
477 on C storage in embankments based on the results of this study. I want to discuss the potential benefits
478 of embankments for C storage and propose guidelines for embankments revegetation, more
479 specifically: i) possible management options to increase C storage in these geotechnical soils and ii)
480 perspectives for future studies on C sequestration.

481

482 *1.3.5. Annex I: Perspectives: the influence of vegetation on soil microstructure and its* 483 *implications on soil carbon sequestration: a geotechnical approach*

484 Annex one is an overview of an ongoing research with UNICAS regarding soil structure. More
485 specifically we investigate the influence of vegetation on soil microstructure and its implications on

486 soil C storage and protection. I propose a multidisciplinary approach including geotechnical
487 engineering and soil science/ecological methods to investigate soil structure in terms of i) soil porosity
488 and void ratio, ii) aggregate stability and C protection, and iii) new C input in different aggregate
489 classes. These results will allow a more comprehensive view on aggregate formation and C protection
490 in revegetated topsoil and subsoil brought to the surface, and understand the role of porosity and void
491 ratio in relation to C protection. Research questions, methodology and preliminary results are outlined
492 in Annex I.

493

494 REFERENCES

- 495 Adams, J.M., Faure, H., Faure-Denard, L., McGlade, J.M., Woodward, F.I. 1990. Increases in terrestrial
496 carbon storage from the Last Glacial Maximum to the present. *Nature* 348: 711–714
- 497 Andersen, T.H., Domsche, K.H. 1989. Ratios of microbial biomass carbon to total organic carbon in
498 arable soils. *Soil Biology and Biochemistry* 21, 471–479
- 499 Anderson, J.M. 1992. Responses of soils to climate change. *Advances in Ecological Research* 22, 163–
500 210
- 501 Balesdent J and Balabane M. 1996. Major contribution of roots to soil carbon storage inferred from
502 maize cultivated soils. *Soil Biology and Biochemistry* 9, 1261–1263.
- 503 Bardgett, R.D., Mommer, L., De Vries, F.T., 2014. Going underground : root traits as drivers of
504 ecosystem processes. *Trends in Ecology & Evolution* 29, 692–699.
- 505 Batjes, N.H. 1996. Total carbon and nitrogen in the soils of the world. *European Journal of Soil Science*
506 47: 151–163
- 507 Blagodatskaya, E., Kuzyakov, Y., 2008. Mechanisms of real and apparent priming effects and their
508 dependence on soil microbial biomass and community structure: Critical review. *Biology and*
509 *Fertility of Soils* 45, 115–131.
- 510 Blankinship, J.C., Fonte, S.J., Six, J., Schimel, J.P., 2016. Plant versus microbial controls on soil aggregate
511 stability in a seasonally dry ecosystem. *Geoderma* 272, 39–50.
- 512 Broadbent, F.E., Nakashima, T., 1974. Mineralisation of carbon and nitrogen in soil amended with
513 carbon-13 and nitrogen-15 labeled plant material. *Soil Science Society of America Journal* 38,
514 313–315.
- 515 Bronick, C.J., Lal, R., 2005. Soil structure and management: a review. *Geoderma* 124, 3–22.
- 516 Caesar-Tonthat, T.C. 2002. Soil binding properties of mucilage produced by a basidiomycete fungus in
517 a model system. *Mycological Research* 106, 930–937.
- 518 Campbell, C.A., Lafond, G.P., Zentner, R.P., Biederbeck, V.O., 1991. Influence of fertilizer and straw
519 baling on soil organic matter in a thick black chernozem in Western Canada. *Soil Biology and*
520 *Biochemistry* 23, 443–446.
- 521 Cardinael, R., Chevallier, T., Barthès, B.G., Saby, N.P.A., Parent, T., Dupraz, C., Bernoux, M., Chenu, C.,
522 2015. Geoderma Impact of alley cropping agroforestry on stocks , forms and spatial distribution
523 of soil organic carbon — A case study in a Mediterranean context. *Geoderma* 259–260, 288–
524 299.
- 525 Castellano, M. J., Mueller, K. E., Olk, D. C., Sawyer, J. E., & Six, J. 2015.. Integrating plant litter quality,
526 soil organic matter stabilization, and the carbon saturation concept. *Global Change Biology*,
527 21(9), 3200–3209.
- 528 Chan, Y. 2008. Increasing soil organic carbon of agricultural land. *Primefact* 735, (JANUARY), 1–5.
529 Retrieved from [http://www.dpi.nsw.gov.au/__data/assets/pdf_file/0003/210756/Increasing-](http://www.dpi.nsw.gov.au/__data/assets/pdf_file/0003/210756/Increasing-soil-organic-carbon.pdf)
530 [soil-organic-carbon.pdf](http://www.dpi.nsw.gov.au/__data/assets/pdf_file/0003/210756/Increasing-soil-organic-carbon.pdf)

- 531 Chapin, F.S. 2003. Effects of plant traits on ecosystem and regional processes: a conceptual framework
532 for predicting the consequences of global change. *Annals of Botany*, 91, 455–463.
- 533 Cheng, W. 1999. Rhizosphere feedbacks in elevated CO₂. *Tree Physiology* 19, 313–320
- 534 Cheng, W., Kuzyakov, Y., 2005. Root effects on soil organic matter decomposition. In: S. Wright, S.,
535 Zobel, R. (Eds.), *Roots and Soil Management: Interactions Between Roots and the Soil*.
536 Agronomy Monograph No. 48, American Society of Agronomy, Madison, Wisconsin, USA 119–
537 143.
- 538 Cheng, W., and D.C. Coleman. 1990. Effect of living roots on soil organic matter decomposition. *Soil*
539 *Biology and Biochemistry* 22, 781–787.
- 540 Clemmensen, K. E. et al. 2013. Roots and associated fungi drive long-term carbon sequestration in
541 boreal forest. *Science* 339, 1615–1618.
- 542 Cotrufo, M. F., Soong, J. L., Horton, A. J., Campbell, E. E., Haddix, M. L., Wall, D. H., & Parton, W. J. 2015.
543 Formation of soil organic matter via biochemical and physical pathways of litter mass loss.
544 *Nature Geoscience*, 8(10), 776–779.
- 545 Cotrufo, M. F., Wallenstein, M. D., Boot, C. M., Deneff, K., & Paul, E. 2013. The Microbial Efficiency-
546 Matrix Stabilization (MEMS) framework integrates plant litter decomposition with soil organic
547 matter stabilization: Do labile plant inputs form stable soil organic matter? *Global Change*
548 *Biology*, 19(4), 988–995.
- 549 De Deyn, G. B., Cornelissen, J. H. C., & Bardgett, R. D. 2008. Plant functional traits and soil carbon
550 sequestration in contrasting biomes. *Ecology Letters*, 11(5), 516–531.
- 551 De Graaff, M.A., Classen, A.T., Castro, H.F., Schadt, C.W., 2010. Labile soil carbon inputs mediate the
552 soil microbial community composition and plant residue decomposition rates. *New Phytologist*
553 188, 1055–1064.
- 554 Dejong, J. T., Soga, K., Banwart, S. A., Whalley, W. R., Ginn, T. R., Nelson, D. C., ... Barkouki, T. 2011. Soil
555 engineering in vivo : harnessing natural biogeochemical systems for engineering solutions,
556 *Journal of The Royal Society Interface* 8(54), 1-15
- 557 Dixit, M.K., Fernandez-Solis, J.L., Lavy, S. and Culp, C.H. 2010 Identification of parameters for embodied
558 energy measurement: A literature review. *Energy and Buildings*, 42, 1238-1247
- 559 Dixit, M.K., Fernandez-Solis, J.L., Lavy, S. and Culp, C.H. 2010. “Identification of parameters for
560 embodied energy measurement: A literature review”, *Energy and Buildings*, 42, 1238-1247.
- 561 Downie, J.A., 2010. The roles of extracellular proteins, polysaccharides and signals in the interactions
562 of rhizobia with legume roots 34, 150–170.
- 563 Ehrenfeld, J.G., W.F.J. Parsons, X. Han, R.W. Parmelee, and W. Zhu. 1997. Live and dead roots in for-
564 est soil horizons: Contrasting effects on nitrogen dynamics. *Ecology* 78, 348–362.
- 565 Ekklund, F., Ronn, R., Christensen, S., 2001 Distribution with depth of protozoa, bacteria and fungi in
566 soil profiles from three Danish forest sites. *Soil Biology and Biochemistry* 33, 475–481

567 Eswaran, H., van den Berg, E., Reich, P. 1993 Organic carbon in soils of the world. Soil Science Society
568 of America Journal 57: 192–194

569 EU-SDG 2018 Sustainable development in the European Union - monitoring report on progress towards
570 the SDGs in an EU context. Luxembourg: Publications Office of the European Union, 2018

571 Eyles, A., Coghlan, G., Hardie, M., Hovenden, M., & Bridle, K. 2015. Soil carbon sequestration in cool-
572 temperate dryland pastures: Mechanisms and management options. Soil Research, 53(4), 349–
573 365.

574 Fang, C., Moncrieff, J.B. 2005 The variation of soil microbial respiration with depth in relation to soil
575 carbon composition. Plant and Soil 268, 243–253

576 Fehrmann, R., Weaver, R., 1978. Scanning electron microscopy of Rhizobium spp. ad-
577 hering to fine silt particles. Soil Science Society of America Journal 42, 279–281.

578 Fierer, N., Allen, A.S., Schimel, J.P., Holden, P.A., 2003. Controls on microbial CO₂ production: A
579 comparison of surface and subsurface soil horizons. Global Change Biology 9, 1322–1332.

580 Fontaine, S., Bardoux, G., Abbadie, L., Mariotti, A., 2004. Carbon input to soil may decrease soil carbon
581 content. Ecology Letters 7, 314–320.

582 Fontaine, S., Barot, S., Barré, P., Bdioui, N., Mary, B., Rumpel, C., 2007. Stability of organic carbon in
583 deep soil layers controlled by fresh carbon supply. Nature 450, 277–280.

584 Fontaine, S., Mariotti, A., Abbadie, L., 2003. The priming effect of organic matter: A question of
585 microbial competition? Soil Biology and Biochemistry 35, 837–843.

586 Fujisaki, K., Chevallier, T., Chapuis-Lardy, L., Albrecht, A., Razafimbelo, T., Masse, D., Ndour, B.Y.,
587 Chotte, J.L. 2018. Soil carbon stock changes in tropical croplands are mainly driven by carbon
588 inputs: A synthesis. Agriculture, Ecosystems & Environment, 259, 147-158

589 Gallipoli, D., & Mendes, J. 2017. A geotechnical perspective of raw earth building, 463–478.

590 Gill RA, Polley HW, Johnson HB et al. 2002 Nonlinear grassland responses to past and future
591 atmospheric CO₂. Nature, 417, 279–282.

592 Henneron, L., Picon-cochard, C., 2019. Plant economic strategies of grassland species control soil
593 carbon dynamics through rhizodeposition.

594 Hodge, A., D. Robinson, and A. Fitter. 2000. Are microorganisms more effective than plants at com-
595 peting for nitrogen? Trends in Plant Science 5, 304–308

596 Högberg P, Nordgren A, Buchmann N, Taylor AFS, Ekblad A, Högberg MN, Nyberg G, Ottosson-
597 Löfvenius M, Read DJ 2001 Large-scale girdling experiment shows that current photosynthesis
598 drives soil respiration. Nature 411:789–792

599 Holden, P.A., Fierer, N. 2005 Microbial processes in the vadose zone. Vadose Zone Journal 4:1–21

600 Holz, M., Zarebanadkouki, M., Kaestner, A., Kuzyakov, Y., Carminati, A., 2018. Rhizodeposition under
601 drought is controlled by root growth rate and rhizosphere water content 429–442.

602 Horrocks, A., Thomas, S., Tregurtha, C., Beare, M.H., Meeken, E., 2010. Implications for dry matter
603 production and nitrogen management as soils develop following 'humping and hollowing' on
604 the West Coast. *Proceedings of the New Zealand Grassland Association* 72, 103–108.

605 Hungate, B. A., Holland, E. A., Jackson, R. B., Chapin, F. S., Mooney, H. A., & Field, C. B. 1997. The fate
606 of carbon in grasslands under carbon dioxide enrichment. *Nature*, 388(6642), 576–579.

607 IPCC. 2014. *Climate change 2014: Mitigation of climate change. Contribution of working group III to
608 the fifth assessment report of the intergovernmental panel on climate change* (O. P. Edenhofer
609 et al., Eds.). Cambridge, UK and New York, NY, USA: Cambridge University Press

610 Jackson, L.E., J.P. Schimel, and M.K. Firestone. 1989. Short-term partitioning of ammonium and ni-
611 trate between plants and microbes in an annual grassland. *Soil Biology and Biochemistry* 21,
612 409–415.

613 Jastrow, J. D., Miller, R. M., Matamala, R., Norby, R. J., Boutton, T. W., Rice, C. W., & Owensby, C. E.
614 2005. Elevated atmospheric carbon dioxide increases soil carbon. *Global Change Biology*, 11(12),
615 2057–2064.

616 Jastrow, J.D., 2006. Soil aggregate formation and the accrual of particulate and mineral-associated
617 organic matter. *Soil Biology and Biochemistry*, 28, 665-676

618 Jones, D.L., Nguyen, C., Finlay, R.D., 2009. Carbon flow in the rhizosphere: Carbon trading at the soil-
619 root interface. *Plant and Soil* 321, 5–33.

620 Kalbitz, K., & Kaiser, K. 2008. Contribution of dissolved organic matter to carbon storage in forest
621 mineral soils. *Journal of Plant Nutrition and Soil Science*, 171(1), 52–60.

622 Kaye, J.P., and S.C. Hart. 1997. Competition for nitrogen between plants and soil microorganisms.
623 *Trends in Ecological Evolution* 12, 139–143

624 Keil, R.G., Mayer, L.M., 2014. Mineral matrices and organic matter. *Treatise on Geochemistry* 12, 337–
625 359.

626 Keiluweit, M., Bougoure, J. J., Nico, P. S., Pett-Ridge, J., Weber, P. K., & Kleber, M. 2015. Mineral
627 protection of soil carbon counteracted by root exudates. *Nature Climate Change*, 5(6), 588–595.

628 Kibert, C.J. 2008. *Sustainable Construction, 2nd Edition* – John Wiley and Sons Inc., New Jersey,

629 Kleber, M., Sollins, P., & Sutton, R. 2007. A conceptual model of organo-mineral interactions in soils:
630 Self-assembly of organic molecular fragments into zonal structures on mineral surfaces.
631 *Biogeochemistry*, 85(1), 9–24.

632 Kögel-Knabner, I., 2002. The macromolecular organic composition of plant and microbial residues as
633 inputs to soil organic matter. *Soil Biology and Biochemistry* 34, 139–162

634 Kuzyakov, Y. V., Larionova, A.A., 2006. Contribution of rhizomicrobial and root respiration to the CO₂
635 emission from soil (A review). *Eurasian Soil Science* 39, 753–764.

636 Kuzyakov, Y., Domanski, G., 2000. Carbon input by plants into the soil. Review. *Journal of Plant
637 Nutrition and Soil Science* 163, 421–431.

638 Kuzyakov, Y., Friedel, J.K., Stahr, K., 2000. Review of mechanisms and quantification of priming effects.
639 Soil Biology & Biochemistry 32, 1485-1498

640 Lal, R. 2004. Soil carbon sequestration impacts on global change and food security. Science 304: 1623-
641 1627., 304(June).

642 Lavorel, S., Díaz, S., Cornelissen, J.H.C., Garnier, E., Harrison, S.P., McIntyre, S. et al. 2007. Plant
643 functional types: are we getting any closer to the Holy Grail? In: Terrestrial Ecosystems in a
644 Changing World (eds Canadell, J., Pitelka, L.F. & Pataki, D.). Springer, Berlin, pp. 171–186

645 Lekkerkerk, L.J.A., Van De Geijn, S.C., Van Veen, J.A. 1990 Effects of elevated atmospheric CO₂-levels
646 on the carbon economy of a soil planted with wheat. In Soils and the Greenhouse Effect. Ed. A F
647 Bouwman. pp 423-429. Wiley and Sons, Chichester, UK

648 Liang, C., Schimel, J.P., Jastrow, J.D., 2017. The importance of anabolism in microbial control over soil
649 carbon storage. Nature Microbiology 2, 1–6.

650 Lorenz, K. and Lal, R. 2005. The depth distribution of soil organic carbon in relation to land use and
651 management and the potential of carbon sequestration in subsoil horizons. Advanced
652 Agronomy, 88, 35–66.

653 Luo Y, Su B, Currie WS et al. 2004 Progressive nitrogen limita- tion of ecosystem responses to rising
654 atmospheric carbon dioxide. BioScience, 54, 731–739.

655 Misra, A., Basu, D., 2011. Sustainability in geotechnical engineering. Internal Geotechnical Report
656 2011-2" Technical Reports. http://digitalcommons.uconn.edu/cee_techreports/1

657 Nichols, K.A., Wright, S.F. 2005 Comparison of glomalalin and humic acid in eight native U.S. soils. Soil
658 Science 170, 985–997.

659 O'Brien, S. L., & Jastrow, J. D. 2013. Physical and chemical protection in hierarchical soil aggregates
660 regulates soil carbon and nitrogen recovery in restored perennial grasslands. Soil Biology and
661 Biochemistry, 61, 1–13.

662 O'Riordan, N. O., Nicholson, D., Hughes, L., Phear, A., & Group, A. 2011. Technical Paper Examining the
663 carbon footprint and reducing the environmental impact of slope engineering options, Ground
664 engineering

665 Poirier, V., Roumet, C., Munson, A.D., 2018. The root of the matter: Linking root traits and soil organic
666 matter stabilization processes. Soil Biology and Biochemistry 120, 246–259.

667 Rasse, D.P., Rumpel, C., Dignac, M., 2005. Is soil carbon mostly root carbon ? Mechanisms for specific
668 stabilization Is soil carbon mostly root carbon ? Mechanisms for a specific stabilisation.

669 Reid, C. P. P., & Mexal, J. G. 1977. Water stress effects on root exudation by lodgepole pine. Soil Biology
670 and Biochemistry, 9(6), 417–421.

671 Reid, J.B., and M.J. Goss. 1982. Suppression of decomposition of ¹⁴C-labelled plant roots in the pres-
672 ence of living roots of maize and perennial ryegrass. Journal of Soil Science. 33, 387–395

673 Reid, J.B., and M.J. Goss. 1983. Growing crops and transformations of ¹⁴C-labelled soil organic matter.
674 Soil Biology and Biochemistry 15, 687–691.

- 675 Riordan, N.O., Nicholson, D., Hughes, L., Phear, A., Group, A., 2011. technical Paper Examining the
676 carbon footprint and reducing the environmental impact of slope engineering options.
- 677 Rumpel, C., Chabbi, A., and Marschner, B. 2012. Carbon storage and sequestration in subsoil horizons:
678 knowledge, gaps and potentials. in Recarbonization of the Biosphere, eds R. Lal, K. Lorenz, R.
679 Hüttil, B. Schneider, and J. von Braun (Dordrecht: Springer)
- 680 Rumpel, C., Kögel-Knabner, I., 2011. Deep soil organic matter-a key but poorly understood component
681 of terrestrial C cycle. *Plant and Soil* 338, 143–158.
- 682 Sallih, Z., and P. Bottner. 1988. Effect of wheat (*Triticum aestivum*) roots on mineralization rates of soil
683 organic matter. *Biology and Fertility of Soils* 7, 67–70.
- 684 Sauerbeck, D.R., 2001. CO₂emissions and C sequestration by agriculture - Perspectives and limitations.
685 *Nutrient Cycling in Agroecosystems* 60, 253–266.
- 686 Schimel, J.P., L.E. Jackson, and M K. Firestone. 1989. Spatial and temporal effects on plant microbial
687 competition for inorganic nitrogen in a California annual grassland. *Soil Biology and Biochemistry*
688 21, 1059– 1066.
- 689 Six, J., Feller, C., Denef, K., Ogle, S.M., Moraes Sa J.C., Albrech, A. 2002. Soil organic matter, biota and
690 aggregation in temperate and tropical soils – effects of no-tillage. *Agronomie* 22, 755–775.
- 691 Six, J., Frey, S.D., Thiet, R.K., Batten, K.M. 2006 Bacterial and fungal contributions to carbon
692 sequestration in agroecosystems. *Soil Science Society of America Journal*, 70, 555–569.
- 693 Smith, P., Powlson, D.S., Smith, J.U., Falloon, P., Coleman, K., 2000. Meeting Europe’s climate change
694 commitments: Quantitative estimates of the potential for carbon mitigation by agriculture.
695 *Global Change Biology* 6, 525–539.
- 696 Solberg, E.D., M. Nyborg, R.C. Izaurralde, S.S. Malhi, H.H. Janzen, and M. Molina-Ayala. 1997. Carbon
697 storage in soils under continuous cereal grain cropping: N fertilizer and straw. p. 235–254. In R.
698 Lal et al. (ed.) *Management of carbon sequestration in soil*. CRC Press, Boca Raton, FL
- 699 Sørensen, L.H., 1974. Rate of decomposition of organic matter in soil as influenced by repeated air
700 drying-rewetting and repeated additions of organic material. *Soil Biology and Biochemistry* 6,
701 287–292.
- 702 Standards Australia, 2003. *Methods of testing soils for engineering purposes – soil compaction and*
703 *density tests – determination of the dry density/moisture content relation of a soil using*
704 *standard compactive effort, AS 1289.5.1.1, Sydney*
- 705 Stewart, C. E., Paustian, K., Conant, R. T., Plante, A. F., & Six, J. 2007. Soil carbon saturation: Concept,
706 evidence and evaluation. *Biogeochemistry*, 86(1), 19–31.
- 707 Swanston, C. W., Castanha, C., Berkeley, L., & Trumbore, S. E. 2009. Storage and Turnover of Organic
708 Matter in Soil, In book: *Biophysico-Chemical Processes Involving Natural Nonliving Organic*
709 *Matter in Environmental System* John Wiley & Sons, Inc.
- 710 Taylor, J.P., Wilson, B., Mills, M.S., Burns, R.G., 2002. Comparison of microbial numbers and enzymatic
711 activities in surface soils and subsoils using various techniques 34.

712 Thomas, S.M., Beare, M.H., Rietveld, V., 2007. Changes in soil quality following humping/hollowing and
713 flipping of pakihī soils on the West Coast, South Island New Zealand. New Zealand Grassland
714 Association Sixty-Ninth Conference 265–270.

715 Tisdall, J. M., & Oades, J. M. 1982. Organic matter and water-stable aggregates in soils. *Journal of Soil*
716 *Science*, 33, 141–163.

717 Van de Geijn, S.C., J. Goudriaan, J. Van der Eerden, and J. Rozema, 1993: Problems and approaches to
718 integrating the concurrent impacts of elevated carbon dioxide, temperature, ultraviolet-B
719 radiation, and ozone on crop production. In: *International Crop Science*, vol. I. Crop Science
720 Society of America, Madison, WI, pp. 333-338

721 Van Veen, J.A., E. Liljeroth, L.J.A. Lekkerkerk, and S.C. Van de Geijn. 1991. Carbon fluxes in plant- soil
722 systems at elevated atmospheric CO₂ levels. *Ecological applications*, 1:175–181

723 Vidal, A., Hirte, J., Bender, S. F., Mayer, J., Gattinger, A., Höschel, C., ... Mueller, C. W. 2018. Linking 3D
724 Soil Structure and Plant-Microbe-Soil Carbon Transfer in the Rhizosphere. *Frontiers in*
725 *Environmental Science*, 6(February), 1–14.

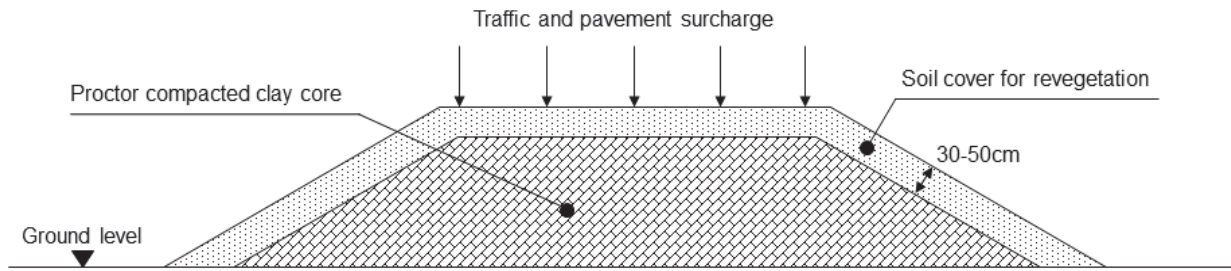
726 von Lützow, M., Kögel-Knabner, I., Ekschmitt, K., Matzner, E., Guggenberger, G., Marschner, B., Flessa,
727 H. 2006. Stabilization of organic matter in temperate soils: Mechanisms and their relevance
728 under different soil conditions—a review. *European Journal of Soil Science* 57, 426–445

729 Wang, J., Chapman, S.J., Yao, H., 2014 The effect of storage on microbial activity and bacterial
730 community structure of drained and flooded paddy soil, *J Soils Sediments*, 15, 880–889

731 Wu, J., Brookes, P.C., Jenkinson, D.S., 1993. Formation and destruction of microbial biomass during
732 decomposition of glucose and ryegrass in soil. *Soil Biology and Biochemistry* 25, 1435–1441.

733 Yin, L., Dijkstra, F.A., Wang, P., Zhu, B., Cheng, W., 2018. Rhizosphere priming effects on soil carbon
734 and nitrogen dynamics among tree species with and without intraspecific competition. *New*
735 *Phytologist* 218, 1036–1048.

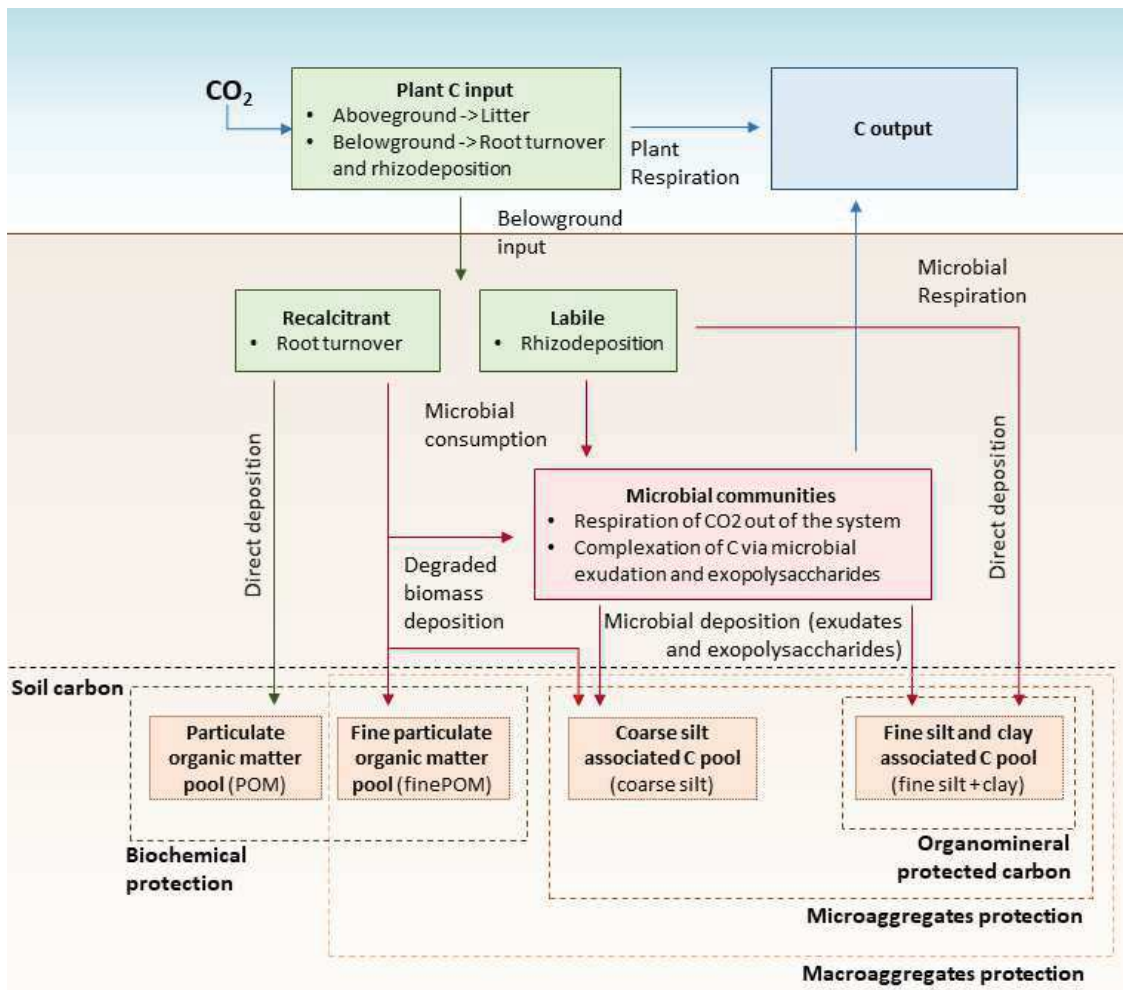
736



738

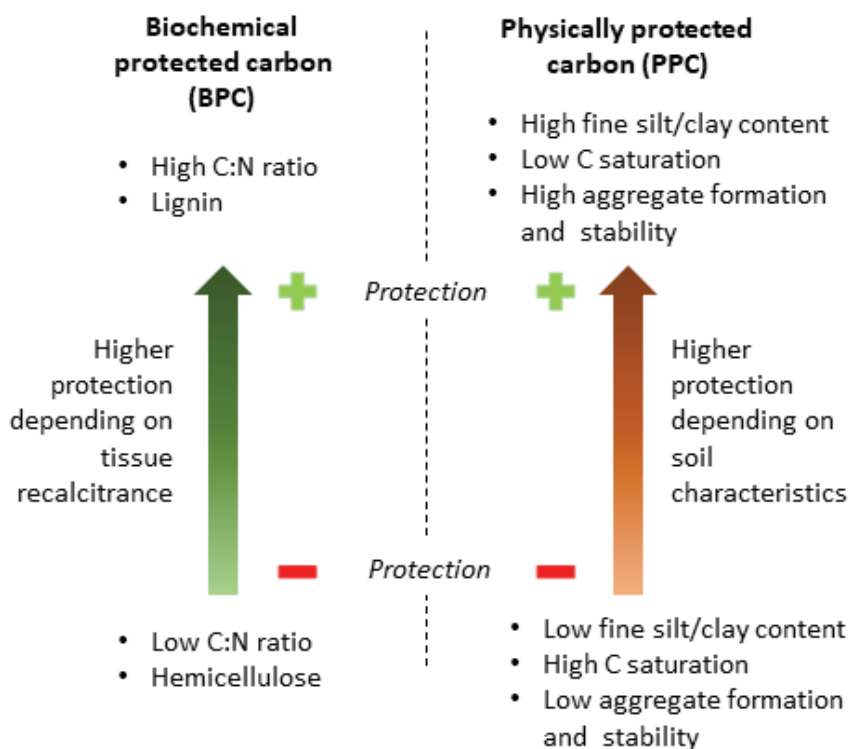
739 **Figure 1:** Section of a geotechnical embankments comprehensive of proctor compacted clay core and cover of soil
 740 for revegetation purposes

741



742

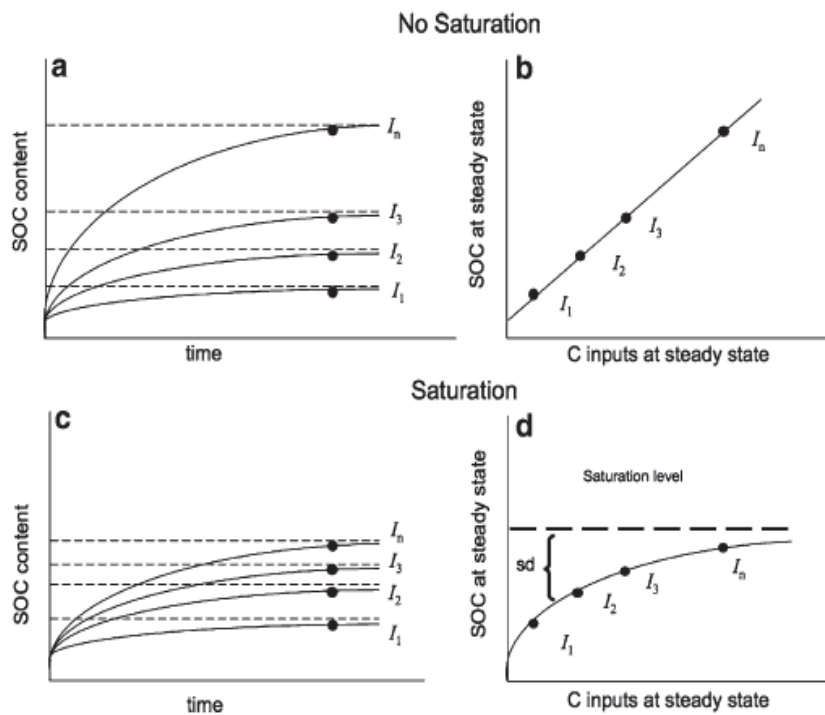
743 **Figure 2:** Flow chart of soil carbon (C) cycle and deposition/complexation in different soil fractions. In green square
 744 boxes, C input from plants is depicted, and green arrow signifies deposition of direct plant inputs. The red box
 745 symbolizes the microbial communities and the red arrows the consumption and deposition of C by microbial
 746 communities. Brown boxes represent the different soil C pools. The green dashed line represents the biochemical
 747 protection of free particulate organic matter (POM) in soil, while the brown dotted lines the soil protection via
 748 aggregate complexation and organomineral absorption on fine silt and clay minerals.



749

750 **Figure 3:** Representation of different types of carbon (C) protection in soil. Biochemically protected carbon (BPC, 751 left) protection depends on the chemical composition of plant tissues, with recalcitrant C having a lower turnover. 752 Physically protected carbon (PPC) depends on soil properties, more specifically on the aggregate formation and 753 the resulting stability, the fine soil fraction in soil and soil C saturation levels.

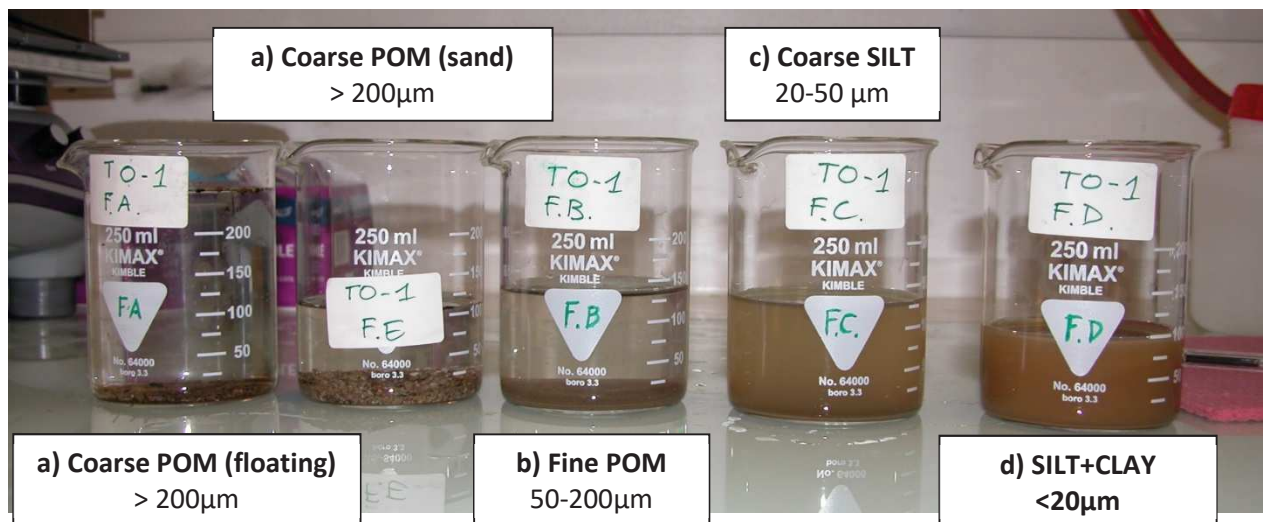
754



755

756 **Figure 4** : Different soil organic C (SOC) evolutions with a constant carbon (C) input for two conditions: a,b, not
 757 considering the effect of C saturation, and c, d including the C saturation effect. Under unsaturated conditions, (a)
 758 a steady state soil C accumulation over time will express a linear relationship if expressed (b) over C input. If the
 759 relationship between SOC and time is analyzed for (c) a C saturated soil it will not be proportional, meaning that a
 760 C input increase will not result in a linear SOC accumulation over time, but (d) in a asymptotic relationship (after
 761 Stewart et al. 2007).

762



763

764 **Figure 5**: Example of soil fractionation following the Gavinelli et al. (2005) methodology. a) coarse POM soil
 765 fraction $> 200\mu\text{m}$ (+ sand fraction), b) finePOM, soil fraction $50\text{-}200\mu\text{m}$, c) the coarse silt fraction $20\text{-}50\mu\text{m}$, d)
 766 silt+clay fraction, $<20\mu\text{m}$.

Embankments as a carbon sink: a study on carbon sequestration pathways and mechanisms in topsoil and exposed subsoil

General research questions:

- What is the effect of plant and soil features on soil C sequestration in terms of quantity and quality of stored C? (Fundamental research question)
- Which are the best possible plant and soil practices that can be implemented to increase soil C storage in embankments and, possibly, in grey soils from geotechnical work? (Applied research question)

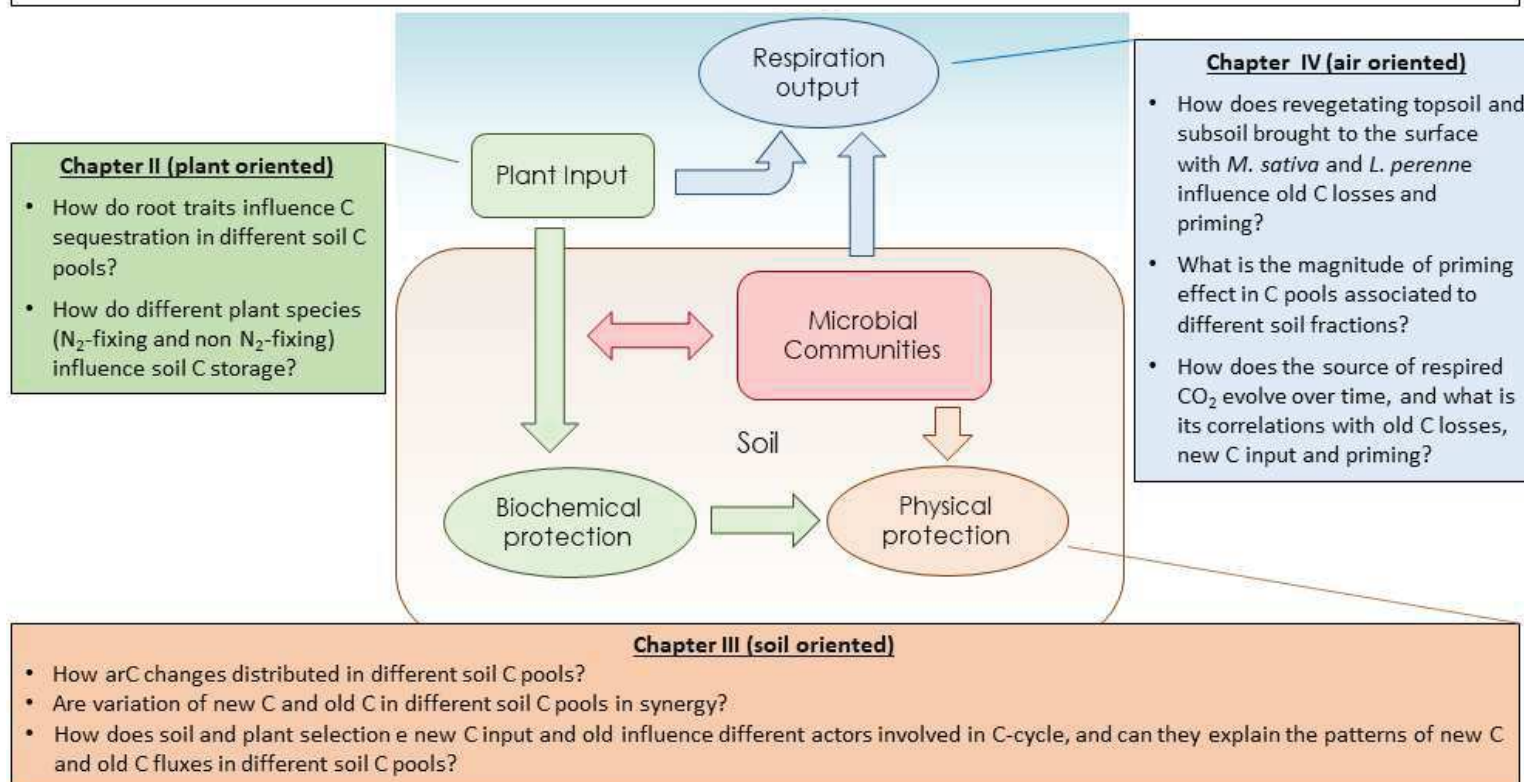


Figure 6: scheme of thesis structure and related research questions (RQ). Applied RQ are presented in the first box, together with the title of the thesis. Fundamental RQ are displayed in the different boxes related to the different chapters of the thesis. The scheme in the middle represents a simplified version of Figure 1. The squared boxes represent the main actors in C-cycle (green plants, red microbes, brown soil) while the circles the pools of C: soil carbon (biochemically and physically protected) and the atmospheric C in CO_2 .

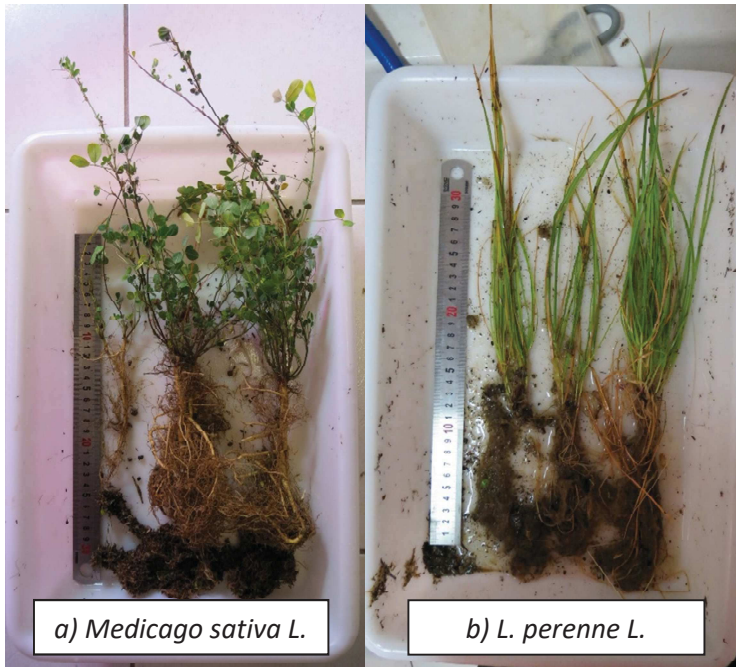


745

746

747

Figure 7: Experimental set up with 12 species grown in monoculture in grow-boxes. The picture shows two of the three blocks of growboxes present in the experiment (Chapter II)



748

749

750

Figure 8: Species grown in ^{13}C constant labelling experiment sampled after 6 months for root traits assessment (Chapter III and IV).



751

752

753

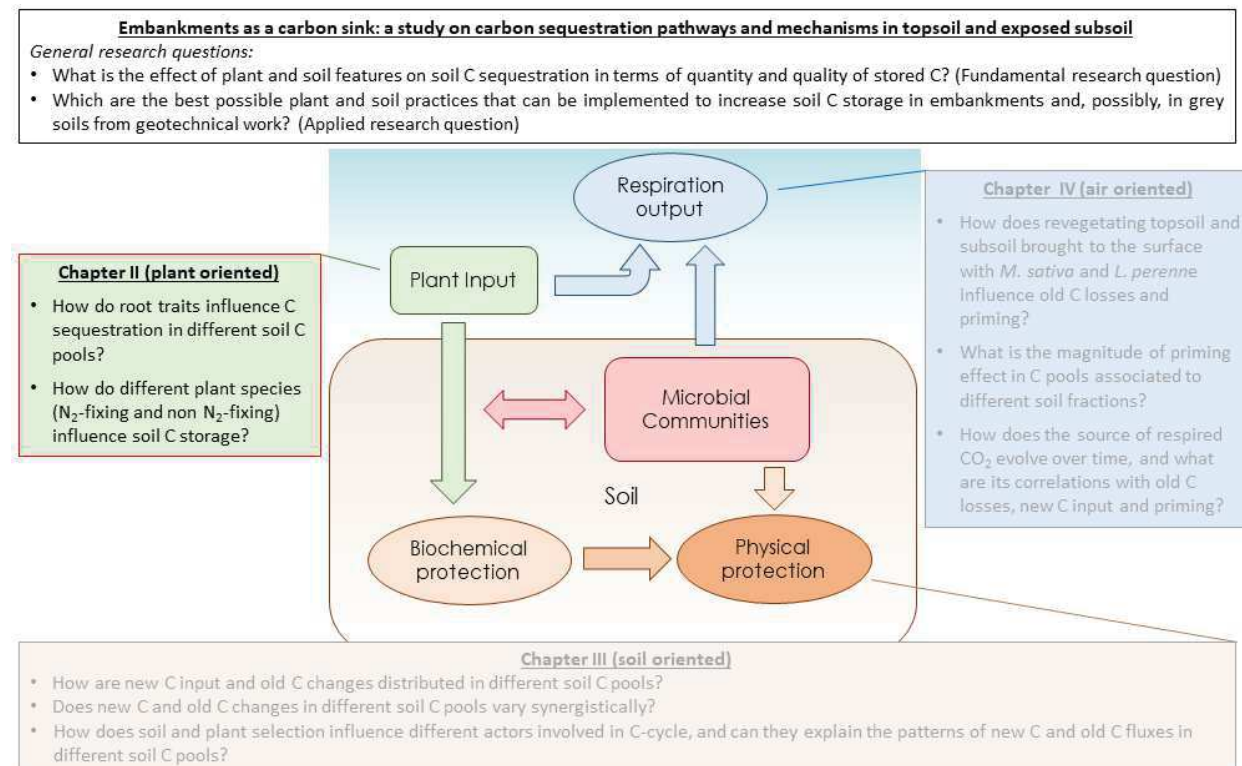
754

755

756

Figure 9: Excavation in Pisciotta (SA), Italy, to collect the soil for the experiment described in Chapter III and IV. Topsoil excavated from 0-30cm depth, subsoil from 110-140 cm depth. On the far right a picture with the main components of soil structure visually isolated.

CHAPTER II: Pathway to persistence: plant root traits alter carbon accumulation in different soil carbon pools through microbial mediation



Plant input is the first step in soil C sequestration. Plant choice influences the final C storage in soil by providing different amounts and quality of C input. In this chapter, we aim to quantify this effect by assessing the C changes in different soil C pools associated with different soil size particle fractions, and relating them to contrasting root traits characterizing 12 different herbaceous species used for embankment revegetation in south of France.

1 **Pathways to persistence: plant root traits alter carbon accumulation in different soil carbon pools**

2 Lorenzo M.W. Rossi^{a,b}, Zhun Mao^a, Luis Merino-Martín^{a,c}, Catherine Roumet^c, Florian Fort^d, Olivier
3 Taugourdeau^e, Hassan Boukcim^e, Stéphane Fourtier^a, Maria Del Rey-Granado^c, Tiphaine Chevallier^f,
4 Rémi Cardinael^{g,h,i}, Nathalie Fromin^c, Alexia Stokes^a

5 Published on Plant and Soil, DOI: 10.1007/s11104-020-04469-5

6 Contact author: Lorenzo MW Rossi

7 [Email: lmw.rossi@gmail.com](mailto:lmw.rossi@gmail.com)

8 Address: AMAP, INRAE Montpellier, PS2 TA/A51, 34 398 Montpellier cedex 5, France

9

10 a) Univ Montpellier, AMAP, INRAE, CIRAD, CNRS, IRD, Montpellier, France.

11 b) University of Cassino, Via Di Biasio 43, 03043 Cassino (Fr), Italy.

12 c) Univ Montpellier, CEFE, CNRS, EPHE, IRD, Univ Paul Valéry Montpellier 3, Montpellier, France.

13 d) Univ Montpellier, CEFE, Montpellier SupAgro, CNRS, EPHE, IRD, Univ Paul Valéry Montpellier 3,
14 Montpellier, France.

15 e) Valorhiz, 1900, Boulevard de la Lironde PSIII, Parc Scientifique Agropolis F-34980 Montferrier sur
16 Lez, France.

17 f) Univ Montpellier, Eco&Sols, IRD, CIRAD, INRA, Montpellier SupAgro, Montpellier, France Eco&ols

18 g) CIRAD, UPR AIDA, Harare, Zimbabwe.

19 h) Univ Montpellier, AIDA, CIRAD, Montpellier, France.

20 i) University of Zimbabwe, Crop Science Department, Box MP167, Mt. Pleasant, Harare, Zimbabwe.

21

22 **Keywords:** *particulate organic matter, mineral-associated organic matter, carbon stabilization,*
23 *physical and density soil fractionation, root biomass, root elongation rate, substrate induced*
24 *respiration, microbial biomass*

25 **ABSTRACT**

26 *Aims:* Mineral-associated organic matter, mainly derived from microbial by-products,
27 persists longer in soil compared to particulate organic matter (POM). POM is highly recalcitrant and
28 originates largely from decomposing root and shoot litter. Theory suggests that root traits and growth
29 dynamics should affect carbon (C) accumulation into these different pools, but the specific traits
30 driving this accumulation are not clearly identified.

31 *Methods:* Twelve herbaceous species were grown for 37 weeks in monocultures. Root
32 elongation rate (RER) was measured throughout the experiment. At the end of the experiment, we
33 determined morphological and chemical root traits, as well as substrate induced respiration (SIR) as a

34 proxy for microbial activity. Carbon was measured in four different soil fractions, following particle-
 35 size and density fractionation.

36 *Results:* In N₂-fixing Fabaceae species, root biomass, RER, root diameter, hemicellulose content
 37 and SIR, were all positively correlated with increased C in the coarse silt fraction. Root diameter and
 38 hemicellulose content were also negatively correlated with C in the POM fraction, that was greater
 39 under non N₂-fixing Poaceae species, characterized by lignin-rich roots with a high carbon:nitrogen
 40 ratio that grew slowly. The accumulation of C in different soil pools was mediated by microbial activity.

41 *Conclusions:* Our results show that root traits determine C input into different soil pools, mediated
 42 primarily by microbial activity, thus determining the fate of soil organic C. We also highlight that C in
 43 different soil pools, and not only total soil organic C, should be reported in future studies to better
 44 understand its origin, fate and dynamics.

45 **Abbreviations**

<i>Abbreviation</i>	<i>Meaning</i>
C	Carbon
POM	Particulate organic matter
C:N	Carbon – nitrogen ratio in plant tissue and/or soil
N ₂ -fixing	Dinitrogen fixing
t0	Time zero, beginning of the experiment
t37	Time 37 weeks, end of the experiment
ΔC	Delta carbon, as difference between carbon at time 0 and carbon at time 37, in different fractions (mg C g ⁻¹ soil)
C _{POM}	Carbon in the coarse POM 200-2000 μm fraction (mg C g ⁻¹ soil)
C _{finePOM}	Carbon in the fine POM 50-200 μm fraction (mg C g ⁻¹ soil)
C _{SILT}	Carbon in the 20-50 μm coarse silt fraction (mg C g ⁻¹ soil)
C _{SILT+CLAY}	Carbon in the fine silt+clay <20 μm fraction (mg C g ⁻¹ soil)
ΔC _{SUM}	Sum of delta carbon in different fractions, ΔC _{SUM} = ΔC _{POM} + ΔC _{finePOM} + ΔC _{SILT} + ΔC _{SILT+CLAY} (mg C g ⁻¹ soil)
RER	Root elongation rate (mm d ⁻¹)
RLP	Root length production (m)
RER _{NEW} , RLP _{NEW}	RER and RLP of 'new' roots initiated during the 2 weeks interval between measurements

RER _{OLD} , RLP _{OLD}	RER and RLP of 'old' roots, initiated more than 2 weeks before the measurement
SIR	Substrate induced respiration ($\mu\text{g C-CO}_2 \text{ g}^{-1} \text{ soil h}^{-1}$)
PCA	Principal component analysis

46

47 2.1.INTRODUCTION

48 Given the current climate change emergency, several international initiatives have been launched to
49 unlock the potential of soils to sequester atmospheric carbon (C) (e.g. 4 per Thousand Initiative,
50 Minasny et al. 2017). Better understanding the interactions between vegetation and soil has become
51 central for sequestering C into anthropogenically disturbed soil, such as agricultural fields, mining
52 waste soil, road embankments and technosols (Paustian et al. 2016; Griscom et al. 2017). Plants act as
53 a major conduit for transferring C into soils via litterfall, root mortality and exudation (Six et al. 2004;
54 Derrien et al. 2016; Sokol et al. 2019). Some C is transformed by soil microbes and released back into
55 the atmosphere by respiration (Jones et al. 2009; Kuzyakov and Larionova, 2005), but C can also be
56 stabilized in soil, increasing its residence time (Besnard et al. 1996; Lal, 2004; Rasse et al. 2005;
57 Bardgett et al. 2014 ; Vidal et al. 2018; Sokol et al. 2019). Carbon persists in soil at different time scales
58 based on recalcitrance (short-term preservation), spatial inaccessibility to decomposers due to
59 occlusion in soil aggregates, and adsorption to mineral and metal surfaces (Kleber et al. 2011, Schmidt
60 et al. 2011, Poirier et al. 2018). These mechanisms are influenced by abiotic and biotic factors and
61 especially by plant roots, since their C is preferentially stabilized compared to aerial parts (Balesdent
62 and Balabane, 1996; Rasse et al. 2005, Kätterer et al. 2011). In a recent review, Poirier et al. (2018)
63 argued that the root traits most influencing C stabilization are those related to chemical composition,
64 root exudation and the presence of symbionts (e.g. mycorrhizas and *Rhizobium* bacteria), whereas the
65 role of morphological traits is not yet clear. More specifically, root traits increasing chemical
66 recalcitrance promote short-term C stabilization by slowing root decomposition rates, whereas root
67 traits increasing exudation rate promote long-term C stabilization faster. Several studies have analysed
68 the link between plant functional traits, microbial activity and C accumulation (Chapin 2003; Lavorel
69 et al. 2007; De Deyn et al. 2008; Poirier et al. 2018). However, as yet, it is not understood how root
70 traits can alter the accumulation and potential persistence of C.

71 Through differences in chemical and physiological traits, roots should affect C accumulation into
72 different C pools depending on soil texture. These pools are defined as: i) coarse particulate organic
73 matter (coarse POM, > 200µm fraction), that is free in the soil at different levels of degradation, ii) fine
74 POM (50-200µm fraction), that comprises free organic C and organic C occluded in soil
75 macroaggregates. These two pools are mostly derived from the decomposition of roots and shoots
76 (Kögel-Knabner, 2002), and their short-term C protection from microbial consumption relies mainly on
77 the recalcitrance of their lignocellulose C structures and the physical protection given by
78 macroaggregate structure (Six et al. 2002). Finally, iii) C protected in the coarse silt and fine silt+clay
79 pools (20-50µm and <20µm fractions, respectively); that is highly processed and protected from

80 microbial consumption via occlusion in microaggregates and through organo-mineral adsorption to
81 clay particles and metals. This C is mostly derived from dissolved organic C originating from the
82 degradation of above and belowground plant C input (Bird et al. 2008; Rubino et al. 2010; Sanderman
83 et al. 2014), from root exudation of labile rhizospheric compounds and from microbial compounds
84 (Simpson et al., 2007; Mambelli et al., 2011; Cotrufo et al. 2013; 2014; Vidal et al. 2018; Rossi 2019). It
85 is now generally accepted that labile low molecular weight compounds persist in soil longer than
86 chemically recalcitrant C structures, when protected by organo-mineral adsorption (Mikutta et al.
87 2006; Kleber et al. 2015; King et al. 2019; Robertson et al. 2019; Sokol et al. 2019). The stability of
88 sequestered C in soil is therefore linked to the fraction of soil to which it is associated, with a greater
89 stability of C pools associated with finer fractions (Torn et al., 2009).

90 As C accumulation into the coarse POM pool is related to the amount of recalcitrant matter present, it
91 should therefore be greater in soils containing roots with high cellulose, lignin and carbon:nitrogen
92 ratio (C:N) (Poirier et al. 2018). However, it is C-rich exudates produced during fine root elongation
93 that promote long-term C stabilization in the coarse silt and fine silt+clay fractions (Mikutta et al. 2006;
94 King et al. 2019; Robertson et al. 2019; Sokol et al. 2019), and together with mucilage and border cells
95 (shed during growth), are important substrates for microbial communities (Dennis et al., 2010). These
96 C substrates that are assimilated by microorganisms close to the root apex are utilized rapidly for
97 respiration and growth, or lost as microbial exudates or exopolysaccharides that are then used as a
98 substrate for subsequent microbial communities. Since microbial byproducts (from activity in any soil
99 C pool) are believed to be the main precursor of protected C due to organo-mineral interactions
100 (Simpson et al., 2007; Mambelli et al., 2011; Cotrufo et al., 2013; Rossi 2019), root exudation should
101 influence the C storage in this fraction. It is however important to mention that exudation and the
102 resulting microbial activity can also negatively influence soil C storage, increasing the consumption of
103 preexistent soil C (i.e. priming effect; Hamer and Marschner, 2005; Shahzad et al. 2017). Root traits
104 related to exudation are however poorly understood; the few studies available showed contrasted
105 results and relate to root morphological traits measured at the whole root system level (Roumet et al.
106 2006; Guyonnet et al. 2018). Because root exudates are mainly released at the elongating root tip,
107 where rhizospheric microbial activity is high (Jones et al. 2009; Canarini et al. 2019), it can be expected
108 that root elongation rate (RER) is a powerful predictor of C deposits in coarse silt and fine silt+clay C
109 pools (Holz et al. 2018). Root elongation rate is affected principally by local abiotic soil conditions such
110 as soil temperature, moisture, and compaction, but also differs among species, although most known
111 data is related to woody species (Steinaker et al. 2011; Mohamed et al. 2016; Wang et al. 2018). Fast

112 growing species with small diameter fine roots, high specific root length and N uptake rate usually have
113 high RER (Larson and Funk 2016).

114 Determining plant traits that increase C accumulation in different soil C pools should therefore enable
115 the selection of species that promote C persistence in soil. Recent debate has focused on the ability of
116 dinitrogen fixing (N₂-fixing) species to sequester large amounts of C in soil (Plaza-Bonilla et al. 2016;
117 King et al. 2018). Bacteria such as *Rhizobium*, present in nodules of N₂-fixing species, produce large
118 amounts of exopolysaccharides (Downie, 2010; Sasse et al. 2018), that are adsorbed onto fine silt and
119 clay particles (Fehrmann and Weaver, 1978). Also, N₂-fixing species have roots that are easily
120 degradable with a high content of hemicelluloses (Hernández et al. 2017) and low C:N ratio
121 (Warembourg et al. 2003; Roumet et al. 2005), therefore enhancing microbial activity (Poirer et al.
122 2018). However, it is not known whether N₂-fixing species promote greater C accumulation in the fine
123 silt and clay soil fractions, thereby enhancing C persistence in soil.

124 We explored the effect of root traits on C accumulation into different soil C pools beneath 12
125 herbaceous species grown in monocultures for 37 weeks. These species had diverse root traits in terms
126 of morphology, chemical composition, and elongation rate and belonged to different plant families:
127 five N₂-fixing Fabaceae, five Poaceae, one Rosaceae and one Plantaginaceae. Our main hypothesis is
128 that C accumulation into different soil C pools is driven by root traits and their effects on microbial
129 activity and biomass. More specifically, we hypothesize that (i) traits related to high RER promote C
130 accumulation in the coarse silt and fine silt + clay C pools, since these traits are expected to favour
131 exudation and subsequent microbial activity, whereas (ii) root traits related to chemical recalcitrance
132 (high lignin and cellulose content and high C:N ratio), promote C accumulation in the unprotected POM
133 pool, and iii) N₂-fixing species favour C accumulation in the coarse silt and fine silt + clay pools. Results
134 should enable us to disentangle the relationships between root growth, traits and the accumulation
135 and stabilization of C in different soil C pools, between different families (Poaceae and Fabaceae) and
136 N₂ and non N₂-fixing species.

137

138

139 2.2. MATERIALS AND METHODS

140 2.2.1. *Experimental setup*

141 The experiment was set up in the experimental garden of CEFÉ-CNRS Montpellier, France (43.6389°
142 N°, 3.864125° E and lasted 37 weeks (from t₀: Sept-2016 to t₃₆: July-2017). Twelve herbaceous species
143 were grown as monocultures in steel boxes (0.7 m length x 0.7 m width x 0.3 m depth): five N₂-fixing

144 species from the Fabaceae family and seven non N₂-fixing species, including five Poaceae, one
145 Plantaginaceae and one Rosaceae species (Table 1). A weather station was set up permanently in the
146 experimental garden, and air humidity, air temperature (minimum, maximum and mean daily) and
147 solar irradiation (measured daily) were monitored throughout the experiment.

148
149 Seventy-eight boxes were prepared: six replicate boxes per species and six additional boxes of bare
150 soil used as controls. Boxes were organized in three blocks with two rows of 13 adjacent boxes in each
151 block, and with a distance of 50 cm between each box. Each row comprised 12 monocultures (one per
152 species) and a bare soil, randomly arranged in each row (Fig S1). Boxes of the first row were used for
153 destructive plant and soil sampling, while the boxes of the second row were equipped with rhizotrons
154 for the study of root elongation (Section 1.1, Fig. S1). In the second block, each box was equipped with
155 soil temperature and humidity sensors placed at a depth of 0.1 m. Soil temperature was recorded
156 every 4 hours with an i-button sensor (iButtonLink, Wisconsin, USA); soil relative humidity was
157 recorded every hour with moisture sensors (Waterscout SM100, Spectrum Technologies Inc.) and a
158 datalogger (WatchDog weather station 200 series, Spectrum Technologies Inc.). These boxes were
159 undisturbed for the duration of the experiment. Rhizotrons comprised a 0.2 m width x 0.3 m depth x
160 0.05 m thick pane of transparent plexiglass set into the lower walls of the boxes, through which roots
161 were observed and root elongation rate (RER, in mm root⁻¹ day⁻¹) and root length production (RLP, in
162 mm mm⁻² day⁻¹), were calculated (Fig. S2). For RER and RLP, only one replicate box per species was
163 analyzed, because the analysis of root images was extremely time consuming.

164 Boxes were inclined at 20° relative to the horizon to encourage the positive geotropism of roots when
165 they came into contact with rhizotron windows (Huck and Taylor, 1982). Boxes were filled with soil
166 sieved to 8 mm. Five layers of soil were successively added and manually compacted to attain a volume
167 of 0.113 m³, i.e., a total of 190 kg of soil per box (bulk density = 1.70 ± 0.02 g cm⁻³). The soil, excavated
168 in Villefort (France; 44°26'25" N, 3°55'58" E), was sandy-loam (62.6 % sand, 26.1 % silt, 11.3 % clay);
169 with 1.36 g kg⁻¹ of total N, 16.9 g kg⁻¹ of total C, 0.069 g kg⁻¹ of phosphorus (P Olsen), pH in water was
170 7.06, and cation-exchange capacity (CEC) was 7.98 cmol_c kg⁻¹.

171 On 17-19 October 2016, 72 boxes were sown as monocultures (12 species x 6 replicates with one
172 replicate species per row). Seeds of each species were sown in lines, the distance between lines was
173 75 mm and the distance between plants within a line was 75 mm, leading to a final plant density of
174 155 plants m⁻². Once seeds had germinated, each box was inoculated with a purified solution of local
175 *Rhizobium* bacteria strains (Incolum Valorhiz™, France) and was netted to avoid birds disturbing seeds.
176 During the experiment, mean air temperature was 13 C° (Figure S3) with a maximum of 30 °C and a

177 minimum of -0.4 °C (Figure S3a), and the cumulative precipitation was 349 mm (Fig S3 for additional
178 information on climatic conditions over the 37 weeks of the experiment). Soil temperature in the boxes
179 followed closely the air temperature over the 37 weeks period, with a mean of 13.5 °C, a maximum of
180 25.9 °C and a minimum of 3 °C (Figure S3a). Air humidity ranged from 53 to 87%, with a mean value of
181 74% (Figure S3a) and solar irradiation ranged from 320 to 897 W m⁻² with a mean value of 568 W m⁻²
182 (Figure S3b). During the experiment, boxes were carefully weeded by hand and plants were cut to
183 ground level every 4 months to maintain a regular aerial cover. In addition, each box was watered with
184 sprinklers when required.

185

186 2.2.2. *Analysis of carbon content in different soil fractions*

187 Soil C content was measured before filling the boxes, as a reference for time 0 (t₀), on three samples
188 from the initial homogenized soil batch, and at the end of the experiment, i.e. at 37 weeks (t₃₇) after
189 sowing. At t₃₇, soil samples were taken at 0-200 mm depth using a soil corer (75 mm in diameter) in
190 each box dedicated to soil and plant sampling. All soil samples were separated into two depths (0-100
191 mm and 100-200 mm), air dried and separately sieved to 2 mm. A subsample of 40 g of soil was
192 collected at a depth of 0-100 mm for subsequent fractioning into POM fractions (coarse POM: 200-
193 2000 µm and fine POM: 50-200 µm), coarse silt (20-50 µm), fine silt + clay (<20 µm) fractions. Soil
194 fractionation was carried out using the method from Gavinelli et al. (1995). Soil samples were
195 presoaked overnight in 300 ml of deionized water at 4°C with 0.5 g of hexametaphosphate to enhance
196 disaggregation. Soil was then shaken at 300 rpm (digital orbital shaker, Intertek) with five agate
197 marbles for 2 h (i.e., the time suggested for sandy soils, to avoid the transfer of C into finer fractions,
198 Gavinelli et al. 1995). The soil was wet sieved with a 200 µm sieve, and the resulting 200-2000 µm
199 fraction was then transferred into a separate container and soaked in deionized water. The floating
200 coarse particulate organic matter (POM) was then carefully collected. The remaining 200-2000 µm
201 fraction represented the coarse sand fraction in soil and was carefully collected by washing the content
202 of the sieve in a beaker using deionized water. Then, the remaining fraction was sieved with a 50 µm
203 sieve, to separate and collect the fine sand fraction and the fine POM fraction (50-200 µm). The
204 remaining fraction <50 µm was sonicated with a 1510E-MT Branson sonicator for 10 minutes to break
205 microaggregates before sieving at 20 µm. The 20-50 µm fraction (coarse silt) was collected and the
206 resulting solution of deionized water and <20 µm fraction collected in a beaker and filled up to 1.0 L.
207 This solution was tumbled 30 times to homogenize it and an aliquot of 100 mL was collected with the
208 aid of a syringe, representing the fine silt + clay fraction. All the fractions were oven dried at 40°C until
209 all the water evaporated. The dried fractions were weighed to check that the sum of the fraction's

210 weight did not differ from +/-5% the initial 40 g total weight. The quality of the soil particle dispersion
211 was checked and did not differ +/-5% compared to the soil texture analysis, being 62.6% in the sand
212 fraction and 37.4% in the fine silt + clay fraction.

213 Carbon content in each of the soil fractions (C_{POM} - carbon in the coarse POM fraction; $C_{finePOM}$ - carbon
214 in the fine POM fraction; C_{SILT} - carbon in the coarse silt fraction and $C_{SILT+CLAY}$ - carbon in the fine silt+clay
215 fraction), was analyzed using an elemental analyzer (CHN model EA 1108; Carlo Erba Instruments,
216 Milan, Italy) to assess the amount of C present in each pool. A subsample of 0.1 g was taken from each
217 40 g sample and analyzed without fractioning to determine the total C in the bulk sample. The
218 difference between total C in bulk soil and the sum of C in the different soil fractions was used to assess
219 the correctness of the fractionation (+/-5%) and was equal to 97.3% (SD=22%; n=34).

220 We calculated soil C changes (ΔC) in each soil fraction as the difference between C content in $mg\ C\ g^{-1}$
221 soil at 0 and 37 weeks ($\Delta C = C_{t37} - C_{t0}$). The sum of ΔC in each soil fraction ($\Delta C_{SUM} = \Delta C_{POM} + \Delta C_{finePOM} +$
222 $\Delta C_{SILT} + \Delta C_{SILT+CLAY}$) was also calculated to investigate the variation in the totality of the soil fractions.
223 Note that ΔC can be either positive (accumulation) or negative (depletion due to the positive priming
224 effect, that is the increase of pre-existing soil C consumption and losses due to vegetation, Kuzyakov,
225 2002).

226 All the raw data can be found in the Harvard Dataverse 'Embankment as a carbon sink: a study on
227 carbon sequestration pathways and mechanisms in topsoil and exposed subsoil', DOI:
228 10.7910/DVN/QTFLVE.

229 *2.2.3. Measurement of root elongation rate (RER) and root length production (RLP)*

230 As soon as the first root of a given species was visible in a rhizotron, roots of that species were scanned
231 every 2 weeks for the experiment experiment (i.e. n = 19 measurement dates) using a smartphone
232 scanner application CamScanner (INTSIG Information Co., Ltd, Shanghai, China; version 3.9.5). A
233 smartphone (Samsung Xcover3, Samsung Electronics, Korea) was kept at a fixed distance from the
234 rhizotron (0.3 m) and a ruler was included in the picture to set the scale (Mohamed et al. 2017). Images
235 were then analyzed with the SmartRoot software (Lobet et al. 2011), a freeware plugin of ImageJ
236 software (Schneider et al. 2012). The images acquired were converted into 8-bit grey scale and, when
237 necessary, color- inverted, so that roots were dark on a lighter background. SmartRoot allows the semi-
238 automatic tracing of roots by clicking on the basal point of each root (Fig. S4a). Data extracted include
239 the length and diameter of the roots. The resulting traced image of roots could then be imported and
240 superimposed onto a new image, allowing analysis of subsequent images and creating a time-
241 dependent dataset acquiring root length at different time steps.

242 Root elongation rate (RER; mm d⁻¹) is indicative of primary root growth and is defined as the difference
 243 in individual root length measured between two dates. RER is a frequent but punctual observation of
 244 root dynamics over time. As soil C storage is a cumulative process, root length production (RLP; m)
 245 after 37 weeks was also calculated for up to 60 roots (randomly chosen) per rhizotron. RLP is the total
 246 length of all roots produced in a specific period of time (Mommer et al. 2015). Of these 60 roots
 247 measured, 30 were selected from the 'new roots', i.e., the roots that were not present in the previous
 248 scan, and so had formed in the previous two weeks. Of the 30 'new roots', 20 were primary and first
 249 order roots and ten were second order laterals (Fig. S4a, according to the developmental centrifugal
 250 protocol of root topology; Berntson, 1997). Then, 30 'old roots' were selected at each subsequent
 251 sampling date. The 'old roots' were the roots already present in the previous scan (again, 20 primary
 252 axes and ten second order lateral roots). Fig. S5 shows an example of rhizotron analysis for new and
 253 old roots. To have a more representative sample of the 'old roots,' ten primary roots were selected
 254 from the 20 primary 'old roots' of the previous scan, ten were selected from the 20 newly emerged
 255 roots of the previous scan, five were chosen from the ten second order lateral 'old roots' of the
 256 previous scan and five were selected from the newly emerged second order laterals of the previous
 257 scan. This method was used to select roots at each subsequent sampling date. If one or more roots
 258 had: 1) reached the boundaries of the rhizotron, or 2) were in a bundle and not distinguishable (Fig.
 259 S4b), or 3) could not be analyzed for any other reason (e.g. soil masking the root), they were discarded
 260 and different roots were then selected.

261 The mean daily RER was calculated by subtracting from the length of a root (L_{t2}) the length of the root
 262 acquired at the previous sampling date (L_{t1}). This result was then standardized dividing by the number
 263 of days between the two sampling dates (t) to have the mean elongation rate of a single root:

$$264 \quad RER(t) = (L_{t2} - L_{t1}) / [t2 - t1] \quad \text{Equation 1}$$

265 Root length production (RLP) of roots over the 37 weeks was chosen as a cumulative indicator for root
 266 dynamics, adapted from Mommer et al. (2015):

$$267 \quad RLP = \sum_{t=1}^T \sum_{r=1}^R (RER(t) * \frac{R_{30}}{R}) \quad \text{Equation 2}$$

268 Where t represents the sampling date ; (t) ; RER(t) is the daily RER; R the real number of roots analyzed
 269 in that interval. Since the number of analyzed roots varied depending on dates and species, we decided
 270 to standardize the analysis of RLP for $R_{30} = 30$ roots.

271 To refine the understanding of root dynamics, the RER and RLP were calculated separately for the new
 272 roots (RER_{NEW} and RLP_{NEW}, i.e. roots initiated during the 2 weeks interval between measurements), old

273 roots (RER_{OLD} and RLP_{OLD} , i.e. roots older than 2 weeks), and also the total root system, regardless of
274 root age. For all species, RER was high during the first two samplings after their initiation and then
275 decreased rapidly or stopped. Therefore, mean RER could be biased by the development of new roots,
276 justifying our decision to separate roots based on age and order for the statistical analysis.

277

278 *2.2.4. Analysis of root traits*

279 After 37 weeks, a soil core (75 mm diameter, 200 mm depth), centered on one individual plant per
280 species and per box was collected. In each core, roots were separated from the aboveground part and
281 washed. Roots were sorted into absorptive roots, typically the first, second and third root orders
282 (defined as the most distal root orders), and transport roots, that were higher order roots (all orders
283 above third order roots, following McCormack et al. 2015). A subsample of absorptive roots (0.1 g dry
284 mass on average) was selected, stained in a solution of methyl violet (0.5 g L^{-1}), spread into a
285 transparent water filled tray and scanned at 800 dpi (Epson Expression 1680, Canada).

286 The software Winrhizo Pro (Regent Instruments, Quebec, Canada) was used to determine the root
287 diameter (from 0 to 2 mm, with a 0.1 mm diameter interval) of absorptive roots. Roots were then oven
288 dried at 40°C for 3 days and weighed to determine the total root dry mass for each core.

289 For each species, determination of root chemical composition was conducted on three subsamples of
290 absorptive roots reserved for chemical analyses. C and N concentrations were determined on ground
291 material using an elemental analyser (CHN model EA 1108; Carlo Erba Instruments, Milan, Italy).
292 Concentrations of water-soluble compounds + hemicelluloses, cellulose and lignin were obtained
293 following the Van Soest method (Van Soest, 1963) and using a fiber analyser (Fibersac 24; Ankom,
294 Macedon, NJ, USA). This method consists of measuring the various plant tissue constituents by
295 sequential extraction with neutral detergent, acid detergent and sulfuric acid (76%).

296 Substrate-induced respiration (SIR) was used as a proxy for potential soil microbial respiration and
297 activity, according to Beare et al. (1990). Briefly, 20 g air-dried 2 mm sieved soil samples were
298 incubated in 150 mL sealed serum flasks with $1.5 \text{ mg C-glucose g}^{-1}$ soil, at 80 % field capacity and at
299 25°C . A 200 μL aliquot of the flask headspace was analyzed for CO_2 concentration after 2 and 6 hours
300 using a microcatharometer (MicroGC Serie S, SRA Industries, Marcy l'Etoile, France), equipped with a
301 PoraPlot column (Agilent, Santa Clara, United States). Substrate induced respiration rates were
302 calculated as the mass of C-glucose converted to C- CO_2 per g of soil dry weight and per hour (in $\mu\text{g C-}$
303 $\text{CO}_2 \text{ g}^{-1} \text{ soil h}^{-1}$).

304 2.2.5. *Statistical analysis*

305 First, a one-way analysis of variance (ANOVA) and post-hoc Tukey honestly significance difference
306 (HSD) tests were performed to test the effects of species on mean RER, mean RLP, root traits and ΔC
307 sequestration in soil C pools. Secondly, one way ANOVAs were conducted on the five Poaceae species
308 and the five Fabaceae species, i.e excluding *P. lanceolata* and *S. minor* (hypothesis 3). In order to select
309 the environmental parameters to be included in the constrained ordination, an initial db-RDA including
310 all parameters was performed followed by a stepwise model selection using Generalized Akaike
311 Information Criterion (AIC, ordistep function with a backward direction). The normal distribution of
312 residuals was verified using a Shapiro-Wilk test ($p = 0.05$). If the data were not normally distributed,
313 one way ANOVA was substituted with a Kruskal-Wallis test. Finally, the same procedure using one way
314 ANOVA was performed to compare the mean effect of N_2 -fixing and non N_2 -fixing species (for the
315 latter, grouping together Poaceae, *P. lanceolata* and *S. minor*) on root traits and C storage (hypothesis
316 3).

317 A principal component analysis (PCA) was performed on 12 variables (six root traits, four ΔC of each
318 soil C pool plus their sum, and SIR) using the mean for three replicate boxes ($n = 12$) to investigate the
319 effect of root traits at the species level. RER and RLP were not included in the PCA since they were
320 measured on one replicate box per species. Then, Pearson's correlation coefficients were calculated
321 to study the relationships between root traits and ΔC in each soil C pool (hypotheses 1 and 2) and
322 linear models of the significant correlations were analyzed to study the data dispersion. To deepen the
323 understanding of these correlations, Pearson's correlation analysis and a study of the linear models
324 were performed on raw data ($n = 34$) to study relationships at the individual level.

325 To investigate the effect of abiotic factors on root growth dynamics, Pearson's correlation coefficients
326 were calculated between mean daily RER, mean RLP, mean daily soil and air temperatures, mean daily
327 soil humidity and mean daily solar irradiation ($n = 12$ for each variable). Means of daily climate data
328 were calculated for the 2 weeks preceding the measurement of RER.

329 All the statistical analyses were performed in the open-source statistical environment R, version 3.4.3
330 (R Development Core Team, 2017) using the packages *Hmisc* (Harrel 2007) and *vegan* (Oksanen et al.
331 2019).

333 2.3. RESULTS

334 *Effect of plant species on soil carbon accumulation (ΔC) in different C pools associated with soil fractions*

335 Plant species did not significantly influence the accumulation of C in different pools, nor in the sum of
336 C pools (Fig. 1). The mean ΔC_{SUM} increase was $1.72 \pm 1.45 \text{ mg C g}^{-1} \text{ soil}$, and was highest in soil beneath
337 *L. corniculatus* ($3.60 \pm 0.70 \text{ mg C g}^{-1} \text{ soil}$) compared to the bare soil control ($0.21 \pm 3.87 \text{ mg C g}^{-1} \text{ soil}$,
338 Fig. 1a). The mean increase in the coarse pool ΔC_{POM} was $0.58 \pm 0.34 \text{ mg C g}^{-1} \text{ soil}$ (Fig. 1b) and in the
339 $\Delta C_{\text{finePOM}}$ was $1.21 \pm 0.74 \text{ mg C g}^{-1} \text{ soil}$ (Fig. 1c). In the protected C_{SILT} pool, the ΔC mean increase was
340 $0.57 \pm 0.34 \text{ mg C g}^{-1} \text{ soil}$ (Fig. 1d), while the $\Delta C_{\text{SILT+CLAY}}$ decreased by $-0.50 \pm 0.77 \text{ mg C g}^{-1} \text{ soil}$ (Fig. 1e).
341 However, no significant differences were found between any species and bare soil with regard to any
342 C pool (Fig. S6, C data in different soil C pools for each species at t37).

343 Significant differences in mean ΔC between N_2 -fixing Fabaceae and non N_2 -fixing Poaceae were found
344 with regard to C_{POM} and C_{SILT} . Mean C_{POM} was significantly higher in soil beneath Poaceae species
345 (ANOVA, $p = 0.024$, Tukey HSD test, Fig. 2a), whilst C_{SILT} was significantly higher in Fabaceae species
346 (ANOVA, $p = 0.060$, Tukey HSD test, Fig. 2b), and no significant differences were found in C_{SILT} between
347 Poaceae and bare soil. When grouping the data for all the non N_2 -fixing species (i.e., Poaceae, *P.*
348 *lanceolata* and *S. minor*), mean C_{POM} was higher compared to N_2 -fixing Fabaceae (ANOVA, $p = 0.06$, $F =$
349 3.61) but C_{SILT} was lower (ANOVA, $p = 0.01$, $F = 7.01$) (Fig. 2), although a Tukey HSD test did not find
350 significant differences between N_2 -fixing and non N_2 -fixing species.

351

352 2.3.1. Root elongation rate (RER) and root length production (RLP)

353 More than a threefold variation in mean daily RER_{TOT} occurred among species, ranging from 0.23 mm
354 d^{-1} (*F. rubra*) to 0.75 mm d^{-1} (*T. repens*) (Table 1). Mean daily RER_{TOT} did not differ between N_2 -fixing
355 Fabaceae ($0.57 \pm 0.08 \text{ mm d}^{-1}$ on average) and non N_2 -fixing Poaceae ($0.42 \pm 0.13 \text{ mm d}^{-1}$, ANOVA, $p =$
356 0.221 , Table 1), even when grouped with non N_2 -fixing species ($0.46 \pm 0.14 \text{ mm d}^{-1}$, ANOVA, $p = 0.075$).
357 Mean daily RER_{TOT} peaked at 0.75 mm d^{-1} in mid-February for Poaceae and then decreased, attaining a
358 value of 0.4 mm d^{-1} from April to June 2017 (Figs. S7). For Fabaceae species, mean daily RER_{TOT} peaked
359 at 1.1 mm d^{-1} in May 2017, before decreasing sharply in June 2017 (Fig. S7, mean RER_{TOT} for Fabaceae
360 and Poaceae species).

361 The mean daily RER for new roots (RER_{NEW} , $0.83 \pm 0.22 \text{ mm d}^{-1}$) was significantly higher than that of old
362 roots (RER_{OLD} , $0.17 \pm 0.09 \text{ mm d}^{-1}$, ANOVA, $p < 0.001$). Mean daily RER_{NEW} ranged from 0.32 mm d^{-1} (*F.*
363 *rubra*) to 1.13 mm d^{-1} (*D. glomerata*) whereas RER_{OLD} ranged from 0.05 mm d^{-1} (*P. pratensis*) to 0.40
364 mm d^{-1} (*T. pratense*). Mean daily RER_{NEW} did not differ in N_2 -fixing Fabaceae compared to non N_2 -fixing
365 Poaceae or all non N_2 -fixing species grouped together. However, mean daily RER_{OLD} was greater in N_2 -

366 fixing Fabaceae ($0.25 \pm 0.09 \text{ mm d}^{-1}$) than in non N₂-fixing Poaceae ($0.13 \pm 0.03 \text{ mm d}^{-1}$, ANOVA, $p =$
367 0.020) or all non N₂-fixing species grouped together ($0.12 \pm 0.04 \text{ mm d}^{-1}$, ANOVA, $p = 0.005$, Table 1).

368 After 37 weeks, the highest cumulative RLP_{TOT} was observed in in *O. viciifolia* (3.62 m) and the lowest
369 in *F. rubra* (1.19 m) (Table 1). N₂-fixing Fabaceae species possessed a greater RLP_{TOT} ($3.37 \pm 2.32 \text{ m}$)
370 compared to non N₂-fixing Poaceae ($2.32 \pm 0.70 \text{ m}$, ANOVA, $p = 0.032$), as well as all the N₂-fixing
371 species grouped together ($2.42 \pm 0.63 \text{ m}$, ANOVA, $p = 0.009$). Root dynamics of only three species were
372 correlated with climate factors. In *L. corniculatus*, mean daily RER_{TOT}, RER_{OLD}, RER_{NEW}, RLP_{TOT}, RLP_{OLD} and
373 RLP_{NEW} were all positively correlated with soil and air temperature and solar irradiation (Tables S1, S2).
374 In *T. repens*, RER_{TOT} and RER_{NEW}, RLP_{NEW} were significantly and positively correlated with soil and air
375 temperature (Tables S1, S2). With regard to Poaceae species, mean RER_{NEW} of *D. glomerata* was
376 negatively correlated with soil and air temperature and solar irradiation (Table S1). In *O. viciifolia*,
377 RLP_{TOT} was slightly and positively correlated with solar irradiation (Table S2). In *D. glomerata*, RLP_{NEW}
378 only, was negatively correlated with soil and air temperature (Table S2).

379

380 2.3.2. Root biomass, diameter and chemical composition

381 At 37 weeks, *M. sativa* had significantly greater mean root biomass ($4.23 \pm 0.42 \text{ g}$) compared to all
382 other species (Tukey HSD test, Table 1). In general, N₂-fixing Fabaceae species had a significantly higher
383 mean root biomass ($2.08 \pm 1.33 \text{ g}$) compared to non N₂-fixing Poaceae ($0.62 \pm 0.11 \text{ g}$) and all the non
384 N₂-fixing species grouped together ($0.65 \pm 0.17 \text{ g}$, ANOVA, $p < 0.001$). The mean diameter of absorptive
385 roots differed significantly between species, with *O. viciifolia* having the thickest absorptive roots and
386 *D. glomerata* the thinnest ($0.21 \pm 0.14 \text{ mm}$, Table 1). Species from the N₂-fixing Fabaceae family had
387 significantly thicker absorptive roots ($0.39 \pm 0.11 \text{ mm}$) compared to non N₂-fixing Poaceae (0.23 ± 0.03
388 mm) or all the non N₂-fixing species grouped together ($0.25 \pm 0.03 \text{ mm}$, ANOVA, $p < 0.001$).

389 The chemical composition of absorptive roots strongly varied among species and between N₂-fixing
390 Fabaceae and non N₂-fixing Poaceae or all the non N₂-fixing species grouped together (Table 1).
391 Absorptive roots of N₂-fixing Fabaceae possessed more hemicelluloses + water-soluble compounds
392 ($705 \pm 74 \text{ mg g}^{-1}$) than non N₂-fixing Poaceae ($543 \pm 33 \text{ mg g}^{-1}$) or all non N₂-fixing species grouped
393 together ($583 \pm 69 \text{ mg g}^{-1}$), a lower mean lignin content (N₂-fixing Fabaceae: $173 \pm 56 \text{ mg g}^{-1}$, non N₂-
394 fixing Poaceae: $302 \pm 59 \text{ mg g}^{-1}$, all non N₂-fixing species grouped together: $264.18 \pm 79.06 \text{ mg g}^{-1}$), and
395 a lower mean C:N ratio (N₂-fixing Fabaceae: 19.15 ± 3.07 , non N₂-fixing Poaceae: 58.67 ± 6.34 , and all
396 non N₂-fixing species grouped together: 62.04 ± 7.41). Mean root cellulose content did not differ either
397 among species or between N₂-fixing Fabaceae and non N₂-fixing Poaceae. However, when all the non

398 N₂-fixing species were grouped together, absorptive roots had a significantly higher mean cellulose
399 content compared to N₂-fixing Fabaceae (Table 1).

400

401 2.3.3. Soil substrate induced respiration (SIR)

402 Mean SIR for soil microbial communities varied significantly among species and between N₂-fixing
403 Fabaceae ($5.28 \pm 1 \mu\text{g C-CO}_2 \text{ g}^{-1} \text{ soil h}^{-1}$) and non N₂-fixing Poaceae ($3.12 \pm 0.41 \mu\text{g C-CO}_2 \text{ g}^{-1} \text{ soil h}^{-1}$,
404 ANOVA, $p < 0.001$, Table 1). Mean SIR ranged from $2.47 \pm 0.34 \mu\text{g C-CO}_2 \text{ g}^{-1} \text{ soil h}^{-1}$ (beneath *B. erectus*)
405 to $6.41 \pm 0.56 \mu\text{g C-CO}_2 \text{ g}^{-1} \text{ soil h}^{-1}$ (beneath *M. sativa*). When grouping all the non N₂-fixing species
406 together, mean SIR was still significantly lower ($3.1 \pm 0.46 \mu\text{g C-CO}_2 \text{ g}^{-1} \text{ soil h}^{-1}$) compared to N₂-fixing
407 Fabaceae ($5.28 \pm 1.02 \mu\text{g C-CO}_2 \text{ g}^{-1} \text{ soil h}^{-1}$, ANOVA, $p < 0.001$, Table 1).

408

409 2.3.4. Relationships between soil carbon accumulation (ΔC), root growth dynamics, 410 root traits, and substrate induced respiration (SIR)

411 The PCA conducted on the ΔC in the different C pools, SIR and root traits explained 64.6% of the
412 variance of the variables analyzed (Fig. 3). The first PCA axis (horizontal), accounting for 44.4% of the
413 variation, opposed $\Delta\text{C}_{\text{POM}}$ (negative) and $\Delta\text{C}_{\text{SILT}}$ (positive), while the remaining C pools, as well as the
414 sum of C pools, covaried and were quite orthogonal to $\Delta\text{C}_{\text{POM}}$ and $\Delta\text{C}_{\text{SILT}}$ and related to the second PCA
415 axis, that accounted for 20.2% of the variation. SIR and root biomass, diameter, and hemicelluloses +
416 water soluble compounds content of absorptive roots all went along the 1st axis (positive) together
417 with $\Delta\text{C}_{\text{SILT}}$. Root traits linked with recalcitrance, lignin, cellulose and C:N ratio, went along the 1st axis
418 (negative) together with $\Delta\text{C}_{\text{POM}}$. Convex hull polygons reflecting intraspecific variations generally had
419 small areas and were segregated over the biplot (Fig. 3). The PCA strongly discriminated Poaceae from
420 Fabaceae. Poaceae were all on the negative end of the first axis and were characterized by high lignin
421 and cellulose contents, high C:N and accumulation of C in the coarse POM fraction. Fabaceae species
422 were at far right of the first axis and were characterized by a higher biomass and thicker roots that
423 were rich in hemicelluloses, favoring accumulation of C in the coarse silt fraction. The two other non
424 N₂-fixing species were situated in intermediate positions on the axis.

425 When analyzing the species effect of root traits on C storage ($n = 12$) regression analyses showed that
426 mean $\Delta\text{C}_{\text{POM}}$ was not related to RER, but was slightly significantly and negatively related to two traits:
427 diameter and hemicelluloses + water-soluble compounds content of absorptive roots (Table S3a,
428 Figure 4a,b). Mean $\Delta\text{C}_{\text{SILT}}$ was significantly and positively correlated with mean daily RER_{OLD} and RLP_{OLD}
429 and with the mean diameter of absorptive roots, root biomass, hemicellulose + water-soluble

430 compounds of absorptive roots, and SIR (Table S3s, Figures 5a,b,c,d,f, h), whereas mean ΔC_{SILT} was
431 negatively correlated with mean lignin and C:N ratio (Table S3s, Figures 5e,g). Linear regressions of
432 mean ΔC_{SILT} and C:N ratio show two segregated clusters of points: one with low C:N related to N_2 -fixing
433 species and one with non N_2 -fixing species having a high C:N ratio and low accumulation in ΔC_{SILT}
434 (Figure 5g). Variations in mean ΔC_{SUM} , $\Delta C_{\text{finePOM}}$ and $\Delta C_{\text{SILT+CLAY}}$ were not explained by any variables.
435 Mean SIR was significantly and positively correlated to mean RER_{OLD} and RLP_{OLD} , root biomass and
436 hemicelluloses + water-soluble compounds (Table S3, Fig. 6a,b,c,e), but negatively correlated with
437 mean lignin and C:N ratio (Table S3a, Figures 6d,f). Mean hemicelluloses + water-soluble compounds
438 were significantly and negatively correlated with mean lignin content and C:N ratio (Table S3a).

439 When considering Pearson's correlations at the individual level ($n = 36$), significant correlations were
440 found only between absorptive root diameter and ΔC_{POM} , SIR and ΔC_{SILT} (Table S3b). Correlations
441 between root traits and mean SIR were similar compared to correlatins of raw data (Table S3b). The
442 data dispersion in linear models showed that at the individual level, even if R^2 was low, the tendency
443 remained the same as that when mean data were used for ΔC_{POM} (Fig. S9), ΔC_{SILT} (Fig. S10), and SIR (Fig.
444 S11).

445

446 2.4. DISCUSSION

447 Total C accumulation in soil did not differ among plant species (Fig. 1), but as expected, C accumulation
448 was significantly greater in the C_{SILT} pool beneath N_2 -fixing Fabaceae, whereas in soil beneath non N_2 -
449 fixing Poaceae species, C accumulation was greater in the C_{POM} pool (Fig. 2). In line with our hypotheses,
450 the accumulation of C into different soil C fractions, specifically C_{POM} and C_{SILT} , was correlated with root
451 traits (Fig. 4, 5, 6). The more rapid RER and greater RLP of older roots promoted C accumulation into
452 the C_{SILT} pool, but smaller root diameter and low content of labile compounds (hemicelluloses and
453 water soluble compounds) enhanced C accumulation into the C_{POM} pool. Although measuring total soil
454 organic carbon can be an easy method to evaluate C storage, it is not as sensitive to short-term C
455 dynamics or effect of plant species and families, as the C changes in different soil fractions. Studies of
456 C sequestration should therefore focus on better estimating C input into different C pools associated
457 with soil textural fractions (Wiesmeier et al. 2019).

458

459 2.4.1. *Hypothesis 1: Root elongation rate and root length production are expected to*
460 *favour carbon accumulation in the C_{SILT} and C_{SILT+CLAY} fractions*

461 We hypothesized that a fast RER would promote C accumulation in coarse silt and fine silt+clay soil
462 fractions, through an increase in exudation and microbial activity along newly initiated roots.
463 Interestingly, RER_{OLD} and RLP_{OLD} were significantly and positively correlated with soil microbial SIR and
464 ΔC_{SILT} (Fig. 5a,b, Table S3a), but not with the RER and RLP of newly initiated roots, that had very high
465 rates of growth. Dennis et al. (2010) hypothesized that rapidly elongating root tips grow quickly out of
466 the main zone of microbial activity, that is established once root exudates have been consumed. These
467 microbial communities then consume rhizodeposits from mucilage and cell senescence as well as
468 exudates from roots growing in proximity. Therefore, slow growing older roots would be maintained
469 in this zone of high microbial activity, and C accumulation in the coarse silt fraction would be higher,
470 especially in N₂-fixing species with populations of bacteria distributed in nodules all along roots. N₂-
471 fixing *Rhizobium* bacteria also increase root elongation (Garrido-Oter et al. 2018), likely inducing a
472 feedback mechanism whereby a stimulated RER results in a higher exudation rate (Garcia et al. 2001),
473 acting as a substrate for newly colonizing *Rhizobium* communities. Although the role of microbial
474 communities is of utmost importance for C input into the soil, differences in the use of C within plants
475 could also explain the lack of a relationship between RER_{NEW}, RLP_{NEW}, SIR and C_{SILT}. In fast-growing,
476 newly initiated roots, we suggest that C in the form of non-structural carbohydrates (NSC, produced
477 during photosynthesis), will be used preferentially for cell production and expansion, as found in a
478 recent seasonal study of root elongation and NSC fluxes (Wang et al. 2018). In older roots with lower
479 RER, less NSC is required for growth, and excess NSC would be freely exuded, reflected in the high SIR
480 that we observed.

481 Contrary to our hypothesis, RER and RLP did not promote accumulation of C in the C_{SILT+CLAY} pool.
482 Surprisingly, the C_{SILT+CLAY} pool was the only pool where C was actually lost over the 37 weeks, in both
483 bare soil and beneath all plant species, and this mineralisation of C could not be explained by microbial
484 activity or by any root traits. When soil was prepared in our study, its excavation, crushing and sieving
485 would have disrupted soil aggregates (Franzluebbers, 1999). This increase in C mineralisation is higher
486 in clays, as organic matter that was highly protected within the clay fraction will be released during
487 disruption, providing a new pool of C available to microorganisms (Hassink, 1992). The presence of
488 plant roots can also lead to an increased mineralization and loss of preexistent soil C due to an
489 increased microbial activity (positive priming effect; Kuzyakov et al., 2000). In our study, the origin of
490 C was not assessed, so it was not possible to quantify any priming effect. The decrease in C was mainly
491 observed in the silt+clay fraction, challenging the assumption that the C pool associated to this soil
492 fraction has greater C stability (Torn et al., 2009). However, these results are in line with the findings

493 from Keiluweit et al. (2015) who observed a major priming effect in the organomineral associated C
494 after the input of oxalic acid, a common component of root exudates. The soil disturbance, together
495 with the input of highly degradable C, may well increase the release and priming of C in the
496 organomineral associated fraction, thereby decreasing the C content in the silt+clay fraction, but
497 further studies are required to better understand this phenomenon.

498

499 *2.4.2. Hypothesis 2: more recalcitrant root traits are expected to favour the* 500 *unprotected coarse POM fraction*

501 Root traits linked to recalcitrance (high cellulose and lignin content and high C:N ratio) did not correlate
502 to C accumulation in the coarse POM fraction (C_{POM}) (Fig. 4), but the PCA showed that this suite of traits
503 was sharing similar coordinates with C_{POM} on axis 1 (Fig. 3). This result is mainly due to the Poaceae
504 species that all have higher C accumulation in the C_{POM} pool, as well as recalcitrant root traits,
505 compared to species from other families. Recalcitrant compounds have all been reported to decrease
506 root decomposition rates (Silver and Miya, 2001; Aulen et al. 2012; Poirier et al. 2018). Lignin-
507 carbohydrate complexes prevent polymer-hydrolyzing enzymes access to substrates, thus reducing the
508 degradability of plant organic matter (Cornu et al. 1994, Malherbe and Cloete, 2002). SIR, as a proxy
509 for microbial activity, was also strongly and negatively correlated to lignin content (Fig. 6f), probably
510 because lignin reduces the accessibility of polysaccharides to microorganisms through the formation
511 of links between lignin and polysaccharides (Bertrand et al. 2006). Products of lignin degradation can
512 also react with ammonia or amino acids to form further recalcitrant complexes that are less available
513 to microorganisms (Nömmik and Vahtras, 1982). The trend observed in the PCA (Fig. 3), that species
514 with recalcitrant tissues were linked to higher C_{POM} accumulation, is in contradiction with the lack of
515 significant correlations between ΔC_{POM} and lignin or C:N ratio. One reason for this lack of correlation
516 might be that the experiment was shorter than the root life span of some or all species, and full
517 accumulation of C in the C_{POM} pool had not yet occurred (Van der Krift et Berendse, 2002). Another
518 reason may be because C_{POM} was derived from the input of fresh C from plants, as well as losses of
519 older C that already existed in soil. While the accumulation of new C in this fraction is influenced by
520 the chemical composition of the root system, the losses of older, pre-existing C are not. A C labeling
521 approach would be helpful to assess the different fluxes of new and old C and to better explain the
522 relationships between root traits and C storage.

523

524 Interestingly, C accumulation in the C_{SILT} pool was negatively correlated with recalcitrant root traits
525 (lignin and C:N ratio, Fig. 5e,g), but positively with hemicelluloses content and root diameter (Fig. 5d,f).

526 Hemicelluloses comprise polysaccharides soluble in alkali and are easily degradable by microorganisms
527 (Dekker, 1985). Hemicelluloses are usually produced to the detriment of lignin and enhance tissue
528 degradability through higher accessibility to amorphous phases in the lignocellulose structure
529 (Malherbe and Cloete, 2002). Microorganisms will use this easily degradable C for growth and
530 respiration and then produce exudates and exopolysaccharides, that are used as a substrate for
531 subsequent microbial communities (Dennis et al. 2010). These exopolysaccharides and low molecular
532 weight compounds are believed to be the main precursors of C in the coarse silt pool (Simpson et al.,
533 2007; Mambelli et al., 2011; Cotrufo et al. 2013, Vidal et al. 2018), probably explaining the high C_{SILT}
534 we found beneath N_2 -fixing species (Fig. 2) with high hemicelluloses + water soluble compounds and
535 low lignin contents. Absorptive roots were negatively correlated with C accumulation in the C_{POM} pool
536 (Fig. 4a) and positively correlated with C accumulation in the C_{SILT} pool (Fig. 5d). Absorptive roots
537 generally have a higher turnover rate and undergo rapid transformation through microbial degradation
538 (McCormack et al., 2015), explaining the low accumulation in the C_{POM} pool and the positive correlation
539 with the C_{SILT} pool. However, this relationship may also be an artefact because Poaceae roots are
540 inherently very fine compared to Fabaceae roots (Roumet et al. 2006; 2016), highlighting that the
541 understanding of relationships between C accumulation and morphological traits is challenging
542 because of their inherent nature and plasticity (Poirier et al. 2018).

543

544 *2.4.3. Hypothesis 3: Fabaceae and Poaceae strongly differ in their influence on* 545 *accumulation of C into different soil fractions*

546 Contrary to that observed in previous studies (Binkley 2005; Fornara and Tilman, 2008; Plaza-Bonilla
547 et al., 2016; King et al., 2018), we did not find evidence of a greater accumulation of total C (ΔC_{SUM}) in
548 soil beneath N_2 -fixing species, because variability was high within Fabaceae. However, we showed that
549 N_2 -fixing species and non N_2 -fixing species (especially Poaceae and Fabaceae) strongly differed in their
550 effect on the accumulation of C into different soil C pools. Roots of Poaceae, as compared to Fabaceae,
551 had a lower RER and RLP. Poaceae produced thinner roots, rich in lignin and cellulose with a high C:N
552 ratio. These more recalcitrant tissues slow down microbial activity and hence root decomposition rate
553 (Roumet et al. 2016; Freschet et al. 2017). Due to their particular chemical composition, non N_2 -fixing
554 species, especially Poaceae species, promote C accumulation in the unprotected C_{POM} pool, and have
555 a lower C accumulation in the more stable C_{SILT} pool (Fig. 4). On the other hand, roots of N_2 -fixing
556 Fabaceae grow faster and produce thick roots that are easily degradable, since they are rich in N (low
557 C:N ratio) and in hemicelluloses and water soluble compounds. These traits favour the development
558 of microbial biomass and enhance their activity, as observed from the SIR that was 40% higher beneath

559 Fabaceae than Poaceae species (see Fig. 7 for a conceptual model describing C accumulation in
560 different pools).

561 Because of the lack of correlations between root traits and C accumulation in $C_{\text{SILT+CLAY}}$ pool, we cannot
562 establish that the $C_{\text{SILT+CLAY}}$ pool increases when there is a higher input of labile C from N_2 -fixing species.
563 C accumulation is the result of the input of new C and losses of pre-existing C that can be influenced
564 by the input of fresh C from plants (priming effect). The difference in behavior between these two
565 pools could result in poor correlations between root traits and C accumulation in the $C_{\text{SILT+CLAY}}$ pool. An
566 isotopic approach differentiating between the changes in new C and old C in different C pools, allowing
567 us to assess the priming effect, would be fundamental to understanding the mechanisms behind soil
568 C storage (Rossi 2019).

569

570 2.5. CONCLUSION

571 Our findings show that specific plant root traits influence the accumulation of C into different pools,
572 largely through the mediation of microbial activity, shaping the C pathway in soil and, finally, its
573 persistence. Our results showed that non N_2 -fixing Poaceae species, characterized by high contents of
574 lignin and cellulose and a high C:N, promoted accumulation of C in the unprotected coarse POM
575 fraction, while root traits associated with high labile C input (high hemicelluloses + water soluble
576 compound contents, high RER_{OLD} and RLP_{OLD}) and microbial activity, typical of N_2 -fixing Fabaceae
577 species, stimulated C accumulation in the protected coarse silt fraction. Root elongation rate and
578 length production promoted microbial activity in older roots only, potentially suggesting either a
579 spatial influence of root exudate accessibility on microbial communities, or a relationship between
580 non-structural carbohydrate use in roots and available exudates for microbial consumption. The
581 planting of vegetation in bare soil also led to a loss of C in the fine silt+clay fraction, commonly believed
582 to be the most stable. Differentiating the source of C loss (pre-existing C in soil or fresh C from live
583 plants), is a fundamental step to assess the priming effect and understand the mechanisms behind C
584 loss in the finer soil fractions, and could be achieved through an isotope labelling approach. Longer
585 term studies on C dynamics are needed to understand these species and root trait effects over time
586 and the consequent C accumulation in different pools. Moreover, the influence of different soils and
587 associated microbial communities need to be taken into consideration for a broader understanding of
588 C pool dynamics. Our results will not only be useful for identifying plant species capable of enhancing
589 long-term C storage in soil, but will also contribute significantly to the understanding of mechanistic
590 processes within the C cycle.

591 **ACKNOWLEDGEMENTS**

592 Funding was provided by the project: TALVEG2 'An innovative approach for the management and
593 monitoring of ecosystems' (Programme Opérationnel Languedoc Roussillon 2014-2020, FEDER-FSE-IEJ
594 2015009142). The authors wish to acknowledge the support of the European Commission via the Marie
595 Skłodowska-Curie Innovative Training Networks (ITN-ETN) project TERRE 'Training Engineers and
596 Researchers to Rethink geotechnical Engineering for a low carbon future' (H2020-MSCA-ITN-2015-
597 675762). Thanks to F. Pailler (INRAE) and D. Degueldre from the Experimental Plots (LabEx CeMEB, an
598 ANR "Investissements d'avenir" program (ANR-10-LABX-04-01) for the technical help and experimental
599 management, and to the staff at the PACE platform (LabEx CeMEB), N. Barthes, R. Leclerc and B.
600 Buatois, for help and assistance with laboratory analyses. Thanks to Ngô Ha My (USTH, Hanoi) and S.
601 Fourcaud-Stokes (AMAP) for their technical assistance.

602 REFERENCES

- 603 Aulen M, Shipley B, Bradley R (2012) Prediction of in situ root decomposition rates in an interspecific
604 context from chemical and morphological traits. *Annals of Botany* 109: 287-297
- 605 Balesdent J and Balabane M (1996) Major contribution of roots to soil carbon storage inferred from
606 maize cultivated soils. *Soil Biol Biochem* 9: 1261–1263.
- 607 Bardgett RD, Mommer L, Vries FT De (2014) Going underground : root traits as drivers of ecosystem
608 processes. *Tends Ecol Evol* 29: 692–699.
- 609 Beare MH, Neely CL, Coleman DC, Hargrove WL (1990) A substrate-induced respiration (SIR) method
610 for measurement of fungal and bacterial biomass on plant residues. *Soil Biol Biochem* 22(5): 585-
611 594
- 612 Berntson GM (1997) Topological scaling and plant root system architecture: developmental and
613 functional hierarchies. *New Phytol* 135: 621–634
- 614 Bertrand I, Chabbert B, Kurek B, Recous S (2006) Can the biochemical features and histology of wheat
615 residues explain their decomposition in soil? *Plant Soil* 281:291–307
- 616 Besnard E, Chenu C, Balesdent J, Puget P, Arrouays D (1996) Fate of particulate organic matter in soil
617 aggregates during cultivation. *Eur J Soil Sci* 47: 495–503.
- 618 Binkley D (2005) How Nitrogen-Fixing Trees Change Soil Carbon. In: Binkley D., Menyailo O. (eds) *Tree
619 Species Effects on Soils: Implications for Global Change*. NATO Science Series IV: Earth Env Sci,
620 vol 55. Springer, Dordrecht
- 621 Bird JA, Kleber M, Torn MS (2008) C-13 and N-15 stabilization dynamics in soil organic matter fractions
622 during needle and fine root decomposition. *Organic Geo- chemistry*, 39, 465–477
- 623 Canarini A, Kaiser C, Merchant A, Richter A, Wanek W (2019) Root exudation of primary metabolites:
624 mechanisms and their roles in plant responses to environmental stimuli. *Front Plant Sci* 10: 157
- 625 Chapin FS III (2003) Effects of plant traits on ecosystem and regional processes: a conceptual
626 framework for predicting the consequences of global change. *Ann Bot* 91: 455–463.
- 627 Cornu A, Besle JM, Mosoni P, Grent E (1994) Lignin- carbohydrate complexes in forages: Structure and
628 consequences in the ruminal degradation of cell-wall carbohydrates. *Reprod Nutr Dev* 24: 385–
629 398
- 630 Cotrufo MF, Wallenstein MD, Boot CM, Deneff K, Paul E (2013) The Microbial Efficiency-Matrix
631 Stabilization (MEMS) framework integrates plant litter decomposition with soil organic matter
632 stabilization: do labile plant inputs form stable soil organic matter? *Global Change Biol* 19: 988–
633 995.
- 634 De Deyn GB, Cornelissen JHC, Bardgett RD (2008) Plant functional traits and soil carbon sequestration
635 in contrasting biomes. *Ecol Lett* 11: 516–531.
- 636 Dekker M (1985) Biosynthesis and Biodegradation of Wood Components: Biodegradation of the
637 Hemicelluloses. Ed. T. Higuchi pp. 505 – 533: Academic Press

638 Dennis PG, Miller AJ, Hirsch PR (2010) Are root exudates more important than other sources of
639 rhizodeposits in structuring rhizosphere bacterial communities? *FEMS Microbiol Ecol* 72: 313–
640 327.

641 Derrien D, Barot S, Chenu C, Chevallier T, Freschet GT, Garnier P, Guenet B, Hedde M, Klumpp K,
642 Lashermes G, et al. (2016) Stocker du C dans les sols : Quels mécanismes, quelles pratiques
643 agricoles, quels indicateurs ? *Étude et Gestion des Sols* 23: 193–224.

644 Downie JA (2010) The roles of extracellular proteins, polysaccharides and signals in the interactions of
645 rhizobia with legume roots. *Fed of Eur Microbiol Soc* 34: 150–170.

646 Dungait JA, Hopkins DW, Gregory AS, Whitmore AP (2012) Soil organic matter turnover is governed by
647 accessibility not recalcitrance. *Global Change Biol* 18: 1781–1796

648 Fehrmann RC and Weaver RW (1978) Scanning electron microscopy of *Rhizobium* sp. adhering to fine
649 silt particles. *Soil Sci Soc Am J* 42: 279-281

650 Fornara D, Tilman D (2008) Plant functional composition influences rates of soil carbon and nitrogen
651 accumulation. *J Ecol* 96: 314–322.

652 Franzluebbers AJ (1999) Potential C and N mineralization and microbial biomass from intact and
653 increasingly disturbed soils of varying texture. *Soil Biol Biochem* 31: 1083-1090,

654 Fujisaki K, Chapuis-Lardy L, Albrecht A, Razafimbelo T, Chotte JL, Chevallier T (2018) Data synthesis of
655 carbon distribution in particle size fractions of tropical soils: implications for soil carbon storage
656 potential in croplands. *Geoderma* 313, 41-51.

657 Garcia JAL, Barbas C, Probanza A, Barrientos ML, Manero FJG (2001) Low molecular weight organic
658 acids and fatty acids in root exudates of two *Lupinus* cultivars at flowering and fruiting stages.
659 *Phytochem Analysis* 12: 305–311.

660 Garrido-Oter R, Nakano RT, Dombrowski N, Ma KW, AgBiome Team, McHardy AC, Schulze-Lefert P
661 (2018) Modular traits of the Rhizobiales root microbiota and their evolutionary relationship with
662 symbiotic rhizobia. *Cell Host Microbe* 24(1): 155-167.

663 Gavinelli E, Feller C, Larré-Larrouy MC, Bacye B, Djegui Z, Nzila JD (1995) Routine method to study soil
664 organic matter by particle-size fractionation: examples for tropical soils. *Comm Soil Sci*
665 *Plan*26(11&12): 1749-1760

666 Gleixner G, Poirier N, Bol R, Balesdent J (2002) Molecular dynamics of organic matter in a cultivated
667 soil. *Org Geochem* 33: 357-366.

668 Griscom BW, Adams, J, Ellis PW, Houghton RA, Lomax G, Miteva DA, Schlesinger WH, Shoch D,
669 Siikamäki J V, Smith P, Woodbury P, Zganjar C, Blackman A, Campari J, Conant RT, Delgado C,
670 Elias P, Gopalakrishna T, Hamsik MR, Herrero M, Kiesecker J, Landis E, Laestadius L, Leavitt SM,
671 Minnemeyer S, Polasky S, Potapov P, Putz FE, Sanderman J, Silvius M, Wollenberg E, Fargione J
672 (2017) Natural climate solutions. *Proceedings of the National Academy of Science of the United*
673 *States of America*. 114, 11645–11650

674 Hamer U, Marschner B, (2005) Priming effects in soils after combined and repeated substrate

675 additions. *Geoderma* 128(1):38-51

676 Harrell FE (2007) Package 'Hmisc'. Harrell Miscellaneous

677 Hassink J (1992) Effects of soil texture and structure on carbon and nitrogen mineralization in grassland
678 soils. *Biol Fertil Soils* 14 : 126–134.

679 Heinze , Gensch S, Weber E, Joshi J (2017) Soil temperature modifies effects of soil biota on plant
680 growth. *J Plant Ecol* 10 (5): 808 – 821

681 Hernández MA, Romero J, Jaime C, León-pulido J (2017) Lignocellulosic biomass from fast-growing
682 species in Colombia and their use as bioresources for biofuel production. *Chem Eng Trans* 58:
683 541–546.

684 Holz M, Zarebanadkouki M, Kaestner A, Kuzyakov Y, Carminati A (2018) Rhizodeposition under drought
685 is controlled by root growth rate and rhizosphere water content. *Plant Soil* 423: 429–442.

686 Huck MG, Taylor HM (1982) The Rhizotron as a Tool for Root Research In *Advances in Agronomy*, ed.
687 NC Brady, pp. 1-35: Academic Press

688 Huo C, Luo Y, Cheng W, (2017) Rhizosphere priming effect: A meta-analysis. *Soil Biology and*
689 *Biochemistry* 111: 78–84

690 Jones DL, Nguyen C, Finlay RD (2009) Carbon flow in the rhizosphere: carbon trading at the soil-root
691 interface. *Plant Soil* 321: 5–33.

692 Kätterer T, Bolinder MA, Andrén O, Kirchmann H, Menichetti L (2011) Roots contribute more to
693 refractory soil organic matter than above-ground crop residues, as revealed by a long-term field
694 experiment. *Agric. Ecosyst. Environ.* 141, 184–192

695 Keiluweit M, Bougoure JJ, Nico PS, Pett-Ridge J, Weber PK, Kleber M (2015) Mineral protection of soil
696 carbon counteracted by root exudates. *Nature Climate Change* 5: 588-595

697 King AE, Blesh J, (2018) Crop rotations for increased soil carbon: Perenniality as a guiding principle.
698 *Ecol. Appl.* 28, 249–261

699 King AE, Congreves KA, Deen B, Dun KE, Voroney RP, Wagner-riddle C (2019) Quantifying the
700 relationships between soil fraction mass , fraction carbon, and total soil carbon to assess
701 mechanisms of physical protection. *Soil Biol Biochem* 135: 95–107.

702 Kleber M, Nico PS, Plante A, Filley T, Kramer M, Swanston C, Sollins P (2011) Old and stable soil organic
703 matter is not necessarily chemically recalcitrant: Implications for modeling concepts and
704 temperature sensitivity. *Glob. Chang. Biol.* 17, 1097–1107

705 Kleber M, Eusterhues K, Keiluweit M, Mikutta C, Mikutta R, Nico PS (2015) Mineral-Organic
706 Associations: Formation, Properties, and Relevance in Soil Environments, *Advances in*
707 *Agronomy*. Elsevier Ltd.

708 Kogel-Knabner I (2002) The macromolecular organic composition of plant and microbial residues as
709 inputs to soil organic matter. *Soil Biol Biochem* 34: 139-162

710 Kuzyakov Y, Friedel JK, Stahr K, (2000) Review of mechanisms and quantification of priming effects. *Soil*

- 711 Biology and Biochemistry 32: 1485-1498
- 712 Kuzyakov Y, Larinova AA (2005) Root and rhizomicrobial respiration: a review of approaches to
713 estimate respiration by autotrophic and heterotrophic organisms in soil. *J Plant Nutr Soil Sci* 168:
714 503 - 520
- 715 Lal R (2004) Soil carbon sequestration impacts on global change and food security. *Science* 304: 1623-
716 1627.
- 717 Larson JE, Funk JL (2016) Seedling root responses to soil moisture and the identification of a
718 belowground trait spectrum across three growth forms. *New Phytol* 210: 827–838.
- 719 Lavorel S, Diaz S, Cornelissen JHC, Garnier E, Harrison SP, McIntyre S, Juli G, Pérez-Harguinde PS,
720 Roumet C, Urcelay C (2007) Plant functional types: are we getting any closer to the Holy Grail?
721 In: *Terrestrial Ecosystems in a Changing World*, eds Canadell, J., Pitelka, L.F. & Pataki, D. Springer,
722 Berlin, pp. 171–186.
- 723 Lobet G, Pagès L, Draye X (2011) A novel image-analysis toolbox enabling quantitative analysis of root
724 system architecture. *Plant Physiol* 157: 29-39
- 725 von Lutzow M, Kogel-Knabner I, Ekschmitt K, Matzner E, Guggenberger G, Marschner B, Flessa H (2006)
726 Stabilization of organic matter in temperate soils: mechanisms and their relevance under
727 different soil conditions – a review. *Eur J Soil Sci* 57: 426–445.
- 728 Malherbe S, Cloete TE (2002) Lignocellulose biodegradation: fundamentals and applications. *Rev*
729 *Environ Sci Bio* 1: 105–114,; 105–114.
- 730 Mambelli S, Bird JA, Gleixner G, Dawson TE, Torn MS (2011) Relative contribution of foliar and fine root
731 pine litter to the molecular composition of soil organic matter after in situ degradation. *Organic*
732 *Geochemistry*, 42: 1099–1108
- 733 McCormack LM, Dickie IA, Eissenstat DM, Fahey TJ, Fernandez CW, Guo D, Erik A, Iversen CM, Jackson
734 RB.(2015) Redefining fine roots improves understanding of below-ground contributions to
735 terrestrial biosphere processes. *New Phytol* 207: 505–518.
- 736 Mikutta R, Kleber M, Torn MS, Jahn R (2006) Stabilization of soil organic matter: association with
737 minerals or chemical recalcitrance?. *Biogeochem* 77: 25-56
- 738 Minasny B, Malone BP, McBratney AB, Angers DA, Arrouays D, Chambers A, Chaplot V, Chen ZS, Cheng
739 K, Das BS, Field DJ, Gimona A, Hedley CB, Hong SY, Mandal B, Marchant BP, Martin M, McConkey
740 BG, Mulder VL, O'Rourke S, Richer-de-Forges AC, Odeh I, Padarian J, Paustian K, Pan G, Poggio L,
741 Savin I (2017) Soil carbon 4 per mille. *Geoderma* 292, 59–86.
- 742 Mohamed A, Monnier Y, Mao Z, Lobet G, Maeght JL, Ramel M, Stokes A (2017) An evaluation of
743 inexpensive methods for root image acquisition when using rhizotrons. *Plant Methods* 13: 1–13.
- 744 Mohamed A, Stokes A, Mao Z, Jourdan C, Sabatier S, Pailler F, Fournier S, Dufour L, Monnier Y (2018)
745 Linking above- and belowground phenology of hybrid walnut growing along a climatic gradient
746 in temperate agroforestry systems. *Plant and Soil* 424: 103
- 747 Mommer L, Padilla FM, van Ruijven J, de Caluwe H, Smit-Tiekstra A, Berendse F, de Kroon H (2015)

748 Diversity effects on root length production and loss in an experimental grassland community.
749 *Funct Ecol* 29: 1560–1568.

750 Nguyen C (2003) Rhizodeposition of organic C by plants: mechanisms and controls. *Agronomie* 23, 375–
751 396.

752 Nömmik H, Vahtras Z (1982) Retention and fixation of ammonium and ammonia in soils. In: Stevenson,
753 F.J. (Ed.),. Nitrogen in agricultural soils. Agronomy monographs, No. 22. Agronomy Society of
754 America, Madison, WI, USA.

755 Oksanen J, Blanchet FG, Friendly M, Kindt R, Legendre P, McGlinn D, Minchin PR, O'Hara RB, Simpson
756 GL, Solymos P, Henry M, Stevens H, Szoecs E, Wagner H (2019) Package 'vegan'. Community
757 Ecology Package, R package version 1.17– 2. <http://CRAN.R-project.org/package=vegan>

758 Paustian K, Lehmann J, Ogle S, Reay D, Robertso GP, Smith P (2016) Climate-smart soils. *Nature* 532:
759 49–57.

760 Plaza-Bonilla D, Nolot JM, Passot S, Raffailac D, Justes E, (2016) Grain legume-based rotations
761 managed under conventional tillage need cover crops to mitigate soil organic matter losses. *Soil*
762 *Tillage Res.* 156, 33–43

763 Poirier V, Roumet C, Munson AD (2018) The root of the matter: linking root traits and soil organic
764 matter stabilization processes. *Soil Biol Biochem* 120: 246–259.

765 R Development Core Team (2013) R: A Language and Environment for Statistical Computing. Vienna,
766 Austria

767 Rasse DP, Rumpel C, Dignac M (2005) Is soil carbon mostly root carbon ? Mechanisms for specific
768 stabilization. *Plant Soil* 269: 341–356

769 Robertson AD, Paustian K, Ogle S, Wallenstein MD, Lugato E , Cotrufo FM (2019) Unifying soil organic
770 matter formation and persistence frameworks: the MEMS model. *Biogeosci* 16: 1225-1248

771 Rossi LMW (2019) Embankment as a carbon sink: a study on carbon sequestration pathways and
772 mechanisms in topsoil and exposed subsoil. Ph. D. Thesis, University of Montpellier, France

773 Roumet C, Urcelay C, Díaz S, Roumet C (2006) Suites of root traits differ between annual and perennial
774 species growing in the field. *New Phytol* 170 : 357–368

775 Roumet C, Birouste M, Picon-Cochard C, Ghestem M, Osman N, Vrignon-Brenas S, Cao K-F, Stokes A
776 (2016) Root structure-function relationships in 74 species: Evidence of a root economics
777 spectrum related to carbon economy. *New Phytol* 210: 815–826.

778 Rubino M, Dungait JAJ, Evershed RP et al. (2010) Carbon input belowground is the major C flux
779 contributing to leaf litter mass loss: evidences from a (13)C labelled- leaf litter experiment. *Soil*
780 *Biology & Biochemistry*, 42: 1009–1016

781 Sanderman J, Maddern T, Baldock J, (2014) Similar composition but differential stability of mineral
782 retained organic matter across four classes of clay minerals. *Biogeochemistry* 121: 409-424

783 Sasse J, Martinoia E, Northen T (2018) Feed Your Friends: Do Plant Exudates Shape the Root

- 784 Microbiome? Trends in Plants Science 23(1): 25-41
- 785 Schmidt MWI, Torn MS, Abiven S, Dittmar T, Guggenberger G, Janssens IA, Kleber M, Kögel-Knabner I,
786 Lehmann J, Manning DAC, Nannipieri P, Rasse DP, Weiner S, Trumbore SE (2011) Persistence of
787 soil organic matter as an ecosystem property. Nature 478, 49–56.
- 788 Schneider CA, Rasband WS, Eliceiri KW (2012) NIH Image to ImageJ: 25 years of image analysis. Nature
789 Methods 9: 671–675
- 790 Shahzad T, Chenu C, Genet P, Barot S, Perveen N, Mougine C, and Fontaine S (2015) Contribution of
791 exudates, arbuscular mycorrhizal fungi and litter depositions to the rhizosphere priming effect
792 induced by grassland species. Soil Biology and Biochemistry, 80: 146–155
- 793 Silver WL, Miya RK (2001) Global patterns in root decomposition: comparisons of climate and litter
794 quality effects. Oecologia 129:407-419
- 795 Simpson AJ, Simpson MJ, Smith E, Kelleher BP (2007) Microbially derived inputs to soil organic matter:
796 are current estimates too low? Environmental Science & Technology, 41: 8070–8076
- 797 Six J, Bossuyt H, Degryze S, Deneff K (2002) A history of research on the link between (micro)aggregates,
798 soil biota, and soil organic matter dynamics. Soil Till Res 79: 7-31
- 799 Sokol NW, Kuebbing SE, Karlsen-ayala E, Bradford MA (2019) Evidence for the primacy of living root
800 inputs, not root or shoot litter, in forming soil organic carbon. New Phytol 221: 233–246.
- 801 Sollins P, Hofmann P and Caldwell BA (1996) Stabilization and destabilization of soil organic matter:
802 mechanisms and controls. Geoderma 74: 65–105.
- 803 Steinaker DF, Wilson SD, Peltzer DA (2010) Asynchronicity in root and shoot phenology in grasses and
804 woody plants. Global Change Biol 16: 2241–2251
- 805 Torn MS, Swanston CW, Castanha C, Trumbore SE (2009) Storage and Turnover of Organic Matter in
806 Soil. In: Biophysico-Chemical Processes Involving Natural Non-living Organic Matter in
807 Environmental Systems, Publisher: John Wiley & Sons
- 808 Van Der Krift TAJ, Berends F (2002) Root life spans of four grass species from habitats differing in
809 nutrient availability. Functional Ecology 16(2): 198 - 203
- 810 Van Soest PJ (1963) Use of detergents in the analysis of fibrous feeds. II. A rapid method for the
811 determination of fiber and lignin. J AOAC Int 46: 829–835.
- 812 Vidal A, Hirte J, Bender SF, Mayer J, Gattinger A, Höschel C, Schädler S, Iqbal TM, Mueller CW (2018)
813 Linking 3D Soil Structure and Plant-Microbe-Soil Carbon Transfer in the Rhizosphere. Front Env
814 Sci 6: 1–14.
- 815 Wang Y, Mao Z, Bakker MR, Kim JH, Brancheriau L, Buatois B, Leclerc R, Selli L, Rey H, Jourdan C, Stokes
816 A (2018) Linking conifer root growth and production to soil temperature and carbon supply in
817 temperate forests. Plant Soil 426: 33–50
- 818 Warembourg FR, Roumet C, Lafont F (2003) Differences in rhizosphere carbon-partitioning among
819 plant species of different families. Plant Soil 256: 347–357.

- 820 Wiesmeier M, Urbanski L, Hobbey E, Lang B, von Lützow A , Marin-Spiotta E, van Wesemael B, Rabot E,
821 Ließ M, Garcia-Franco N, Wollschläger U, Vogel HJ, Kögel-Knabner I (2019) Soil organic carbon
822 storage as a key function of soils - A review of drivers and indicators at various scales. *Geoderma*
823 333: 149-162,
- 824 Žifc'áková L, Ve'trovský T, Howe A, Baldrian P (2016) Microbial activity in forest soil reflects the
825 changes in ecosystem properties between summer and winter. *Env Microbiol* 18: 288-301
- 826
- 827

828 FIGURES AND TABLES

829 **Table 1:** Plant root traits and microbial activity for the 12 herbaceous species. Mean data are also given for species from Fabaceae and Poaceae families.

830

Family Species Acronym code	Fabaceae					Poaceae					Rosaceae	Plantaginaceae	Effect of species (ANOVA)			Fabaceae	Poaceae	Effect of families (ANOVA)		
	<i>Lotus corniculatus</i> Lc	<i>Trifolium repens</i> Tr	<i>Trifolium pratense</i> Tp	<i>Onobrychis viciifolia</i> Ov	<i>Medicago sativa</i> Ms	<i>Bromus erectus</i> Be	<i>Festuca rubra</i> Fr	<i>Dactylis glomerata</i> Dg	<i>Poa pratense</i> Pp	<i>Lolium perenne</i> Lp	<i>Sanguisorba minor</i> Sm	<i>Plantago lanceolata</i> Pl	Df	F	p			Df	F	p
RERTOT (mm d ⁻¹)	0.55±1.1 (a)	0.75±1.5 (a)	0.59±1 (a)	0.53±10 (a)	0.57±0.9 (a)	0.42±0.6 (a)	0.23±0.50 (a)	0.58±0.9 (a)	0.66±2.90 (a)	0.42±0.8 (a)	0.39±0.5 (a)	0.5±0.7 (a)	11,175	18.9	0.06 ¹	0.57±0.08	0.42±0.13	2,9	1.8	0.22
REROLD (mm d ⁻¹)	0.17±0.07 (a)	0.2±0.08 (a)	0.4±0.11 (a)	0.21±0.05 (a)	0.26±0.08 (a)	0.12±0.03 (a)	0.09±0.04 (a)	0.14±0.06 (a)	0.05±0.02 (a)	0.11±0.04 (a)	0.13±0.04 (a)	0.16±0.04 (a)	11,178	17.9	0.08 ¹	0.25±0.09	0.13±0.03	2,9	6.3	0.02
RERNEW (mm d ⁻¹)	0.99±0.27 (a)	0.91±0.21 (a)	0.73±0.15 (a)	0.81±0.16 (a)	0.97±0.12 (a)	1.06±0.29 (a)	0.32±0.08 (a)	1.13±0.25 (a)	0.96±0.31 (a)	0.67±0.11 (a)	0.66±0.08	0.76±0.11	11,178	17.4	0.1 ¹	0.88±0.11	0.79±0.33	2,9	0.37	0.7
RLP_{TOT} (m)	3.03	3.26	3.36	3.62	3.61	2.55	1.19	2.76	2.16	2.95	2.31	3.04	-	-	-	3.37±2.32	2.32±0.7	2,9	5.17	0.03
RLP_{OLD} (m)	4.51	4.91	4.26	4.96	5.23	3.47	1.05	3.30	2.76	4.29	3.32	4.50	-	-	-	1.33±0.61	0.61±0.2	2,9	7.5	0.01
RLP_{NEW} (m)	0.89	1.05	1.78	1.35	1.60	0.78	0.53	0.81	0.32	0.62	0.47	0.99	-	-	-	4.78±2.97	2.97±1.21	2,9	5.12	0.03
Root biomass (g)	1.53±2.6 (bc)	0.55±1.13 (c)	2.01±0.62 (b)	2.06±1.1 (b)	4.23±0.42 (a)	0.65±0.08 (c)	0.70±1.6 (c)	0.58±0.51 (c)	0.60±0.83 (c)	0.57±0.57 (c)	0.91±2.13 (c)	0.49±0.60 (c)	11,24	27.3	<0.001	2.08±1.33	0.62±0.11	1,28	10.9	<0.001 ¹
Diametre absorptive roots (mm)	0.47±0.05 (b)	0.28±0.05 (de)	0.32±0.04 (cd)	0.55±0.18 (a)	0.35±0.18 (c)	0.27±0.02 (def)	0.22±0.05 (fg)	0.21±0.14 (g)	0.22±0.19 (g)	0.22±0.05 (fg)	0.26±0.09 (efg)	0.28±0.14 (de)	11,23	98.7	<0.001	0.39±0.11	0.23±0.03	1,27	31.7	<0.001
Hemicell. +H₂O soluble compounds (mg g ⁻¹)	779.5±58.1 (a)	612±8.3 (bcde)	674.5±44.6 (abc)	704.1±78.8 (ab)	755.1±31 (a)	533.9±12.1 (de)	572.3±27.3 (cde)	530.4±57.6 (de)	562.4±31.2 (cde)	520.5±31.7 (e)	703.2±NA (ab)	639.4±12.7 (bcd)	11,21	17.4	<0.001	705.11±74.39	543.51±33.56	1,25	51.5	<0.001
Cellulose (mg g ⁻¹)	101.6±6.3 (a)	163.2±8.7 (a)	102.5±17.7 (a)	120±69.3 (a)	123.9±27.7 (a)	177.9±76.5 (a)	160.7±44.8 (a)	137.5±7.7 (a)	89.1±6 (a)	181.6±32.3 (a)	140±NA (a)	151.2±54 (a)	11,21	1.7	0.13	122.39±33.61	154.89±50.8	1,25	3.9	0.06
Lignine (mg g ⁻¹)	118.9±57.8 (c)	224.8±0.4 (abc)	223±33.7 (abc)	175.9±9.4 (abc)	120.9±3.5 (c)	288.3±88.5 (ab)	267±39.5 (ab)	332.1±65.3 (a)	348.4±25.1 (a)	297.9±62.1 (ab)	156.8±NA (bc)	209.3±66.7 (abc)	11,21	6.7	<0.001	172.5±56.53	301.6±59.02	1,25	33.7	<0.001
C:N ratio	15.4±0.8 (c)	21.2±1.1 (c)	17.6±3.20 (c)	20.5±3.2 (c)	21.4±2 (c)	50.8±7.6 (b)	61.3±2.6 (ab)	62.5±6.4 (ab)	59.1±4.1 (ab)	61±4.4 (ab)	69.8±3.2 (a)	68.9±3.1 (a)	11,21	96.4	<0.001	19.15±3.07	58.67±6.34	1,25	436	<0.001
SIR (µg C-CO ₂ g ⁻¹ soil h ⁻¹)	5.37±0.46 (ab)	4.43±0.48 (bc)	6.11±0.35 (a)	4.07±0.18 (bcd)	6.41±0.56 (a)	2.47±0.34 (d)	3.22±0.11 (cd)	3.58±0.28 (cd)	3.15±0.15 (cd)	3.17±0.1 (cd)	3.16±0.23 (cd)	2.99±0.11 (cd)	9,20	16	<0.001	5.28±1	3.12±0.4	1,28	45.9	<0.001

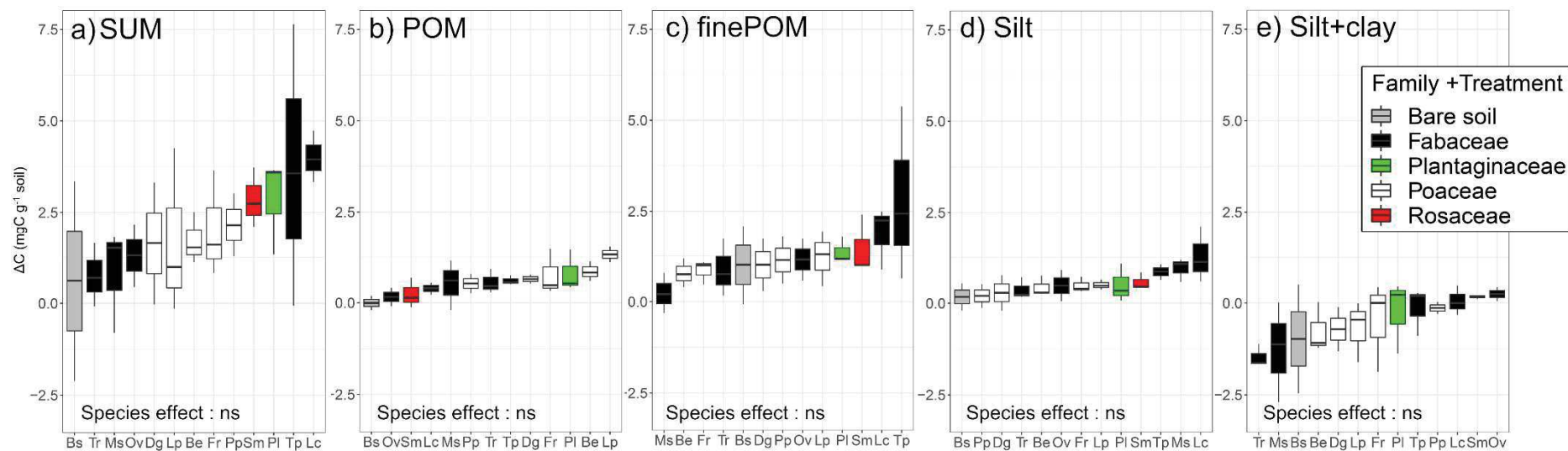
831 ¹ Distribution not normal, Kruskal-Wallis test instead of ANOVA

832 Mean data ± standard deviation are given for species from N₂-fixing Fabaceae , N₂-fixing Poaceae families, and N₂-fixing species aggregated (Poaceae
833 species, *P. lanceolata* and *S. minor*). For each species and for N₂-fixing Fabaceae , N₂-fixing Poaceae families, and N₂-fixing species aggregated, mean and
834 standard deviation are given. Abbreviations: RER_{TOT} – root elongation rate of the entire root system; RER_{OLD} – of old roots older than 2 weeks; RER_{NEW} – of

835 new roots younger than 2 weeks; RLP_{TOT} root length production of the entire root system; RLP_{OLD} – of old roots; RLP_{NEW} – of new roots; Root biomass –
836 total root biomass of a core sampled after 37 weeks; Diameter absorptive – mean diameter of absorptive roots after 37 weeks; Hemicell. + H₂O –
837 concentration of hemicelluloses and water soluble compounds in absorptive roots; Cellulose, Lignin – concentrations of cellulose and lignin in absorptive
838 roots; C:N – ratio of carbon and nitrogen in absorptive roots; SIR – microbial substrate induced respiration. Different letters next to the average value
839 indicate statistically significant differences ($p < 0.05$) between species or families according to Tukey HSD tests. DF – degree of freedom (number of species
840 - 1, number of observations). Statistically significant values ($p < 0.05$) are indicated in bold text.

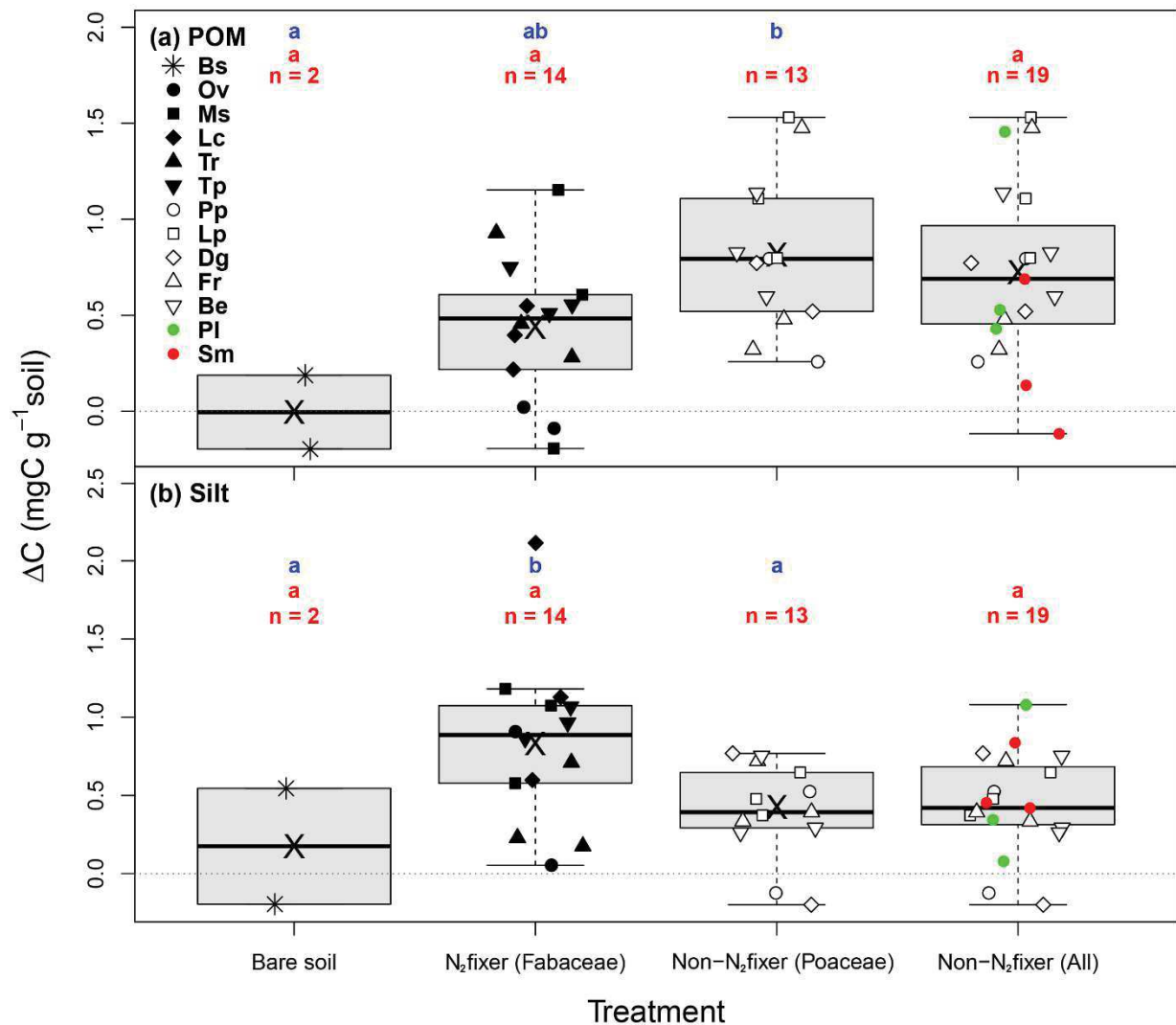
841 .

842



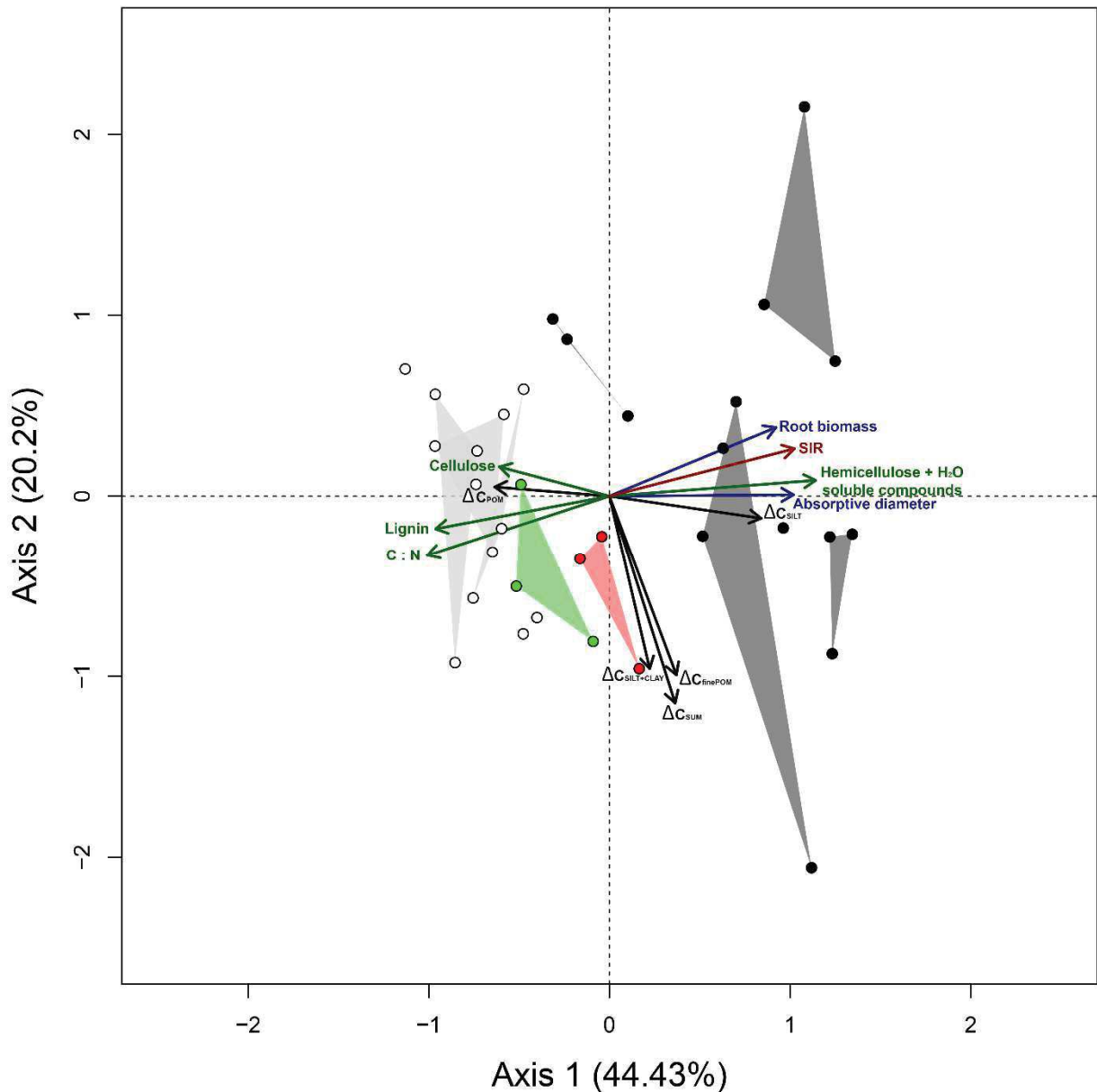
843

844 **Fig.1:** Comparison of the difference ($\Delta C = C_{t37} - C_{t0}$) in carbon (C) after 37 weeks between different soil fractions for each species. a) total C (ΔC_{SUM}), b) C in
 845 the coarse POM fraction (ΔC_{POM}), c) C in the fine POM fraction ($\Delta C_{finePOM}$), d) C in the coarse silt fraction (ΔC_{SILT}) and e) C in the fine silt+clay fraction
 846 ($\Delta C_{SILT+CLAY}$). In each boxplot, the lower edge of the box corresponds to the 25th percentile data point, while the top edge of the box corresponds to the 75th
 847 percentile data point. The line within the box represents the median.



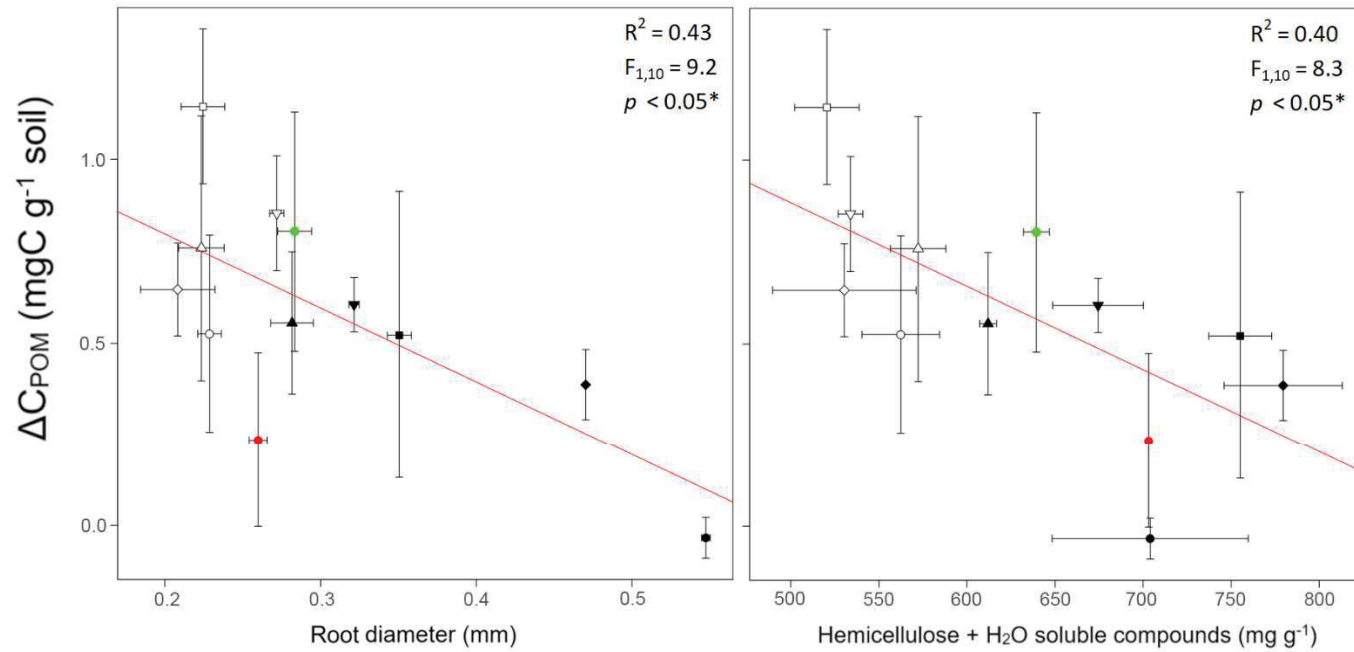
848

849 **Fig.2:** Comparison of the difference ($\Delta C = C_{t37} - C_{t0}$) in carbon (C) after 37 weeks among N_2 -fixing Fabaceae,
 850 non N_2 -fixing Poaceae species only and non N_2 -fixing species aggregated (Poaceae, *P. lanceolate*, *S.*
 851 *Minor*), and control. a) C in the coarse POM fraction (ΔC_{POM}) and b) C in the silt fraction (ΔC_{silt}). No
 852 significant differences were found in total C (ΔC_{SUM}), C in the fine POM fraction ($\Delta C_{finePOM}$), or in C in the
 853 silt+clay fraction ($\Delta C_{silt+clay}$). In each boxplot, the lower edge of the box corresponds to the 25th percentile
 854 data point, while the top edge of the box corresponds to the 75th percentile data point. The line within
 855 the box represents the median and black dots indicate outliers. Different letters above the boxplots
 856 indicate statistically significant differences ($p < 0.05$) among families and control according to a Tukey
 857 HSD test. The blue letters refer to the Tukey HSD test performed between control, N_2 -fixing Fabaceae
 858 species and N_2 -fixing Poaceae species only, while the red letters refer to the Tukey HSD test performed
 859 between control, N_2 -fixing Fabaceae species and N_2 -fixing species aggregated together. Note the
 860 graduation differences in y-axis between a) and b).



861

862 **Fig.3:** Principal Component Analysis of six soil variables (five carbon pool changes and SIR) and six root
 863 variables measured on 12 species. Black dots are Fabaceae, white dots are Poaceae, red dots are
 864 *Sanguisorba minor*, and green dots are *Plantago lanceolata*. The Hull polygons unify the different
 865 replicates for the same species. Abbreviations: SIR – microbial substrate induced respiration;
 866 Hemicelluloses + H₂O – concentration of hemicelluloses and water soluble compounds in absorptive
 867 roots, cellulose, lignin – concentrations of cellulose and lignin in absorptive roots; C:N – ratio of carbon
 868 and nitrogen in absorptive roots; ΔC_{POM} – difference ($\Delta C = C_{t37} - C_{t0}$) in carbon (C) after 37 weeks for the
 869 coarse POM C pool; $\Delta C_{finePOM}$ – for the fine POM C pool; ΔC_{SILT} – for the silt C pool; $\Delta C_{SILT+CLAY}$ – for the silt
 870 + clay f C pool; ΔC_{SUM} – sum of different fractions, ΔC as the total change in C concentration in soil.



Fabaceae

- ◆ *L. corniculatus*
- *O. viciifolia*
- *M. sativa*
- ▼ *T. pratense*
- ▲ *T. repens*

Poaceae

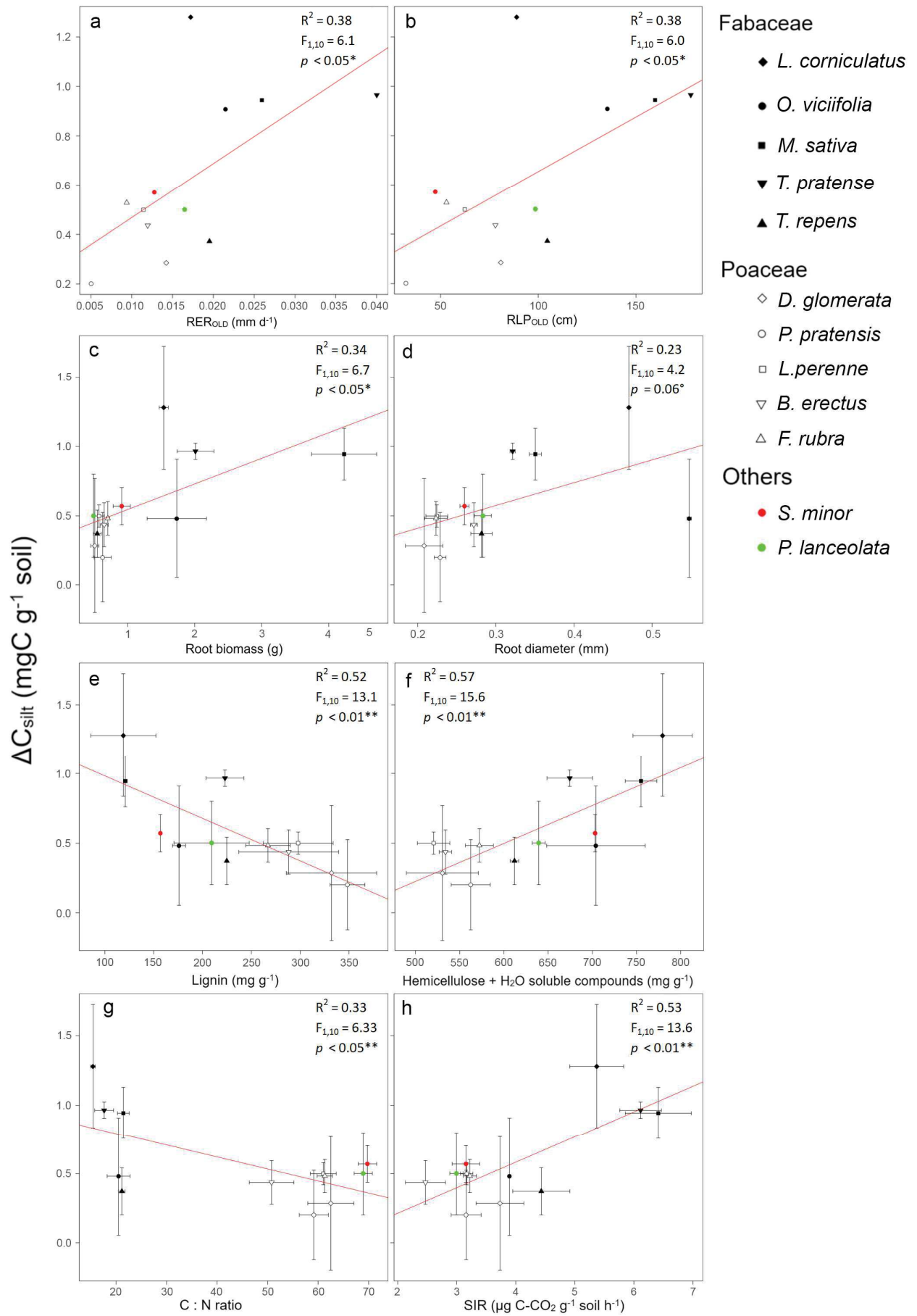
- ◇ *D. glomerata*
- *P. pratensis*
- *L. perenne*
- ▽ *B. erectus*
- △ *F. rubra*

Others

- *S. minor*
- *P. lanceolata*

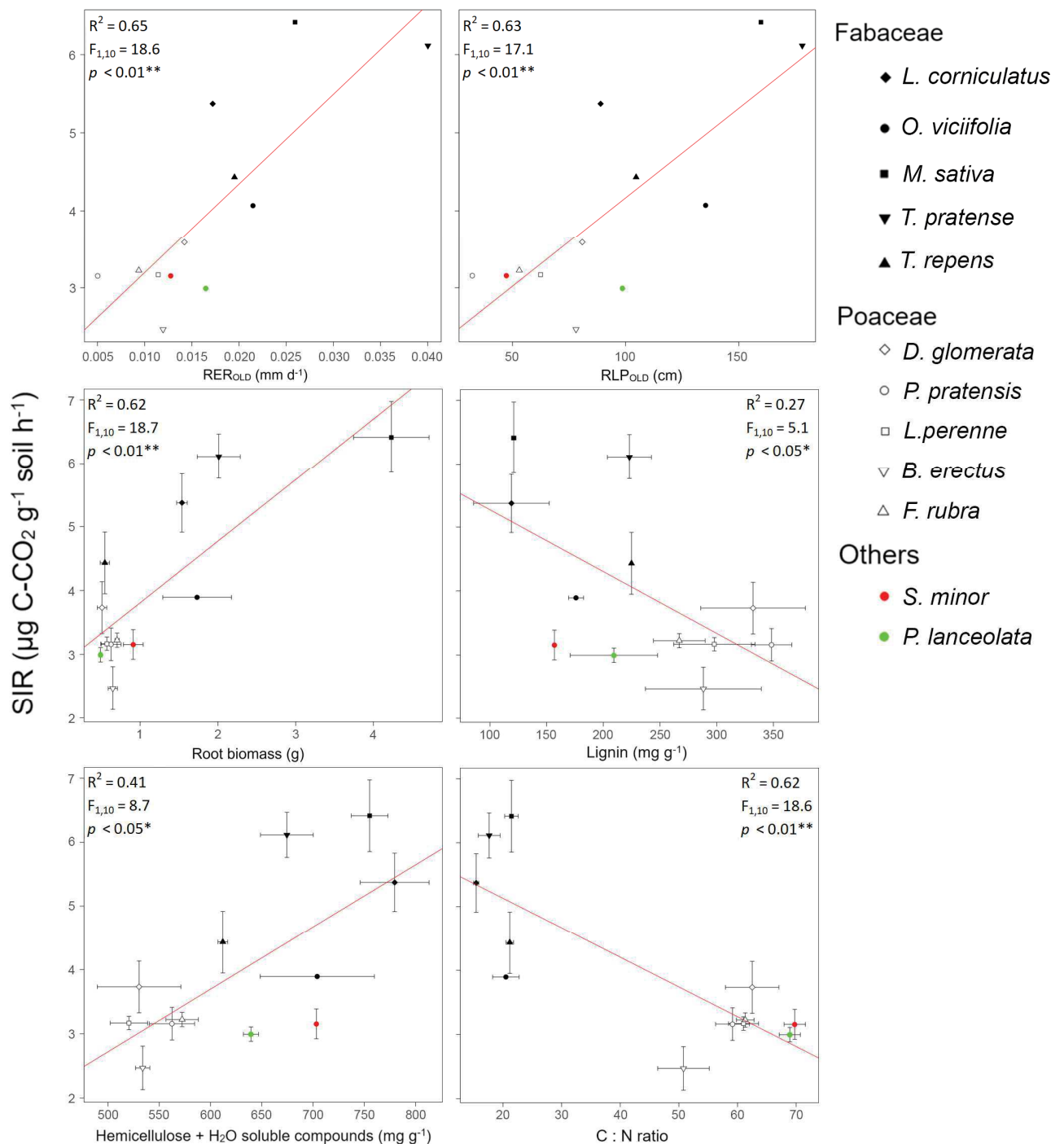
871

872 **Fig. 4:** Linear regression at species level (n=12) between ΔC_{POM} as the difference ($\Delta C = C_{t37} - C_{t0}$) in carbon (C) after 37 weeks for the coarse POM C pool and a)
 873 diameter of absorptive roots and b) hemicelluloses + water soluble compounds. The black symbols are the N₂-fixing Fabaceae species, the white symbols the
 874 non N₂-fixing Poaceae species, the red dots are *S. minor* and the green dots are *P. lanceolata*. The red line is the linear model function of the variables and R²,
 875 F and p of the linear model are shown.



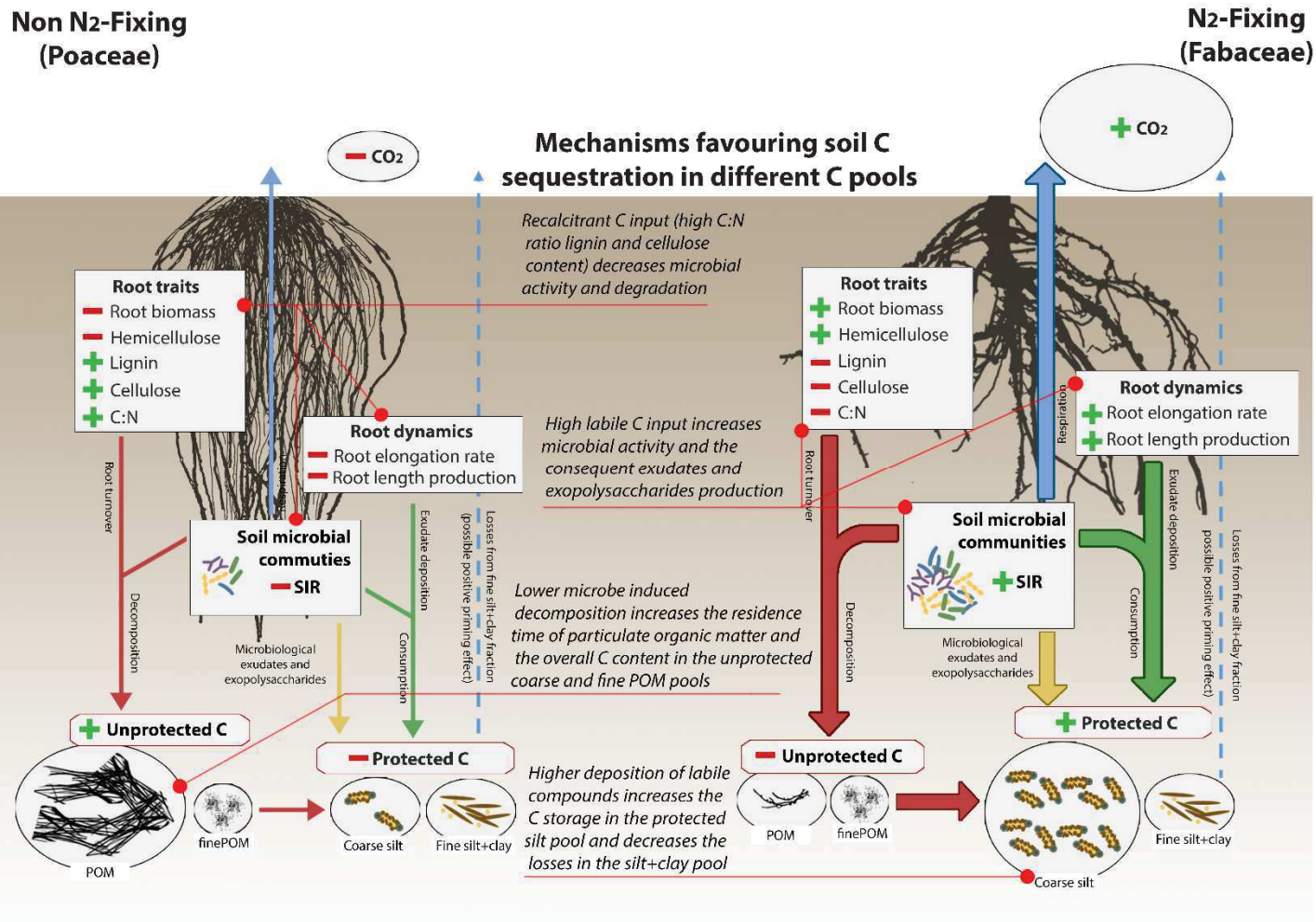
877 **Fig. 5:** Linear regression at species level (n=12) between ΔC_{silt} as difference ($\Delta C = C_{t37} - C_{t0}$) in carbon (C)
878 after 37 weeks for the coarse silt C pool and a) root elongation rate of old roots (RER_{OLD}), b) root length
879 production of old roots (RLP_{OLD}), c) root biomass, d) diameter of absorptive roots, e) lignin content, f)
880 hemicelluloses + water soluble compounds, g) C:N ratio and h) substrate induced respiration rate (SIR).
881 The black symbols are the N₂-fixing Fabaceae species, the white symbols the non N₂-fixing Poaceae
882 species, the red dots are *S. minor* and the green dots are *P. lanceolata*. The red line is the linear model
883 function of the variables and R², F and p of the linear model are shown.

884



885

886 **Fig. 6:** Linear regression at species level ($n=12$) between substrate induced respiration rate (SIR) and a
 887 root elongation rate of old roots (RER_{OLD}), b) root length production of old roots (RLP_{OLD}), c) root biomass,
 888 d) lignin content, e) hemicelluloses + water soluble compounds, f) C:N ratio. The black symbols are the
 889 N_2 -fixing Fabaceae species, the white symbols the non N_2 -fixing Poaceae species, the red dots *S. minor*
 890 and the green dots *P. lanceolata*. The red line is the linear model function of the variables and R^2 , F and
 891 p of the linear model are shown.



892

893 **Fig.7:** Conceptual scheme of carbon (C) sequestration mechanisms into different soil pools under N₂-fixing (Fabaceae) and non N₂-fixing (Poaceae) species.
 894 Square boxes refer to the major factors affecting C sequestration. Ellipses show the destination of C into unprotected pools (POM and finePOM) and protected
 895 pools (coarse silt and fine silt+clay). Text in the central column describes the mechanisms favoring C sequestration into soil C pools. The arrows symbolize the
 896 processes of transformation or transport of C into different pools. Arrow colors represent the nature of the C: red C derived from root turnover, green C from
 897 rhizodeposition, yellow C from microbial exudates and exopolysaccharides and blue the C respired back into the atmosphere as CO₂. The thickness of the
 898 arrows is qualitative, with wider arrows reflecting higher C fluxes. The signs: “+” (in green) means an increase and “-” (in red) means a decrease

899 **Supplementary Materials**

900 **Article: Pathways to persistence: plant root traits alter carbon accumulation in different soil carbon**
901 **pools**

902 Lorenzo M.W. Rossi^{a,b}, Zhun Mao^a, Luis Merino-Martín^{a,c}, Catherine Roumet^c, Florian Fort^d, Olivier
903 Taugourdeau^e, Hassan Boukcim^e, Stéphane Fourtier^a, Maria Del Rey-Granado^c, Tiphaine Chevallier^f,
904 Rémi Cardinael^{g,h,i}, Nathalie Fromin^c, Alexia Stokes^a

905

906 Contact author: Lorenzo MW Rossi

907 [Email: lmw.rossi@gmail.com](mailto:lmw.rossi@gmail.com)

908 Address: AMAP, INRAE Montpellier, PS2 TA/A51, 34 398 Montpellier cedex 5, France

909

910 j) Univ Montpellier, AMAP, INRAE, CIRAD, CNRS, IRD, Montpellier, France.

911 k) University of Cassino, Via Di Biasio 43, 03043 Cassino (Fr), Italy.

912 l) Univ Montpellier, CEFÉ, CNRS, EPHE, IRD, Univ Paul Valéry Montpellier 3, Montpellier, France.

913 m) Univ Montpellier, CEFÉ, Montpellier SupAgro, CNRS, EPHE, IRD, Univ Paul Valéry Montpellier 3,
914 Montpellier, France.

915 n) Valorhiz, 1900, Boulevard de la Lironde PSIII, Parc Scientifique Agropolis F-34980 Montferrier sur
916 Lez, France.

917 o) Univ Montpellier, Eco&Sols, IRD, CIRAD, INRA, Montpellier SupAgro, Montpellier, France Eco&sols

918 p) CIRAD, UPR AIDA, Harare, Zimbabwe.

919 q) Univ Montpellier, AIDA, CIRAD, Montpellier, France.

920 r) University of Zimbabwe, Crop Science Department, Box MP167, Mt. Pleasant, Harare, Zimbabwe.

921

922 **Table S1:** Pearson's correlation coefficients (r) showing relationships between mean root elongation rate and climatic variables.

923 Variables tested include: mean daily soil temperature, mean daily air temperature, minimum daily air temperature, maximum daily air temperature, mean
 924 daily solar radiation and a) RER_{TOT}: mean root elongation rate of a single root, b) RER_{OLD}: mean root elongation rate of a single root that was already present
 925 at the previous sampling date (i.e. that were older than 14 days), c) RER_{NEW}: mean root elongation rate of a single newly initiated root (i.e. that were aged 1
 926 to 14 days). The correlations were performed for data from each RER sampling date, i.e. every 2 weeks for each species over the 10 month period.

a - Correlation between climate factors and RER _{TOT} of the total root system							b - Correlation between climate factors and RER _{OLD} of the old roots						
		Soil temperature	Mean air temperature	Minimum air temperature	Maximum air temperature	Mean solar radiation	Family	Species	Soil temperature	Mean air temperature	Minimum air temperature	Maximum air temperature	Mean solar radiation
Poaceae	<i>Dactylis glomerata</i>	-0.23	-0.21	-0.1	-0.18	-0.1	Poaceae	<i>Dactylis glomerata</i>	-0.27	-0.26	-0.17	-0.22	-0.12
	<i>Lolium perenne</i>	0.01	-0.04	-0.03	0.09	0.38		<i>Lolium perenne</i>	0.14	0.13	0.31	0.09	0.21
	<i>Festuca rubra</i>	-0.21	-0.27	-0.34	-0.2	0.15		<i>Festuca rubra</i>	-0.25	-0.3	-0.41	-0.25	0.05
	<i>Bromus erectus</i>	-0.02	-0.05	-0.01	0.02	0.29		<i>Bromus erectus</i>	0.17	0.28	-0.07	0.2	0.29
	<i>Poa pratensis</i>	0.1	0.08	0.34	0.1	0.43		<i>Poa pratensis</i>	-0.03	0	0.4	0.04	0.21
Fabaceae	<i>Trifolium repens</i>	0.76***	0.81***	0.45	0.68**	0.33	Fabaceae	<i>Trifolium repens</i>	0.28	0.28	0.15	0.4	0.45
	<i>Trifolium pratense</i>	0.02	-0.02	-0.02	0.09	0.4		<i>Trifolium pratense</i>	0.18	0.25	-0.07	0.24	0.38
	<i>Lotus corniculatus</i>	0.70**	0.70**	0.44	0.68**	0.72**		<i>Lotus corniculatus</i>	0.73**	0.71**	0.51	0.74**	0.89***
	<i>Onobrychis viciifolia</i>	0.13	0.09	0.3	0.17	0.54*		<i>Onobrychis viciifolia</i>	0.04	0.02	0.26	0.07	0.36
	<i>Medicago sativa</i>	0.01	0.01	-0.05	0.02	0.22		<i>Medicago sativa</i>	0.03	0.01	-0.05	0.03	0.23
Rosaceae	<i>Sanguisorba minor</i>	-0.06	-0.06	-0.06	-0.04	0.16	Rosaceae	<i>Sanguisorba minor</i>	0.13	0.2	-0.08	0.1	-0.33
Plantaginaceae	<i>Plantago lanceolata</i>	0	-0.04	0	0.04	0.3	Plantaginaceae	<i>Plantago lanceolata</i>	-0.05	-0.07	-0.05	-0.03	0.21

c - Correlation between climate factors and RER _{NEW} of new roots						
		Soil temperature	Mean air temperature	Minimum air temperature	Maximum air temperature	Mean solar radiation
Poaceae	<i>Dactylis glomerata</i>	-0.55*	-0.54*	-0.47	-0.60*	-0.66**
	<i>Lolium perenne</i>	0.03	0	-0.05	0.1	0.29
	<i>Festuca rubra</i>	-0.11	-0.16	-0.04	-0.15	0.26
	<i>Bromus erectus</i>	-0.06	-0.07	-0.08	-0.05	0.17
	<i>Poa pratensis</i>	0.09	0.08	0.36	0.06	0.38
Fabaceae	<i>Trifolium repens</i>	0.59*	0.67**	0.17	0.57*	0.17
	<i>Trifolium pratense</i>	0.11	0.1	0.37	0.08	0.41
	<i>Lotus corniculatus</i>	0.76***	0.75**	0.48	0.76***	0.76**
	<i>Onobrychis viciifolia</i>	0.13	0.1	0.3	0.15	0.51
	<i>Medicago sativa</i>	0.04	0.06	-0.35	0.04	0.21
Rosaceae	<i>Sanguisorba minor</i>	0.09	0.16	0.04	0.06	-0.05
Plantaginaceae	<i>Plantago lanceolata</i>	-0.05	-0.06	-0.06	-0.03	0.19

927

928

929 **Table S2:** Pearson's correlation coefficients (r) showing relationships between cumulative root length production and climatic variables.

930 Variables tested include: mean daily soil temperature, mean daily air temperature, minimum daily air temperature, maximum daily air temperature, mean
 931 daily solar radiation and a) RLP_{TOT}: cumulative root length production of the 30 roots that were analysed, b) RLP_{OLD}: cumulative root length production of roots
 932 that were already present at the previous sampling date (i.e. that were older than 14 days), c) RLP_{NEW}: cumulative root length production of newly initiated
 933 roots (i.e. that were aged 1 to 14 days). The correlations were performed for data from each RLP sampling date, i.e. every 2 weeks for each species over the
 934 10 month period.

a - Correlation between climate factors and RLP _{TOT} of the total root system						
		Soil temperature	Mean air temperature	Minimum air temperature	Maximum air temperature	Average solar radiation
Poaceae	<i>Dactylis glomerata</i>	-0.4	-0.41	-0.46	-0.45	-0.38
	<i>Lolium perenne</i>	-0.02	-0.05	-0.08	0.04	0.29
	<i>Festuca rubra</i>	-0.19	-0.25	-0.32	-0.18	0.18
	<i>Bromus erectus</i>	-0.01	-0.05	0.01	0.03	0.31
	<i>Poa pratensis</i>	0.12	0.09	0.35	0.12	0.46
Fabaceae	<i>Trifolium repens</i>	0.36	0.37	-0.01	0.33	0.38
	<i>Trifolium pratense</i>	0.03	0	0.03	0.07	0.34
	<i>Lotus corniculatus</i>	0.72**	0.72**	0.46	0.70**	0.74**
	<i>Onobrychis viciifolia</i>	0.13	0.09	0.3	0.17	0.54*
	<i>Medicago sativa</i>	0.01	-0.01	-0.04	0.02	0.24
Rosaceae	<i>Sanguisorba minor</i>	-0.06	-0.07	-0.05	-0.04	0.18
Plantaginaceae	<i>Plantago lanceolata</i>	0	-0.04	0	0.04	0.31

b - Correlation between climate factors and RLP _{OLD} of the old roots						
		Soil temperature	Mean air temperature	Minimum air temperature	Maximum air temperature	Mean solar radiation
Poaceae	<i>Dactylis glomerata</i>	-0.29	-0.34	-0.38	-0.28	0
	<i>Lolium perenne</i>	0	-0.07	-0.02	-0.08	0.24
	<i>Festuca rubra</i>	-0.16	-0.22	-0.31	-0.15	0.19
	<i>Bromus erectus</i>	0.18	0.25	0	0.23	0.38
	<i>Poa pratensis</i>	0.02	0.03	0.4	0.1	0.31
Fabaceae	<i>Trifolium repens</i>	0.28	0.26	0.2	0.41	0.51*
	<i>Trifolium pratense</i>	0.22	0.26	0.02	0.29	0.47
	<i>Lotus corniculatus</i>	0.72**	0.69**	0.52	0.75***	0.90***
	<i>Onobrychis viciifolia</i>	0.06	0.03	0.28	0.1	0.42
	<i>Medicago sativa</i>	0.04	0	0.02	0.08	0.33
Rosaceae	<i>Sanguisorba minor</i>	-0.04	-0.05	-0.06	-0.02	0.18
Plantaginaceae	<i>Plantago lanceolata</i>	0	-0.04	0.02	0.05	0.33

c - Correlation between climate factors and RLP _{NEW} of new roots						
		Soil temperature	Mean air temperature	Minimum air temperature	Maximum air temperature	Mean solar radiation
Poaceae	<i>Dactylis glomerata</i>	-0.52*	-0.51*	-0.51	-0.54*	-0.48
	<i>Lolium perenne</i>	-0.25	-0.3	-0.43	-0.27	0.04
	<i>Festuca rubra</i>	-0.08	-0.14	-0.03	-0.1	0.33
	<i>Bromus erectus</i>	0.01	-0.03	0.01	0.05	0.33
	<i>Poa pratensis</i>	0.13	0.1	0.34	0.12	0.46
Fabaceae	<i>Trifolium repens</i>	0.51*	0.57*	0.11	0.49	0.26
	<i>Trifolium pratense</i>	0.17	0.14	0.36	0.17	0.51*
	<i>Lotus corniculatus</i>	0.69**	0.69**	0.41	0.70**	0.77***
	<i>Onobrychis viciifolia</i>	0.06	0.01	0.02	0.13	0.43
	<i>Medicago sativa</i>	0.03	0.02	-0.03	0.05	0.27
Rosaceae	<i>Sanguisorba minor</i>	0.17	0.14	0.19	0.22	0.46
Plantaginaceae	<i>Plantago lanceolata</i>	0.01	-0.03	0.01	0.05	0.32

935

936 **Table S3:** Pearson's correlation coefficients (*r*) showing relationships between root variables and soil variables. Table S3a) shows the significant correlations
 937 obtained with the means of the three replicates for every soil and root characteristic for a total of n=12. Table S3b) shows the significant Pearson's correlations
 938 obtained using all data where n = 34. Abbreviations: RER_{TOT} – root elongation rate of the entire root system; RER_{OLD} – of roots older than 14 days; RER_{NEW} – of
 939 new roots aged 1 – 14 days; RLP_{TOT} – root length production of the entire root system; RLP_{OLD} – of old roots; RLP_{NEW} – of new roots; Root biomass – total root
 940 biomass of a core sampled at 37 weeks; absorptive root diameter– mean diameter of absorptive roots at 37 weeks; hemicellulose + water soluble compounds
 941 – concentration of hemicellulose and water soluble compounds in absorptive roots; cellulose, lignin – concentrations of cellulose and lignin in absorptive
 942 roots; C:N – ratio of carbon to nitrogen in absorptive roots; SIR – microbial substrate induced respiration.

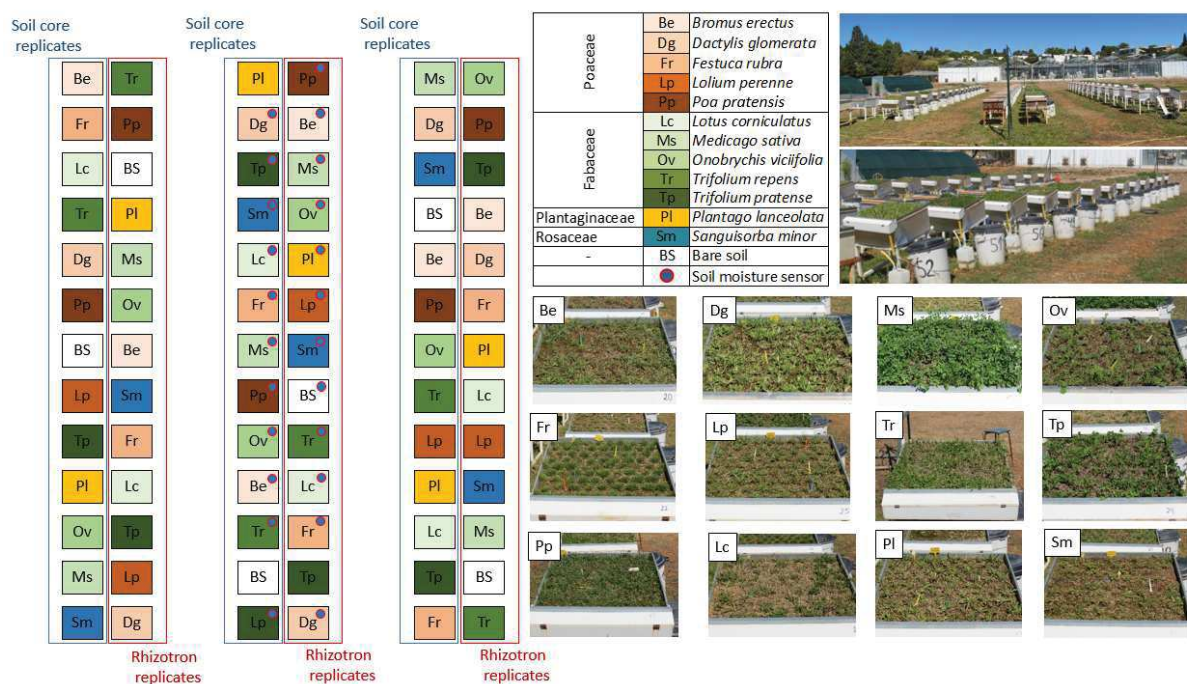
a) Pearson's correlations at species level (n = 12, mean of three replicates)								b) Pearson's correlations at individual level (n = 34)					
		ΔC_{SUM}	ΔC_{POM}	$\Delta C_{finePOM}$	ΔC_{silt}	$\Delta C_{silt+clay}$	SIR	ΔC_{SUM}	ΔC_{POM}	$\Delta C_{finePOM}$	ΔC_{silt}	$\Delta C_{silt+clay}$	SIR
Root growth dynamics	RER _{TOT}	-0.32	-0.2	-0.06	-0.1	-0.17	0.45	-0.32	-0.2	-0.06	-0.1	-0.17	0.45
	RER _{OLD}	-0.17	-0.25	-0.04	0.72**	0.37	0.74**	-0.17	-0.25	-0.04	0.72**	0.37	0.74**
	RER _{NEW}	-0.24	-0.13	-0.2	-0.12	-0.55	0.18	-0.24	-0.13	-0.2	-0.12	-0.55	0.18
	RLP _{TOT}	-0.34	-0.33	-0.18	0.37	0.34	0.51	-0.34	-0.33	-0.18	0.37	0.34	0.51
	RLP _{NEW}	-0.3	-0.3	-0.15	0.33	0.17	0.43	-0.3	-0.3	-0.15	0.33	0.17	0.43
	RLP _{OLD}	-0.32	-0.25	-0.22	0.66*	0.34	0.70*	-0.32	-0.25	-0.22	0.66*	0.34	0.70*
Root morphological traits	Root biomass	-0.2	-0.46	-0.37	0.78**	0.3	0.80**	0.18	-0.08	0.02	0.3	-0.07	0.69***
	Absorptive roots diameter	-0.2	-0.72**	-0.17	0.79**	0.14	0.56	0.08	-0.44*	0.21	0.14	0.36	0.50**
	Hemicelluloses +H ₂ O soluble	-0.06	-0.61*	-0.13	0.82**	-0.3	0.68*	0.26	-0.3	0.25	0.22	0.23	0.60***
Root chemical compounds traits	Cellulose	-0.18	0.47	-0.14	-0.22	0.19	-0.53	-0.24	0.13	-0.16	-0.03	0.18	-0.31
	Lignin	0.15	0.56	0.26	-0.84***	0.49	-0.60*	-0.19	0.18	-0.17	-0.21	-0.26	-0.46**
	Root C:N ratio	0.26	0.37	0.09	-0.68*	0.29	-0.86***	-0.06	0.28	-0.07	-0.3	-0.17	-0.79***
	SIR	-0.16	-0.19	-0.11	0.65*	-0.57		0.27	-0.15	0.18	0.48**	0.12	

943

944 In bold, significant *r* values: * *p* < 0.05, ***p* < 0.01, *** *p* < 0.001

945 **Fig. S1:** Spatial disposition of growth boxes.

946 In left panel, replicates are depicted in different colours according to their family (green: N₂-
 947 fixing Fabaceae, brown: non N₂-fixing Poaceae, yellow: non N₂ fixing *P. lanceolata*, blue: non
 948 N₂-fixing *S. minor*). The different shades of colour representing different species are shown in
 949 the legend. The blue dot on the upper right-hand corner of the different colored squares shows
 950 the boxes that were equipped with air/soil temperature and soil moisture sensors. Soil cores
 951 were removed from each row of ‘soil core replicates’ growth boxes. Half the boxes were fitted
 952 with rhizotrons (‘rhizotron replicates’). Photographs of each species can be seen in the bottom
 953 right panel of the figure.



954

955

956 **Fig. S2:** Growth boxes used in the experiment.

957 Above a gravel layer, soil was homogeneously compacted into growth boxes. Seeds were
958 sown at a density of 155 plants m⁻². Panes of plexiglass on the front of the box allowed root
959 elongation to be observed over the 37 week long experiment.

960

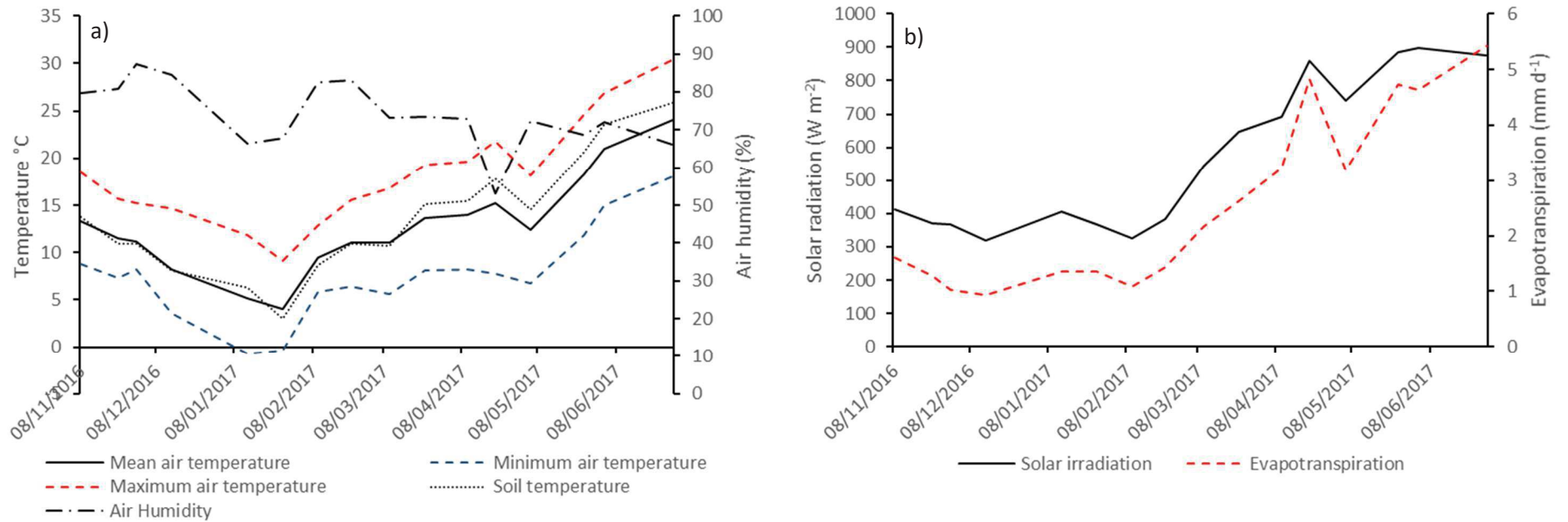


961

962

963 **Fig. S3:** Climatic conditions over the 37 weeks of experimentation.

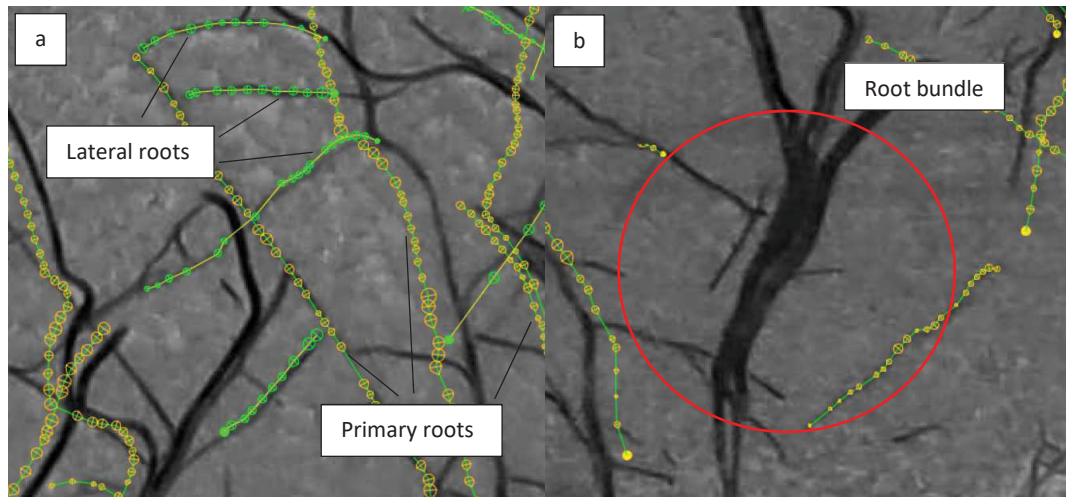
964 a) Mean daily air temperature (solid black line), minimum air temperature (segmented blue line), maximum air temperature (segmented red line),
965 mean daily soil temperature (dotted black line) and mean daily air humidity (segmented black, dotted line). In b), mean daily solar irradiation (solid
966 black line) and evapotranspiration (segmented red line).



967

968 **Fig. S4:** Example of an image analyzed using SmartRoot software.

969 a) primary roots (in orange) from which lateral roots are initiated (in green). Each orange circle along
970 the root axis represents a single 'mouse click' for root selection. b) A bundle of roots growing close
971 together, where the number and diameter of roots cannot be recognized by the SmartRoot software.



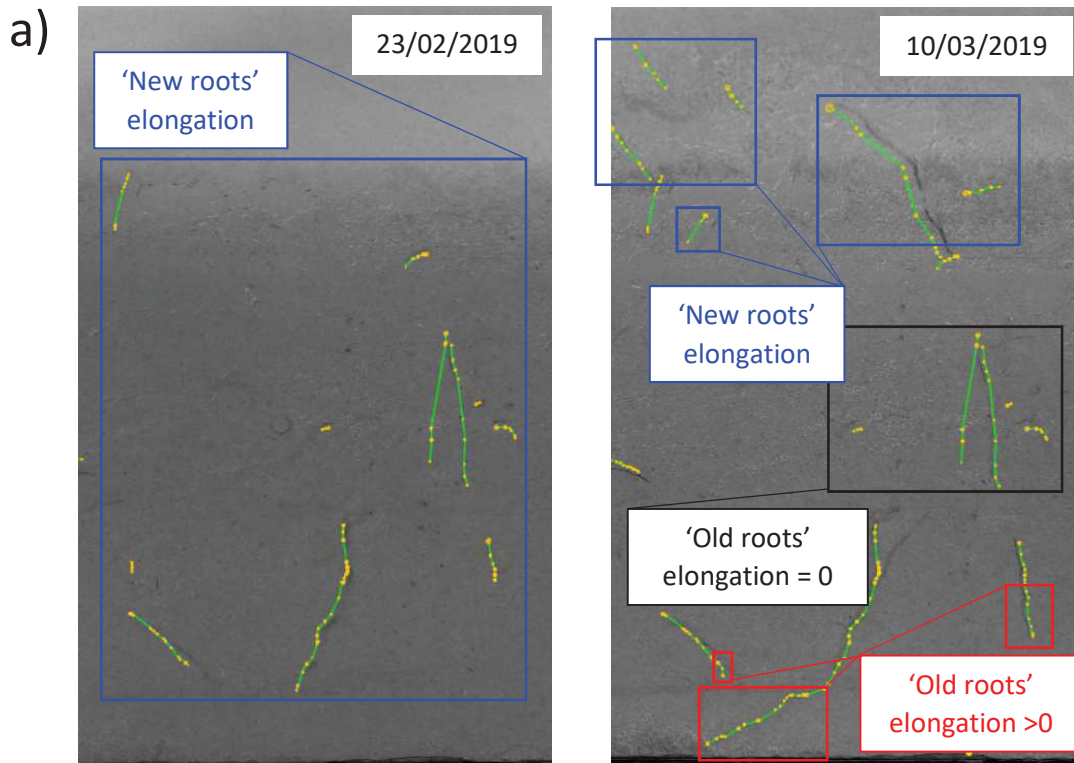
972

973

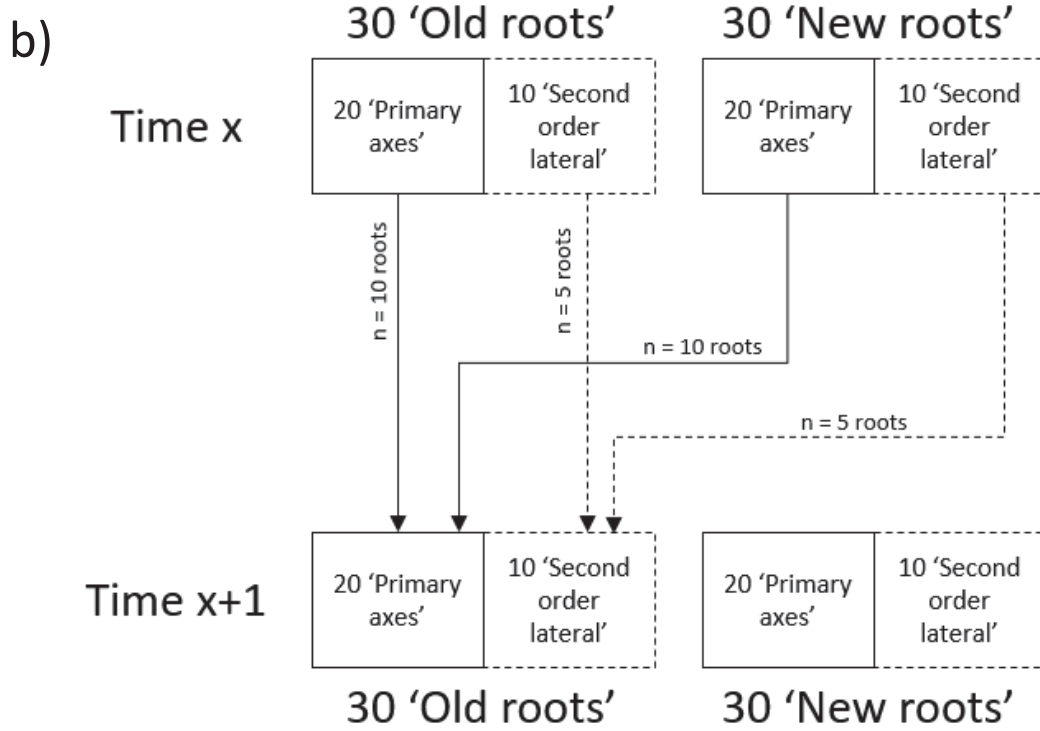
974

975

976 **Fig.S5:** a) Example of two subsequent images of roots of *Bromus erectus* taken on 23/02/2019 and
977 10/03/2019 and b) conceptual scheme to explain root selection procedure.. a) The figure on the left
978 shows newly initiated roots that will be analyzed to calculate the RER_{NEW} and RLP_{NEW} on 23/02/2019.
979 At the next date for image analysis (10/03/2019), some of the previously analyzed roots were the same
980 length ($RER=0$, middle of the rhizotron), whereas other roots elongated ($RER>0$, bottom of the
981 rhizotron), and were used to calculate RER_{OLD} and RLP_{OLD} . On the top part of the rhizotron, some new
982 roots were initiated, and analyzed to calculate the RER_{NEW} and RLP_{NEW} on 10/03/2019. b) Conceptual
983 scheme showing the procedure to select 'old roots' at each sampling: at Time x 30 new roots and 30
984 old roots have been analyzed. Of these 30 roots, 20 are primary axis roots while 10 second order lateral
985 (Fig. S4a). 10 roots from Time x primary old roots and 10 from Time x primary new roots are randomly
986 selected to be analyzed and constitute the Time x+1 old primary roots. 5 roots from Time x secondary
987 old roots and 5 from Time x new secondary roots are selected and analyzed and constitute the Time
988 x+1 secondary old roots.



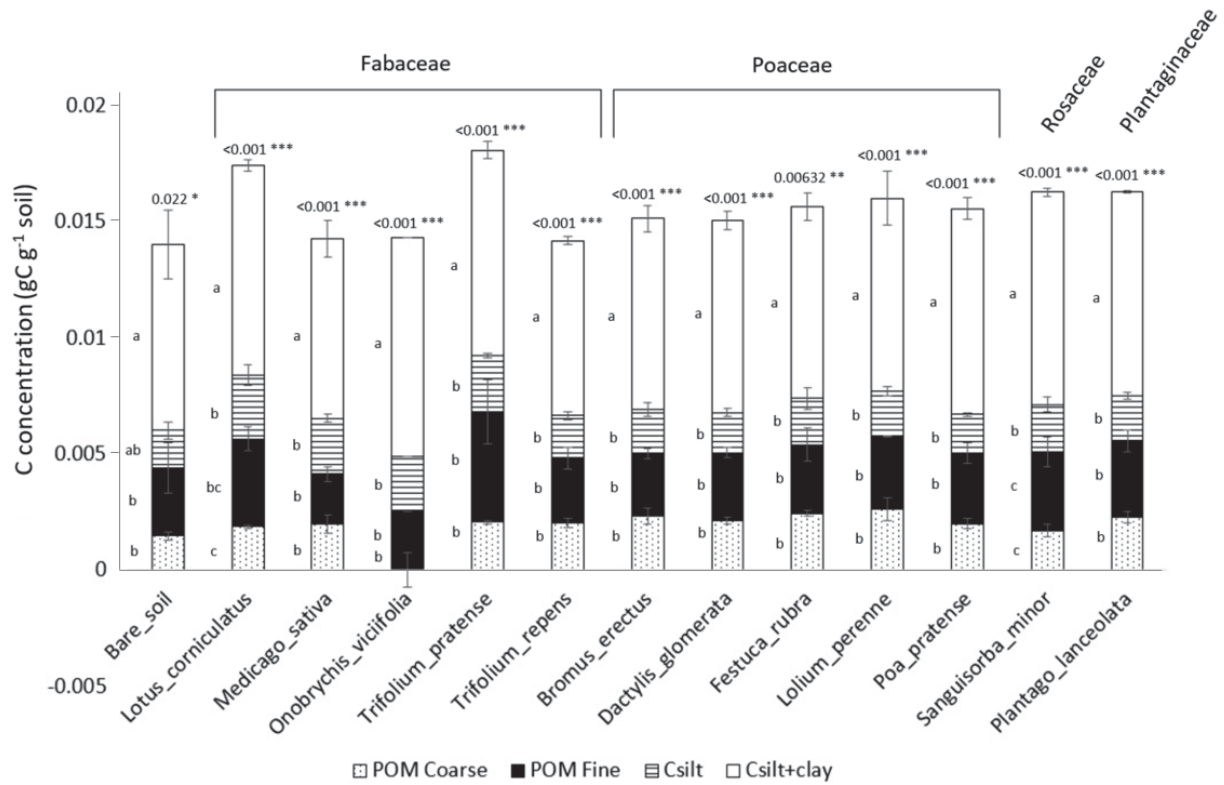
989



990

991 **Fig. S6:** Carbon (C) content in each soil C pool beneath the 12 species and in the control bare soil, 37
 992 weeks after sowing.

993 The C pools analyzed are C_{POM} in the coarse particulate organic matter $>200\mu\text{m}$), C_{finePOM} (C in the fine
 994 particulate organic matter $200\text{-}50\mu\text{m}$), C_{SILT} (in the coarse silt fraction $50\text{-}20\mu\text{m}$) and $C_{\text{SILT+CLAY}}$ (C in the
 995 fine silt + clay fraction $<20\mu\text{m}$). The letters on the left hand side of the fraction bars indicate significant
 996 differences (Tukey HSD, $p < 0.05$) between C pools and within species.

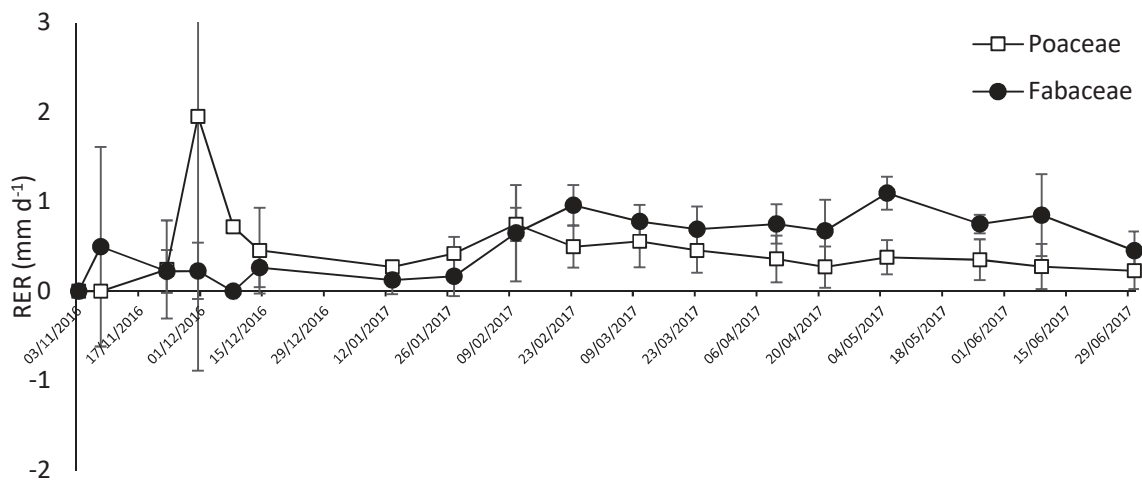


997
 998

999 **Fig. S7:** Mean daily root elongation rate (RER_{TOT}) for all the roots analyzed in the rhizotrons (without
1000 distinguishing between old and new roots) in Fabaceae (N_2 -fixing, black circles) and Poaceae (non N_2 -
1001 fixing, white squares) family.

1002 Mean daily RER_{TOT} in Fabaceae peaked in May - June, whereas in Poaceae, mean daily RER_{TOT} was fairly
1003 constant between February and June, with no marked peaks. Data are means \pm standard error of the RER
1004 data in the 2 weeks prior to the measurement of root elongation.

1005

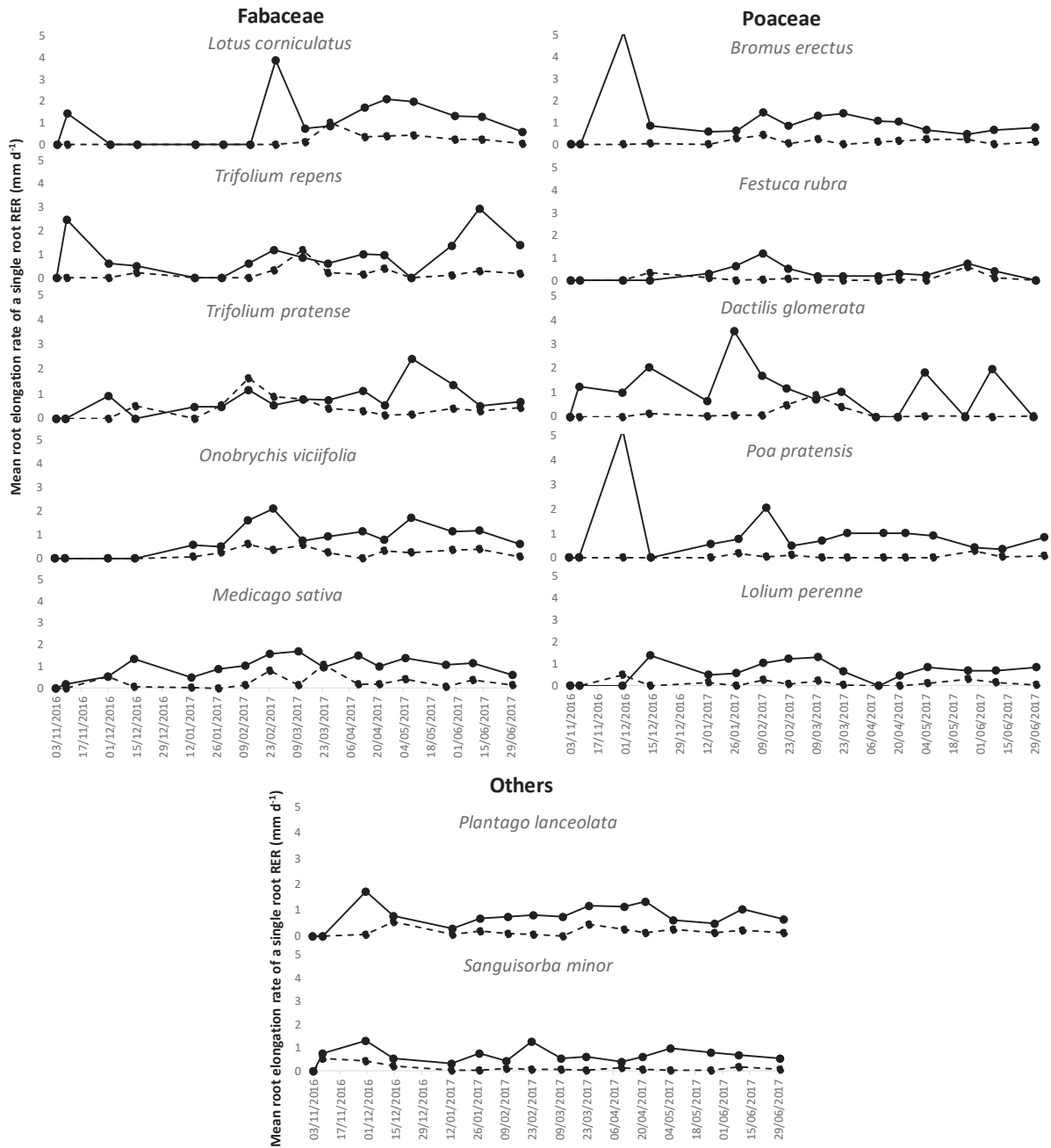


1006

1007

1008 **Fig.S8:** Mean root elongation rate of individual roots (RER, measured every 2 weeks) for each of the 12
 1009 species.

1010 The solid black line is the RER_{NEW} of the roots that were newly initiated (aged 1 to 14 days), and were not
 1011 present at the previous sampling date. The dotted black line represents the RER_{OLD} of the roots that were
 1012 already present at the previous sampling date, and so were older than 14 days.

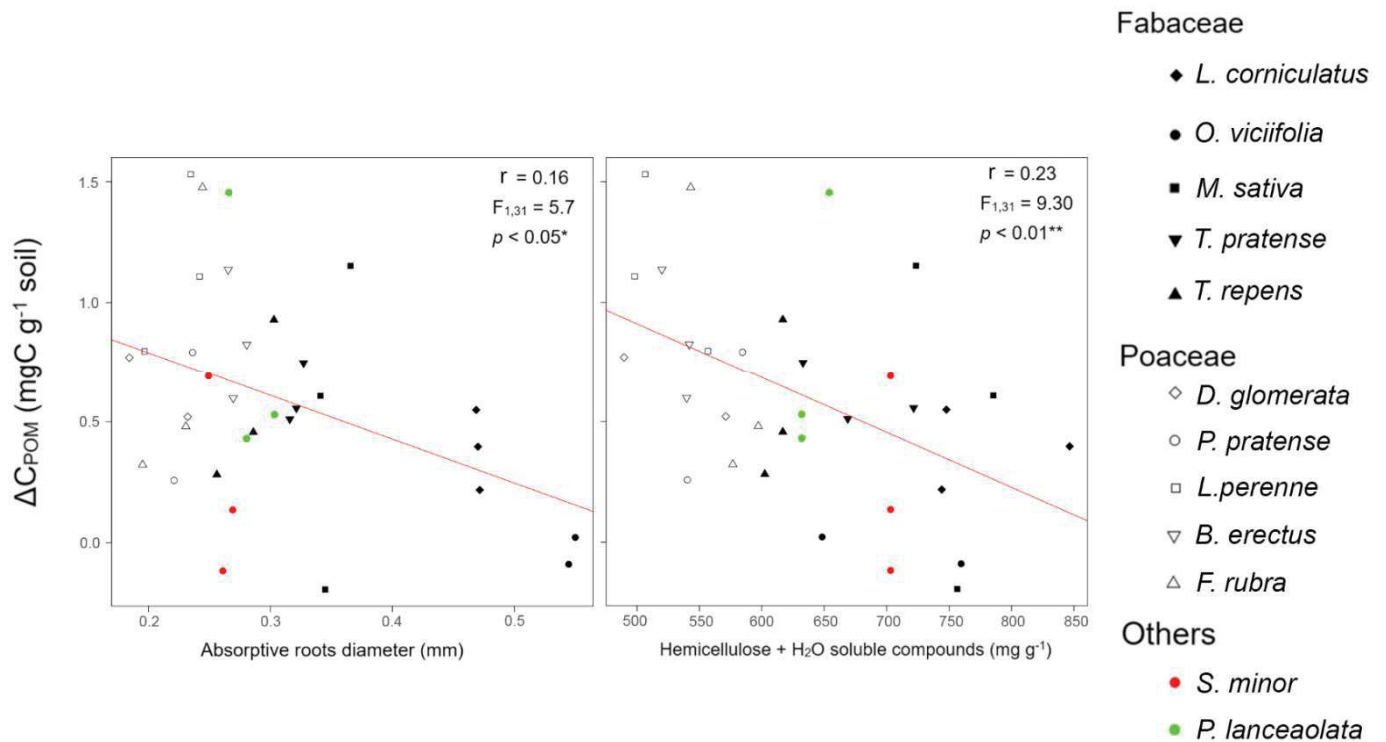


1013

1014 **Fig. S9:** Linear regression at the individual level (n = 34 samples), between ΔC_{POM} (as the difference in
 1015 carbon (C) in the coarse POM C pool, $\Delta C = C_{t37} - C_{t0}$, after 37 weeks), and a) diameter of absorptive
 1016 roots and b) hemicelluloses + water soluble compounds.

1017 The black symbols are the N₂-fixing Fabaceae species, the white symbols the non N₂-fixing Poaceae
 1018 species, the red dots are *S. minor* and the green dots are *P. lanceolata*. The red line is the linear model
 1019 function of the variables and R², F and p of the linear model are shown.

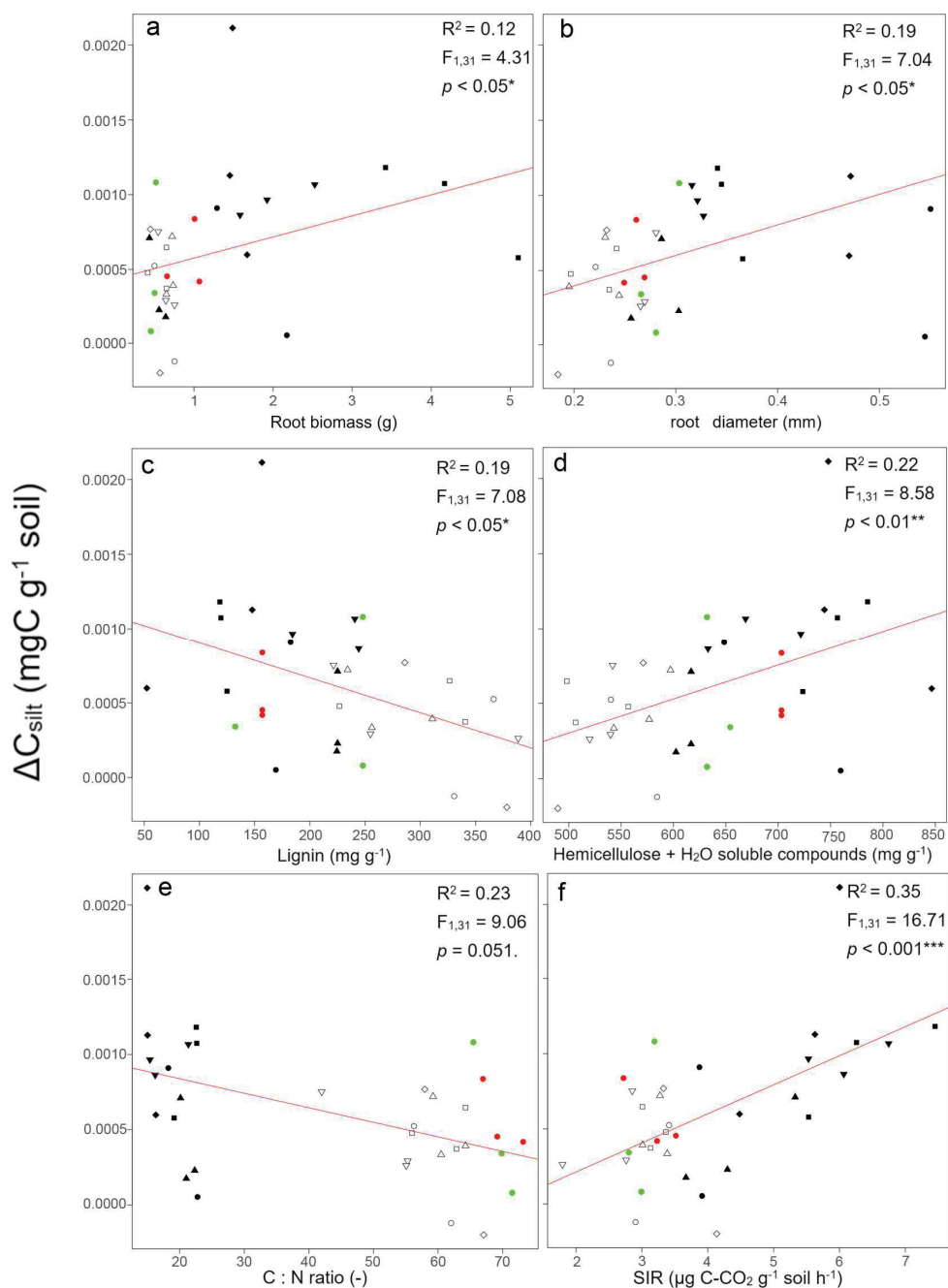
1020



1021

1022 **Fig. S10:** Linear regression at individual level (n = 34 samples) between ΔC_{silt} (as the difference in carbon
 1023 (C) in the coarse silt C pool, $\Delta C = C_{t37} - C_{t0}$, after 37 weeks), and a) root biomass, b) diameter of
 1024 absorptive roots, c) lignin content, d) hemicelluloses + water soluble compounds, e) C:N ratio and f)
 1025 substrate induced respiration rate (SIR).

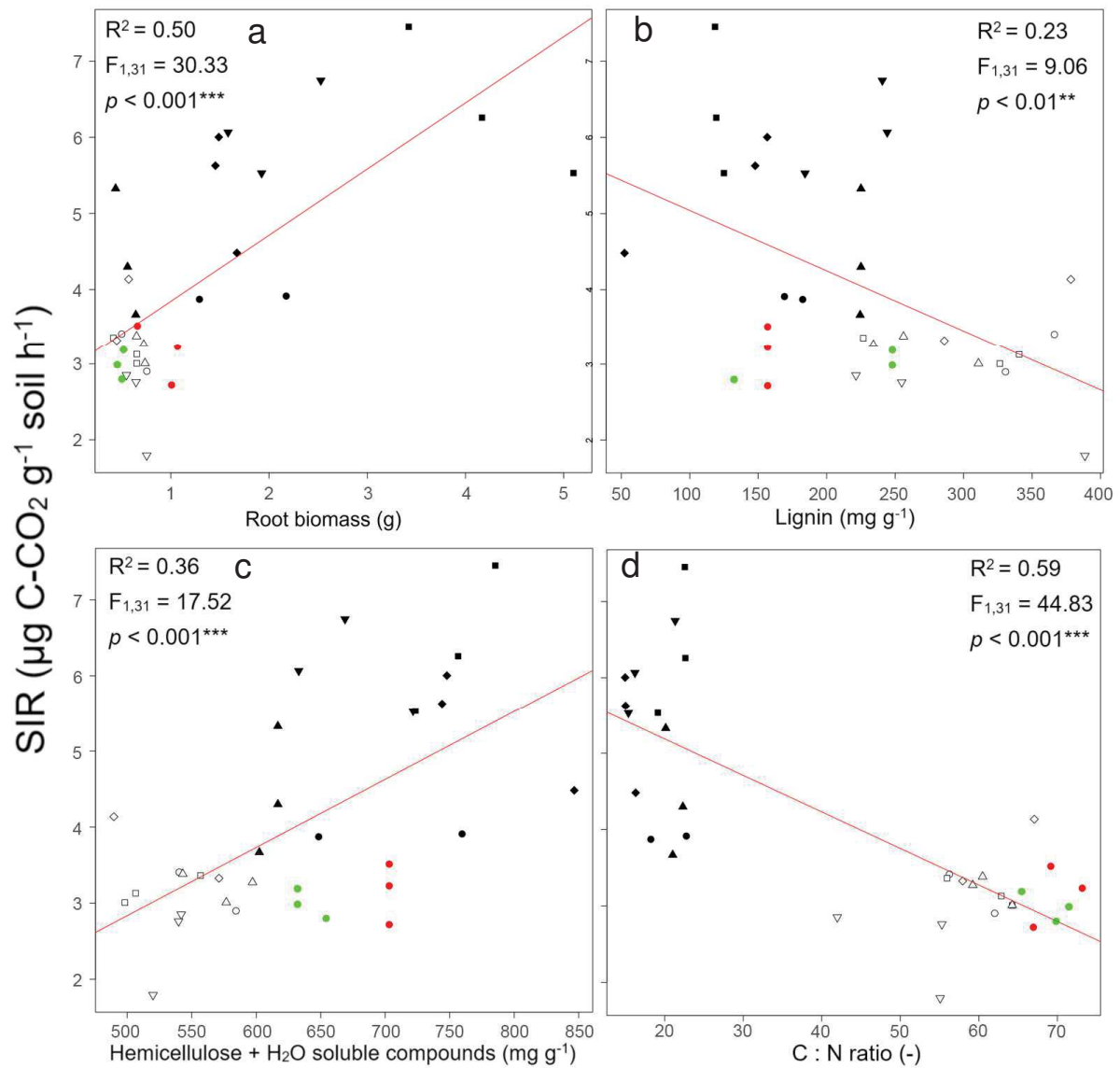
1026 The black symbols are the N₂-fixing Fabaceae species, the white symbols the non N₂-fixing Poaceae
 1027 species, the red dots are *S. minor* and the green dots are *P. lanceolata*. The red line is the linear model
 1028 function of the variables and R², F and p of the linear model are shown. For the legend refer to figure
 1029 S9.



1030

1031 **Fig. S11:** Linear regression at individual level (n = 34 samples) between substrate induced respiration
1032 rate (SIR) and a) root biomass, b) lignin content, c) hemicelluloses + water soluble compounds, d) C:N
1033 ratio.

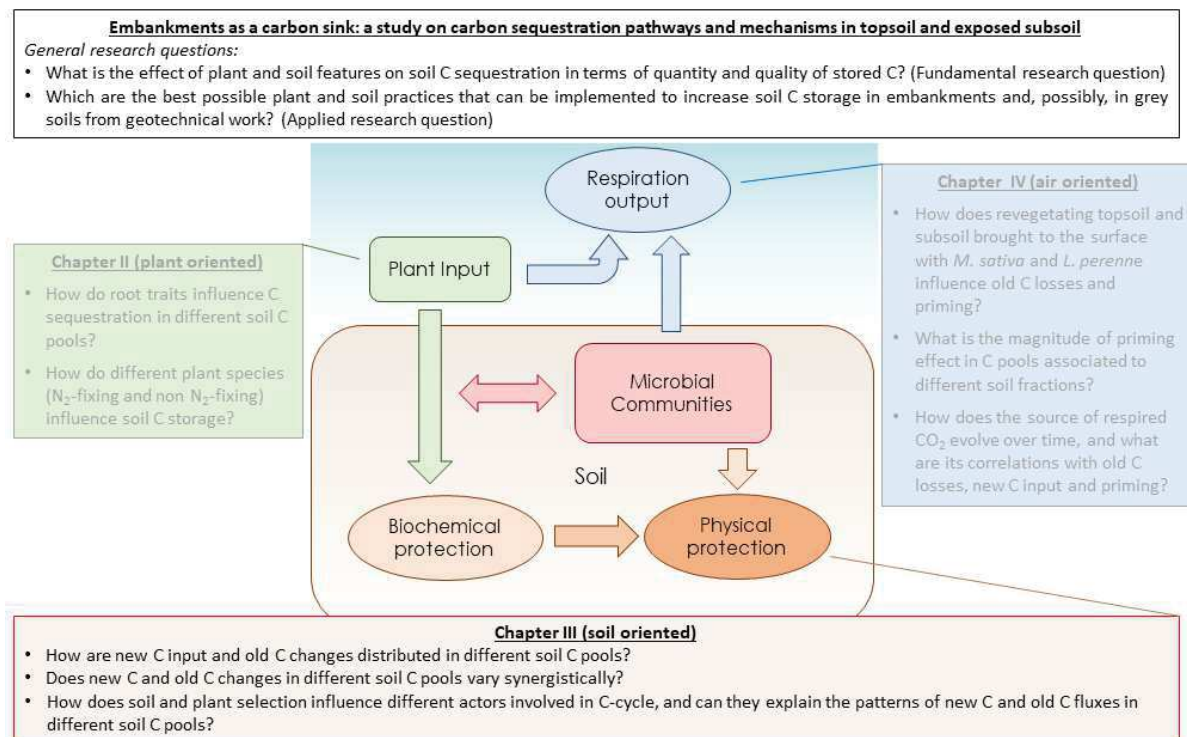
1034 The black symbols are the N₂-fixing Fabaceae species, the white symbols the non N₂-fixing Poaceae
1035 species, the red dots *S. minor* and the green dots *P. lanceolata*. The red line is the linear model function
1036 of the variables and R², F and p of the linear model are shown. For the legend refer to figure S9.



1037

1038

Chapter III: The fates of fresh new carbon and old soil carbon differ in topsoil and newly exposed subsoil and are explained by root, microbial, and soil particle size



In Chapter II we studied the effect of revegetation on C storage in different soil C pools. In Chapter III we aim to refine the understanding of C pathways in soil by selecting two species with contrasting root characteristics (among the species in Ch. II) and sowing them on two soils showing contrasting characteristics (fertile topsoil and poor subsoil) in a ^{13}C constantly enriched environment. We will differentiate the input of fresh new C and changes in preexistent old C in the different soil C pools and study their relationships with root traits, microbiological and soil characteristics.

Abbreviation	Definition	Corresponding symbol
C	Carbon; soil carbon refers to soil organic carbon in this study	
C pool	Soil carbon contents associated with different soil particle fraction sizes: particulate organic matter fraction (50-200 μm), fine particulate organic matter fraction (20-50 μm), coarse silt fraction (20-50 μm) and fine silt and clay fraction (<20 μm)	$X = \text{POM}, \text{finePOM}, \text{SILT}$ and SILT+CLAY
C content	Soil carbon concentration (in $\text{mgC g}^{-1}\text{soil}$) per unit weight of soil for each C pool or pool summed	$C_{\text{POM}}, C_{\text{finePOM}}, C_{\text{SILT}}, C_{\text{SILT+CLAY}}, C_{\text{SUM}}$
C change	Difference in soil carbon contents (in $\text{mgC g}^{-1}\text{soil}$) between the end and beginning of the experiment	$\Delta C_{\text{POM}}, \Delta C_{\text{finePOM}}, \Delta C_{\text{SILT}}, \Delta C_{\text{SILT+CLAY}}, \Delta C_{\text{SUM}}$
C quality	Proportion (in %) of soil carbon content belonging to each carbon pool	$\%C_{\text{POM}}, \%C_{\text{finePOM}}, \%C_{\text{SILT}}, \%C_{\text{SILT+CLAY}}$
new C	Fresh soil carbon due to plant inputs	$\Delta \text{New } C_x$ (new C gain for the pool X)
old C	Existing soil carbon before plant growth	$\Delta \text{Old } C_x$ (old C change for the pool X)
t_0	Time zero, beginning of the experiment	
t_6	Time after 6 months, end of the experiment	
POM	Particulate organic matter	
C:N	Carbon – nitrogen ratio in plant tissue	
GMA	Global Metabolic Activity of microbial communities	
SIR	Substrate induced respiration	
ANOVA	Analysis of variance	
PCA	Principal component analysis	
H	Shannon metabolic diversity index	

1 3.1.INTRODUCTION

2 3.1.1. *General context in soil organic carbon sequestration on embankments: can* 3 *subsoil brought to the surface be used as a C sink?*

4 Soil is the largest terrestrial carbon (C) reservoir and soil organic C (SOC) exchanges rapidly with C in
5 the atmosphere and biosphere (Torn et al. 2009). In the context of global warming, knowing the fate
6 of SOC is essential for greenhouse gasses mitigation. So far, national and supranational programs have
7 been developed to maintain soil organic C stability and promote C sequestration in soil (e.g. 4p1000).
8 Appropriate soil and vegetation management that favors C transfer from air to soil via plants has been
9 shown to be a promising way to increase the soil C sink (Rees et al., 2005; Minasny et al., 2017). Most
10 of the research has been carried out on agricultural and 'natural' soils, while heavily disturbed
11 antropized soils, i.e.. soils related to geotechnical operations. In this work we focus on the revegetation
12 of geotechnical road and railroad embankments, and their potential for soil C storage. Topsoil has
13 often been used for the revegetation of embankments, however, subsoil can be brought to the surface
14 and revegetated directly. We argue that revegetating subsoil brought to the surface has a high
15 influence on the C-cycle due to the different characteristics of subsoil compared to topsoil: lower
16 fertility levels, different aggregate characteristics, microbiological communities and their evolution
17 and dynamics (Taylor et al. 2002, Murray et al. 2004, Chabbi et al. 2009, Jones et al. 2018) and, most
18 notably, C saturation (Lorenz and Lal 2005; Rumpel and Kögel-Knabner 2011, Beare et al. 2016). It has
19 been hypothesized that soil has a C saturation level associated to its fine particle size partition (i.e.,
20 clay content) and the initial old C content (Six et al. 2002; Stewart et al. 2007). Protection via
21 organomineral interactions relays on surface area of soil particles, and after the available areas and
22 reactive surfaces are occupied by C, further C input will not be adsorbed anymore and therefore will
23 not be protected (Six et al. 2002). The potential amount of C protected via organomineral complexation
24 depends on the amount of the <20µm fraction and the initial amount of C in the associated soil C pool.
25 We argue that subsoils have a lower C saturation compared to topsoil due to higher clay content and
26 lower C content (Lorenz and Lal 2005; Rumpel and Kögel-Knabner 2011, Lawrence-Smith et al. 2015)

27 and, therefore, could store stable C more efficiently via organomineral interactions in the finer silt and
28 silt+clay soil fractions (<20 μ m). For this reason, subsoil brought to the surface could be an interesting
29 feature for C storage, and we aim to investigate the influence of excavating and revegetating subsoil
30 on the main actors involved in C-cycle and their influence on C storage in different soil C pools
31 associated to granulometry of soil fractions.

32

33 *3.1.2. New and old carbon in soil*

34 The soil C stock within a defined time frame is the balance between input and transformation of newly
35 photosynthesized C from plants to soil (new C) and losses of existing soil organic C (old C) through
36 microbial and plant respiration (Kuzyakov and Domansky, 2000; Fontaine et al., 2004). Although total
37 soil C sequestration is increasingly measured as an important ecosystem service, few studies have
38 quantified the proportions of new C input from plants and the losses of old soil C during respiration. It
39 is unclear how the input of new C and the losses of old C participate to the final soil C sequestration
40 and if trade off or synergetic patterns exist between new C input in soil and old C losses. The underlying
41 mechanisms behind these processes are poorly understood, but are crucial if we wish to improve soil
42 C sequestration.

43

44 *3.1.3. Soil organic carbon quality: carbon pools are associated to different soil granular* 45 *fractions*

46 More and more studies have highlighted the importance of C quality in soil (Chapter II, this thesis;
47 Cardinael et al.,2015). High quality soil C refers to organic C compounds that have long mean residence
48 time and good stability against mineralization because of their physical or physiochemical associations
49 with soil particles. Characterizing absolute and relative sizes of soil C pools associated to soil particle
50 size fractions is a powerful instrument to evaluate soil C quality. The commonly used classification of
51 soil pools in literature refers to (i) C in particulate organic matter (POM) (C_{POM} , 2000-200 μ m), (ii) C in

52 fine POM ($C_{finePOM}$, 200-50 μ m), (iii) C in coarse silt (C_{SILT} , 50-20 μ m) and (vi) C in fine silt+clay ($C_{SILT+CLAY}$,
53 <20 μ m). In the POM and finePOM pools, C is usually supposed to originate from plant litter debris at
54 different levels of degradation, and is more exposed to decomposers (Kögel-Knabner, 2002), whereas C
55 in the SILT and SILT+CLAY pools is considered more stable due to the organomineral binding with fine
56 soil particles (Sollins et al., 1996; von Lützow et al., 2006; Cotrufo et al. 2013). Although recent studies
57 have quantified soil C in different pools instead of that in total soil C (Cardinael et al., 2015; Chapter II,
58 this thesis), no study to our knowledge has bridged the link between C pools and the fates of new C
59 and old C. Speculating such an association is reasonable, as fates of new C and old C should have
60 different sensitivities to fresh plant C inputs, that has been shown to have a significant impact on the
61 relative size of soil C pools, i.e., soil C quality (Cardinael et al., 2015). To differentiate the inputs of new
62 C and the changes of old C in different C pools, stable isotopic labelling has proven to be a powerful
63 methodology. Growing plants in an atmosphere with increased % of ^{13}C in the CO_2 allows to
64 differentiate the new C inputted in soil from the preexistent old C (Staddon 2004). Being able to
65 differentiate old C is very interesting, since it allow to quantify even the changes in the old C pool in a
66 determined timeframe, other than the input of new C.

67

68 **3.1.4. New old carbon distribution in different soil pools: drivers and mechanisms**

69 Besides understanding the fates of new and old soil C in different soil fractions, we also need to
70 determine how plant and soil characteristics affect the trajectory of new and old C. The dynamics of
71 new C in soil is assumed to be jointly determined by plant performance and soil C storage capacity.
72 Plants transform atmospheric C via litter decomposition or root exudation, therefore, traits related to
73 decomposition and exudation should be examined in soil C sequestration studies (De Deyn et al., 2008;
74 Roumet et al. 2016; Henneron et al., 2019). Roumet et al. (2016) suggested that species with
75 contrasting growth strategies and tissue quality, i.e., N_2 -fixing fast-growing species with a low tissue
76 carbon:nitrogen (C:N) ratio versus non N_2 -fixing slow-growing species with a high tissue C:N ratio,

77 result in contrasting soil C sequestration. However, the relative importance of such traits on soil C
78 sequestration is not yet known. In this regard, studying the effects of N₂-fixing and non N₂-fixing species
79 is of particular interest, since they are placed at the two opposite ends of the root economic spectrum
80 (Roumet et al. 2016, Rossi et al., submitted, Chapter II) and expected to significantly influence the C
81 sequestration quantity and quality in different soil fractions. The capacity of soil to influence new C
82 storage is related, as already mentioned, to its C saturation levels. New C input increase soil
83 aggregation that, with a double feedback effect, in turn protect the C from microbial mineralization via
84 physical protection in the aggregate structure (Tisdall and Oades 1979,1982; Chevallier et al., 2004).
85 Aggregate stability, as a proxy for aggregation resistance to disruption, might very well be associated
86 with C protection in soil. Furthermore, N levels in soil will affect the soil fertility, and therefore, plant
87 development and microbial biomass and activity (Sarker et al., 2017).

88 Studies over the last 20 years have greatly focused on the priming effect, i.e., the phenomenon that
89 fresh biomass may, in most cases, stimulate microbial activities and thus accelerate the loss of old C
90 existing in soil (i.e., positive priming) (Kuzyakov et al. 2000; Blagodatskaya & Kuzyakov, 2008). Positive
91 priming can offset the gain of new C in soil and result in a net negative C balance (Cheng et al., 2003,
92 Fontaine et al., 2004). Many factors, from fresh tissue recalcitrance to soil physical properties are found
93 to influence the loss of old C. In particular, fresh tissue recalcitrance greatly affects the proliferation
94 rate of the microbial population and subsequent soil respiration rate. However, soil aggregate and
95 particle size determine the ability of soil to protect old C from microbial mineralization (Six et al., 2002).
96 For example, aggregates act as a physical barrier that separate occluded C from microbes and enzymes
97 (Besnard *et al.*, 1996; Rasse *et al.*, 2005; Bardgett *et al.*, 2014; Sokol *et al.*, 2019

98 I ask therefore, if plant traits, and soil characteristics (as aggregate stability, N content, and particle
99 size fractions) alter new C and old C dynamics in different soil fractions through their direct effect and
100 indirect influence on microbial communities. Microbial abundance (in terms of biomass that can be
101 calculated as concentration of DNA in soil), the global metabolic activity as the amount of respired CO₂

102 per g of soil in a specific timeframe (GMA), and the diversity in metabolic substrate consumption, often
103 represented by the Shannon index (H), will be deeply influenced by soil (Liang et al. 2017) and plant
104 species (Cotrufo et al. 2013). Microbial communities have a pivotal role determining the mineralization
105 and losses of old and new C, its subsequent transformation in degraded POM or the C input in the
106 protected silt and silt+clay fractions. The theory of the 'microbial carbon pump' (Liang et al., 2017) put
107 microbial communities at the center of C sequestration mechanisms. It state that microbial
108 communities, consume and input C in protected structure (aggregates) or transform it in recalcitrant
109 structure that are stabilized in soil as microbial necromass, the so called 'entombing effect' (Liang et
110 al., 2017).

111 *3.1.5. Research hypothesis*

112 Using a microcosm experiment, coupled with stable isotopic (¹³C) labelling, we aim at characterizing
113 the fates of new C from plant roots (root debris and exudations) and old C (pre-existing C in soil), as
114 well as their interdependence, across different soil fractions under a fully crossed soil and vegetation
115 treatment: two types of natural soils (subsoil and topsoil) × three vegetation treatments (bare soil,
116 *Medicago sativa* and *Lolium perenne*). Soil and microbial community characteristics and plant root
117 traits were measured to disentangle the effects of different drivers on changes in new and old C. I
118 hypothesize that:

119 i) Soil particle size can regulate the fates of old and new C within fractions. We hypothesize that the
120 input of new C will be higher in the particulate organic matter and in the SILT+CLAY fraction due to
121 exudation and microbial in vivo transformation of C. Old C is expected to be depleted from coarser
122 fractions (POM and finePOM) via microbial mineralization, and transferred to finer fractions, increasing
123 the old C in the SILT and SILT+CLAY fractions.

124 ii) The fates of new and old C show independent patterns: old C losses are expected to be more related
125 to microbial characteristics than to input of new C, however the influence of new C on microbial activity
126 might show an indirect effect decreasing old C concentration due ti priming effect.

127 iii) the patterns of new C and old C fluxes in different soil C pools could be explained by plant, micro-
128 organism and soil characteristics. More specifically, root traits connected to high root biomass and
129 labile input (i.e. acquisitive resource strategies N₂-fixing species) are expected to increase new C in the
130 soil, especially in the SILT and SILT+CLAY pools. We suppose subsoil to have a higher new C
131 accumulation in the SILT+CLAY fraction due to higher fine fraction and lower initial C content,
132 decreasing soil C saturation. In this respect, we think the percentage of the fine soil fraction (FF) will
133 be positively correlated with new C in the SILT+CLAY fraction. Aggregate stability (measured as mean
134 weight diameter, MWD) is expected to be positively correlated with new and old C accumulation in silt
135 and silt+clay fractions due to C protection. We believe soil N content will increase the overall input of
136 new C in all the fractions due to its connection with soil fertility and biomass production. Microbial
137 characteristics (GMA, H and DNA concentration) are expected to be positively correlated with the
138 accumulation of new C in the SILT and SILT+CLAY fraction and and decrease the old C content due to
139 metabolism and respiration of C.

140

141 3.2. MATERIALS AND METHODS

142 3.2.1. *Soil and plant preparation, experimental design and set-up*

143 The soil used in the experiment was excavated from a grassland in Pisciotta (Italy, 40°07'N, 15°14'E,
144 178 m a.s.l.) at two depths of the same soil profile: topsoil (0.0 – 0.3 m depth) and subsoil (1.1 – 1.4 m
145 depth). The soil was a clay loam soil (USDA) with a comparable granulometric texture between topsoil
146 and subsoil (topsoil: 27.3% clay, 31.1% silt, 41.6% sand; subsoil: 34.8% clay, 36.8% silt, 28.4% sand).
147 Topsoil (7.0) had a lower pH than subsoil (8.4).

148 Both top- and subsoil were sieved to 5 mm prior and then placed in containers (20 cm x 20 cm x 20
149 cm), where it was packed manually to a depth to 10 cm. Pots were weighed to ensure that they
150 contained the same amount of soil (+/- 2.5 %). N₂-fixing *Medicago sativa* L. and non N₂-fixing *Lolium*

151 *perenne* L. were planted as monocultures with exactly the same pattern. In each pot, three seeds were
152 put at six equidistant spots. After germination, one seedling was removed with scissors at ground level,
153 at each spot. For each soil type (i.e. top- and subsoil) and species, six replicate containers were
154 prepared and six bare containers per soil type were used as controls (n = 36 in total).

155 Containers were placed into three identical microcosms at the Ecotron growth facility at Montpellier,
156 France (<http://www.ecotron.cnrs.fr/>). In each microcosm, two replicates of all treatments, i.e., 12 pots,
157 were placed randomly to avoid any effect of microcosm on plant growth and soil processes. Plants
158 were grown at a constant air temperature of 21°C and at 80% humidity (to reduce the soil water loss
159 by evapotranspiration). Artificial light was provided by three lamps (Gavita PRO 300 LEP 02,
160 Netherlands) in each microcosm with a 12h day/night cycle, shifted to allow air sampling at the same
161 moment of the plant's circadian rhythm (data not shown in this study, see Chapter 4). A shade was
162 placed on the lamps and the distance of the lamps from the plants was adjusted to achieve the most
163 possible homogenous light intensity on the foliage ($300 \mu\text{mol m}^{-2} \text{s}^{-1}$). Soil moisture was kept at $45 \pm$
164 10% of the soil water holding capacity for the entire duration of the experiment (that was previously
165 calculated for topsoil and subsoil separately, data not shown). To minimize disturbances to the ^{13}C
166 concentration due to the opening of microcosm, a system of plastic pipes was installed into the
167 microcosm for watering. Every two weeks, pots were taken out to assess their evapotranspiration rate
168 and weight (data not shown). Each time pot position was randomized when they were put back to the
169 microcosm. Air enriched with enriched ^{13}C (with a concentration of 2%, approximately two times
170 higher than the natural ^{13}C abundance of 1.1%, in other words $\delta^{13}\text{C}$ of CO_2 in the chamber was roughly
171 +760%, as compared to the ambient -8) was supplied into the microcosms once the first emergence of
172 seedlings was observed in any microcosm (approximately three weeks). The air enrichment with ^{13}C
173 was supplied only during the 12h day cycle and the ^{13}C infusion was stopped during the night period.

174 The whole experiment lasted for 183 days, or six months from 29 September 2017, (t_0) to 31 March
175 2018 (t_6). Experiment length enabled us to (i) track the changes in soil C immediately after seedling

176 emergence (ii) avoid the effect of plant leaf and flower litter on soil C, which was not our study
177 objective. Any plant litter was removed manually every 2 weeks from the soil surface.

178

179 3.2.2. *Soil fractionation and assessment of soil carbon and $\delta^{13}C$*

180 Before the experiment, three soil samples per soil type were sampled for the measurement of carbon
181 content in different fractions, mean weight diameter of aggregates, nitrogen content, microbial
182 activity, DNA concentration and Shannon metabolic diversity at t_0 . Each sample was mixed and divided
183 into four parts, and an equal amount of soil from each part was collected and mixed to obtain a
184 homogenized sample of soil.

185 At t_6 , soil was removed from each pot, weighed and then cut into two equal-size half blocks with a saw
186 and a ruler: one half was air dried and used for soil analyses and the other half was used for plant trait
187 and microbiological measurements. A mixed sample from each pot was collected from a depth of 3.5-
188 10 cm depth. The soil samples at t_0 and t_6 were then sieved at 2 mm and 40g were sub-sampled and
189 fractioned using the Gavinelli et al. (1995) method (Supplementary material, Method S1, Fig. S1). The
190 resulting four fractions (POM: >200 μ m, finePOM: 200-50 μ m, SILT: 50-20 μ m, SILT+CLAY: <20 μ m) were
191 analyzed for both C content and $\delta^{13}C$ using an elemental analyzer Isoprime100 coupled with an
192 Elementar Varo Isotope Cube (machine reference no). The sum of C in different fractions represents
193 the total C in the sample. A subsample of 0.1 g was taken from each 40 g sample and analyzed without
194 fractioning to determine the total C in the bulk sample. We checked the accordance between the mean
195 difference between total C in bulk soil and the sum of C in the different soil fractions and the results
196 were satisfactory (mean 93.3% of recovery).

197 To assess the changes in total C in each fraction, the differences between C content at t_0 and t_6 were
198 assessed:

$$199 \Delta C_x = \Delta C_{x,t6} - \Delta C_{x,t0} \quad [1]$$

200 Where ΔC_x is the change in C content (mg C g^{-1} soil) in a given soil C pool. All the raw data can be found
201 in the Harvard Dataverse 'Embankment as a carbon sink: a study on carbon sequestration pathways
202 and mechanisms in topsoil and exposed subsoil', DOI: 10.7910/DVN/QTFLVE.

203

204 Every Fractionation method present some advantages and drawbacks. We chose the Gavinelli et al.
205 (1995) methodology for several reasons: it allows to reducing the shaking time of the sample to avoid
206 transfer of C from the sand to the clay fraction, an important factor given the sandy texture of the soil
207 used in this experiment (Gavinelli et al. 1995). The soil sieving at 2mm prior to fractionation decrease
208 the amount of unprotected POM, up to 50% (Duddigan et al., 2019). However, this problem is
209 particularly relevant for soils having a high C content and high organic fertilization; the soil used in this
210 experiment have low C content and no fertilization, therefore the issue is sensibly reduced (Duddigan
211 et al., 2019). The use of an aliquot to assess the silt-clay fraction allowed to less time consuming and
212 more economical procedure, a key element when a high number of samples need to be fractionated.
213 It is possible, however, using a wet sieving fractionation method, that part of the OM was transferred
214 in the SILT+CLAY fraction, overestimating its C content (Duddigan et al., 2019). However, the
215 fractionation has been performed by the same operator using the same protocol at time 0 and time
216 37, therefore the overestimation should be considered a standard error that does not affect the
217 difference in C between the two sampling times. Since the separation of POM in the Gavinelli et al.
218 (2005) methodology via density fractionation happens after soaking soil with exametaphosphate and 2
219 hours shaking with agate balls, the POM fraction includes also the POM occluded in macroaggregates.
220 However, this methodology allows assessing the amount of C protected in microaggregates after their
221 breaking via sonication, and this fraction is considered the most important for physically protected C
222 (Kong et al., 2005; Six and Paustian, 2014).

223

224 **3.2.3. Estimation of new and old carbon in soil fractions**

225 The increased atmospheric $\delta^{13}\text{C}$ signature in the microcosm allowed a calculation of the proportions
226 of new C in the different soil fractions. We used an isotope mixing model (Balesdent and Mariotti,
227 1996):

$$228 \quad \%NewC = \frac{\delta(t6) - \delta(t0)}{\delta B - \delta(t0)} \quad [2]$$

229 Where %New C is the percentage of new C in a specific fraction, $\delta(t6)$ is the $\delta^{13}\text{C}$ signature of C
230 measured in a specific fraction at $t6$, $\delta(t0)$ is the $\delta^{13}\text{C}$ signature of C of a specific soil fraction $t0$, δB is
231 the $\delta^{13}\text{C}$ signature of the new C input in the system (in our case the signature of the absorptive and
232 transport root biomass). The δB was specific for each pot based on the analysis of the root biomass,
233 and the mean was 615 ± 38 . The choice of root biomass as the $\delta^{13}\text{C}$ reference for C input was made
234 because root material was considered to be the main input of C, given that shoot litter was negligible,
235 and comparable with exudates signature.

236 The new C at $t0$ was zero. To calculate the gain of new C (mgC g^{-1} soil) in a specific soil C pool X, we
237 multiplied %Cnew by the total amount of C at $t6$ (C_X) of the pool X:

$$238 \quad \Delta NewC_X = C_X(t6) \times \%NewC \quad [3]$$

239 To assess the changes in the old C in different soil C pools, we subtracted the new C from the ΔC of
240 each soil C pool.

$$241 \quad \Delta OldC_X = \Delta C_X - \Delta NewC_X \quad [4]$$

242

243 The isotope labeling approach was chosen since it allows following the path of C when the desired C
244 input is 'traced' with an increased (or decreased) C isotope ratio (Staddon, 2004; Hungate, 1996). The
245 different ^{13}C levels, compared with the natural abundance and input ^{13}C signal, allow following the
246 carbon from the atmosphere to the different plant systems, the trophic transfer via microorganisms,

247 to end up in soil or in respired carbon (Leake et al., 2006; Bradford et al., 2007; Högberg et al., 2008).
248 We chose stable labeling methodology since pulse labeling, even if more economically convenient and
249 easier to implement than stable labeling, cannot achieve a uniform labeling distribution in the system
250 as stable labeling does, and this can result in a bias results analysis (Meharg, 1994). Stable isotope
251 labeling has been extensively used to trace respired CO₂ and understand its origins, separating root
252 respiration from microbiological respiration of old or new carbon (Rygiewicz and Andersen, 1994;
253 Kuzyakov et al., 2001; Trubore, 2006; McDowell et al., 2004; Subke et al., 2004; review from Hanson
254 et al. 2004). However, different challenges can be encountered when using stable ¹³C labelling in CO₂,
255 more specifically the stability of the enrichment, possible leaking, and different photosynthetic
256 efficiency and ¹³C adsorption from plants. For this reason, the chambers have been open as fewer times
257 as possible and only when the ¹³C enrichment was not in place (in chambers 'night hours').

258 *3.2.4. Microbial global metabolic activity (GAM) and Shannon metabolic diversity index* 259 *(H)*

260 To analyze functional diversity, precisely GAM and H from microbial communities, 20 g of soil were
261 collected immediately after sampling from each container at t6 and t0 from the half of soil collected
262 for chemical analyses. We used a Microresp system that comprises a Deepwell plate (Fisher Scientific
263 E39199) holding soil subsamples saturated with a solution with different substrates, a detection plate
264 containing the detection gel, a rubber seal to connect the deepwell and the detection plate and metal
265 clamp to keep the two parts tightly together (MicroResp™, Aberdeen, UK) (Fig. S2). The output of
266 Microresp is to assess the respiration rate of soil saturated (at 80% of field capacity) with different
267 substrates presenting different levels of recalcitrance and biological properties. Detailed methodology
268 is provided in supplementary materials, Method S2. Substrates utilized for MicroResp are shown in
269 Table S1.

270 To have a proxy of the global metabolic activity (GAM) of the microbial communities, the respiration
271 rates from the different 15 C substrates were summed (mg C-CO₂ g⁻¹ soil h⁻¹; Frac et al. 2012, Ammar
272 et al. 2017). For each replicate, a Shannon metabolic diversity index was calculated as:

273 $H = -\sum_{i=1}^{15} \pi \times \log(\pi)$ [5]

274 Where π is the standardized respiration rate for substrate (i) (Shinan et al. 2017).

275 MicroResp was chosen since is a method that allows a convenient, sensitive, rapid methodology to
276 determine microbial activity and functional diversity, assessing their substrate utilization (Campbell et
277 al. 2008). SIR, instead, allow only to assessing the potential activity with glucose. The method has been
278 utilized in a wide range of soils and land uses, and always demonstrated its value (Chapman et al. 2007;
279 Creamer et al. 2016; Shinnan at al. 2017).

280 However, MicroResp suffers from three main limitations according to Renault et al. (2013) that needs
281 to be taken into account: first, the method consider the CO₂ in the well air space to be only of microbial
282 origin (Campbell et al., 2003). The volume of the deep well that is not filled with soil is neglected and
283 given the low volume of soil solution this can lead to overestimation of respired CO₂. Second, the
284 increasing CO₂ in the air decrease the pH of the solution (Stumm and Morgan, 1996) and, again, could
285 lead to overestimate the CO₂ in solution. Third, there was no check done to see if the transfer between
286 calcite, soil solution, air and gel is in equilibrium, otherwise calibration would be impossible (Renault
287 et al. 2013).

288 *3.2.5. Microbial DNA concentration as proxy for microbial biomass*

289 To examin microbial biomass in different communities, 10g of soil was immediately frozen at -20°C
290 after sampling, and kept until samples were processed for DNA extraction. Total DNA was extracted
291 from soil (0.5 g). DNA extraction was performed using FastDNA® SPIN Kit for Soil Isolation Kit according
292 to manufacturer's instructions (MP Biomedicals, USA). An additional step to wash the DNA binding
293 matrix with 500 µl of guanidine thiocyanate 5.5M was added following Tournier et al. (2015). The
294 concentration of extracted DNA in solution (ng/µL) were measured using a Quant-iT™ PicoGreen™
295 dsDNA Assay Kit for DNA quantification and used as a proxy for microbial biomass (Bohórquez et al.
296 2017).

297 The main drawback of using DNA concentration as a proxy of microbial biomass is that this
298 methodology does not make the distinction between intracellular DNA of live microbial cells, dead
299 microbial cells, and extracellular DNA released via cellular lysis (Torti et al., 2015). This bias can result
300 in an overestimation of microbial biomass. However, the aim of this analysis is not to precisely estimate
301 microbial biomass (for which other methodologies are more suitable) but to compare the changes in
302 biomass. As a general comparative biomass growth indicator, this methodology has proven to be valid
303 and easy to implement (Bohórquez et al., 2017).

304

305 *3.2.6. Percentage of fine fraction in soil, soil nitrogen and aggregate stability*

306 After the wet sieving and weighing of the different soil fractions, the percentage of fine fraction (FF, in
307 %) was determined as the ratio of the SILT+CLAY soil fraction weight (<20 μm) and the total mass of
308 the fractioned soil sample (in average 40g). When analyzing C content and $\delta^{13}\text{C}$ for each bulk soil
309 fraction, the amount of nitrogen in soil (N; mg g^{-1} soil) was also determined.

310 As a proxy for aggregate stability, mean weight diameter (MWD) of aggregates was assessed following
311 the conventional methodology according to Le Bissonnais et al. (2006). 20g of aggregates were
312 collected from the half pot for soil analysis, air dried and sieved first at 5 mm and then at 3 mm, to
313 isolate the 3 - 5mm aggregates fractions. This aggregate fraction were put in the oven for 24h to reach
314 the same water matrix potential. First, 5g of 3-5mm fraction are weighed and gently immerse in a 250
315 cm^3 beaker filled with 50 cm^3 of ethanol for 10 minutes. After ethanol was carefully sucked off with a
316 pipette and the sample transferred in a 250 cm^3 Erlenmeyer flask containing 50 cm^3 of deionized water,
317 and brought to 200 cm^3 . The flask was agitated 20 times and left 30 minutes for sedimentation of
318 coarse particles. Water was sucked off with a pipette and the mixture of soil and water transferred to
319 a 50 μm sieve previously immersed in ethanol. The disaggregated soil was sieved gently by moving 5
320 times the sieve in the ethanol to separate the <50 μm soil fraction from the >50 μm . The >50 μm
321 aggregate fraction was collected from the 50- μm sieve, oven-dried and gently dry-sieved by hand on a

322 column of six sieves: 2000, 1000, 500, 200, 100 and 50 μm . The mass percentage of each aggregate
323 fraction was calculated, and by subtracting the mass of soil collected on sieves from the initial mass
324 analyzed mass we calculated even the $<50\mu\text{m}$ fraction. MWD is calculated as the sum of the mass
325 fraction of soil remaining on each sieve after sieving multiplied by the mean aperture of the adjacent
326 mesh:

$$327 \quad MWD = \frac{\sum_{f>2mm}^{f0.05-1mm} (Af * df)}{100} \quad [6]$$

328 Where Af is the aggregate fraction abundance in % of the total weight of the analyzed sample
329 remaining in a specific f aggregate fraction ($f = >2\text{mm}$, $1-2\text{mm}$, $0.5-1\text{mm}$, $0.2-0.5\text{mm}$, $0.1-0.2\text{mm}$, and
330 $0.05-0.01\text{mm}$), and df the diameter in mm of the smaller sieve characterizing the lower boundary of
331 the f aggregate fraction.

332 To assess aggregate stability we chose Le Bissonais (1996) methodology since it unifies different
333 previously utilized methodologies that sum up the main aggregate disruption processes and it is
334 applicable to a wide range of soils (le Bissonais et al., 1996). This methods allow to simulate the main
335 mechanisms for aggregate disruption: slacking due to compression of entrapped air during wetting, 2)
336 micro cracking originating from swelling, 3) breaking due to mechanical action and 4) dispersion due
337 to osmotic stress (Rohošková and Valla, 2004). Being one of the most complete and comprehensive
338 tests for aggregate stability assessment it is widely used, however it present a major drawback: it
339 might overestimate MWD due to the fact that sand particles are not removed from its calculation
340 (Rohošková and Valla, 2004)

341 *3.2.7. Root traits*

342 For each species, three out of the six plants in each pot were sampled and their root system carefully
343 washed and separated from the aboveground part. Roots were water-rinsed in a plate container. A 0.1
344 g composite subsample of roots was cut off from several parts of the root systems with scissors. After
345 being carefully washed, they were stained with a solution of methyl violet (0.5 g L^{-1}). Following

346 McCormack *et al.* (2015), we visually separated transporting (long, thick, high-order roots (>3) and
347 absorptive roots (short, thin, low-order roots 1 – 3). Both types of roots were separately extended over
348 a transparent water filled tray and scanned at 800 dpi (Epson® perfection V700 PHOTO, Canada). The
349 software Winrhizo Pro® (Regent Instruments, Quebec, Canada) was used to determine root length (L,
350 in mm) per diameter class stretching from 0 to 2 mm with a 0.1 mm interval. . Winrhizo Pro® also
351 provides the mean diameter of the analyzed root sample (Prieto *et al.*, 2016). We then calculated the
352 mean diameter of adsorptive roots (D_{ad}), for in each soil and species type.

353

354 Specific root length (SRL, $m\ g^{-1}$) was calculated as the ratio between root length and dry root mass
355 (Esseinstat, 1992). Only absorptive root data were then used in the data analysis as they are most
356 short-lived and active in exudation, thus should be the main contributor of new C deposition to soil.

357 Following the same sampling and sorting manner, another sample of 0.1 g absorptive roots from the
358 same plants was obtained and then finely ground. The ground samples were analyzed with an
359 elemental analyzer Isoprime100 coupled with an Elementar Varo Isotope Cube to determine root C
360 and N contents and root $\delta^{13}C$.

361 The remaining roots in the half pot were then oven dried at 60°C for three days and weighed to
362 determine the total root dry mass (in g) for each pot

363 Finally the amount of new C moved into the SILT+CLAY pool by g of root was calculated by standardizing
364 the $\Delta New\ C_{SILT+CLAY}$ for the g of dry root weight per gram of soil (DRW; $g\ dry\ roots\ g^{-1}\ soil$). Also the
365 amount of new C moved into the SILT+CLAY pool by cm of root was calculated by standardizing the
366 $\Delta New\ C_{SILT+CLAY}$ for the length of the root (L, $cm\ of\ roots\ g^{-1}\ soil$) per gram of soil. To calculate the root
367 L, we multiplied SRL per the DRW.

368

369 3.2.8. *Statistical analysis*

370 One way analysis of variance (ANOVA) was performed to test the effects of plant and soil treatments
371 on

- 372 1) C content: ΔC_x , $\Delta New C_x$ and $\Delta Old C_x$ for the C pool X and all pool summed (*SUM*)
- 373 2) C quality: %C_x each C pool X
- 374 3) Soil, root and microorganism feature indicators, including initial SOC stock, FF, soil N content,
375 MWD, total root biomass, mean absorptive diameter, C:N ratio of absorptive roots, SRL of
376 absorptive roots, concentration of extracted DNA in ml⁻¹ of soil solution as proxy for microbial
377 biomass, microbial activity (GMA) and metabolic community diversity (H) .

378 The normality of distribution of residues was verified using a Shapiro-Wilk test ($\alpha_p = 0.05$). Principal
379 component analysis (PCA) and Pearson's correlations factors were used to study the relationships
380 between C sequestration indicators and soil type, root and microbial indicators. All the statistical
381 analyses were performed using the open-source statistical environment 'R', version 3.4.3 (R
382 Development Core Team, 2017) using the packages *vegan* and *Hmisc*. (Oksanen et al. 2019, Harrel
383 2007).

384

385 3.3. RESULTS

386 3.3.1. *Changes in total soil carbon*

387 In general, a decrease in mean total soil C content occurred after 6 months in subsoils (Fig. 1a,b). The
388 mean negative ΔC in bare subsoil (-0.37 ± 0.18 mgC g⁻¹ soil) was not significantly different to that with
389 either *L. perenne* (-0.38 ± 0.11 mgC g⁻¹ soil) or *M. sativa* (-0.17 ± 0.25 mgC g⁻¹ soil) present. Although the
390 presence of vegetation did not significantly affect total C in subsoil (ANOVA, $p \geq 0.05$) (Figure 1b), mean
391 ΔC had a significant increase in topsoil (ANOVA, $p < 0.05$), with the highest increase in C content under
392 *M. sativa* ($+0.68 \pm 0.36$ mgC g⁻¹ soil), followed by *L. perenne* ($+0.1 \pm 0.51$ mgC g⁻¹ soil). In bare soil, ΔC was

393 negative ($-0.47 \pm 0.28 \text{ mgC g}^{-1} \text{ soil}$) (Figure 4.1a,b). ΔC_{SUM} was significant lower under *M. sativa* subsoil
394 compared to *M. sativa* topsoil (ANOVA, $p < 0.05$), but no difference between soil types where observed
395 under *L. perenne* (ANOVA, $p \geq 0.05$) due to the high variability in data. There was no effect of soil type
396 on ΔC_{SUM} in bare soil (ANOVA, $p \geq 0.05$) (Fig. 1b).

397 Mean old C decreased in all treatments (Fig. 1a), although a slight positive $\Delta \text{Old C}$ could be occasionally
398 found in some pots (Fig. 2a). In topsoil, the increase in new C was sufficient to compensate for the loss
399 of old C, but it was not the case in subsoil, where $\Delta \text{New C}$ was less than the $\Delta \text{Old C}$ (Figure 1a). As
400 expected, bare soil had a negligible input of new C, while topsoil under *M. sativa* had both the smallest
401 lower negative $\Delta \text{Old C}$ and the highest positive $\Delta \text{New C}$. Data were highly variable with regard to
402 negative $\Delta \text{Old C}$ in topsoil under *L. perenne* (Fig. 2a). The effect of species, $\Delta \text{Old C}$ and $\Delta \text{New C}$ were
403 less pronounced in subsoil than in topsoil. In vegetated soils, positive $\Delta \text{New C}$ was accompanied by a
404 smaller loss of old C (lower $\Delta \text{Old C}$) (Fig. 2a). However, there were no consistent relationships between
405 changes in old C and in new C in either soil type or plant species (Fig. 2a).

406 Over 6 months, the amount of active C (i.e., $|\Delta C_{\text{New}}| + |\Delta C_{\text{Old}}|$) represented 9.1% and 6.1% of the total
407 C contents for subsoil and topsoil, respectively. The amount of active C in topsoil was 1.5 times higher
408 than that in subsoil.

409

410 3.3.2. Changes in soil carbon in different soil C pools associated to soil fractions

411 In subsoil, $\Delta C_{\text{finePOM}}$ was significantly lower than in the other pools, (ANOVA, $p < 0.05$). The ΔC between
412 pools was not significant for *M. sativa* and bare soil due to the high variability in data (Figure 3a). In
413 topsoil, mean $\Delta C_{\text{finePOM}}$ was not significantly different with that in the ΔC_{POM} or ΔC_{SILT} . $\Delta C_{\text{SILT+CLAY}}$ was
414 usually the highest among all the four C pools (Fig. 3a,b).

415 Regardless of soil type, plant species had a limited effect on $\Delta C_{\text{finePOM}}$ and ΔC_{SILT} (Figure 3a, b). In subsoil,
416 plants increased ΔC_{POM} (Fig. 3a), but not in topsoil. However, in topsoil, plants increased $\Delta C_{\text{SILT+CLAY}}$

417 (1.28±0.63 mgC g⁻¹ soil for *M. sativa*, 1.00 ± 0.44 mgC g⁻¹ soil for *L. perenne*), compared to bare soil
418 (0.90±0.29 mgC g⁻¹ soil). In the remaining C pools, ΔC significantly decreased (Figure 3b).

419 The only significant difference in soil planted with either species, was the increase in ΔC_{SILT+CLAY} in the
420 topsoil compared to subsoil (ANOVA, *p* < 0.01).

421 ΔNew C_{finePOM} and ΔNew C_{SILT} changed negligibly with regard to soil type and plant species (Fig. 4a,c).
422 Compared to bare soil, new C gain in planted subsoil soil was mainly located in the POM pool, while
423 new C gain in planted topsoil was located in both POM and CLAY+SILT C pools (Fig. 4a,c). Soil under *M.*
424 *sativa* had significantly higher ΔNew C_{POM} and ΔNew C_{SILT+CLAY} pools compared to *L. perenne* (Fig. 4a,c).

425 The effect of soil type on old C was more accentuated compared to New C. In subsoil, neither C pool
426 and plant species had any effect on old C loss, which was always negative (C depletion). In topsoil,
427 instead, here was a positive accumulation for ΔOld C_{SILT+CLAY}, while this decreased in all the other pools
428 which did not differ among each other (Fig. 4b,d). Plant species had no effect on old C loss in any C
429 pool (ANOVA, *p* ≥ 0.05).

430

431 3.3.3. Changes in carbon quality

432 *M. sativa* increases the % of C stored in the POM C pool over the total amount of C in the soil thanks
433 to high input of new C, while *L. perenne* and bare soil decreased the % of C in this pool (Fig. 5a). The %
434 of C stored in the finePOM and SILT pools decreased over at t6, with negligible inputs of new C (Fig.
435 5b,c). Finally, every treatment increased the % of C stored in the SILT+CLAY pool over the 6 months
436 compared to t0 (Fig. 5d).

437

438 3.3.4. Root, soil and microbial characteristics

439 Root biomass of both plant species was significantly higher in topsoil (*M. sativa* 17.53±2.03 g pot⁻¹, *L.*
440 *perenne* 4.09±1.43 g pot⁻¹) than in subsoil (*M. sativa* 5.13±1.36 g pot⁻¹, *L. perenne* 1.05±1.36 g pot⁻¹)

441 (Tables 1, 2). In *M. sativa* soil type did not influence mean SRL, diameter or C:N ratio of absorptive
442 roots. In *L. perenne*, greater SRL (topsoil +11.97 m g⁻¹) and C:N ratio (+39.30) in subsoil was found
443 compared to topsoil (Tables 1, 2). In *L. perenne*, absorptive roots were thinner in subsoil compared to
444 topsoil (-0.01 mm; Tables 1, 2). *M. sativa* had greater root biomass (topsoil +13.44 g pot⁻¹, subsoil
445 +4.08 g pot⁻¹) and mean diameter, but lower SRL and C:N ratio than *L. perenne*, in both soils (Tables 1,
446 2). In topsoil, GMA, H and DNA mass were all significantly greater compared to subsoil once plants had
447 grown. In bare soil, GMA did not significantly differ among topsoil and subsoil (Tables 1, 2). In topsoil,
448 the presence of both species significantly increased GMA (*M. sativa* +10.39±4.63 µgC-CO₂ g⁻¹ soil h⁻¹,
449 *L. perenne* +3.01±2.19 µgC-CO₂ g⁻¹ soil h⁻¹) and DNA concentration (*M. sativa* +5.33±5.29 µgC-CO₂ g⁻¹
450 soil h⁻¹, *L. perenne* +4.73±6.37 µgC-CO₂ g⁻¹ soil h⁻¹) that did not differ between treatments (Tables 1, 2).
451 In subsoil, GMA decreased over the 6 months (*M. sativa* -1.59±1.53 µgC-CO₂ g⁻¹ soil h⁻¹, *L. perenne* -
452 0.16±2.73 µgC-CO₂ g⁻¹ soil h⁻¹) while DNA concentration increased (*L. perenne* +2.00±1.41 ng µL⁻¹; *M.*
453 *sativa* 4.20±1.64 ng µL⁻¹), and they did not differ between plant species (Table 2). In subsoil H was
454 significantly higher in soil planted with either species compared to bare soil (Tables 1, 2).

455 Soil type significantly influenced the soil structural and characteristics and N content: topsoil had a
456 higher MWD and N content regardless of plant species (Table 1, 2). The fine fraction (FF) was higher in
457 subsoil compared to topsoil (Tables 1, 2). There was a significant increase in MWD with both the
458 species in topsoil (*M. sativa* +0.52±0.29 mm, *L. perenne* +0.62±0.20 mm), while in subsoil MWD was
459 not significantly different from t0 or between treatment (Table 1, 2). Soil N and FF were not
460 significantly different among treatments (Tables 1 and 2) and soil N was depleted during the 6 months,
461 with subsoil showing an homogeneous depletion among treatments (-0.1±0.8 mgN g⁻¹ soil) while in
462 subsoil *L. perenne* had higher decrease in soil N (-0.13±0.12 mgN g⁻¹ soil) compared to bare soil and *M.*
463 *sativa*. In subsoil, the presence of vegetation did not influence any of the soil characteristics.

464

465 3.3.5. *Relationship between changes in new C and old C and soil, microorganism and*
466 *root variables*

467 The PCA conducted on the Δ New C and Δ Old C in the different soil C pools, root traits, DNA mass, H
468 and GMA, and soil structural characteristics explained 83.9% of the total variance (Fig. 6). The first PCA
469 axis (horizontal) accounted for 63.3% of the variation. On the negative end, results were governed by
470 the Δ New C_{POM} , Δ New C_{finePOM} and Δ New $C_{\text{SILT+CLAY}}$, and Δ Old C_{finePOM} . At the positive end, results were
471 driven by total Δ Old C_{SUM} and Δ Old $C_{\text{SILT+CLAY}}$, while the remaining new C and old C pools were orthogonal
472 and more related to the second PCA axis (vertical), that accounted for 20.6%. Microbial traits (GMA,
473 DNA and H), MWD, soil N and root biomass, went all along the first axis (negative). Root traits linked
474 with recalcitrance (C:N ratio and SRL) and fine fraction percentage FF went along the 1st axis (positive)
475 together with Δ Old C_{SUM} and Δ Old $C_{\text{SILT+CLAY}}$.

476 The PCA strongly discriminated top- and subsoil at the two extremes of the first axis, with topsoil on
477 the negative end of the first axis, characterized by high GAM, H and DNA concentration, high MWD,
478 soil N and root biomass, correlated with Δ New C and Δ Old C_{finePOM} . Subsoil was on the positive end of
479 the first axis, with FF, root C:N and SRL, suggesting a loss of Δ Old C_{SUM} and Δ Old $C_{\text{SILT+CLAY}}$. Species were
480 discriminated mostly by the second axis, with *L. perenne* on the positive end of the axis together with
481 higher C:N ratio, SRL, and Δ Old C_{POM} and *M. sativa* on the negative end, with high root biomass and
482 diameter of absorptive roots, illustrating a positive Δ New C_{POM} pool and the Δ New C_{SUM} , and negative
483 Δ Old C_{SILT} and Δ Old $C_{\text{SILT+CLAY}}$.

484 The gain in new C, regardless of total new C, or within each soil C pool, was better related to every
485 analyzed variable than the loss of old C (Table 3). The gain in Δ New C in every C pool was positively
486 correlated with microbial traits (GMA, H and DNA), except for Δ New C_{POM} and H (Table 3). Δ New C_{POM} ,
487 Δ New $C_{\text{SILT+CLAY}}$, and Δ New C_{SUM} were significantly and negatively correlated with SRL and C:N ratio of
488 absorptive roots. Apart from Δ New C_{POM} , the gain in new C in every soil fraction was positively
489 correlated with MWD and soil N content (Table 3), but negatively correlated with FF. The negative
490 Δ Old C was significantly and positively correlated with H in Δ Old C_{POM} and with GMA in Δ Old C_{finePOM} ,

491 but was negatively correlated with every microbial trait (GAM, H, DNA concentration) in $\Delta\text{Old } C_{\text{SILT+CLAY}}$
492 and $\Delta\text{Old } C_{\text{SUM}}$. Root variables were poor predictors of total old C losses, except for root biomass, which
493 was positively correlated with the loss in $\Delta\text{Old } C_{\text{finePOM}}$ and negatively with that in $\Delta\text{Old } C_{\text{SILT+CLAY}}$. Soil
494 variables were all correlated with the losses in $\Delta\text{Old } C_{\text{SILT+CLAY}}$ and $\Delta\text{Old } C_{\text{SUM}}$ demonstrating an opposing
495 pattern compared with correlations with the gain in new C. The losses in $\Delta\text{Old } C_{\text{finePOM}}$ and in $\Delta\text{Old } C_{\text{SILT}}$
496 were poorly correlated with most of the variables.

497 Finally, when standardized by dry root weight, $\Delta\text{New } C_{\text{SILT+CLAY}}$ in subsoil planted with either *M. sativa*
498 and *L. perenne* was different than that found in topsoil, but the difference was not significant (Fig. S5a;
499 ANOVA, $p > 0.05$). When the $\Delta\text{New } C_{\text{SILT+CLAY}}$ was standardized for every cm of root, no differences could
500 be observed between top- and subsoil planted with either species (Fig. S5b; ANOVA, $p > 0.05$).

501

502 3.4. DISCUSSION

503 Soil, with its biotic and abiotic characteristics, had the highest influence on C sequestration. New C
504 accumulation, old C and total C changes in terms of both absolute (C quantity) and relative (C quality)
505 values significantly differ among soil C pools, thus validating our Hypothesis 1. The most reactive pools
506 were POM and SILT+CLAY for new C accumulation. We examined the correlations between new C and
507 old C for total soil C and each C pool and found synergetic patterns in a generally consistent manner,
508 thus rejecting our Hypothesis 2. Finally, we showed that new C and old C changes could be partially
509 explained by multiple soil, microorganism and root variables despite their disparities in drivers,
510 validating our Hypothesis 3. In general, the main drivers for C storage were N content and microbial
511 activity, which influenced soil quality. Root biomass development was the third driver showing high
512 correlations with new C storage in soil fractions, but subdued to soil characteristics. We did not observe
513 a positive effect of lower C saturation on C storage in SILT+CLAY in subsoil, due to the lower biomass
514 development and microbial activity, resulting in a lower new C input. Regarding the applied aspect, we

515 found topsoil had relatively higher new C gain and lower old C loss compared to subsoil and *M. sativa*
516 had a better performance in gain of new C and limit of old C loss than *L. perenne*, although such an
517 effect of species was moderated by soil type. Understanding and assessing the choice of plant and soil
518 on C sequestration will help shape practical guidelines in revegetation and restoration programs of
519 geotechnical systems, notably road embankments.

520

521 *3.4.1. Importance of differentiating soil carbon origin and pools (Hypothesis 1)*

522 Here, we clearly confirm the importance of disentangling the C fates of different origins and pools.

523 Taking the vegetated topsoil as an example, we found that the increase in total C after six months was
524 mainly attributed to a high input of new C in POM and to the high increase of new and old C in the
525 most stable SILT+CLAY pool. This result is in line with previous studies on either C origins (De Deyn et
526 al., 2008; Cotrufo et al., 2013; Liang et al., 2017; Vidal et al., 2018) or C quality by taking into account
527 C pools (O'Brien and Jastrow, 2013; Cardinael et al., 2015; Saenger et al., 2015; Chapter II this thesis).

528 In topsoil, the total old C change was close to zero, but was actually an offset between an active and
529 high gain in old C in the SILT+CLAY pool and an active and high loss in old C in the POM pool. As the
530 fate of old C was not estimated in the different C pools, it is possible to wrongly diagnose that old C
531 was little active during the whole revegetation process.

532 The correlations between total ΔC and diverse soil, root and microbial characteristics, did not reveal
533 the relationships in most of the C pools. (e.g. Cardinale et al., 2015, Rossi et al., submitted). Being able
534 to separate new C and old C fluxes thanks to isotopic enrichment have proved fundamental to
535 investigate correlations that are hidden when considering the total ΔC as the sum of new and old C
536 changes in the system. Jointly considering C origins and pools enabled us to better depict the pathways
537 of C flux from plant roots to soil and among soil C pools. We found that, once soil was vegetated (either
538 topsoil or subsoil), the increase in total soil new C was mainly due to the increase in the least stable
539 POM pool. This result confirms the key role of plant roots in supply of C to the POM pool via root

540 turnover, and is in line with results by e.g. De Deyn et al. (2008), Cotrufo et al. (2013) and Rees et al.
541 (2005). Surprisingly, we found a high $\delta^{13}\text{C}$ signal in the SILT+CLAY pool for both soil types, which
542 corresponds to a minor, but non-negligible amount of new C supply into the most stable pool. Given
543 that this phenomenon is more pronounced for *M. sativa* (N_2 -fixing species, lower tissue recalcitrance
544 due to lower C:N ratio) than for *L. perenne* (non N_2 -fixing species, higher tissue recalcitrance due to
545 higher C:N ratio), we may partially attribute this phenomenon to the higher mineralization rate of the
546 POM pool, that supplies the SILT+CLAY pool. However, in this case, we argue that POM is not the only
547 cause of the new C increase in the SILT+CLAY pool, as POM, consisting of plant residues rich in cellulous
548 and lignin, has a mean residence time much higher than six months, i.e., the experiment duration
549 (Cotrufo et al., 2015). Instead, it would be more likely that such new C increase in the SILT+CLAY pool in
550 the short term be a consequence of the higher microbial proliferation and activity induced by a higher
551 root exudation / microbial symbiosis with *Rhizobium* in *M. sativa* (Cotrufo et al., 2015). Such a
552 mechanism is incorporated as a part of the entombing effect in the recent “Soil Microbial Pump”
553 hypothesis (Liang et al. 2017). As an alternative pathway to the routinely characterized ex vivo C flux
554 from plant tissue to soil C pools via decomposition, the entombing effect refers to the in vivo C flux
555 from triggered microbial necromass and metabolites to the very stable soil C pools (Liang et al. 2017).
556 Although the estimation of microbial necromass was not available in this study and still remains a
557 technical bottleneck (Liang et al. 2019), we may expect a higher level of microbial necromass due to
558 the observed high GAM, H, DNA indicators in *M. sativa*, compared to *L. perenne* and bare soil.
559 Accordingly, our observed new C enhancement in both POM and the very stable SILT+CLAY C pools in
560 our experiment could be considered as novel data supporting the importance of the entombing effect.

561 **3.4.2. Generally a strong synergy exists between new and old carbon (Hypothesis 2)**

562 We found that soil that gained new C usually had a significantly smaller loss in old C. In topsoil sowed
563 with *M. sativa*, that had more new C input, , more labile tissues (low C:N content) and higher microbial
564 activity, old C loss in soil was much less than that in the vegetated subsoil treatment. This result is in
565 accordance with substrate utilization hypothesis developed by Cheng and Kuzyakov (2005) and

566 observed in an incubation experiment by De Graaf et al. (2010). However, to our knowledge, this is the
567 first time we observed this mechanism in an *in vivo* experiment. According to this hypothesis,
568 microorganisms prefer labile C to stable C, thus resulting in a limited consumption of old C, especially
569 old C protected by fine soil particles. This mechanism is observed in soils with high fertility and mineral
570 nutrients, and when the input of fresh new C is adequate, which is our case in the topsoil treatment.
571 However, when mineral nutrients are low and fresh C input is low and insufficient to switch substrate
572 utilization preference, the low input of C increases the activity of microbes, that augment the
573 consumption of old C (Cheng and Kuzyakov 2005; De Graaf et al. 2010), as in our subsoil treatment. In
574 addition to the preexisting hypothesis, due to the use of fractionation, we can argue that the
575 entombing effect in the soil microbial pump hypothesis (Liang et al., 2017) can expand the
576 comprehension of the synergetic pattern. We observed that the synergetic pattern between new C
577 and old C changes was largely due to the same pattern existing in the SILT+CLAY C pool that received
578 more than 50% of total soil C. Due to the entombing effect, the maintenance of old C content against
579 old C loss in the SILT+CLAY pool may be a consequence of increased microbial biomass relying on the
580 old C resource that consumes the old C in unprotected coarser fractions and transfers to the SILT+CLAY
581 fraction via entombing of microbial exudates, exopolysaccharides and necromass (Cotrufo et al. 2013;
582 Liang et al. 2017; Vidal et al., 2018). Accordingly, soil with a greater microbial biomass (in our study,
583 topsoil) may have more advantages to maintain the size of the stable C pool via entombing effect
584 (necromass, microbial exudates and exopolysaccharides). Such a kind of increase in C due to microbial
585 necromass based old C should not be considered a part of old C. However, to what extent the increase
586 in microbial necromass relies on old C and new C is unknown, hindering the validity of the speculation.
587 Overall, understanding the role of microbial necromass and its underlying mechanism is an important
588 scientific lacuna in soil ecology to explore in the future.

589

590 3.4.3. *Root traits influence new carbon gain and old carbon changes, and are strongly*
591 *mediated by soil variables (Hypothesis 3)*

592 The two plant species that we examined had contrasting functional root traits, i.e., SRL, diameter of
593 absorptive roots and C:N ratio that were negatively correlated with the gain of new C in the POM pool,
594 and with new C in the SILT+CLAY C pool, however not with high significance. While this finding may be
595 possibly due to the short-term experiment in which species impact is not yet fully exerted, it could also
596 be attributed to the nature of these traits. Functional traits such as C:N ratio, diameter of absorptive
597 roots, and SRL are classified as morpho-physio-phenological (MPP) traits according to Violle et al.,
598 (2007), and the impact of these functional traits can be compensated by the effect of biomass, i.e., a
599 performance trait (Violle et al., 2007). In agreement with this hypothesis, we found root biomass a
600 much better predictor of new C gain in every soil C pool compared to the C:N ratio and SRL.

601 We found that the effect of species on new C gain is much less pronounced in the subsoil than in the
602 topsoil treatments, although the disparity of trait values between the two species in subsoil was still
603 very clear. This result suggests that the effect of root traits on C sequestration is strongly mediated by
604 soil characteristics. In the previous studies working on similar subjects soil treatment was usually
605 excluded (Roumet et al., 2016; Henneron et al., 2019; Rossi et al. submitted, Chapter II, this thesis). In
606 this study, we used two soil types that were similar in granulometric texture, but greatly differed in
607 physical, chemical and biological qualities. Topsoil had greater initial C and N contents, aggregate
608 stability and soil biodiversity than subsoil, suggesting that better soil quality is a primordial factor in
609 influencing plant performance in C sequestration.

610 Compared to new C, Δ old C were generally much less sensitive to plant traits, including MPP traits e.g.,
611 C:N ratio, SRL and mean diameter and biomass. This result suggests that Δ old C does not share the
612 same mechanism with Δ new C and was less dependent on ex vivo C flux from plants. Compared to the
613 MPP traits, root biomass was a slightly better predictor of Δ old C . This result can also be explained by
614 the preferential substrate utilization hypothesis (Cheng and Kuzyakov, 2005) and the boosting effect
615 of root biomass on microbial proliferation and activity (Fontaine and Barot 2005, De Deyn et al. 2008).

616 Microbial communities may prefer consuming new C to old C, resulting in better maintenance of old
617 C.

618 *M. sativa*, as a N₂ fixing species increases microbial activity via symbiosis with *Rhizobium* bacteria
619 (Poirer *et al.* 2018), augmenting microbial exudation and input of exopolysaccharides in the SILT+CLAY
620 protected pool (Fehrmann and Weaver, 1978; Downie, 2010; Cotrufo *et al.*, 2013). The increased
621 biomass of *M. sativa* and its lower C:N ratio (due to its N fixing ability) increases the labile C input in
622 soil (Warembourg *et al.* 2003; Roumet *et al.* 2005; Hernández *et al.* 2017) again increasing
623 mineralization and deposition in the SILT+CLAY protected pool. Being able to differentiate fluxes of old
624 C and new C in soil allowed to observe the increased input of new C from N₂-fixing *M. sativa*. This
625 higher input, when analyzing the total ΔC , was hidden by the changes in old C that were soil dependent
626 and not species dependent. This result helps to explain why different studies have discrepant results
627 regarding the C storage from N₂ fixing and non N₂ fixing species, where not always N₂ fixing species
628 significantly increased ΔC compared to non N₂-fixing species (e.g. Binkley, 2005; Fornara and Tilman,
629 2008; Chapter II, this thesis). The higher input of new C that N₂ fixing species provided due to a higher
630 root biomass, lower C:N ratio and fastest growth, might have been hidden by soil dependent old C
631 changes.

632 Overall, our finding highlights the necessity of studying the effect of functional traits on C sequestration
633 in a more refined manner (i) differentiating soil C origins and pools for a given soil enables us to better
634 identify soil C flux pathways that are more susceptible to vegetation; (ii) including the effect of soil
635 type can allow us to determine the magnitude of influence of plant trait disparities so as to take into
636 account more complex effects of interaction between soil features and root traits in future
637 experimental design.

638

639 *3.4.4. Microbiological activity can explain the disparity in new C and old C changes*
640 *between topsoil and subsoil*

641 The soil C saturation theory states that a soil with lower amount of C in the fine SILT+CLAY particle
642 fraction has a higher potential for organomineral interactions and the derived C storage in the fine
643 SILT+CLAY C pool (Six et al 2002). Given the lower initial C content in the SILT+CLAY pool at t0 and the
644 significant slightly higher fine fraction ratio in subsoil, we expected a faster increase in new C in the
645 SILT+CLAY pool given the same amount of C input from biomass. Our results support the C saturation
646 theory to a certain extent, as the increase in new C in the SILT+CLAY per unit root biomass or length in
647 subsoil was slightly higher than that in topsoil but not significant (Fig. S5). This difference was
648 disproportionately less than the difference in initial C content between two soil types. We argue that
649 the fine fraction abundance and soil C saturation can have a positive influence on C stored via
650 organomineral interactions if other conditions, especially soil microbiological conditions are previously
651 met. Recent studies have highlighted the importance of considering the robustness of soil microbial
652 diversity as a soil quality indicator (Bouchez et al., 2016; Karimi et al., 2017), thus challenging the
653 conventional use of only physical and chemical soil quality indicators. In this study, we have shown
654 that microorganisms play a central role in the gain of new C and loss of old C in the SILT+CLAY pool.
655 The higher microbial activity and diversity in topsoil from t0 to t6 may compensate the less favorable
656 physical and chemical quality (lower fine fraction and higher initial C content) for C sequestration.
657 Therefore, if microbial communities are not considered in the prediction of soil C sequestration, results
658 will be flawed.

659 Along with greater microbial diversity, an increase in aggregate stability (MWD) and N content in
660 topsoil could also promote a synergetic effect that augments C sequestration. The physical protective
661 role of aggregates for C stock is widely documented (Hassink et al., 1992; Six et al., 2002; Chevallier et
662 al. 2004; Rasse et al. 2005; O'Brien et al., 2013; King et al., 2019). A high soil N content in topsoil will
663 also improve plant development and subsequent biomass, thus affecting C input and microbial

664 diversity. We suggest therefore, that a comprehensive indicator of soil health for plant performance
665 and C sequestration should incorporate physical, chemical and microbiological characteristics.

666

667 **3.4.5. Practical applications**

668 This study provides useful implications for future engineers to choose appropriate soil and species in
669 road embankment revegetation to favor C sequestration. First, with the dominant effect over months
670 of soil over species found in this study, choosing healthy and functional soil is of primary importance
671 for C sequestration. Topsoil has shown a clearly better performance in C sequestration than subsoil.
672 However, implementing topsoil over large scales is unrealistic when revegetating a site, because the
673 amount of topsoil is relatively limited and over-exploitation of topsoil may further provoke
674 environmental issues for the location where the topsoil is removed. Although subsoil has higher C
675 sequestration potential due to its lower initial C content, attention should be paid to the microbial
676 diversity and functioning in subsoil. Inoculation of soil with suitable microbial communities and
677 fertilizer would therefore be necessary to favor both revegetation and soil C sequestration (Dou et al.
678 2016, Guo et al., 2019).

679 Once soil quality is ensured, choosing appropriate species will be a bonus for boosting new C input and
680 protecting old C against priming. In our experiment that lasted 6 months, and so corresponds to the
681 initial planting stage in the field, *M. sativa* had a better performance than *L. perenne*, and also
682 enhanced soil aggregate stability, thus decreasing soil erodibility. However, the long-term effects of
683 revegetation on long-term soil C fates should also be investigated.

684

685 **3.5. CONCLUSIONS**

686 We designed an experiment with fully crossed treatments between vegetation and soil in microcosms
687 and used stable isotopic (¹³C) labelling to assess new C input and old C changes in the soil system. We

688 revealed the distinct fates of new C and old C in soil, in both absolute values and relative values, among
689 different soil C pools related to soil fractions, highlighting:

- 690 • The major influence of soil, with the topsoil treatment having a higher C storage capacity
691 compared to the subsoil treatment due to higher soil quality that increase biomass
692 development and C input in POM C pool, and higher microbial biomass and activity that
693 favors entombing of C in the stable SILT+CLAY pool.
- 694 • We evidence the necessity of considering both C fluxes in pools associated to soil fractions
695 and origin of C (new and old C) when studying C dynamics in soil. An example being old C
696 decreasing in the POM C pool and increasing in the SILT+CLAY C pool in the topsoil
697 treatment. If only ΔC or $\Delta \text{old C}$ in bulk soil was considered no changes would have been
698 observed, and the old C would have been considered inactive, masking the real mechanisms
699 behind soil C sequestration in the topsoil treatment.
- 700 • New C increased not only in the POM C pool, but also in the more stable SILT+CLAY pool.
701 Given the short duration of the experiment, this flux is probably due to entombing of
702 microbial necromass and microbial exudates and exopolysaccharides more than
703 degradation of POM.
- 704 • New C and old C covaried similarly in the SILT+CLAY C pool. A higher increase of new C
705 resulted in a lower decrease of old C due to a microbiological switch of substrate
706 preference.
- 707 • Changes in new and old C differed depending on plant and soil characteristics. N_2 fixing *M.*
708 *sativa* higher root biomass labile input in soil increased the amount of new C in soil. N_2 fixing
709 *M. sativa* also increased microbial biomass and activity that favor the mineralization of C
710 from exudates or POM and transport into the SILT+CLAY protected fraction. Root biomass
711 was the trait better correlated with new C input in soil C pools.

712 • The lack of microbiological activity and the lower root biomass decreased the transfer of
713 new C in the SILT+CLAY pool in the subsoil treatment. For this reason, the lower C saturation
714 did not increase the total new C content in SILT+CLAY pool in the subsoil treatment as
715 expected. When normalized for the root biomass, however, the system showed the
716 opposite behavior, and the subsoil treatment had a higher amount of new C stored in
717 SILT+CLAY for g of root. We argue that C saturation effect might be present but is subdued
718 to soil fertility and microbiological activity.

719 Such a fundamental understanding of plant-soil interactions may help us to better optimize soil and
720 vegetation management for road embankment revegetation. Long-term observations are now needed
721 for a better assessment of the roles of plant and soil characteristics in soil C cycling and long-term
722 sequestration.

723

724 REFERENCES

- 725 Balesdent, J. & Mariotti, A. 1996. Measurement of soil organic matter turnover using ^{13}C natural
726 abundances. In: *Mass Spectrometry of Soils* (eds T.W. Boutton & S. Yamasaki), pp. 83-111.
727 Marcel Dekker Inc., New York.
- 728 Bardgett, R.D., Mommer, L., Vries, F.T. De., 2014. Going underground: root traits as drivers of
729 ecosystem processes. *Trends in Ecology & Evolution* 29, 692–699.
- 730 Beare, M.H., Lawrence-Smith, E.J., Curtin, D., Kelliher, F.M., 2016. Potential use of full inversion tillage
731 during pasture renewal to increase soil carbon storage in New Zealand. Ministry for Primary
732 Industries - Soil C Workshop.
- 733 Besnard, E., Chenu, C., Balesdent, J., Puget, P., Arrouays, D., 1996 Fate of particulate organic matter in
734 soil aggregates during cultivation. *Eur. J. Soil Sci.* 47, 495–503.
- 735 Binkley, D., 2005. How nitrogen-fixing trees change soil carbon. In: Binkley, D., Menyailo, O. (Eds.), *Tree
736 Species Effects on Soils: Implications for Global Change*. NATO Science Series. Kluwer Academic
737 Publishers, Dordrecht, pp. 155–164.
- 738 Blagodatskaya, E., Kuzyakov, Y., 2008. Mechanisms of real and apparent priming effects and their
739 dependence on soil microbial biomass and community structure: Critical review. *Biology and
740 Fertility of Soils* 45, 115–131. doi:10.1007/s00374-008-0334-y
- 741 Bohórquez, J., Mcgenity, T.J., Papaspyrou, S., García-robledo, E., 2017. Different types of diatom-
742 derived extracellular polymeric substances drive changes in heterotrophic bacterial
743 communities from intertidal sediments 8. *Frontiers in Microbiology* 2017; 8 - 245.
- 744 Bouchez, T., Bliex, A.L., Dequiedt, S., Domaizon, I., Dufresne, A., Ferreira, S., Godon, J.J., Hellal, J.,
745 Joulain, C., Quaiser, A. Martin-Laurent, F., (2016). Molecular microbiology methods for
746 environmental diagnosis. *Environmental Chemistry Letters*, 14(4), pp.423-441.
- 747 Bradford M.A., Tordoff G.M., Black H.I.J, Cook R., Eggers T., Garnett M.H., Grayston S.J., Hutcheon K.A.,
748 Ineson P., Newington J.E. et al., 2007, 'Carbon dynamics in a model grassland with functionally
749 different soil communities', *Functional Ecology* 21, 690–697.
- 750 Campbell, C.D., Chapman, S.J., Cameron, C.M., Davidson, M.S., Potts, J.M., 2003. A rapid microtiter
751 plate method to measure carbon dioxide evolved from carbon substrate amendments so as to
752 determine the physiological profiles of soil microbial communities by using whole soil. *Applied
753 and Environmental Microbiology* 69, 3593–3599.
- 754 Campbell C.D., Cameron C.M., Bastias B.A., Chen C., Cairney J.W.G., 2008, Long term repeated burning
755 in a wet sclerophyll forest reduces fungal and bacterial biomass and responses to carbon
756 substrates. *Soil Biol Biochem* 40:2246–2252.
- 757 Cardinael, R., Chevallier, T., Barthès, B.G., Saby, N.P.A., Parent, T., Dupraz, C., Bernoux, M., Chenu, C.,
758 2015. Geoderma Impact of alley cropping agroforestry on stocks, forms and spatial distribution
759 of soil organic carbon — A case study in a Mediterranean context. *Geoderma* 259–260, 288–
760 299. doi:10.1016/j.geoderma.2015.06.015

- 761 Chabbi, A., Kögel-Knabner, I., Rumpel, C., 2009 Stabilised carbon in subsoil horizons is located in
762 spatially distinct parts of the soil profile. *Soil Biology and Biochemistry* 41:256–271
- 763 Chapman S.J., Campbell C.D., Artz R.R.E., 2007, Assessing CLPPs using MicroReSp (TM)—a comparison
764 with biology and multi-SIR. *J Soils Sediments* 7:406–410
- 765 Cheng, W., Kuzyakov, Y., 2005. Root effects on soil organic matter decomposition. In: S. Wright, S.,
766 Zobel, R. (Eds.), *Roots and Soil Management: Interactions Between Roots and the Soil*. Agronomy
767 Monograph No. 48, American Society of Agronomy, Madison, Wisconsin, USA 119–143.
- 768 Cheng, W.X., Johnson, D.W., Fu, S.L., 2003. Rhizosphere effects on decomposition: controls of plant
769 species, phenology, and fertilization. *Soil Science Society of America Journal* 67 (5), 1418–1427.
- 770 Chevallier, T., Blanchart, E., Albrecht, A., Feller, C., 2004. The physical protection of soil organic carbon
771 in aggregates: A mechanism of carbon storage in a Vertisol under pasture and market gardening
772 (Martinique, West Indies). *Agriculture, Ecosystems and Environment* 103, 375–387
- 773 Cotrufo, M.F., Soong, J.L., Horton, A.J., Campbell, E.E., Haddix, M.L., Wall, D.H., Parton, W.J., 2015.
774 Formation of soil organic matter via biochemical and physical pathways of litter mass loss.
775 *Nature Geoscience* 8, 776–779. doi:10.1038/ngeo2520
- 776 Cotrufo, M.F., Wallenstein, M.D., Boot, C.M., Deneff, K., Paul, E., 2013. The Microbial Efficiency-Matrix
777 Stabilization (MEMS) framework integrates plant litter decomposition with soil organic matter
778 stabilization: Do labile plant inputs form stable soil organic matter? *Global Change Biology* 19,
779 988–995.
- 780 Creamer R.E., Stone D., Berry P., Kuiper I., 2016, Measuring respiration profiles of soil microbial
781 communities across Europe using MicroResp™ method. *Appl Soil Ecol* 97:36–43
- 782 De Deyn, G.B., Cornelissen, J.H.C., Bardgett, R.D., 2008. Plant functional traits and soil carbon
783 sequestration in contrasting biomes. *Ecology Letters* 11, 516–531.
- 784 De Graaff, M.A., Classen, A.T., Castro, H.F., Schadt, C.W., 2010. Labile soil carbon inputs mediate the
785 soil microbial community composition and plant residue decomposition rates. *New Phytologist*
786 188, 1055–1064
- 787 Dou, X., He, P., Cheng, X., Zhou, W., 2016. Long-term fertilization alters chemically-separated soil
788 organic carbon pools: Based on stable C isotope analyses. *Scientific Reports* 6, 1–9.
789 doi:10.1038/srep19061
- 790 Downie, J.A., 2010. The roles of extracellular proteins, polysaccharides and signals in the interactions
791 of rhizobia with legume roots 34, 150–170. doi:10.1111/j.1574-6976.2009.00205.x
- 792 Duddigan S., Shaw L.J., Alexander P.D., Collins C.D., 2019, A Comparison of Physical Soil Organic
793 Matter Fractionation Methods for Amended Soils, *Applied and Environmental Soil Science*
- 794 Esseinstat, D.M., 1991 On the relationship between root length and the rate of root proliferation: a
795 field study using citrus rootstocks. *New Phytol.* 188, 63–68.
- 796 Fehrmann, R., Weaver, R., 1978. Scanning electron microscopy of *Rhizobium* spp. ad-hering to fine silt
797 particles. *Soil Science Society of America Journal* 42, 279–281.

798 Fontaine, S., Bardoux, G., Abbadie, L., Mariotti, A., 2004. Carbon input to soil may decrease soil carbon
799 content. *Ecology Letters* 7, 314–320

800 Fontaine, S., Barot, S., 2005. Size and functional diversity of microbe populations control plant
801 persistence and long-term soil carbon accumulation. *Ecology Letters* 8, 1075e1087.

802 Fornara, D. A. and Tilman, D.: Plant functional composition influences rates of soil carbon and nitrogen
803 accumulation, *J. Ecol.*, 96, 314–322

804 Gavinelli, E., Feller, C., Larré - Larrouy, M.C., Bacye, B., Djegui, Z., Nzila, J.D., 1995. Routine method to
805 study soil organic matter by particle - size fractionation: Examples for tropical soils. *Soil Science*
806 *Plant Analysis* 26(11&12), 1749-1760

807 Guo, Z., Zhang, Z., Zhou, H., Wang, D., Peng, X., 2019. The effect of 34-year continuous fertilization on
808 the SOC physical fractions and its chemical composition in a Vertisol. *Scientific Reports* 9, 1–10.

809 Harrell, F.E., 2007. Package 'Hmisc'. Harrell Miscellaneous

810 Hanson P.J., Edwards N.T., Garten C.T., Andrews J.A., 2000, 'Separating root and soil microbial
811 contributions to soil respiration: A review of methods and observations', *Biogeochemistry*, 48,
812 115-146

813 Hassink, J., 1992. Effects of soil texture and structure on carbon and nitrogen mineralization in
814 grassland soils 126–134.

815 Henneron, L., Picon-cochard, C., 2019. Plant economic strategies of grassland species control soil
816 carbon dynamics through rhizodeposition.

817 Hernández, M.A., Romero, J., Jaime, C., León-pulido, J., 2017. Lignocellulosic Biomass from Fast-
818 Growing Species in Colombia and their Use as Bioresources for Biofuel Production 58, 541–546.

819 Höggberg P., Höggberg M.N., Göttlicher S.G., Betson N.R., Keel S.G., Metcalf D.B., Campbell C.,
820 Schindlbacher A., Hurry V., Lundmark T. et al., 2008, 'High temporal resolution tracing of
821 photosynthate carbon from the tree canopy to forest soil microorganisms', *New Phytologist*,
822 220–228.

823 Hungate BA, et al. 1996'Detecting changes in soil carbon in CO₂ enrichment experiments.' *Plant Soil*
824 187, 135–145

825 Jones, D.L., Magthab, E.A., Gleeson, D.B., Hill, P.W., Sánchez-rodríguez, A.R., Roberts, P., Ge, T.,
826 Murphy, D. V, 2018. Microbial competition for nitrogen and carbon is as intense in the subsoil
827 as in the topsoil 117, 72–82.

828 Karimi, B., Maron, P.A., Boure, N.C.P., Bernard, N., Gilbert, D. Ranjard, L., (2017). Microbial diversity
829 and ecological networks as indicators of environmental quality. *Environmental Chemistry*
830 *Letters*, pp.1-17.

831 King, A.E., Congreves, K.A., Deen, B., Dun, K.E., Voroney, R.P., Wagner-riddle, C., 2019. Quantifying the
832 relationships between soil fraction mass , fraction carbon , and total soil carbon to assess
833 mechanisms of physical protection. *Soil Biology and Biochemistry* 135, 95–107.

834 Kong A. Y. Y., Six J., Bryant D. C., Denison R. F., van Kessel C., 2005, "The relationship between carbon
835 input, aggregation, and soil organic carbon stabilization in sustainable cropping systems," *Soil*
836 *Science Society of America Journal* 69 (4), 1078–1085,

837 Kogel-Knabner, I., 2002. The macromolecular organic composition of plant and microbial residues as
838 inputs to soil organic matter. *Soil Biology and Biochemistry* 34, 139-162

839 Kuzyakov, Y., Domanski, G., 2000. Carbon input by plants into the soil. Review. *Journal of Plant*
840 *Nutrition and Soil Science* 163, 421–431

841 Leake J.R., Ostle N.J., Rangel-Castro J.I., Johnson D., 2006, 'Carbon fluxes from plants through soil
842 organisms determined by field ¹³CO₂ pulse labeling in an upland grassland', *Applied Soil Ecology*
843 33, 152–175.

844 Le Bissonnais, Y., 2016. Aggregate stability and assessment of soil crustability and erodibility: I. Theory
845 and methodology. *European Journal of Soil Science* 67, 11–21

846 Liang, C., Amelung, W., Lehmann, J., Kästner, M., 2019. Quantitative assessment of microbial
847 necromass contribution to soil organic matter. *Global Change Biology*.

848 Liang, C., Schimel, J.P., Jastrow, J.D., 2017. The importance of anabolism in microbial control over soil
849 carbon storage. *Nature Microbiology* 2, 1–6.

850 Lorenz, K., Lal, R., 2005 The depth distribution of soil organic carbon in relation to land use and
851 management and the potential of carbon sequestration in subsoil horizons

852 McCormack, L.M., Dickie, I.A., Eissenstat, D.M., Fahey, T.J., Fernandez, C.W., Guo, D., Erik, A., Iversen,
853 C.M., Jackson, R.B., 2015. Redefining fine roots improves understanding of below-ground
854 contributions to terrestrial biosphere processes. *New Phytologist* 207, 505–518.

855 McDowell N.G., Bowling D.R., Bond B.J. et al., 2004, 'Response of the carbon isotopic content of
856 ecosystem, leaf, and soil respiration to meteorological and physiological driving factors in a *Pinus*
857 *ponderosa* ecosystem.' *Global Biogeochemical Cycles*, 18, GB1013.

858 Meharg A.A., 1994, 'A critical review of labelling techniques used to quantify rhizosphere carbon-flow',
859 *Plant and Soil* 166, 55-62

860 Minasny, B., Malone, B.P., McBratney, A.B., Angers, D.A., Arrouays, D., Chambers, A., Chaplot, V., Chen,
861 Z.S., Cheng, K., Das, B.S., Field, D.J., Gimona, A., Hedley, C.B., Hong, S.Y., Mandal, B., Marchant,
862 B.P., Martin, M., McConkey, B.G., Mulder, V.L., O'Rourke, S., Richer-de-Forges, A.C., Odeh, I.,
863 Padarian, J., Paustian, K., Pan, G., Poggio, L., Savin, I., 2017, Soil carbon 4 per mille. *Geoderma*
864 292, 59–86.

865 Murray, P.J., Hatch, D.J., Dixon, E.R., Stevens, R.J., Laughlin, R.J., Jarvis, S.C., 2004. Denitrification
866 potential in a grassland subsoil : effect of carbon substrates 36, 545–547.

867 O'Brien, S.L., Jastrow, J.D., 2013. Physical and chemical protection in hierarchical soil aggregates
868 regulates soil carbon and nitrogen recovery in restored perennial grasslands. *Soil Biology and*
869 *Biochemistry* 61, 1–13

870 Oksanen, J., Blanchet, F.G., Friendly, M., Kindt, R., Legendre, P., McGlenn, D., Minchin, P.R., O'Hara,
871 R.B., Simpson, G.L., Solymos, P., Henry, M., Stevens, H., Szoecs, E., Wagner, H., 2019. Package
872 'vegan'. Community Ecology Package

873 Prieto, I., Stokes, A., Roumet, C., 2016. Root functional parameters predict fine root decomposability
874 at the community level. *Journal of Ecology* 104, 725–733

875 Rasse, D.P., Rumpel, C., Dignac, M., 2005. Is soil carbon mostly root carbon ? Mechanisms for specific
876 stabilization. *Plant and Soil* 269, 341–356

877 Rees, R.M., Bingham, I.J., Baddeley, J.A., Watson, C.A., 2005. The role of plants and land management
878 in sequestering soil carbon in temperate arable and grassland ecosystems. *Geoderma* 128, 130–
879 154

880 Renault, P., Ben-Sassi, M., Bérard, A., 2013, Improving the MicroResp™ substrate-induced respiration
881 method by a more complete description of CO₂ behavior in closed incubation wells. *Geoderma*,
882 207-208

883 Rohošková M., Valla M., 2004, 'Comparison of two methods for aggregate stability measurement - A
884 review', *Plant Soil and Environment* 50(8):379-382

885 Roumet, C., Birouste, M., Picon-Cochard, C., Ghestem, M., Osman, N., Vrignon-Brenas, S., Cao, K. fang,
886 Stokes, A., 2016. Root structure-function relationships in 74 species: Evidence of a root
887 economics spectrum related to carbon economy. *New Phytologist* 210, 815–826.

888 Rumpel, C., Kögel-Knabner, I., 2011. Deep soil organic matter-a key but poorly understood component
889 of terrestrial C cycle. *Plant and Soil* 338, 143–158.

890 Rygielwicz P.T., Andersen C.P., 1994, 'Mycorrhizae alter quality and quantity of carbon allocated below
891 ground.', *Nature* 369, 58–60

892 Saenger, A., Cécillon, L., Poulénard, J., Bureau, F., De Daniéli, S., Gonzalez, J.M., Brun, J.J., 2015.
893 Surveying the carbon pools of mountain soils: A comparison of physical fractionation and Rock-
894 Eval pyrolysis. *Geoderma* 241–242, 279–288.

895 Sarker, J.R., Singh, B.P., He, X., Fang, Y., Li, G.D., Collins, D., Cowie, A.L. 2017. Tillage and nitrogen
896 fertilization enhanced belowground carbon allocation and plant nitrogen uptake in a semi-arid
897 canola crop–soil system. *Nature* 7, 1-13

898 Shihan, A., Hättenschwiler, S., Milcu, A., Joly, F., Santonja, M., Fromin, N., 2017. Changes in soil
899 microbial substrate utilization in response to altered litter diversity and precipitation in a
900 Mediterranean shrubland. *Biology and Fertility of Soils* 53, 171–185.

901 Six, J., Feller, C., Denef, K., Ogle, S.M., Moraes Sa, J.C., Albrecht, A. 2002. Soil organic matter, biota and
902 aggregation in temperate and tropical soils effects of no-tillage. *Agronomie* 22, 755–775.

903 Six J. and Paustian K., 2014, "Aggregate-associated soil organic matter as an ecosystem property and a
904 measurement tool," *Soil Biol. Biochem*, 68, A4–A9

- 905 Sokol, N.W., Kuebbing, S.E., Karlsen-ayala, E., Bradford, M.A., 2019. Evidence for the primacy of living
906 root inputs, not root or shoot litter, in forming soil organic carbon. *New Phytologist* 221, 233–
907 246.
- 908 Sollins, P., Hofmann, P., and Caldwell, B.A., 1996. Stabilization and destabilization of soil organic
909 matter: mechanisms and controls. *Geoderma* 74, 65–105.
- 910 Staddon, P.L., 2004. Carbon isotopes in functional soil ecology. *Trends in Ecology and Evolution* 19,
911 148–154.
- 912 Stewart, C.E., Paustian, K., Conant, R.T., Plante, A.F., Six, J., 2007. Soil carbon saturation: Concept,
913 evidence and evaluation. *Biogeochemistry* 86, 19–31
- 914 Stumm, W., Morgan, J.J., 1996. Dissolved carbon dioxide, In: Shnoor, J.L., Zehnder, A.J.B. (Eds.), *Aquatic
915 chemistry. Chemical Equilibria and Rates in Natural Waters*, 3rd edition. John Wiley & Sons, New
916 York, pp. 148–205
- 917 Subke J.A., Hahn V., Battipaglia G. et al. 2004, 'Feedback interactions between needle litter
918 decomposition and rhizosphere activity'. *Oecologia*, 139, 551–559.
- 919 Taylor, J.P., Wilson, B., Mills, M.S., Burns, R.G., 2002. Comparison of microbial numbers and enzymatic
920 activities in surface soils and subsoils using various techniques. *Soil Biology and Biochemistry* 34,
921 387–401.
- 922 Tisdall, J. M., Oades, J. M., 1979. Stabilization of soil aggregates by the root systems of ryegrass.
923 *Australian Journal of Soil Research* 29, 729–743.
- 924 Tisdall, J.M., Oades, J.M., 1982. Organic matter and water-stable aggregates in soils. *J. Soil Sci.* 33, 141–
925 163.
- 926 Torn, M.S., Swanston, C.W., Castanha, C., Trumbore, S.E., 2009. Storage and turnover of organic
927 matter in soil. In: Senesi, N., Xing, B., Huang, P.M. (Eds.), *Biophysico-Chemical Processes
928 Involving Natural Nonliving Organic Matter in Environmental System*. John Wiley & Sons, Inc.,
929 Hoboken, NJ, USA, pp. 215–269.
- 930 Trumbore S., 2006, 'Carbon respired by terrestrial ecosystems – recent progress and challenges',
931 *Global Change Biology*, 12, 141-153
- 932 Vidal, A., Hirte, J., Bender, S.F., Mayer, J., Gattinger, A., Höschel, C., Schädler, S., Iqbal, T.M., Mueller,
933 C.W., 2018. Linking 3D Soil Structure and Plant-Microbe-Soil Carbon Transfer in the Rhizosphere.
934 *Frontiers in Environmental Science* 6, 1–14.
- 935 Violle, C., Navas, M.L., Vile, D., Kazakou, E., Fortunel, C., Hummel, I., Garnier, E., 2007 Let the concept
936 of trait be functional! *Oikos*, 116, 882–892.
- 937 von Lutzow, M., Kogel-Knabner, I., Ekschmitt, K., Matzner, E., Guggenberger, G., Marschner, B., Flessa,
938 Hassink J 1997 The capacity of soils to preserve organic C and N by their association with clay
939 and silt particles. *Plant Soil* 191, 77–87.
- 940 Warembourg, F.R., Roumet, C., Lafont, F., 2003. Differences in rhizosphere carbon-partitioning among
941 plant species of different families 347–357.

943 FIGURES AND TABLES

944 **Table 1:** Root, microbial and soil characteristics analyzed at time 0, after 183 days of experiment (time 6 months),
 945 and the difference between time 0 and time 6, for *M. sativa*, *L. perenne* sowed on tospoil and subsoil, plus bare soil
 946 controls. Root traits: Root biomass (g), specific root length (SRL, m g⁻¹), diameter of absorptive roots (mm),
 947 adsorptive roots C:N ratio; Microbial characteristics: global metabolic activity (GMA, µgC-CO₂ g⁻¹ soil h⁻¹), Shannon
 948 metabolic diversity (H), concentration of DNA in solution as proxy for microbial biomass (DNA, ng µL⁻¹); Soil
 949 characteristics: mean weight diameter of aggregates (MWD, mm), soil nitrogen content (Soil N, mg N g⁻¹ soil),
 950 percentage of fine fraction <20µm in soil (FF, %).

		SUBSOIL			TOPSOIL			
		Bare soil	<i>L. perenne</i>	<i>M. sativa</i>	Bare soil	<i>L. perenne</i>	<i>M. sativa</i>	
Time 0	<i>Micorbial characteristics</i>	GMA (µgC-CO ₂ g ⁻¹ soil h ⁻¹)	7.56±1.1	-	-	8.68±1.94	-	-
		H (-)	0.85±0.17	-	-	1.14±0.05	-	-
		DNA concentration (ng µL ⁻¹)	1.00±0.00	-	-	13.67±3.06	-	-
	<i>Soil characteristics</i>	MWD (mm)	0.82±0.03	-	-	1.55±0.02	-	-
		Soil N (mg N g ⁻¹ soil)	0.75±0.04	-	-	1.25±0.06	-	-
		FF (%)	51.00±1.00	-	-	43.00±1.00	-	-
<i>Root traits</i>	Root biomass (g)	-	1.05±0.34	5.13±1.36	-	4.09±1.43	17.53±2.03	
	SRL absorptive roots (m g ⁻¹ soil)	-	34.92±4.72	14.77±7.87	-	23.25±2.98	10.25±0.57	
	Diameter absorptive roots (mm)	-	0.09±0.02	0.27±0.04	-	0.10±0.02	0.26±0.01	
	Absorptive roots C:N	-	90.78±15.53	20.12±2.42	-	51.48±10.73	20.23±1.31	
Time 6 months	<i>Micorbial characteristics</i>	GMA (µgC-CO ₂ g ⁻¹ soil h ⁻¹)	6.77±0.72	7.41±2.50	5.98±1.06	7.41±1.72	11.69±1.02	19.06±4.21
		H (-+)	0.78±0.07	0.93±0.08	0.90±0.04	1.16±0.01	1.17±0.00	1.17±0.00
		DNA concentration (ng µL ⁻¹)	4.00±2.22	3.00±1.41	5.20±1.64	18.40±5.90	18.40±5.59	19.00±4.32
	<i>Soil characteristics</i>	MWD (mm)	0.84±0.10	0.78±0.07	0.89±0.08	1.64±0.08	2.17±0.20	2.07±0.29
		Soil N (mg N g ⁻¹ soil)	0.63±0.05	0.65±0.08	0.65±0.05	1.19±0.14	1.12±0.10	1.23±0.10
		FF (%)	49.84±1.17	50.62±1.16	50.77±0.58	42.24±1.26	42.01±1.31	41.87±1.42
Δ t0-t6	<i>Micorbial characteristics</i>	GMA (µgC-CO ₂ g ⁻¹ soil h ⁻¹)	3.00±2.22	-0.16±2.73	-1.59±1.53	-1.27±2.59	3.01±2.19	10.39±4.63
		H (-)	-0.07±0.18	0.08±0.18	0.06±0.17	0.02±0.05	0.03±0.05	0.03±0.05
		DNA concentration (ng µL ⁻¹)	3.00±2.22	2.00±1.41	4.20±1.64	4.73±6.64	4.73±6.37	5.33±5.29
	<i>Soil characteristics</i>	MWD (mm)	0.02±0.1	-0.03±0.08	0.08±0.08	0.1±0.08	0.62±0.20	0.52±0.29
		Soil N (mg N g ⁻¹ soil)	-0.11±0.07	-0.1±0.09	-0.1±0.07	-0.06±0.15	-0.13±0.12	-0.02±0.12
		FF (%)	-0.01±0.02	-0.01±0.01	0.00±0.01	0.00±0.02	-0.01±0.02	-0.01±0.02

951 For Δt0-t6 the red values indicate a loss in 6 months, black value a gain

952

953 **Table 2:** Statistical analysis of the effect of treatments (soil and species) on on root, microbial and soil characteristics
 954 analyzed after 183 days of experiment for *M. sativa*, *L. perenne* sowed on topsoil and subsoil, plus bare soil controls.
 955 Root traits: Root traits: Root biomass (g), specific root length (SRL, m g⁻¹), diameter of absorptive roots (mm),
 956 adsorptive roots C:N ratio; Microbial characteristics: global metabolic activity (GMA, µgC-CO₂ g⁻¹ soil h⁻¹), Shannon
 957 metabolic diversity (H), concentration of DNA in solution as proxy for microbial biomass (DNA, ng µL⁻¹); Soil
 958 characteristics: mean weight diameter of aggregates (MWD, mm), soil nitrogen content (Soil N, mg N g⁻¹ soil),
 959 percentage of fine fraction <20µm in soil (FF, %).. Data where normal according to the Shapiro-Wilk test and the
 960 ANOVA test was utilized to asses statistical differences.

	Soil	Variable	df	F	p
Effect of treatment	Topsoil	Root biomass	1,7	136.8	<0.001***
		SRL absorptive roots	1,6	73.33	<0.001***
		Diameter absorptive roots	1,6	224.6	<0.001***
		Absorptive roots C:N	1,7	32.61	<0.001***
		GMA	2,11	24.19	<0.001***
		H	2,11	5.925	0.0179 *
		DNA concentration	2,11	0.018	0.983
		MWD	2,11	9.953	0.00341 **
		Soil N	2,11	1.168	0.347
	FF	2,11	0.034	0.967	
	Subsoil	Root biomass	1,8	42.13	<0.001***
		SRL absorptive roots	1,7	22.98	0.00198 **
		Diameter absorptive roots	1,7	64.44	<0.001***
		Absorptive roots C:N	1,7	104	<0.001***
		GMA	2,11	0.914	0.429
		H	2,11	6.827	0.0118 *
		DNA concentration	2,11	2.181	0.159
MWD		2,11	2.263	0.15	
Soil N		2,11	0.079	0.925	
FF	2,11	0.662	0.535		
Effect of Soil	<i>M.sativa</i>	Root biomass	1,7	120.9	<0.001***
		SRL absorptive roots	1,6	1.314	0.295
		Diameter absorptive roots	1,6	0.098	0.765
		Absorptive roots C:N	1,7	0.006	0.939
		GMA	1,7	46.22	<0.001***
		H	1,7	150.6	<0.001***
		DNA concentration	1,7	44.35	<0.001***
		MWD	1,7	80.22	<0.001***
		Soil N	1,7	129.6	<0.001***
	FF	1,7	159.8	<0.001***	
	<i>L.perenne</i>	Root biomass	1,8	21.33	<0.001***
		SRL absorptive roots	1,7	18.3	0.00366 **
		Diameter absorptive roots	1,7	0.738	<0.001***
		Absorptive roots C:N	1,7	20.3	0.00278 **
		GMA	1,8	12.57	0.00757 **
		H	1,8	40.75	<0.001***
		DNA concentration	1,8	35.61	<0.001***
		MWD	1,8	220.4	<0.001***
		Soil N	1,8	72.42	<0.001***
	FF	1,8	132.1	<0.001***	
	Bare soil	GMA	1,7	0.398	0.548
		H	1,7	149	<0.001***
		DNA concentration	1,7	18.83	0.0034 **
		MWD	1,7	178.9	<0.001***
		Soil N	1,7	56.59	<0.001***
		FF	1,7	45.36	<0.001***

961

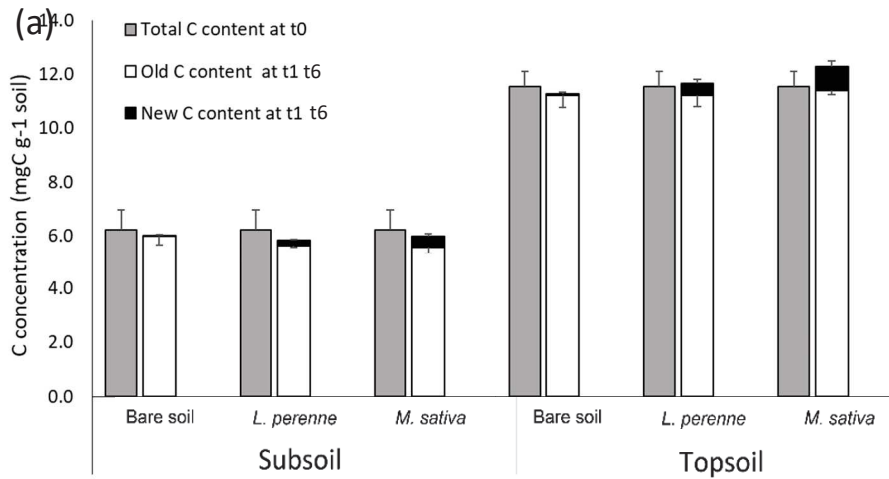
962

963 **Table 3:** Pearson's correlation coefficients (r) showing relationships between microbial characteristics, root
 964 variables, soil structural characteristics and New, Old C, and ΔC in different soil C pools. Root traits: Root biomass
 965 (g), specific root length (SRL, m g⁻¹), diameter of absorptive roots (mm), absorptive roots C:N ratio; Microbial
 966 characteristics: global metabolic activity (GMA, $\mu\text{gC-CO}_2 \text{ g}^{-1} \text{ soil h}^{-1}$), Shannon metabolic diversity (H),
 967 concentration of DNA in solution as proxy for microbial biomass (DNA, ng μL^{-1}); Soil characteristics: mean weight
 968 diameter of aggregates (MWD, mm), soil nitrogen content (Soil N, mg N g⁻¹ soil), percentage of fine fraction <20 μm
 969 in soil (FF, %). Data where normal according to the Shapiro-Wilk test and the ANOVA test was utilized to asses
 970 statistical differences.

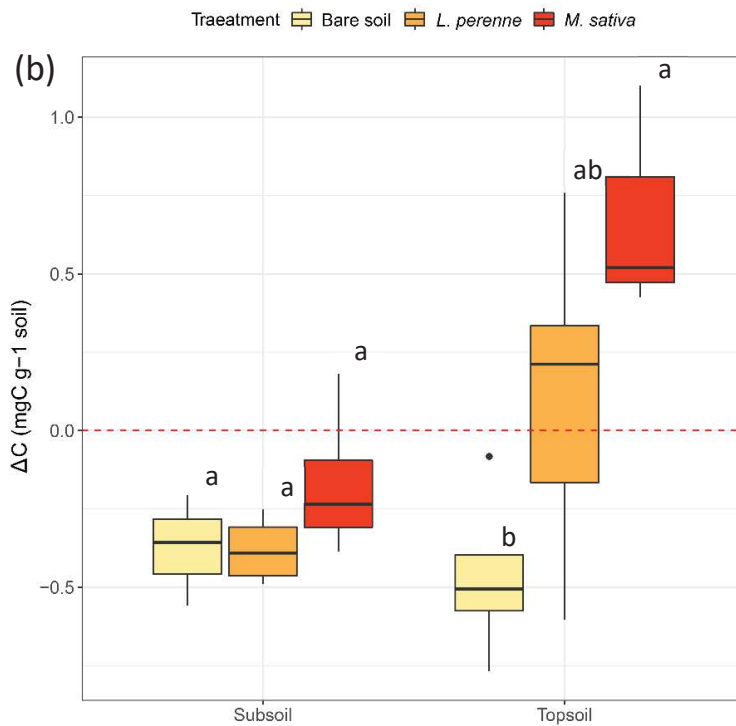
	Root biomass (R_bio)	Specific root length of absorptive roots (SRL_AD)	Diameter of absorptive roots (Diam_AD)	C:N ratio of absorptive roots(C:N_A D)	Global metabolic activity (GMA)	Shannon metabolic diversity index (H)	Microbial DNA concentration (DNA)	Aggregates mean weight diameter (MWD)	Soil nitrogen (Soil_N)	Fine fraction percentage (FF)
<i>NewC_{POM}</i>	0.77***	-0.69**	0.59**	-0.66**	0.57*	0.34	0.53*	0.36	0.43	-0.36
<i>NewC_{finePOM}</i>	0.57*	-0.4	0.06	-0.39	0.71***	0.90***	0.87***	0.97***	0.94***	-0.94***
<i>NewC_{silt}</i>	0.60**	-0.37	0.06	-0.35	0.73***	0.86***	0.85***	0.94***	0.94***	-0.90***
<i>NewC_{silt+clay}</i>	0.83***	-0.61**	0.45	-0.57*	0.84***	0.69**	0.71***	0.74***	0.82***	-0.76***
<i>NewC_{SUM}</i>	0.88***	-0.73***	0.56*	-0.69**	0.76***	0.57*	0.71***	0.61**	0.69**	-0.62**
<i>OldC_{POM}</i>	0.25	-0.08	-0.08	-0.04	0.38	0.53*	0.38	0.57*	0.59**	-0.57*
<i>OldC_{finePOM}</i>	0.58**	-0.3	0.14	-0.17	0.51*	0.36	0.33	0.38	0.43	-0.38
<i>OldC_{silt}</i>	0.06	-0.2	0.05	-0.17	-0.09	0.05	0.05	-0.02	-0.11	0.02
<i>OldC_{silt+clay}</i>	-0.55*	0.28	0	0.21	-0.71***	-0.83***	-0.70***	-0.87***	-0.87***	0.86***
<i>OldC_{SUM}</i>	-0.44	0.24	-0.07	0.23	-0.59**	-0.57*	-0.60**	-0.58**	-0.59**	0.56*
ΔC_{POM}	0.02	-0.13	0.24	-0.17	-0.16	-0.36	-0.16	-0.39	-0.38	0.39
$\Delta C_{finePOM}$	-0.47*	0.22	-0.13	0.09	-0.37	-0.17	-0.37	-0.17	-0.24	0.18
ΔC_{silt}	0.01	0.16	-0.04	0.13	0.17	0.05	0.17	0.12	0.21	-0.12
$\Delta C_{silt+clay}$	0.60**	-0.33	0.05	-0.26	0.74***	0.83***	0.74***	0.87***	0.89***	-0.87***
ΔC_{SUM}	0.72***	-0.52*	0.33	-0.50*	0.74***	0.63**	0.74***	0.66**	0.70***	-0.65**

971

972

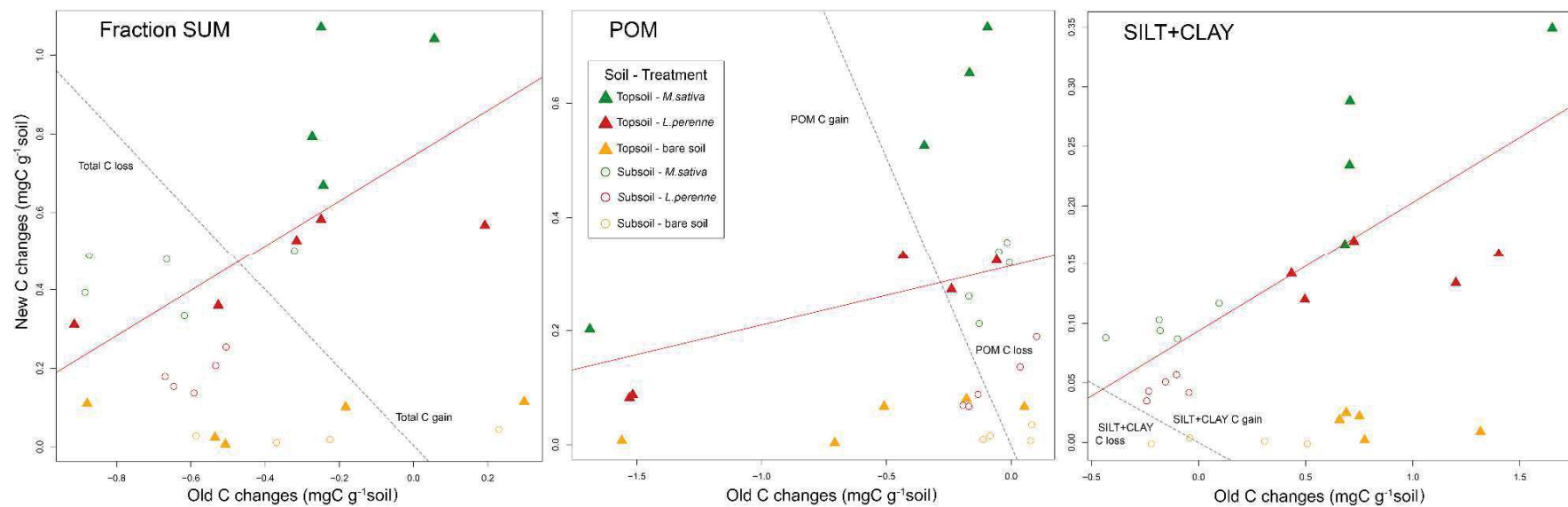


973



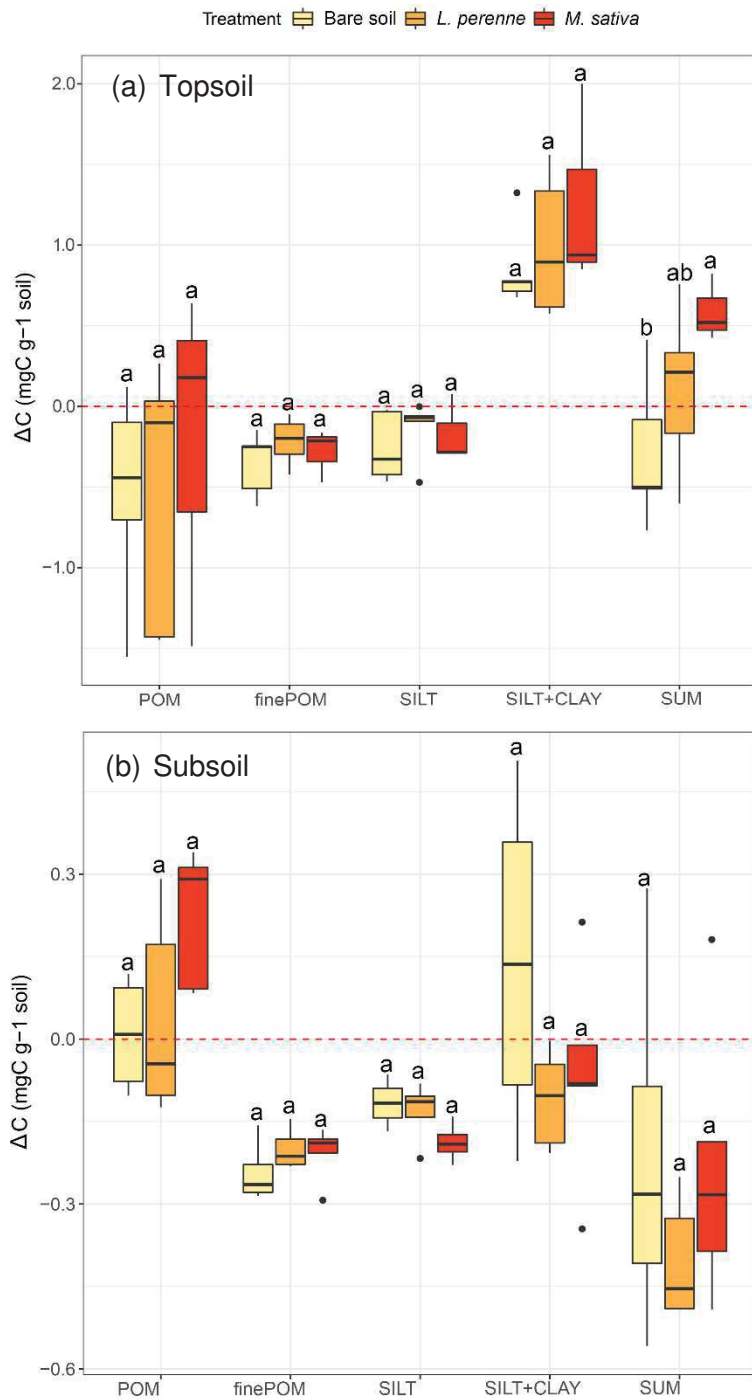
974

975 **Figure 1.** Total soil carbon (C) concentration (a) and concentration changes (b) among different soil types and
 976 vegetation treatments from t_0 (experiment set-up) to t_6 (harvest, i.e. 183 days after). In (a): total C concentration at
 977 t_0 , corresponding to old C concentration at t_0 , are all identical within each soil type. In (b), for each boxplot, the
 978 lower edge of the box corresponds to the 25th percentile data point, while the top edge of the box corresponds to
 979 the 75th percentile data point; the upper and lower vertical lines corresponds to the 90th and 10th percentile data
 980 points, respectively; the horizontal line within the box represents the median and black dots indicate outliers. Letters
 981 above the boxplots indicate statistically significant differences ($p < 0.05^*$) between species and controls according
 982 to Tukey HSD test.



824

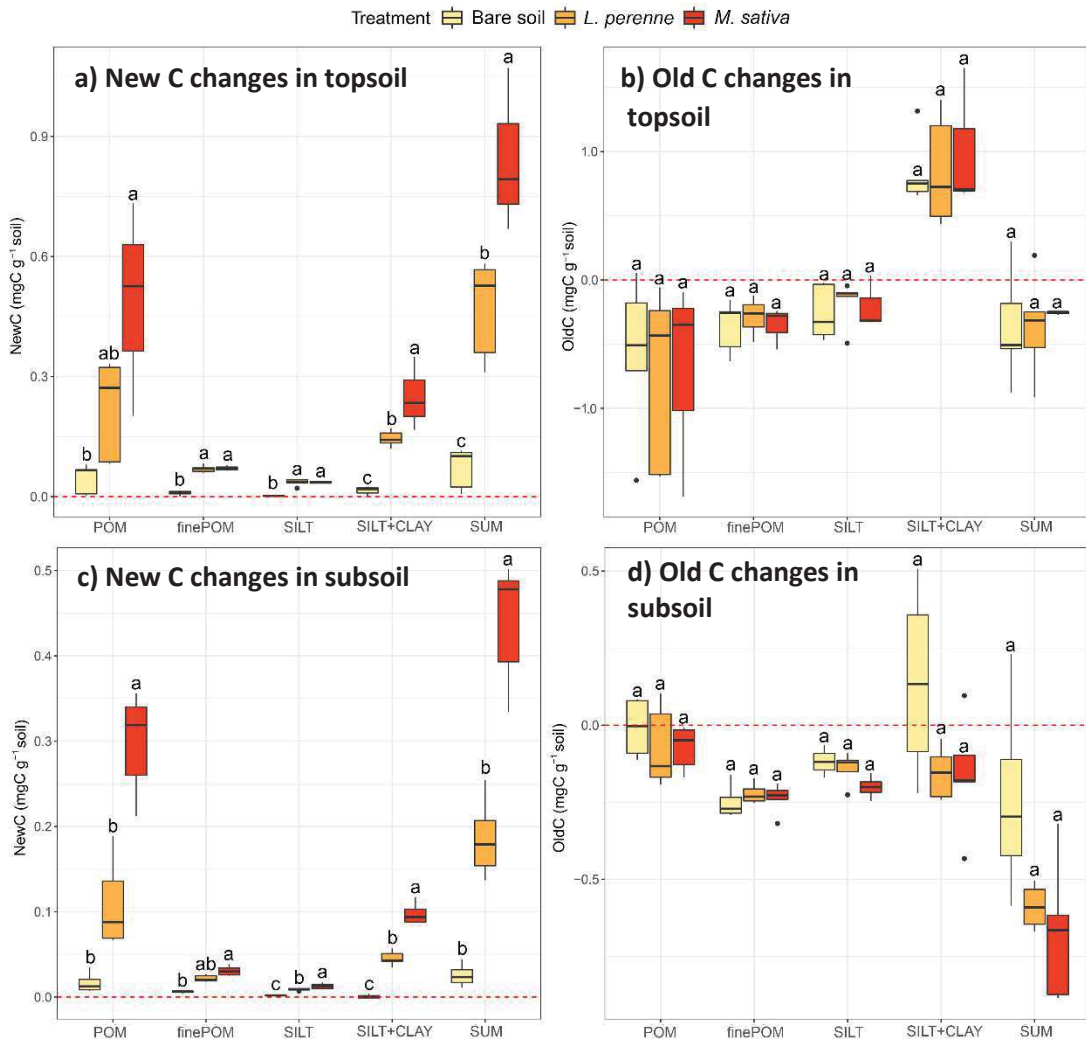
825 **Figure 2.** Relationships between the loss of OldC and gain in NewC in soil for (a) the sum of old and new C in every pool, (b) the POM pool and (c) the SILT+CLAY pool. The red
 826 solid line shows correlation between old c decrease and new c input for the vegetated treatment (without considering bare soil control). The grey dashed line shows the divide of
 827 the data between C gain (on the right) and loss (on the left) on sum of fraction, POM and SILT+CLAY pools. The red line show the linear correlations between data.



828

829 **Figure 3:** Comparison of the difference in carbon (ΔC) after 6 months in different soil C pools and for each treatment
 830 in a) subsoil and b) topsoil. In each boxplot, the lower edge of the box corresponds to the 25th percentile data point,
 831 while the top edge of the box corresponds to the 75th percentile data point. The line within the box represents the
 832 median and black dots indicate outliers. Different letters above the boxplots indicate statistically significant
 833 differences ($p < 0.05$) between families and controls according to Tukey HSD test.

834

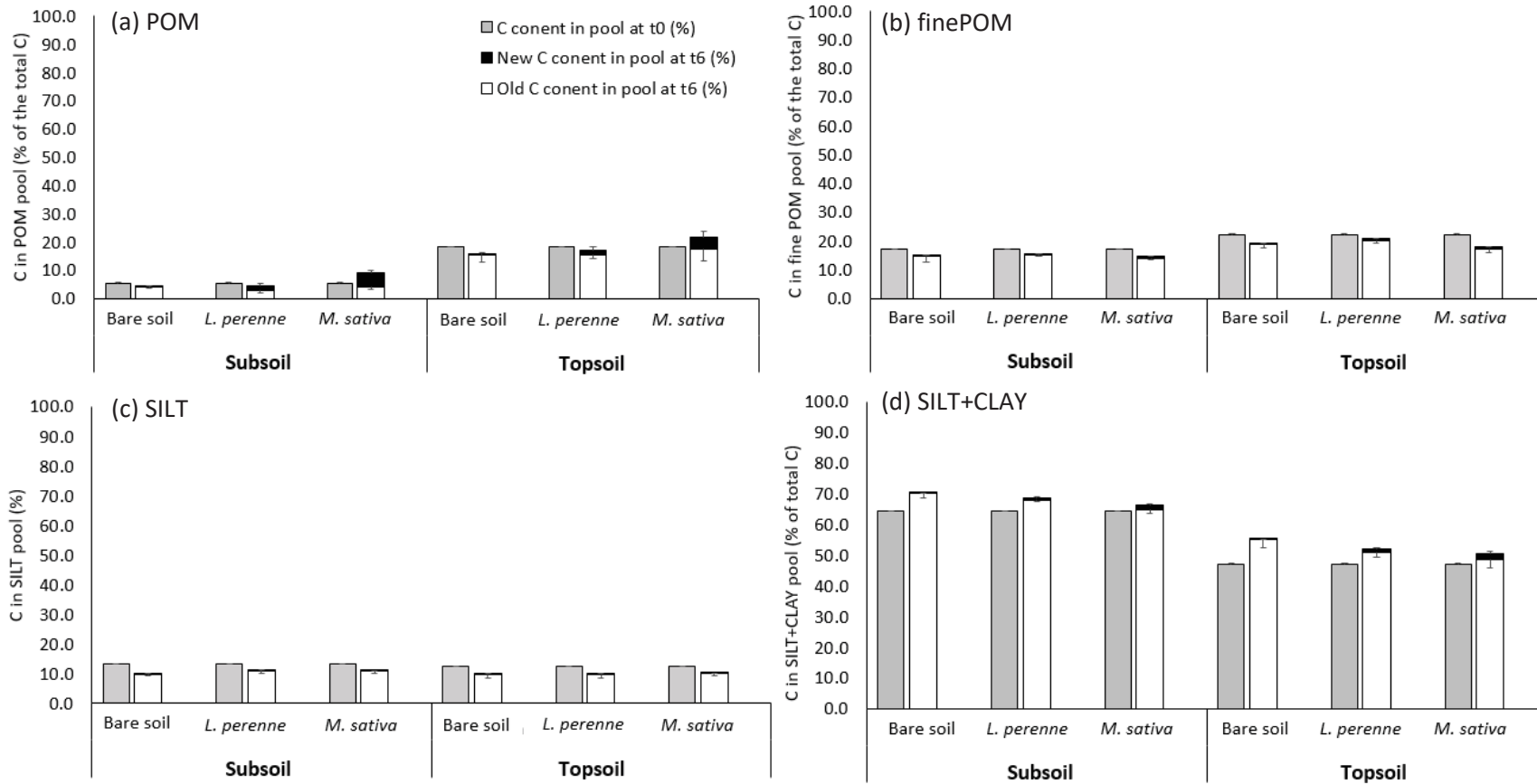


835

836 **Figure 4:** Gain of new C and changes in old C in 4 different C pools (POM, finePOM, SILT, SILT+CLAY) and in the
 837 total bulk soil (as sum of the different pools, Sum) for bare soil control (light yellow), *L. perenne* (orange), and *M.*
 838 *sativa* (red). a) shows the fluxes of new C in topsoil, b) the fluxes of old C in topsoil, c) the fluxes of new C in subsoil,
 839 and d) the fluxes of old C in subsoil. In each boxplot, the lower edge of the box corresponds to the 25th percentile
 840 data point, while the top edge of the box corresponds to the 75th percentile data point. The line within the box
 841 represents the median and black dots indicate outliers. Different letters above the boxplots indicate statistically
 842 significant differences (p < 0.05) between species treatments according to Tukey HSD test.

843

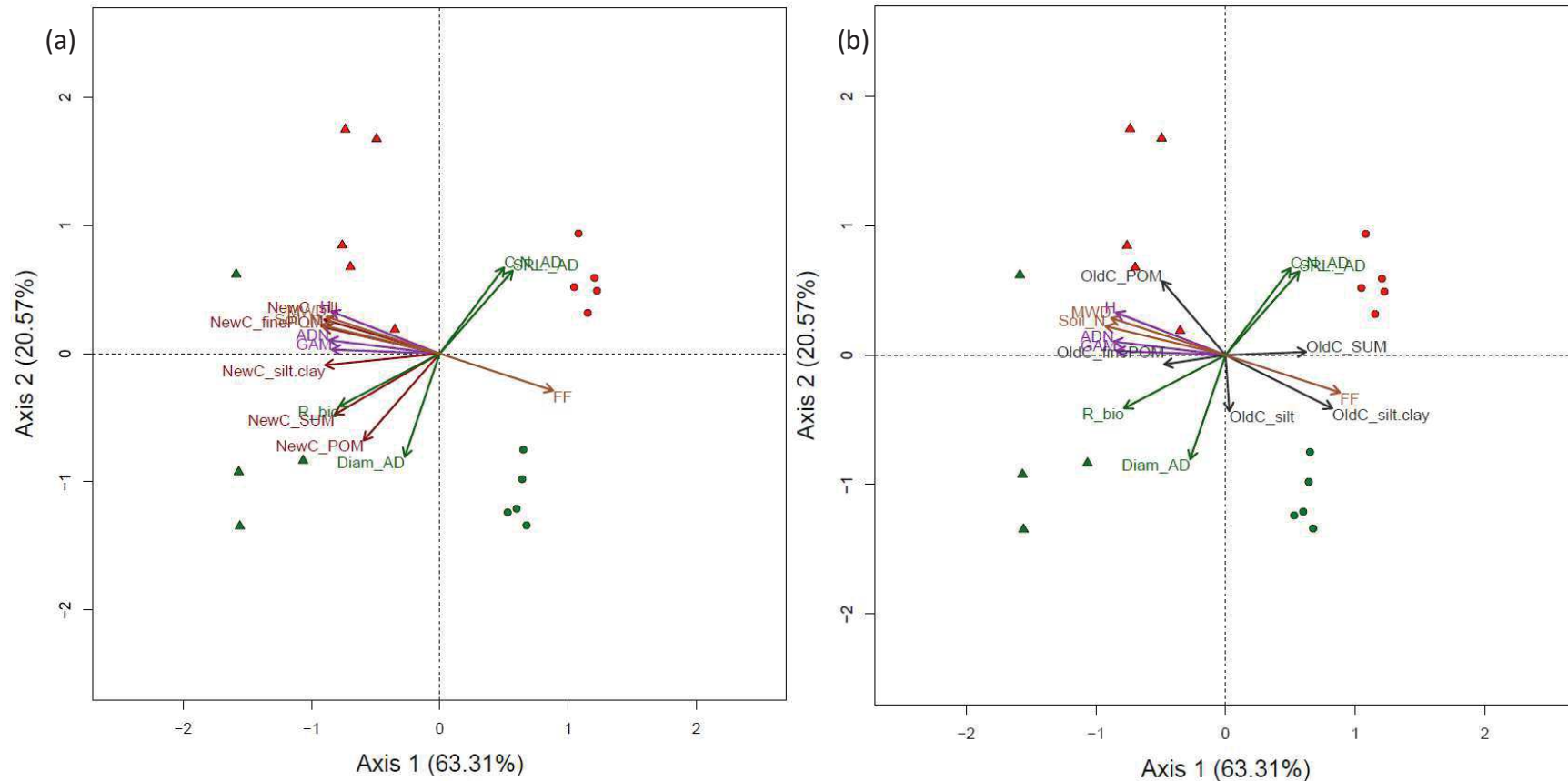
844



845

846 **Figure 5:** C concentration in % of total C in the different soil C pools at t0 and t6 (after 183 days of experiment). At t6 the C is divided in % of new C in soil (black) and old C in
 847 soil (white). (a) shows the C concentration in % in POM pool, (b) in fine POM pool, (c) in SILT pool, and (d) in SILT+CLAY pool.

848



850

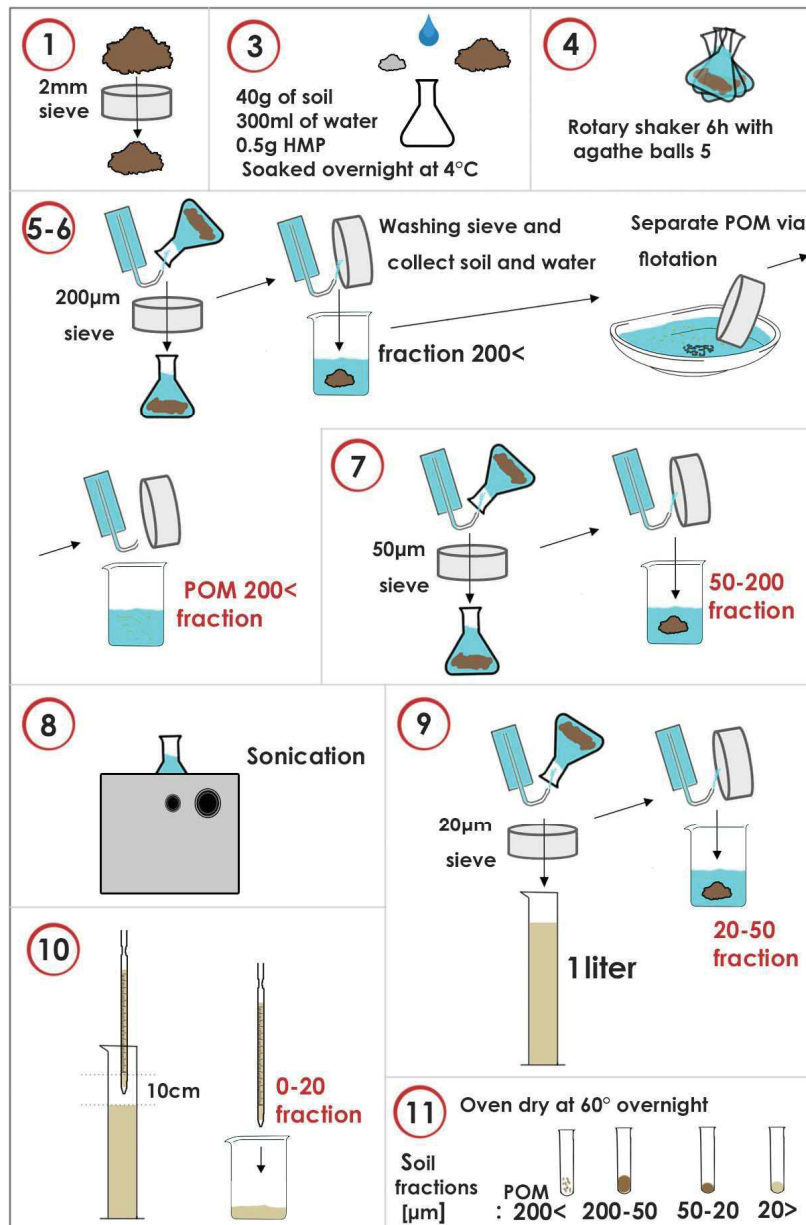
851 **Figure 6:** Principal Component Analysis of (a) new C input and (b) old C fluxes in different soil C pools and root traits (SRL_AD: specific root length of absorptive roots, C:N_AD:
 852 C:N ratio of absorptive roots, R_bio: root biomass and Diam_AD: diameter of absorptive roots), microbial processes indicators (ADN: concentration of DNA as proxy for microbial
 853 biomass, GMA: global metabolic activity, H: Shannon metabolic diversity), and soil structure indicators (MWD: mean weight diameters of aggregates, Soil_N: nitrogen content in
 854 soil, and FF: percentage of fine fraction <20 μm) in soil. Triangles are topsoil and dots subsoil. Green is *M. sativa* and red is *L. perenne*. (a) and (b) shows the same PCA analysis,
 855 but in (a) only the arrows of new C are shown, while in (b) only the arrows for old C, for a better comprehension of the graph.

857 **SUPPLEMENTARY MATERIALS**

858 **Method S1:** Soil fractionation according to Gavinelli et al. (1995) methodology

859 Gavinelli et al. (1995) methodology:

- 860 1. Soil is sieved at 2mm and 40g are collected for fractionation
- 861 2. Soil presoaked overnight at 4 °C in 300 mL of deionized water with 0.5g HMP (sodium
862 metaphosphate)
- 863 3. Shaken with 5 agate balls (d 10 mm) in a rotary shaker, maximum frequency for 2h in case of sandy
864 soils, 6h for other soils.
- 865 4. Soil suspension wet sieved through a 200 µm
- 866 5. Fraction remaining on sieves (2000-200 µm) washed with water in a bowl for POM separation via
867 flotation, while the remaining >200 µm fraction is collected in a beaker for further farctioning
- 868 6. The POM is separated from the sand fractions by submerging the 2000-200 µm fraction in deionized
869 water. The POM will float while the sand will drown. Carefully collect the POM using a sieve and
870 separate it from the sand (**coarse POM fraction**). The sand fraction is collected in a glass beaker
871 after separation from POM (sand fraction)
- 872 7. >200 µm suspension is sieved at 50 µm and the 200-50 µm is gently washed with deionized water
873 from the sieve and collected in a glass beaker (**finePOM fraction**)
- 874 8. >50 µm suspension sonicated for 10 minutes
- 875 9. >50 µm suspension sieved with 20 µm screen and 50-20 µm is gently washed with deionized water
876 from the sieve and collected in a glass beaker (**coarse SILT fraction**)
- 877 10. Transfer of >20 µm suspension in 1 L glass cylinder and add water to bring the volume to 1 L
- 878 11. >20 µm suspension shaken by hand (30 tumbling) and collection of 100 ml immediately after
879 (aliquot for the **fine SILT+CLAY fraction**)
- 880 12. The resulting beakers containing the soil suspension of the different fractions are collected and
881 oven dried at 60 °C until all the water evaporates

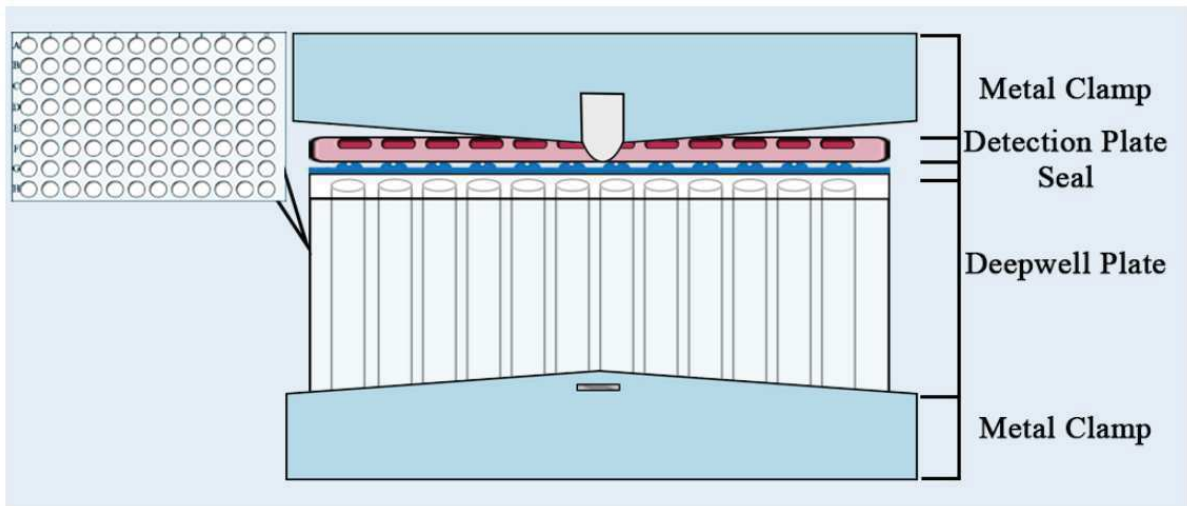


882

883

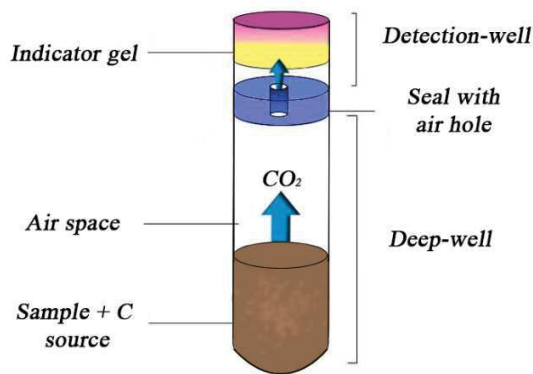
884

Figure S1: Soil fractionation according to the Gavinelli et al. (1995) methodology



885

886 **Figure S2** (ONICA et al.2018): scheme of a MicroResp system



887

888 **Fig. S3** (ONICA et al.2018): scheme of the functioning of a deep well detection system. Soil is placed in a deepwell and
 889 sealed, the CO₂ respired and accumulating in the detection well change the colour of the detection gel according to the
 890 equation [4.5]

891 **Method S2**

892 The principle of the MicroResp is to utilize a colored detection gel (Cresol red) that change color when
 893 changing pH or increasing the CO₂ concentration according to the equation:



895 When the pH diminishes, the Cresol red turns from pink to yellow. (Fig. S3)

896 The first step in the process is to prepare the detection gel in the MicroResp plaques. The preparation of
 897 detection gel is a fundamental step to assess the calibration curve of each detection plaque and calibrate
 898 the results based on the gel preparation, where $\% \text{CO}_2 = A + B / (1 + D * \text{DO}_{\text{norm}})$. First an Agar solution is
 899 prepared, mixing 3g of agar with 100ml of deionized water, mixed in an autoclave for 20minutes at 120°C.
 900 After the indicator solution is prepared mixing 0.315 g NaHCO₃ (final: 2.5 mM), 16.77 g KCl (final: 150 mM)

901 and 18.75 mg cresol red (final: 12.5 $\mu\text{g ml}^{-1}$ or 20 ppm), in 900 ml of deionized water and brought at 65°C
902 to dissolve. The 1000ml solution is transferred to an open bottle and stored at 4°C for 6 months maximum.
903 To prepare the gel 100ml of the 3% agar solution are melted and kept at 60°C. Separately, other 200ml of
904 the indicator solution are melted at 6°C while stirring, and after mixed with the agar solution. The mixture
905 is then distributed in the detection plaques, 150 μl of solution for each one of the 96 detection well of each
906 plaque. To avoid the formation of bubbles the gel is kept throughout the process in a baker of boiling water
907 and the tip of the pipette used to distribute the solution is preheat in boiling water. When the gel is solidified
908 (2-3h) the plaques are stored in a dessicator at room temperature in a dark room with a baker of soda and
909 a cup of water for 2-3 days to allow each microplate to reach CO₂ equilibrium. After they are covered in
910 parafilm.

911 After the detection plaque are prepared a calibration process is needed for every new detection plaque. 12
912 strips (8 wells each) made for calibration containing the indicator gel are scanned used a Victor 1420
913 Multilabel Counter (PerkinElmer, Massachusetts, USA) to asses the initial DO₅₉₀ (DO_{initial}). Twenty-four
914 150ml serum vials are prepared, each containing ½ a strip of detection gel (4 wells), and injected with known
915 CO₂ concentration with a syringe in order to have a CO₂ concentration range (from 0% CO₂ concentration
916 to 4% CO₂ concentration, 6040 vol CO₂ (μl), increasing the concentration in each vial of 0.1%). The strips
917 are incubated for 2h at 25°C to achieve balance with the CO₂ in each serum vial. After 2h the concentration
918 of CO₂ is assessed in the vials using the GC-microcatha measurement. The detection strips are then retrieve
919 and immediately read at 590nm to assess the DO_{final}. Finally the calibration is finalized as follow:

- 920
- Normalize DO data: $DO_{norm} = DO_{final} / DO_{initial} * average(DO_{initial})$
 - Draw the DO_{norm} vs [CO₂] calibration curve in %.
 - Fit the curve (rectangular hyperbola regression $\%CO_2 = A + B / (1 + D * DO_{norm})$)
- 921
- 922

923

924 The next step in the MicroResp protocol is to prepare the different substrate solutions. The idea is to give
925 1.5 mg of C for each g of dry soil (substrate saturation) and reach a humidity level of 80% of field capacity.
926 For each soil type is therefore necessary to determine 1) the field capacity in g of water per g of soil and 2)
927 the soil mass distributed in each well by the MicroResp filling device. Field capacity for the soil was
928 calculated at 28.3%. Three plaques for each soil where filled with the MicroResp filling device and weighted
929 to estimate the average soil content in each MicroResp well, set at $0.5 \pm 0.04\text{g well}^{-1}$. 1.2ml of solution have
930 been added to each MicroResp well. The solution have been prepared using miliQ water and sterilized using
931 0.45 μm paper filters, stored in sterilized falcon tubes at 4°C.

932 The substrates used for the MicroResp analyses were chosen based on their biological properties and are
933 reported in Table S1. In every detection plate an extra substrate with pure MillQ water were added as
934 control. In each plaque (96 wells) we tested 2 samples, one in each half of the plaque, for a total of 48 wells
935 per samples organized as follow: 3 sub replicates per substrate (15 substrate) plus 3 sub replicate per the
936 millQ water control (Fig.S4).

937 Each sample was prepared as follow:

- 938 • Identify the deepwell plate and the sample used
- 939 • Tare the deepwell plate
- 940 • Hide half of the filling device, place it above a deepwell plate, covered with plastic sheeting, fill
941 half of the filling device with the ground and remove the excess with a spatula.
- 942 • Pull the plastic sheet to drop the soil into the wells, then weigh and record the mass of soil used
943 for the half plate (48 wells). Tare again before filling the second half of the plate with the other
944 soil sample.

945 The samples are analyzed as follow:

- 946 • At time 0 the substrate are added using a multichannel pipette to each wells of the deepwell
947 plate, cover with the parafilm and incubated at 25°C in the dark for 2h
- 948 • Before the end of the 2h incubation, the DO_{590t0} of each detection placed is taken with a Victor
949 1420 Multilabel Counter (PerkinElmer, Massachusetts, USA). After two hours the detection plate
950 is placed above the analysis plate with and sealed with a clamp. Resume incubation at 25°C for an
951 additional 4 hours.
- 952 • At time 6h: the detection plate are detached from the deepweell and immediately read using a
953 Victor 1420 Multilabel Counter (PerkinElmer, Massachusetts, USA) to determine the DO_{590t6}

954 For the data analysis the following steps were taken:

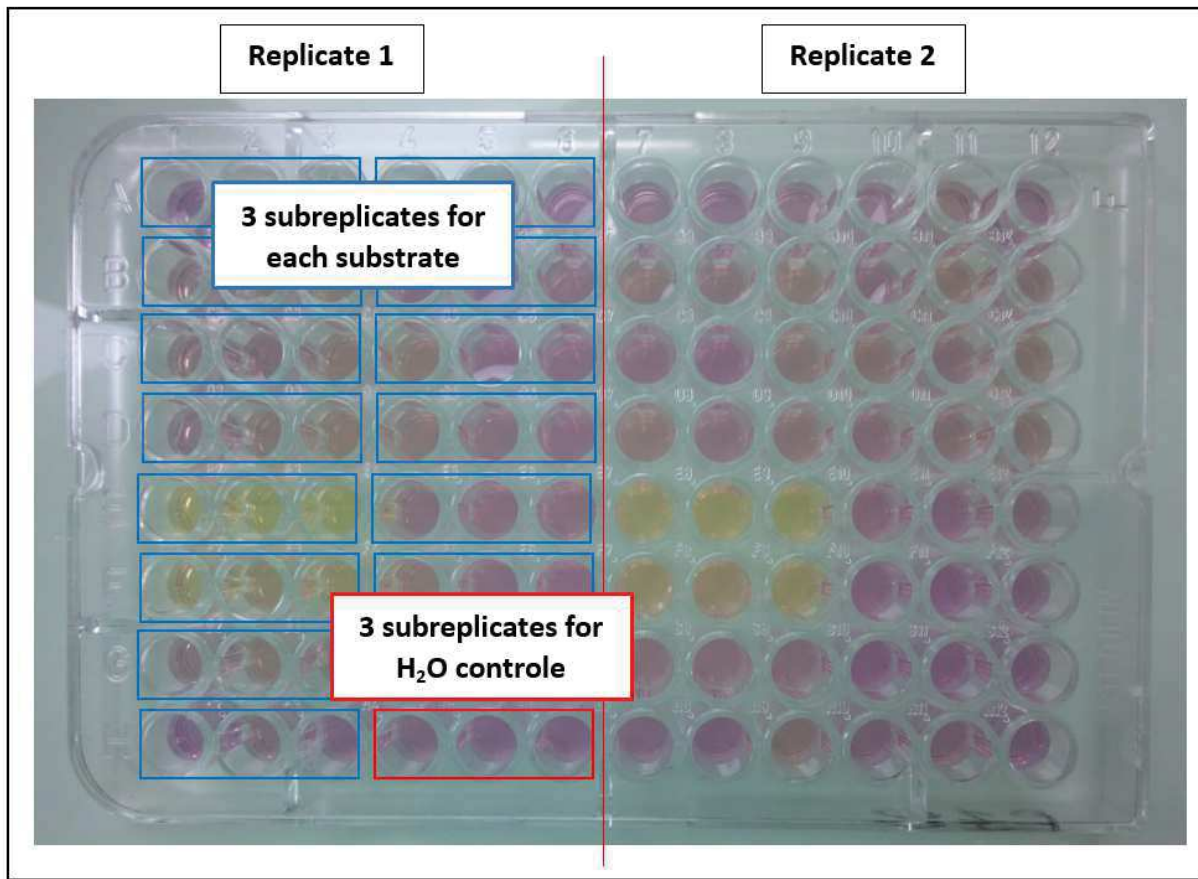
- 955 • Retrieve DO data at t0 and t6 for each plate. Check that the coefficient of variation of the DO_{590} of
956 each detection half plate at t0 does not exceed 5% (otherwise, remove the outliers DO values).
- 957 • Normalize the data: $DO_{norm} = DO_{t6}/DO_{t2} * \text{average}(DO_{t2})$
- 958 • Convert DO_{norm} to % CO2 from calibration data: $\%CO2 = A + B / (1 + D * DO_{norm})$. The data for the
959 calibration curve were A = -0.29, B = -0.87, D = -7.72
- 960 • Convert these %CO2 to SIR ($\mu\text{g C-substrate g}^{-1} \text{ soil h}^{-1}$) according to the incubation time and soil
961 mass in each well.

962 The aim of the MicroResp is to characterize the differences in functional activity of microbiological
963 communities. The activity was assessed on soil sampled and t0 and t6.

964

Table S1: Substrates used for the MicroResp

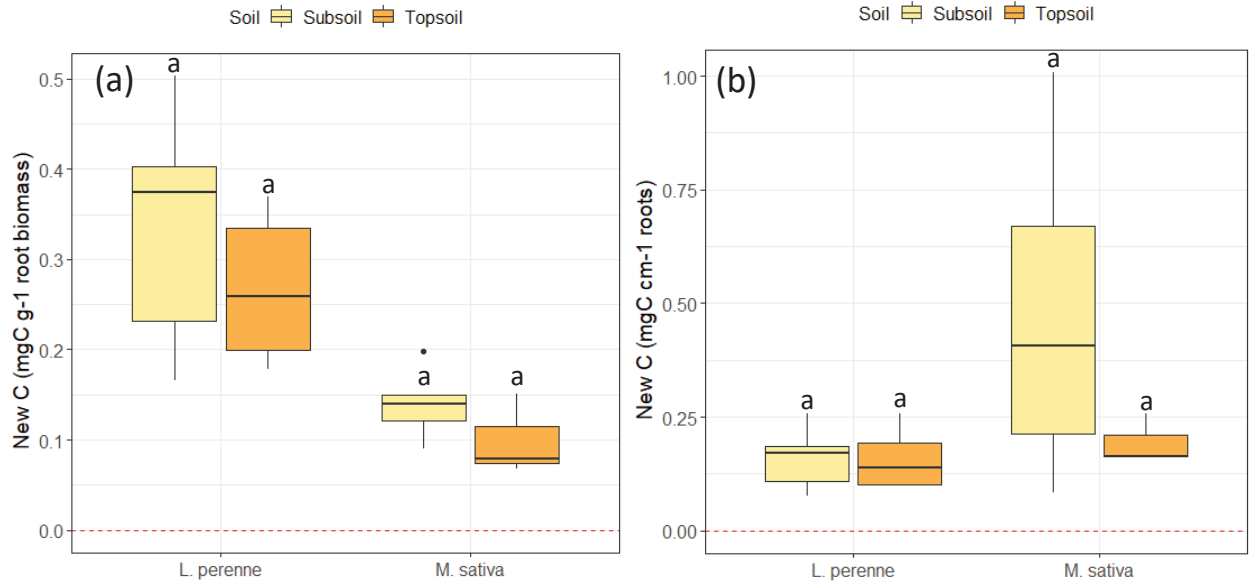
Code	Substrate	Interest and biological properties	Reference	Formula
Carbohydrates :				
GLU	D-glucose	Potential comparison with SIR and cellulose compound	Reactive to different soils	C ₆ H ₁₂ O ₆
XYL	Xylan	Compost of hemicellulose, changes strongly according to the seasons	Reactive to different soils	(C ₅ H ₈ O ₅) _n
CEL	Cellulose	plus dur à dégrader et comparaison potentielle avec résultats DCP	Bérard	(C ₆ H ₁₀ O ₅) _n
Amino acid				
ASP	L-Asparagine	Reactive to different soils		C ₄ H ₈ N ₂ O ₃
SER	L-Serine	Reactive to different soils		C ₃ H ₇ N ₁ O ₃
LYS	L-Lysine	Reactive to different soils		C ₆ H ₁₄ N ₂ O ₂
GLY	Glycine	responds well when decomposed results Berard, precursor ac uric	Bérard, article	C ₂ H ₅ NO ₂
GLUT	L-Glutamine	Linked to the metabolism of nitrogen and ammonia fixation on glutamic acid	données terrain	C ₅ H ₁₀ N ₂ O ₃
Nac	N-acetyl glucosamine	Chitin monomer, found in insects exoskeleton and fungi	Dalmonech	C ₈ H ₁₅ NO ₆
Carboxylic acid (more recalcitrant)				
OX	Oxalic acid	Root and exudates component linked with Malic acid	From field trial, Dalmonech, Bérard	C ₂ H ₂ O ₄
UR	Ureic acid	extruded by isopods (and diplopods)	From field trial, Dalmonech, Bérard	C ₅ H ₄ N ₄ O ₃
MAL	Malique acid	Root and exudates component, useful in fermentation processes		C ₆ H ₆ O ₅
Phenolic acid (strongly recalcitrant)				
CAF	Cafeic acid	Close to rosemaric acid (extruded by Lamiaceae)	Bérard	C ₉ H ₈ O ₄
SYR	Syringic acid	produit de la dégradation de pigments végétaux la malvidine	Dalmonech	C ₉ H ₁₀ O ₅
VAN	Vanillic acid	produit de dégradation de la lignine par les champignons	Oren	C ₈ H ₈ O ₄



967

968 **Figure S4:** Scheme representing the organization of the MicroResp detection plate, showing the three replicates for each
 969 substrate used, the three for the H₂O control and the separation of 2 replicates analyzed in the same MicroResp system.

970



971

972

973

974

975

976

977

978

979

Figure S5: (a) New C moved in the SILT+CLAY fraction in subsoil (light ocra) and tospoil (orange) for g of root biomass for the two different treatments (*L. perenne*, *M. sativa*) in 183 days of experiment. (b) New C moved in the SILT+CLAY fraction in subsoil (light ocra) and tospoil (orange) for cm of root for the two different treatments (*L. perenne*, *M. sativa*) in 183 days of experiment. , for each boxplot, the lower edge of the box corresponds to the 25th percentile data point, while the top edge of the box corresponds to the 75th percentile data point; the upper and lower vertical lines corresponds to the 90th and 10th percentile data points, respectively; the horizontal line within the box represents the median and black dots indicate outliers. Letters above the boxplots indicate statistically significant differences ($p < 0.05^*$) between species and controls according to Tukey HSD test.

980

981

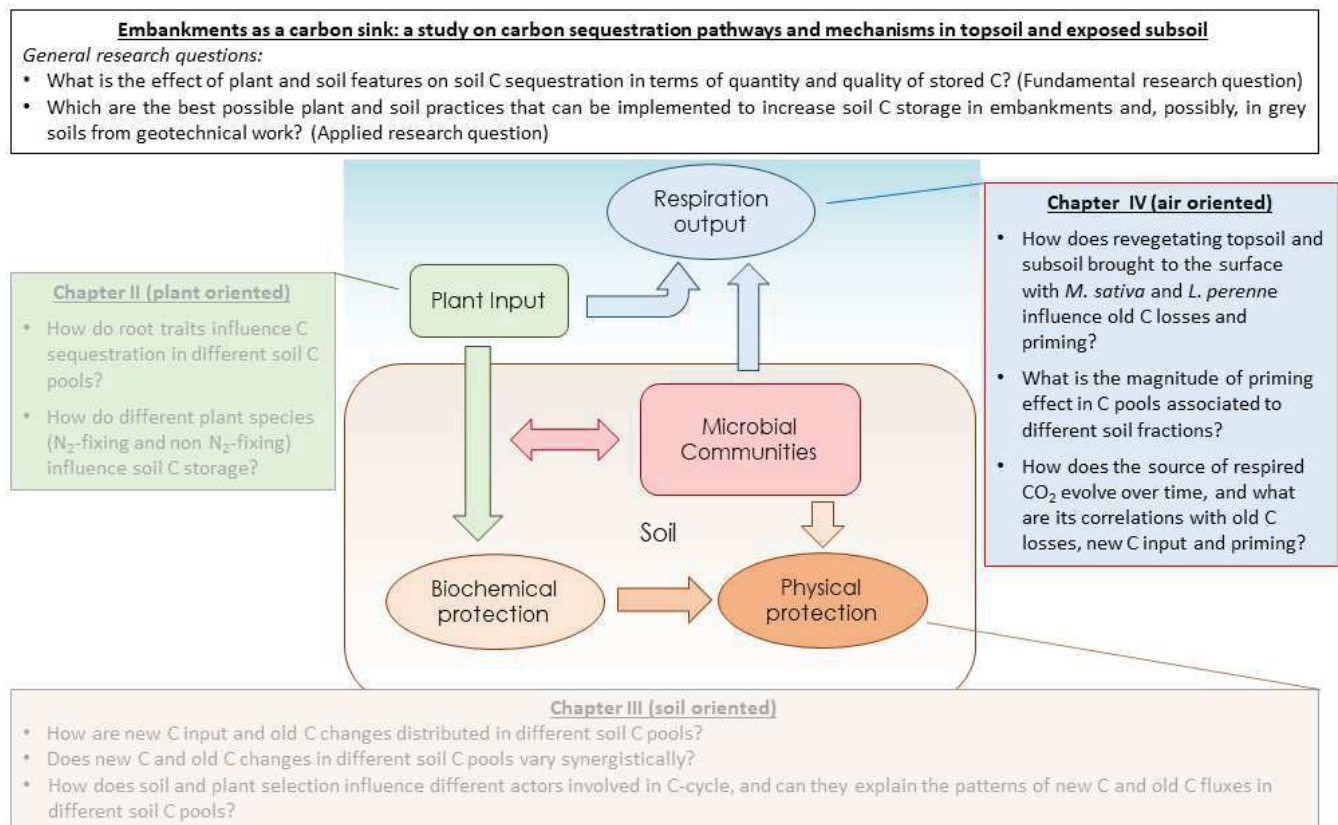
982

983

984

985

Chapter IV: Soil quality drives the priming effect and plant species refine it



In Chapters II and III we investigated the C storage in different C pools and its relationship with soil, root and microbiological characteristics. However, vegetation can also have a negative effect on soil C storage increasing the preexistent old C mineralization and loss compared to bare soil - the so called 'priming effect'. In Chapter IV we aim to tackle this aspect, and study the how plant species and soil showing contrasting characteristics influence the priming effect, analyzing soil respiration origin and changes in soil old C in bulk soil and different soil C pools, and describing the main factors that influence our plant-soil system: microbiological substrate preference and N competition.

4.1. INTRODUCTION

Using vegetation to increase soil C sequestration in soil is recognized as an efficient method to mitigate atmospheric CO₂ content. Accordingly, national and supranational organizations designed international programs to promote C storage in soil e.g., the 4p1000 initiative (www.4p1000.org, Minasny et al. 2017). The net input of C in an ecosystem is jointly determined by fresh biomass input of new C via plant biomass turnover and labile rhizodeposition (new C) and losses of old preexistent C in soil (old C) (Kuzyakov and Domanski, 2000; De Deyn et al., 2008; Lal 1994; Smith et al., 2000; De Deyn et al., 2008). Both processes are not independent, but can have strong interactions. Especially, concerns about the fate of the preexisting old C loss due to such a fresh new C input from plants have been raised increasingly. Such a phenomenon, called the priming effect (PE), refers to input of labile C from plants that can accelerate (positive PE) or decelerate (negative PE) mineralization and losses of preexistent old C from soil (Kuzyakov et al., 2000, Fig. 1).

The PE depends on the nature of the substrate consumed by the soil microorganisms, which could be altered by plant and soil conditions (Hamer and Marschner, 2005; Shahzad et al., 2015; Huo et al., 2017). Therefore, understanding the impact of plant and soil characteristics on the amount of primed C has become a key research objective. Among the diverse factors affecting C sequestration, soil particle size and associated C pools is considered as a major factor affecting PE. The commonly used classification of soil C pools associated to soil particle size fractions in literature refers to four C pools. First C in particulate organic matter (POM) (C_{POM} , 2000-200 μ m), and C in fine POM ($C_{finePOM}$, 200-50 μ m) originating from plant litter debris at different levels of degradation, and less protected from degradation (Kögel-Knabner, 2002). After the pools more stable due to their organomineral binding with fine soil particles: C in coarse SILT (C_{SILT} , 50-20 μ m) and C in fine SILT + CLAY ($C_{SILT+CLAY}$, <20 μ m), deriving from exudation and processed C from microbiological communities in form of exudates, exopolysaccharides and microbial necromass (Sollins et al., 1996; von Lützow et al., 2006; Cotrufo et al. 2013, Liang et al., 2017). For example, Huo et al. (2017), found that rhizospheric PE was significantly

26 greater in finely grained soil. Surprisingly, the effect of soil particle size fraction on PE has seldom been
27 investigated (but see Ohm et al. 2007; Perveen et al., 2019), nor the interactions with soil type and
28 plant species. Perveen et al. (2019) tested the effect of 35 different soils coming from all over the world
29 and from different land uses. They found no effect of landuse on PE, but a significant effect of soil type,
30 with positive priming effect increasing in any soil with increasing C and N content (Perveen et al., 2019).
31 However, the incubation experiment was carried on in a heavily artificial environment, without the
32 presence of living plants and with the addition of a nutrient solution to all the soils . The addition of an
33 N rich solution excluded the possibility of competition between plants and microbes for N and the
34 possible reduction of positive PE from this competition ('competition hypothesis' from Cheng and
35 Kuzyakov, 2005; Perveen et al., 2019).

36 In a framework of soil C sequestration, both soils that differ in initial old C quantity in different soil C
37 pools, and species of contrasted root growing strategies, have been shown to have significant effects
38 on the sequestration of C in soil and relative size of C pools (De Deyn et al., 2008; Prieto et al. 2016;
39 Poirier et al. 2018;. Henneron et al. 2019 ; Perveen et al., 2019). We argue that, to better understand
40 the effects of revegetation on C-cycle and storage, even the influence of soil and species on priming
41 effect needs to be examined, considering the changes of old C in different C pools related to soil
42 particle size fractions.

43 To quantify the PE, knowing the fate of old C in soil is essential and usually performed using a stable
44 isotopic labelling approach (Kuzyakov, 2006). Monitoring respired CO₂ reflecting the source of the
45 consumed substrate and the remaining old C changes in soil are two major means to assess the PE.
46 When plants are growing in an atmosphere constantly enriched with ¹³C atmosphere, the input of plant
47 derived C has a higher abundance of ¹³C. Consequently, the abundance of ¹³C in respired CO₂ (A¹³C, %)
48 depends on the mineralized C source: a higher A¹³C if the main respiration source is the consumed
49 plant new C input, and a lower A¹³C if the source is the preexistent old C in soil (e.g. Fontaine et al.
50 2004, 2007; de Graaf et al. 2010). Another effective way to study priming effect is assessing the losses

51 of preexistent old C in soil with and without vegetation. When analyzing the C in bulk soil, the ¹³C signal
52 also allows the differentiation between preexistent old C, and fresh new C derived from plant input.
53 Comparing losses of old C in a vegetated soil allows for the quantification of the priming effect and
54 whether it is positive or negative PE.

55 On newly constructed road embankments, subsoil is increasingly used to replace topsoil that is
56 stripped off during the construction process. Compared to topsoil, subsoil contains less C, but the old
57 C present is more stable than in topsoil for several reasons. C in subsoil is associated with the finest
58 soil particles and stabilized via organomineral interactions (i.e., SILT and SILT+CLAY) (Eusterhues et al.,
59 2005; Chabbi et al., 2009). Subsoil has less microbial biomass (Taylor et al. 2002; Andersen and
60 Domsche 1989; Ekklund et al. 2001), and activity due to oxygen limitation (Rumple and Kögel-Knabner,
61 2010), and reduced plant inputs (Fontaine et al. 2007) increasing C residence time. Finally, physical
62 separation of microbes and C decrease the possibility for C mineralization (Von Lützow et al. 2006;
63 Holden and Fierer 2005). Subsoil excavation, mixing and revegetation alter all of these protection
64 mechanisms. How the revegetation influences PE and the fate of old C in subsoil, especially in the
65 SILT+CLAY pool remains unclear. To the best of our knowledge, no studies on the priming effect of
66 subsoil brought to the surface have been performed.

67 We aim at comparing the priming processes in two soils with same origin but contrasting
68 characteristics (topsoil with typical fertility, high microbial biomass and nitrogen (N) content versus
69 subsoil with low fertility, microbial biomass and N content). The soils were vegetated with two
70 herbaceous species: the di-nitrogen (N₂) fixing species *Medicago sativa* L., and the non N₂-fixing grass
71 *Lolium perenne* L.. Soil respiration, changes in new C, old C and the priming effect for total C and that
72 in each C pool were quantified. We hypothesize that (i) topsoil will have higher losses of old C due to
73 greater root biomass and microbial biomass and activity; however, (ii) subsoil will have a greater
74 positive priming effect because it is very highly disturbed compared to the initial conditions, and (iii)
75 the C priming effect will differ among soil fractions due to different protection potential.

4.2. METHODOLOGY

4.2.1. *Experimental setup*

Soil used for growing plants was excavated from Pisciotta (Italy, 40°07'N 15°14'E/40.116667°N) at two depths of the same soil profile: topsoil (0-30cm depth) and subsoil (110-140cm depth). The soil is a clay loam soil (USDA) with a slightly different granulometry between topsoil and subsoil (topsoil: 27.3% clay, 31.1% silt, 41.6% sand; subsoil: 34.8% clay, 36.8% silt, 28.4% sand). The pH in topsoil was 7.0 and in subsoil was 8.4.

Air dried soil was crushed and sieved to 5mm to homogenize it. We mixed and divided the soil in four sections (quartiles) and 36 different pots were prepared collecting one scoop of soil from each section until the desired weight in each pot has been reached (Fig. S1). We added 6.9 kg of soil into each pot. During the preparation, three soil samples were removed and put aside for chemical analyses. These samples represent the initial soil, or time zero (t_0). Inside each pot, a 60 mm deep plastic ring with a diameter of 80 mm was fitted that could be closed with an airtight dome for subsequent measurements of soil respiration (Fig. S2).

N_2 -fixing *Medicago sativa* L. and non N_2 -fixing *Lolium perenne* L. were sowed as monocultures with exactly the same pattern. In each pot, three seeds were put at six equidistant spots. After germination, one seedling was removed with scissors at ground level, at each spot. For each soil type (i.e. top- and subsoil) and species, six replicate containers were prepared and six bare containers per soil type were used as controls (n = 36 in total)

Containers were placed into three identical microcosms at the Ecotron growth facility at Montpellier, France (<http://www.ecotron.cnrs.fr/>) (Fig. S3). In each microcosm, two replicates of all treatments, i.e., 12 pots, were placed randomly to avoid any effect of microcosm on plant growth and soil processes. Plants were grown at a constant air temperature of 21°C and at 80% humidity (to reduce the soil water loss by evapotranspiration). Artificial light was provided by three lamps (Gavita PRO 300

101 LEP 02, Netherlands) in each microcosm with a 12h day/night cycle, shifted to allow air sampling at the
102 same moment of the plant's circadian rhythm (data not shown in this study, Fig. S4). A shade was
103 placed on the lamps and the distance of the lamps from the plants was adjusted to achieve the most
104 possible homogenous light intensity on the foliage ($300 \mu\text{mol m}^{-2} \text{s}^{-1}$). Soil moisture was kept at $45 \pm$
105 10% of the soil water holding capacity for the entire duration of the experiment. A system of plastic
106 pipes was installed in the chamber to allow irrigation without having to open the chamber and disturb
107 the ^{13}C concentration (Fig.S5). Pots were irrigated every 2-3 days, according to their evaporation rate.
108 However, with the growth of plants, the increase in biomass and in transpiration had to be considered
109 to calculate the amount of water needed to keep the soil at the desired moisture content. For this
110 reason, every 2 weeks, pots (in correspondence with the air sampling) were removed from the
111 chamber, weighted and randomized inside the chambers. Knowing the amount of water added in the
112 previous 2 weeks, the initial soil moisture content, and the final soil moisture content, we were able
113 to calculate the increase in evapotranspiration every 2 weeks and adjust the amount of water needed
114 (data not shown).

115 After the germination of seedlings, the atmosphere was enriched with ^{13}C , reaching a concentration of
116 2% (approximately two times higher than the natural ^{13}C abundance of 1.1% , in other words $\delta^{13}\text{C}$ of
117 CO_2 in the chamber was roughly $+760$, as compared to the ambient -8). The air enrichment with ^{13}C
118 was infused during the photoperiod and the ^{13}C infusion stopped during the night period. The
119 experiment was carried out for 183 days, starting the 29 September 2017 and ending the 31 March
120 2018.

121

122 *4.2.2. Air sampling*

123 Air sampling rings were built with two openings in their belowground section to allow root growth in
124 their perimeter, and a double ring structure (one inside the other) that could be filled with water.
125 Inserting the plastic dome inside the double ring structure filled with water ensures an airtight sealing,

126 allowing soil respiration to accumulate inside the chamber (the plastic ring cover had an area of 8.5cm
127 and a height of 6cm, for a volume of 340 cm³) (Fig. S6). Every two weeks, we assessed the percentage
128 of ¹³C in the respired CO₂.

129 To conduct the air sampling, ¹³C enrichment was stopped 24h before the sampling procedure to allow
130 the ¹³C accumulated in soil to leak out of macropores and cracks that could pollute the results.

131 The day of the sampling, each chamber was open and the air sampling of the time 0 (t₀) was performed
132 as soon as the photoperiod stopped. The protocol for the air sampling consisted of:

- 133 1. Pour water in the ring (Fig. S7a)
- 134 2. Close the ring with the plastic dome (Fig. S7b)
- 135 3. Insert the syringe in the rubber cap of the plastic dome and collect 5ml of air to set the reference
136 time 0 (t₀) (Fig. S7c)
- 137 4. Immediately transfer the collected 5ml sample from the syringe to an Exitainer under vacuum to
138 store gas (Fig. S7d)
- 139 5. After 2 hours of incubation, without moving the dome, insert the syringe in the rubber cap of the
140 dome, collect 5ml of gas enriched with the soil respiration, and transfer it in the exitainer following
141 steps 3 and 4. This sample will represent the Time 1 (t₁) air sample, as the amount of CO₂ in the
142 chamber atmosphere after a 2h incubation period.
- 143 6. Samples analyzed with an elemental analyzer Isoprime100 coupled with an Elementar Varo
144 Isotope Cube

145 Results from the isotope analyzer provided the CO₂ concentration in ppmV at time 0 (CO_{2t0}) and time
146 2 hours (CO_{2t1}). The abundance of ¹³C in respired CO₂ was given in δ¹³C, according to the equation:

$$147 \quad \delta^{13}C = \frac{R_{sample}}{R_{VPDB}} - 1 \quad [1]$$

148 Where R_{sample} is the carbon isotope ratio of the sample ($^{12}C/^{13}C$) and R_{VPDB} the ratio of the international
 149 standard reference Vienna Pee Dee Belemnite ($R_{VPDB} = 0.0111802$, Werner and Brand, 2001). The $\delta^{13}C$
 150 was adjusted according to the CO_2 concentration of the analyzed samples as $\delta^{13}C_{SR}$:

$$151 \quad \delta^{13}C_{SR} = \frac{(CO_{2t1} * \delta^{13}C_{t1}) - (CO_{2t0} * \delta^{13}C_{t0})}{(CO_{2t1} - CO_{2t0})} \quad [2]$$

152 Where $\delta^{13}C_{t1}$ is the isotopic composition of CO_2 at after 2 hours of soil respiration and $\delta^{13}C_{t0}$ the isotopic
 153 composition at time 0.

154 To calculate the fractional abundance of ^{13}C in the respired CO_2 ($A^{13}C$), first the carbon isotope ratio
 155 was derived from [1] as follows:

$$156 \quad R_{sample} = \left(1 + \frac{\delta^{13}C_{SR}}{10^3}\right) * R_{VPDB} \quad [3]$$

157 Finally, to calculate the isotope abundance $A^{13}C$ (%):

$$158 \quad A^{13}C = R_{sample} / (1 + R_{sample}) \quad [4]$$

159 To calculate the percentage of CO_2 derived from fresh plant input mineralization (fPlant) first the soil
 160 derived CO_2 concentration (CO_{2C}) in μmol have been calculated as:

$$161 \quad CO_{2C} = \Delta CO_{2P} \times \frac{P \times Vc}{R \times T} \quad [5]$$

162 Where ΔCO_{2P} is the CO_2 concentration in (ppmV) is the difference of CO_2 concentration in the sampling
 163 chamber (in ppmV) at time 0 and after 2h of incubation time; P the atmospheric pressure in Pa; Vc the
 164 volume of the chamber in m^3 ; R the ideal gas constant $8.314 J K^{-1}$; and T the temperature in K.

165 After the amount we calculated the quantity C(C_Q in μg) in the respired CO_2 as:

$$166 \quad C_Q = (CO_{2C} \times 12 \times (1 - A^{13}C)) \times (CO_{2C} \times 13 \times A^{13}C) \quad [6]$$

167 Where 12 and 13 are the atomic weight of ^{12}C and ^{13}C . The ^{13}C amount ($^{13}C_Q$ in μg) in the respired CO_2
 168 have been determined as:

169 $^{13}C_Q = C_Q \times E^{13}C$ [7]

170 Where the $E^{13}C$ is the excess of ^{13}C (in %) compared to the bare soil control at the beginning of the
171 experiment t_0 ($E^{13}C = A^{13}C$ at time x - $A^{13}C$ of bare soil control at time 0, equal to 1.076 in topsoil and
172 1.082 in subsoil). After the plant derived C (pC in μg) was calculated as:

173 $pC = \frac{^{13}C_{\mu g}}{E^{13}C_{atm}}$ [8]

174 Where $E^{13}C_{atm}$ is the excess of ^{13}C in the chamber atmosphere (average of +0.8%). Finally, to calculate
175 the percentage of C in CO_2 deriving from plants C input (f_{plant} , in %):

176 $f_{plant} = \frac{pC}{C_{\mu g}}$ [9]

177 The design of the ring did not allow to calculate in a reliable way the amount of respired C due to
178 several technical issues. The clay soil, being kept at 45% of soil water content, formed a superficial
179 crust that did not allowed the soil respiration to freely flow in the plastic dome used for sampling,
180 reducing the respiration rate. Moreover, the presence of cracks that act as preferential pathways for
181 gas dispersion made the diffusion of respiration unreliable. However, the percentage of ^{13}C in air was
182 reliable independently from the amount of respired CO_2 , and allowed the calculation of the
183 percentage of new and old C in the respired CO_2 .

184 **4.2.3. Soil and biomass sampling**

185 The volume of soil in each pot ($20 \times 20 \times 10 \text{ cm}^3$) was divided in two halves vertically with a saw. One
186 half was air dried and used for the soil analysis and microbial measurements, and the other half was
187 used for the measurement of plant traits. Plants were cut at the root collar to divide aboveground and
188 belowground biomass. The resulting mixed sample of soil and roots were placed on a 2 mm sieve and
189 carefully washed to disperse the soil, and the plant individuals were divided (if possible). Above- and
190 belowground biomass was collected, oven dried at $60^\circ C$, and weighed to determine dry weight.).
191 Following McCormack *et al.* (2015), we visually separated and sampled transporting (long, thick, high-

192 order roots (>3) and absorptive roots (short, thin, low-order roots 1 – 3),, finely ground and analyzed
193 with an Elementar Varo Isotope Cube to determine their C and $\delta^{13}\text{C}$ signal.

194 The soil half used for soil sampling was subsequently divided into shallow soil (0-3.5 cm) and deep soil
195 (3.5-10 cm). Deep soil was air dried, crushed, mixed, and divided into four sections. One 5 ml scoop
196 from every section was collected to form a composite subsample, then sieved at 2 mm. Three
197 subsamples were collected for each replicate pot, and analyzed with an elemental analyzer
198 Isoprime100 coupled with an Elementar Varo Isotope Cube, to determine C content, nitrogen (N)
199 content and $\delta^{13}\text{C}$ signal. Samples collected at time 0 and at the end of the experiment (after 183 days,
200 t_6) were analyzed. The difference between t_0 and t_6 gave the changes in C after 6 months (ΔC).

201 Simultaneously, 40g of soil from the same deep layer of the pot of the bulk soil samples were collected
202 and fractionated after Gavinelli et al. (1995) (See Chapter III: Method S1, Figure S1). The resulting five
203 fractions (POM: >200 μm , finePOM: 200-50 μm , SILT: 50-20 μm , SILT+CLAY: <20 μm) were analyzed for
204 C and $\delta^{13}\text{C}$ with an elemental analyzer Isoprime100 coupled with an Elementar Varo Isotope Cube. The
205 sum of C in different fractions represents the total C in the fraction sample (SUM). A subsample of 0.1
206 g was taken from each 40 g sample and analyzed without fractioning to determine the total C in the
207 bulk sample. The difference between total C in bulk soil and the sum of C in the different soil fractions
208 was used to assess the correctness of the fractionation and was equal to 93.3%.

209 The increased $\delta^{13}\text{C}$ signature of the atmosphere in the microcosm chamber, allowed the calculation of
210 the proportion of C stored in soil directly derived from the input of *M. sativa* and *L. perenne* (new C),
211 to differentiate it from the carbon already present in the soil at the beginning of the experiment (old
212 C). To calculate the proportion, an isotope mixing model (after Balesdent and Mariotti 1996) was used:

$$213 \quad \%C_{new} = \frac{\delta(t_1) - \delta(t_0)}{\delta_B - \delta(t_0)} \quad [10]$$

214 Where %Cnew is the percentage of new carbon in the measured SOC of a specific fraction, $\delta(t_1)$ is the
215 $\delta^{13}\text{C}$ signature of the SOC measured in a specific fraction at the end of the experiment (t_1), $\delta(t_0)$ is the

216 $\delta^{13}\text{C}$ signature of the SOC of a specific soil fraction before the experiment (t_0), δ_B is the $\delta^{13}\text{C}$ signature
217 of the new C input in the system, in our case, the signature of the root biomass (i.e., the mean signature
218 of absorptive and transport roots). The choice of root biomass as the $\delta^{13}\text{C}$ reference for C input was
219 made since root material was considered the main source of fresh C, given that litter was removed
220 every two weeks from the pots. Multiplying the total soil C by %C_{new} provides the amount of new C
221 in mgC g^{-1} soil.

222 Since the changes in carbon in the system (ΔC in mgC g^{-1} soil) are composed of the two fluxes: input of
223 new C ($\Delta\text{C}_{\text{NEW}}$) and changes in oldC, the changes of preexistent carbon in soil ($\Delta\text{C}_{\text{OLD}}$) were calculated
224 as:

$$225 \quad \Delta\text{C}_{\text{OLD}} = \Delta\text{C} - \Delta\text{C}_{\text{NEW}} \quad [11]$$

226 The effect of vegetation regarding the losses of old C (priming, PE in mgC g^{-1} soil) was calculated as:

$$227 \quad \text{PE} = \Delta\text{C}_{\text{OLDV}} - \Delta\text{C}_{\text{OLDBS}} \quad [12]$$

228 Where $\Delta\text{C}_{\text{OLDV}}$ is the change in old C in the vegetated soil fraction (in mgC g^{-1} soil), while $\Delta\text{C}_{\text{OLDBS}}$ is the
229 mean of old C changes in the bare soil controls (in mgC g^{-1} soil). If priming has positive values (positive
230 PE) – it means that vegetation increases old C mineralization, with the value corresponding to an
231 increased loss of old C in vegetated soil compared to bare soil. Likewise, if priming has negative values
232 (negative PE), it means that vegetation decreases old C mineralization and losses, with the value
233 corresponding to a decrease in old C loss in vegetated soil compared to bare soil.

234

235 **4.2.4. Statistical analysis**

236 The normal distribution of residues was verified using a Shapiro-Wilk test ($\alpha_p = 0.05$). If data were
237 normally distributed, a one way analysis of variance (ANOVA) was performed to test the effects of soil
238 type (topsoil versus subsoil) and plant species (*M. sativa*, *L. perenne*, bare soil) on C priming and A^{13}C
239 in respired CO_2 .

240 If data were not normal a Kruskal – Wallis test was used. Linear regressions ΔC , new C, old C and
241 priming with $A^{13}C$ in respired CO_2 were analyzed and R^2 and p values calculated. All the statistical
242 analyses were performed using the open-source statistical environment 'R', version 3.4.3 (R
243 Development Core Team, 2017) using the packages *vegan* and *Hmisc*. (Oksanen et al. 2019, Harrel
244 2007).

245

246 4.3. RESULTS

247

248 4.3.1. *Soil characteristics and changes in carbon content*

249 A positive increase in C in bulk soil after six months was found in topsoil planted with *M. sativa* only
250 (ΔC , Table 1). However, on subsoil, a net loss of total ΔC over 6 months was found. In bare soil and soil
251 planted with *L. perenne*, losses of total ΔC were higher in topsoil than subsoil, with the greatest loss in
252 bare topsoil (Tables 1, 2). In bulk soil, new C was significantly greater in topsoil than in subsoil (Tables
253 1, 2) and regardless of soil type, new C input was always greater in soils planted with *M. sativa*
254 compared to *L. perenne* (Table 2).

255 Based on bulk soil data, the losses of old C in topsoil are the highest in bare soil compared to *L. perenne*
256 and *M. sativa*, which are not statistically different (Table 1, Table 2). In subsoil, old C losses were
257 significantly lower than in topsoil, with the most losses in soil planted with *M. sativa*, compared to bare
258 soil and *L. perenne* (Table 1).

259 The losses of old C in SUM of fractions were lower in topsoil and not significantly different among
260 fractions or between species and bare soil (Table 1). In subsoil, SUM was comparable in soils planted
261 with *L. perenne* and *M. sativa*, however the losses in bare soil are lower in the SUM compared to bulk
262 soil data.

263 After 6 months we observed that vegetation significantly influenced N content in both subsoil and
264 topsoil when sowed with *M. sativa*, compared to bare soil. Soil N content at t6 for *L. perenne* did not
265 show any significant change compared to that at t0 (Fig. S8).

266 4.3.2. *Priming effect*

267 In bulk soil that had vegetation present, PE was negative in topsoil and there was no significant effect
268 of species (Fig. 2a). In bulk soil subsoil planted with *M. sativa*, PE was positive and old C loss was
269 significantly greater than bare soil, but in subsoil planted with *L. perenne*, old C loss was not
270 significantly different from bare soil and there was no PE (Fig. 2b). In topsoil SUM, PE was negative but

271 was not significant different between plant species, although it had a lower intensity compared to bulk
272 soil (Fig. 2a). In subsoil, the PE in SUM was positive, although there were no differences among species
273 (Fig. 2b). In topsoil fractions, PE was negative except in SILT+CLAY, and no significant differences
274 occurred in fractions between *L. perenne* and *M. sativa*, except in fine POM (Fig. 2a). In subsoil, priming
275 was positive in each fraction, with the highest effect in SILT and SILT+CLAY fractions, and the only
276 difference between *L. perenne* and *M. sativa* occurred in the POM fraction (Fig. 2b).

277

278 4.3.3. Evolution of ^{13}C abundance in respired CO_2 ($A^{13}\text{C}$) over 6 months

279 There was a significant effect of both soil type (Kruskal-Wallis, $p < 0.001$) and vegetation treatment
280 (Kruskal-Wallis, $p < 0.001$) on the abundance of ^{13}C in respired CO_2 ($A^{13}\text{C}$). In topsoil, the abundance of
281 ^{13}C in the respired CO_2 increased over 6 months, with the highest $A^{13}\text{C}$ from *L. perenne* (2.02%) and *M.*
282 *sativa* on 20/02/18 (1.99%), while in bare soil, $A^{13}\text{C}$ was greatest on 09/02/18 (1.96%). In topsoil there
283 was a significant effect of treatment (Kruskal-Wallis, $p < 0.001$) (Fig. 3a,b,c). Over six months, in topsoil
284 planted with *M. sativa*, the abundance of ^{13}C in CO_2 increased from 1.55 ± 0.05 % to 1.73 ± 0.03 % (with
285 an increment of +11.2%). In the same period, the abundance of ^{13}C in CO_2 from *L. perenne* increased
286 from 1.51 ± 0.07 % to 1.7 ± 0.02 % (with an increment of +13%), and bare soil increased from 1.43 ± 0.13
287 % to 1.61 ± 0.07 % (+13%).

288 In subsoil, the highest peak of $A^{13}\text{C}$ was found under *M. sativa* the 20/02/18 (1.49 ± 0.07 %), followed by
289 bare soil on 06/03/18 (1.41 ± 0.07 %) and *L. perenne* on 23/01/18 (1.37 ± 0.04) (Fig. 3d,e,f). The effect of
290 treatment was significant (Kruskal-Wallis, $p < 0.001$), with the highest $A^{13}\text{C}$ under *M. sativa*. No
291 significant differences between bare soil and that planted with *L. perenne* were found. In subsoil, $A^{13}\text{C}$
292 of soil respiration under *M. sativa* increased from 1.31 ± 0.01 % to 1.41 ± 0.05 % (with an increment of
293 +9%) and bare soil from 1.26 ± 0.01 % to 1.32 ± 0.03 % (with an increment of +5%), while *L. perenne*
294 decreased from 1.32 ± 0.04 % to 1.31 ± 0.02 % (with a decrement of -0.2%), however the decrease was
295 not significant (Fig. 3e).

296 **4.3.4. Evolution of ratio of CO₂ derived from fresh plant new C input (f_{Plant})**
297 There is a significant increase of respired CO₂ derived from fresh plant inputs (f_{Plant}) in the vegetated
298 treatments over the 6 month period. Topsoil had a +152% increase of f_{Plant} , and subsoil had a +84%
299 increase. When observing the trend over time, topsoil had a greater increase than subsoil in f_{Plant} (Fig.
300 4; $p < 0.001$)

301

302 **4.3.5. Correlations between OldC loss, NewC input, priming and $A^{13}C$**
303 In bulk soil, both new C and old changes in soil and the $A^{13}C$ were positively and significantly correlated
304 with the $A^{13}C$ of respired CO₂ (all data grouped together). Data points from different species were
305 clearly segregated, with more changes in new C and old C and $A^{13}C$ in respired CO₂ for *M. sativa* (Fig.
306 5a,b). In the respired CO₂, $A^{13}C$ was negatively correlated with priming effect (Fig. 5c; Kruskal - Wallis,
307 $p < 0.01$).

308

309 4.4. DISCUSSION

310 We observed a strong influence of soil type on old C stability and soil priming for both total C and that
311 in the SILT+CLAY pool, which masked the effect of plant species. Revegetating topsoil results in a
312 negative priming effect, with a lower mineralization of old C compared to the bare soil control.
313 However, in subsoil, the priming effect depends on the species, with no priming effect under *L.*
314 *perenne*, and a positive priming effect under *M. sativa*, that increased old C losses compared to the
315 bare soil control. We will tackle these effects separately for the sake of clarity, but they are nonetheless
316 closely linked and the C-cycle depends on a feedback mechanism between soil, plants and microbial
317 communities.

318

319 4.4.1. *Subsoil and topsoil revegetation: identifying the substrate preference of* 320 *microbial communities*

321 The priming effect was highly negative in topsoil, but was marginally positive in subsoil. On topsoil a
322 high input of fresh new C allowed microbiological communities to change the substrate preference for
323 energy and nutrients requirements from old C in soil to fresh new C inputted by plants. This
324 phenomenon seems to support the Preferential Substrate Utilization hypothesis (Cheng, 1996; Cheng
325 and Kuzyakov, 2005). However, negative PE is usually for a short period of time; and after positive PE
326 starts (Cheng, 1996; Kuzyakov and Cheng, 2001, 2004; Wang et al., 2016). It is therefore crucial to have
327 long term experiment with living plants to assess the PE over a longer period of time. Subsoil had less
328 N than topsoil, resulting in reduced plant development (Chapter III, this thesis), and a consequent
329 lower input of labile C into soil from rhizodeposition. As subsoil is subjected to long-term limitation of
330 nutrients, microbial functioning is decreased, thus promoting the development of oligotrophic
331 communities with high metabolic diversity (Blagodatskaya and Kuzyakov, 2008). This set of conditions
332 makes subsoil a perfect candidate for positive priming effect. Specific dormant microbial groups can
333 be activated by the input of low available substrates, such as oxalic acid, that have a high impact on
334 community shift, and synthesize a broad variety of enzymes that promote old C decomposition and a

335 positive priming (Falchini et al., 2003; Landi et al., 2006; Blagodatskaya and Kuzyakov, 2008). Finally,
336 fungi have been shown to play an important role in C degradation and priming (Panikov 1995; Bell et
337 al. 2003; Blagodatskaya and Kuzyakov, 2008). The input of fresh C might activate spore or cysts
338 dormant in subsoil, which can penetrate previously inaccessible micro zones with hyphae development
339 (Blagodatskaya and Kuzyakov, 2008). The low amount of labile C input, together with the low N
340 availability, will not be enough to shift the increased microbial metabolism towards labile C input in a
341 significant way, and microbial communities will increase old C mineralization to acquire energy and
342 nutrients (De Graaf et al., 2010). In topsoil, instead, the higher biomass development and the
343 consequent high input of labile fresh C from plants will enhance fungal: bacterial gene copy ratios
344 (Griffiths et al., 1998; Broeckling et al., 2008; Chiginevaa et al., 2009). Our data showed higher microbial
345 abundance and diversity, as well as a higher level of activity (Chapter III, this thesis), corresponding
346 well to such a phenomenon. The higher inputs of labile C in the system may, nevertheless, shift the
347 microbial preferential consumption from preexistent old C to fresh C input (as shown in Fig. 5), and
348 result in a negative priming effect. This phenomenon is well supported by the A¹³C and percentage of
349 plant derived C in respired CO₂, that was always higher in topsoil compared to subsoil.

350 Experiments investigating substrate preference or competition mechanisms effect on PE have usually
351 been performed in controlled incubation conditions (e.g., Fontaine et al., 2007; De Graaf et al., 2010).
352 Our study is novel in that plants were grown in different types of non-sterilised soil. Also, we
353 demonstrate that the SILT and SILT+CLAY C pools played a pivotal role in determining the amount and
354 trajectory of PE. Particularly in subsoil, where PE was positive in SILT and SILT+CLAY C pools, thus
355 questioning the point of view that these C pools are highly stable (Chapters II and III, this
356 thesis). However, SILT+CLAY C pools is very reactive to input of new C (Chapter III, this thesis) and
357 Fontaine et al. (2007) showed how input of fresh C in subsoil can increase the mineralization of stable C
358 and lead to positive PE. Our results suggest that SILT+CLAY pool is stable when conditions are not
359 abruptly changed: in topsoil positive PE is present only in POM. An abrupt change of conditions,

360 however, can bring to instability of C associated with fine soil fractions and the resulting PE, as
361 observed in subsoil SILT and SILT+CLAY.

362

363 4.4.2. *The impact of plants on the two soil types: competition for nitrogen*

364 The effect of vegetation on PE was largely influenced by soil type. We did not observe any significant
365 difference in PE between topsoil planted with *M. sativa* or *L. perenne*. Plant species had more influence
366 on PE in subsoil, despite the disparity between the results from bulk soil and from fractionation. *L.*
367 *perenne* better mitigated the undesired positive PE than *M. sativa*, especially in bulk soil, where no PE
368 occurred in subsoil sown with *L. perenne*. This result on of plant species effect on PE in subsoil, however
369 limited, is in line with the competition hypothesis (Cheng and Kuzyakov, 2005). When plants are grown
370 on an N poor soil, mineralization of old SOC from microbial communities can be reduced due to more
371 efficient N removal by plant roots, that hinders microbial activity, resulting in a negative priming effect
372 (Cheng & Kuzyakov, 2005). This phenomenon can explain the effect of *L. perenne* on positive PE
373 mitigation in subsoil. Increased rhizodeposition will increase old C consumption and can result in a
374 positive PE. This mechanism is exactly what we observe when planting soil with *M. sativa* which has a
375 higher biomass development than *L. perenne* on subsoil (Chapter III, this thesis), and therefore lowers
376 rhizodeposition (Fu and Cheng, 2002; Cheng et al., 2003; Dijkstra et al., 2006). Moreover, *M. sativa* is
377 associated with *Rhizobium* bacteria that allow fixation of N₂ directly from the atmosphere, and rely
378 less on N mining for growth. In this case, the 'competition effect' is avoided because *M. sativa* can
379 acquire N from a different source. To test this hypothesis, we analyzed the difference in N content in
380 soil between time 0 and time 6 months under the three different treatments and two soils (Fig. S8).
381 We observed that bare soil and *L. perenne* do not significantly differ from t0 and between each other.
382 However, *M. sativa* increased the amount of soil N, strengthening our hypothesis that competition for
383 N was decreased. Also, substrates from fresh plants' new C input become available, and it increases
384 microbial activity but do not permit a substrate preference switch, resulting in higher mineralization

385 of old C and a positive priming effect (De Graaf et al., 2010). These results are supported in several
386 studies, where N-rich rhizodeposition is believed to be linked with higher PE (Fu and Cheng, 2002;
387 Cheng et al., 2003; Cheng and Kuzyakov, 2005). In topsoil, such a phenomenon was not observed. We
388 speculate that higher fertility levels and rhizodeposition level (Chapter III, this thesis) mask the
389 competitive effect between roots and microorganisms, providing enough nutrients via plants fresh C
390 deposition to the microorganisms to allow them not to have to rely on mining soil C and compete with
391 plants (Cheng and Kuzyakov, 2005; De Graaf et al., 2010).

392 Such a framework considering both soil and vegetation features incorporate the two hypotheses: the
393 Substrate Preferential Utilization hypothesis and the Competition hypothesis (Fig.6), supporting the
394 reconciliation between the two proposed by Cheng and Kuzyakov (2005): in fertile soils,
395 the substrate preference will drive the PE, while in poor soil competition will shape the trajectory and
396 magnitude of PE.

397

398 *4.4.3. The priming effect and its implication in practice*

399 From an applied point of view, when revegetating soil in geotechnical constructions, especially subsoil,
400 it is necessary to consider soil fertility, as it will affect i) biomass development, ii) nutrient competition
401 in soil and fresh substrate availability and, consequently, iii) the priming effect. In nutrient poor
402 subsoils, the use of non N₂-fixing species (e.g. *L. perenne*) will result in a low priming effect. A possible
403 solution to avoid the priming effect when revegetating subsoil (or nutrient poor soils in general) could
404 be to couple inoculation of microbial strains that consume labile C with N fertilization, to increase
405 fertility and nutrient availability, and try to switch the microbial consumption from preexistent oldC to
406 new C.

407

408 4.5. CONCLUSIONS

409 We examined the priming effect in a crossed experimental design with two soil types and two plant
410 species. We highlighted the complex interactions between the two sources of factors and
411 demonstrated the importance of soil quality (in terms of N content and microbiological activity and
412 biomass) in determining the trajectory and magnitude of PE over that of plant species. When soil
413 quality is high, such as topsoil, positive PE can be mitigated and negative PE can occur thanks to high
414 fresh new C input. However, in N-poor subsoils, old soil C, especially the stable old C in the SILT+CLAY
415 pool, can be susceptible to the PE, depending on the competition between plants and soil
416 microorganisms. Therefore, plant species could play a non-negligible role in influencing the tendency
417 and magnitude of PE.

418 Our results suggest that topsoil, with higher rhizodepositions, allows microbial communities to switch
419 from consuming old C to new C mineralization, resulting in a negative priming effect. In subsoil,
420 microbes will mine old C for nutrients due to low new C input. Competition for N is fundamental to
421 shape the priming effect, and in poor subsoil, *L. perenne* had no priming effect due to N competition
422 between plants and microbes. Therefore, when a soil is severely limited in nutrients the competition
423 effect will be predominant; while when conditions are not so limiting the substrate preference will
424 dominate. These findings are in line with the reconciliation of hypothesis from Cheng and Kuzyakov
425 (2005). The $A^{13}C$ and its correlations with old C losses and priming helps to understand the processes
426 in different soils, but alone this is not enough to investigate the effects of priming. Old C losses of
427 vegetated and bare soil control need to be taken into account.

428

429 REFERENCES

- 430 Andersen, T.H., Domsche, K.H. 1989. Ratios of microbial biomass carbon to total organic carbon in
431 arable soils. *Soil Biology and Biochemistry*21:471–479
- 432 Balesdent, J. & Mariotti, A. 1996. Measurement of soil organic matter turnover using ^{13}C natural
433 abundances. In: *Mass Spectrometry of Soils* (eds T.W. Boutton & S. Yamasaki), pp. 83-111.
434 Marcel Dekker Inc., New York.
- 435 Bell, J.M., Smith, J.L., Bailey, V.L., Bolton, H 2003. Priming effect and C storage in semi-arid no-till spring
436 crop rotations. *Biology and Fertility of Soils* 37:237–244
- 437 Blagodatskaya, E., Kuzyakov, Y., 2008. Mechanisms of real and apparent priming effects and their
438 dependence on soil microbial biomass and community structure: Critical review. *Biology and*
439 *Fertility of Soils* 45, 115–131.
- 440 Broeckling, C.D., Broz A.K., Bergelson, J., Manter, D.K., Vivanco, J.M., 2008 Root exudates regulate soil
441 fungal community composition and diversity. *Applied and Environmental Microbiology* 74: 738–
442 744
- 443 Chabbi, A., Kögel-Knabner, I., Rumpel, C., 2009 Stabilised carbon in subsoil horizons is located in
444 spatially distinct parts of the soil profile. *Soil Biology and Biochemistry*41:256–271
- 445 Cheng W., 1996 Measurement of rhizosphere respiration and organic matter decomposition using
446 natural ^{13}C 263–268.
- 447 Cheng, W., Johnson, D.W., Fu, S., 2003 Rhizosphere effects on decomposition: controls of plant species,
448 phenology, and fertilisation. *Soil Science Society of America Journal* 67, 1418e1427
- 449 Cheng, W., Kuzyakov, Y., 2005 Root effects on soil organic matter decomposition. In: S. Wright, S.,
450 Zobel, R. (Eds.), *Roots and Soil Management: Interactions Between Roots and the Soil*.
451 *Agronomy Monograph No. 48*, American Society of Agronomy, Madison, Wisconsin, USA 119–
452 143.
- 453 Chiginevaa, N.I., Aleksandrovab, A.V., Tiunovc, A.V., 2009. The addition of labile carbon alters residue
454 fungal communities and decreases residue decomposition rates. *Applied Soil Ecology* 42: 264–
455 270.
- 456 De Deyn, G.B., Cornelissen, J.H.C., Bardgett, R.D., 2008. Plant functional traits and soil carbon
457 sequestration in contrasting biomes. *Ecology Letters* 11, 516–531.
- 458 De Graaff, M.A., Classen, A.T., Castro, H.F., Schadt, .CW., 2010. Labile soil carbon inputs mediate the
459 soil microbial community composition and plant residue decomposition rates. *New Phytologist*
460 188, 1055–1064.
- 461 Dijkstra, F.A., Cheng, W.X., Johnson, D.W., 2006. Plant biomass influences rhizo- sphere priming effects
462 on soil organic matter decomposition in two differently managed soils. *Soil Biology and*
463 *Biochemistry* 38, 2519e2526.
- 464 Ekklund, F., Ronn, R., Christensen, S. 2001. Distribution with depth of protozoa, bacteria and fungi in
465 soil profiles from three Danish forest sites. *Soil Biology and Biochemistry*33:475–481

466 Eusterhues, K., Rumpel, C., Kögel-Knabner, I., 2005b. Organo–mineral associations in sandy acid
467 forest soils: importance of specific surface area, iron oxides and micropores. *European Journal*
468 *of Soil Science* 56, 753–763

469 Falchini, L., Naumova, N., Kuikman, P.J., Bloem, J., Nannipieri P. 2003. CO₂ evolution and denaturing
470 gradient gel electrophoresis profiles of bacterial communities in soil following addition of low
471 molecular weight substrates to simulate root exudation. *Soil Biology and Biochemistry* 35:775–
472 782

473 Fang, C., Moncrieff, J.B. 2005. The variation of soil microbial respiration with depth in relation to soil
474 carbon composition. *Plant and Soil* 268:243–253

475 Fontaine, S., Bardoux, G., Abbadie, L., Mariotti, A., 2004. Carbon input to soil may decrease soil carbon
476 content. *Ecology Letters* 7, 314–320.

477 Fontaine, S., Barot, S., Barré, P., Bdioui, N., Mary, B., Rumpel, C. 2007. Stability of organic carbon in
478 deep soil layers controlled by fresh carbon supply. *Nature* 450, 277–280.

479 Fu, S. and Cheng, W. 2002. Rhizosphere priming effects on the decomposition of soil organic matter
480 in C₄ and C₃ grassland soils. *Plant Soil* 238, 289–294.

481 Gavinelli, E., Feller, C., Larré, - Larrouy, M.C., Bacye, B., Djegu, Z., Nzila, J.D., 1995. Routine method to
482 study soil organic matter by particle - size fractionation: Examples for tropical soils. *Soil Science*
483 *Plant Analysis* 26(11&12), 1749-1760

484 Griffiths, B.S., Ritz, K., Ebbelwhite, N., Paterson, E., Killham, K., 1998.: Ryegrass rhizosphere microbial
485 community structure under elevated carbon dioxide concentrations, with observations on
486 wheat rhizosphere. *Soil biology and Biochemistry*. 30, 315±321

487 Hamer, U., Marschner, B., 2005. Priming effects in soils after combined and repeated substrate
488 additions, *Geoderma* 128, 38–51

489 Harrell, F.E., 2007. Package ‘Hmisc’. Harrell Miscellaneous

490 Holden, P.A., Fierer, N. 2005. Microbial processes in the vadose zone. *Vadose Zone Journal* 4, 1–21

491 Huo, C., Luo, Y., Cheng, W., 2017. *Soil Biology & Biochemistry* Rhizosphere priming effect : A meta-
492 analysis. *Soil Biology and Biochemistry* 111, 78–84.

493 Kuzyakov, Y., Domanski, G. 2000.. Carbon input by plants into the soil. Review. *Journal of Plant*
494 *Nutrition and Soil Science* 163, 421–431.

495 Kuzyakov, Y., Friedel, J.K., Stahr, K., 2000. Review of mechanisms and quantification of priming effects
496 . *Soil Biology and Biochemistry* 32, 1485-1498

497 Kuzyakov, Y., Cheng, W.X., 2001. Photosynthesis controls of rhizosphere respiration and organic matter
498 decomposition. *Soil Biology & Biochemistry* 33, 1915–1925.

499 Kuzyakov, Y., Cheng, W.X., 2004. Photosynthesis controls of CO₂ efflux from maize rhizosphere. *Plant*
500 *and Soil* 263, 85–99.

501 Kuzyakov, Y., 2006. Sources of CO₂ efflux from soil and review of partitioning methods. *Soil Biology and*
502 *Biochemistry* 38, 425–448.

503 Lal, R, 2004. Soil carbon sequestration impacts on global change and food security. *Science* 304: 1623-
504 1627. 304.

505 Landi, L., Valori, F., Ascher, J., Renella, G., Falchini, L., Nannipieri, P. 2006. Root exudate effects on the
506 bacterial communities, CO₂ evolution, nitrogen transformations and ATP content of rhizo-
507 sphere and bulk soils. *Soil Biology and Biochemistry* 38:509–516

508 Le Bissonnais, Y., 2016. Aggregate stability and assessment of soil crustability and erodibility: I. Theory
509 and methodology. *European Journal of Soil Science* 67, 11–21.

510 Liang, C., Schimel, J.P., Jastrow, J.D., 2017. The importance of anabolism in microbial control over soil
511 carbon storage. *Nature Microbiology* 2, 1–6.

512 Minasny, B., Malone, B.P., McBratney, A.B., Angers, D.A., Arrouays, D., Chambers, A., Chaplot, V., Chen,
513 Z.S., Cheng, K., Das, B.S., Field, D.J., Gimona, A., Hedley, C.B., Hong, S.Y., Mandal, B., Marchant,
514 B.P., Martin, M., McConkey, B.G., Mulder, V.L., O'Rourke, S., Richer-de-Forges, A.C., Odeh, I.,
515 Padarian, J., Paustian, K., Pan, G., Poggio, L., Savin, I., Stolbovoy, V., Stockmann, U., Sulaeman,
516 Y., Tsui, C.C., Vågen, T.G., van Wesemael, B., Winowiecki, L., 2017.. Soil carbon 4 per mille.
517 *Geoderma* 292, 59–86.

518 . Ohm, H., Hamer, U., Marschner, B. 2007. Priming effects in soil size fractions of a podzol Bs horizon
519 after addition of fructose and alanine. *Journal of Plant Nutrition and Soil Science*. 170: 551–559.

520 Oksanen, J., Blanchet, F.G., Friendly, M., Kindt, R., Legendre, P., McGlenn, D., Minchin, P.R., O'Hara,
521 R.B., Simpson, G.L., Solymos, P., Henry, M., Stevens, H., Szoecs, E., Wagner, H., 2019. Package
522 'vegan'. *Community Ecology Package*

523 Panikov, N.S. 1995. *Microbial growth kinetics*. Chapman & Hall, London

524 Perveen, N., Barot S., Maire V., Cotrufo M.F., Shahza T., Blagodatskaya T., Stewart C.E, Ding W., Siddiq,
525 Dimassi B, Mary B, Fontaine S., 'Universality of priming effect: An analysis using thirty five soils
526 with contrasted properties sampled from five continents', *Soil Biology and Biochemistry journal*,
527 134, 162-171

528 Rumpel, C., Kögel-Knabner, I., 2011. Deep soil organic matter-a key but poorly understood component
529 of terrestrial C cycle. *Plant and Soil* 338, 143–158.

530 Shahzad, T., Chenu, C., Genet, P., Barot, S., Perveen, N., Mougin, C., and Fontaine, S., 2015.
531 Contribution of exudates, arbuscular mycorrhizal fungi and litter depositions to the rhizosphere
532 prim- ing effect induced by grassland species. *Soil Biology and Biochemistry* 80, 146–155, 2015

533 Smith, P., Powlson, D.S., Smith, J.U., Falloon, P., Coleman, K., 2000. Meeting Europe's climate change
534 commitments: Quantitative estimates of the potential for carbon mitigation by agriculture.
535 *Global Change Biology* 6, 525–539.

- 536 Taylor, J.P., Wilson, B., Mills, M.S., Burns, R.G., 2002. Comparison of microbial numbers and enzymatic
537 activities in surface soils and subsoils using various techniques. *Soil Biology and Biochemistry* 34,
538 387-401
- 539 von Lutzow, M., Kogel-Knabner, I., Ekschmitt, K., Matzner, E., Guggenberger, G., Marschner, B., Flessa,
540 H. 2006. Stabilization of organic matter in temperate soils: mechanisms and their relevance
541 under different soil conditions—a review. *European Journal of Soil Science*, 57, 426–445
- 542 Wang, X., Tang, C., Severi, J., Butterly, C.R., Baldock, J.A., 2016. Rhizosphere priming effect on soil
543 organic carbon decomposition under plant species differing in soil acidification and root
544 exudation. *New Phytologist* 211, 864–873
- 545

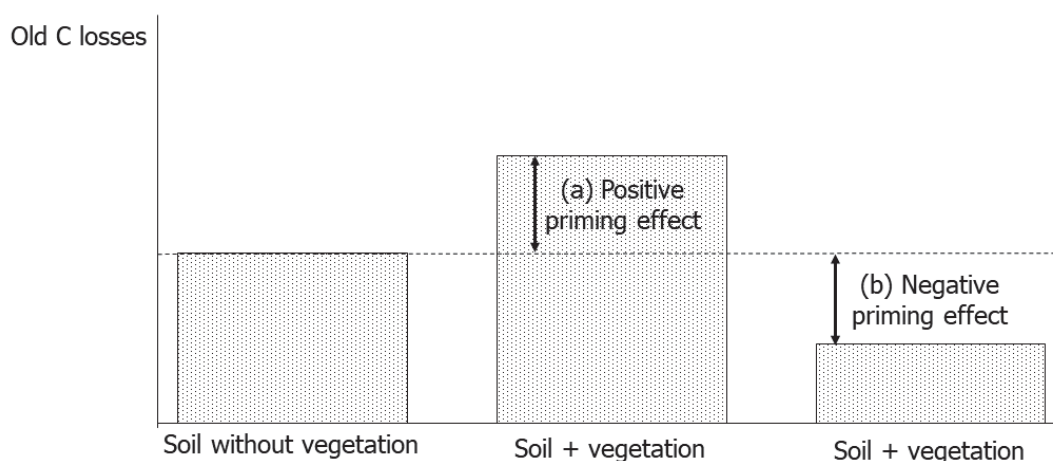
546 FIGURES AND TABLES

547 **Table 1:** ΔC is the difference of C content in bulk soil between time 0 and time 6 months in mgC g^{-1} soil. New C is
 548 the input of C in bulk soil deriving from the vegetation growth during the 6 months of the experiment in mgC g^{-1} soil.
 549 Old C is the losses of old C in bulk soil. The last column shows the losses of old C in the sum of fractions data. ΔC
 550 new C, and old C have been calculated for each treatment (*M.sativa*, *L. perenne* and bare soil) and each soil
 551 (topsoil: 0-30cm depth, subsoil: 110-140cm depth). Different letters next to the average value indicate statistically
 552 significant differences ($p < 0.05$) between species or families according to Tukey HSD tests.

Soil	Data set:		Bulk soil data			SUM of fractions
	Treatment	ΔC (mgC g^{-1} soil)	New C (mgC g^{-1} soil)	Old C (mgC g^{-1} soil)	Old C (mgC g^{-1} soil)	
Topsoil	bare soil	(c) -1.60 ± 0.20	(c) 0.10 ± 0.05	(b) -1.70 ± 0.15	(a) -0.36 ± 0.44	
	<i>L. perenne</i>	(b) -0.48 ± 0.33	(b) 0.68 ± 0.09	(a) -1.16 ± 0.27	(a) -0.36 ± 0.40	
	<i>M. sativa</i>	(a) 0.01 ± 0.41	(a) 1.22 ± 0.16	(a) -1.21 ± 0.29	(a) -0.26 ± 0.02	
Subsoil	bare soil	(b) -0.50 ± 0.07	(c) 0.04 ± 0.03	(ab) -0.54 ± 0.08	(a) -0.24 ± 0.35	
	<i>L. perenne</i>	(a) -0.26 ± 0.08	(b) 0.22 ± 0.03	(b) -0.49 ± 0.06	(ab) -0.59 ± 0.07	
	<i>M. sativa</i>	(a) -0.17 ± 0.18	(a) 0.45 ± 0.11	(a) -0.61 ± 0.1	(b) -0.67 ± 0.23	

553

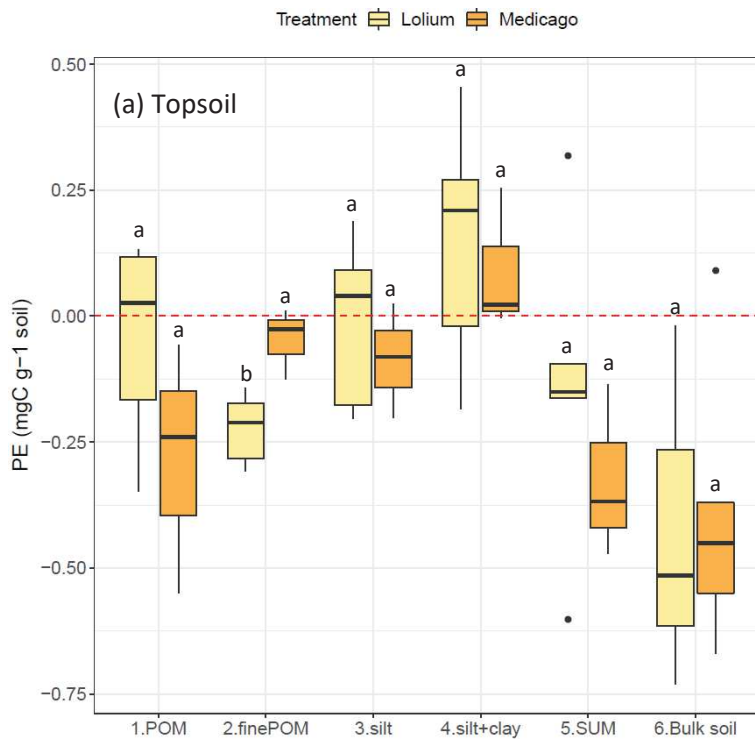
554



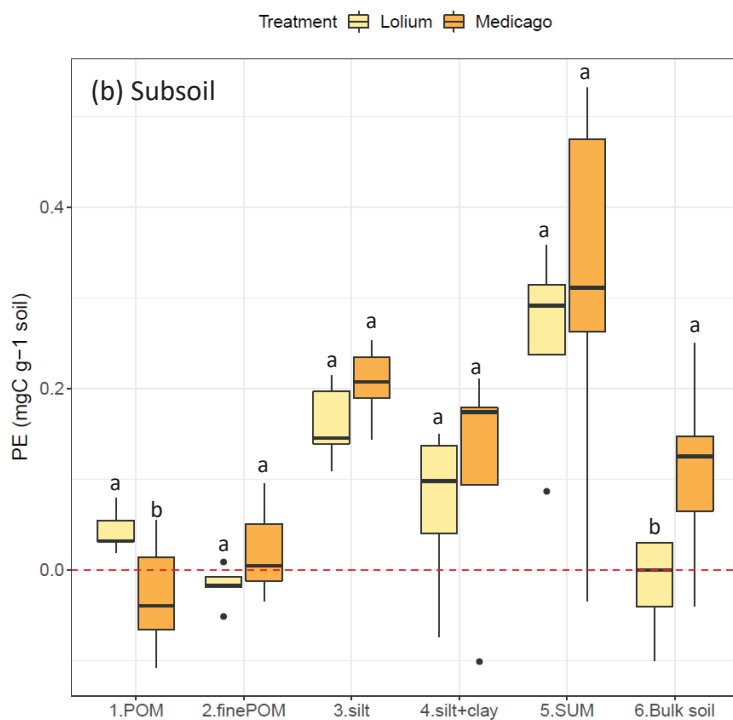
555

556 **Figure 1:** Graphic explanation of positive priming effect (a) and negative priming effect (b).

557



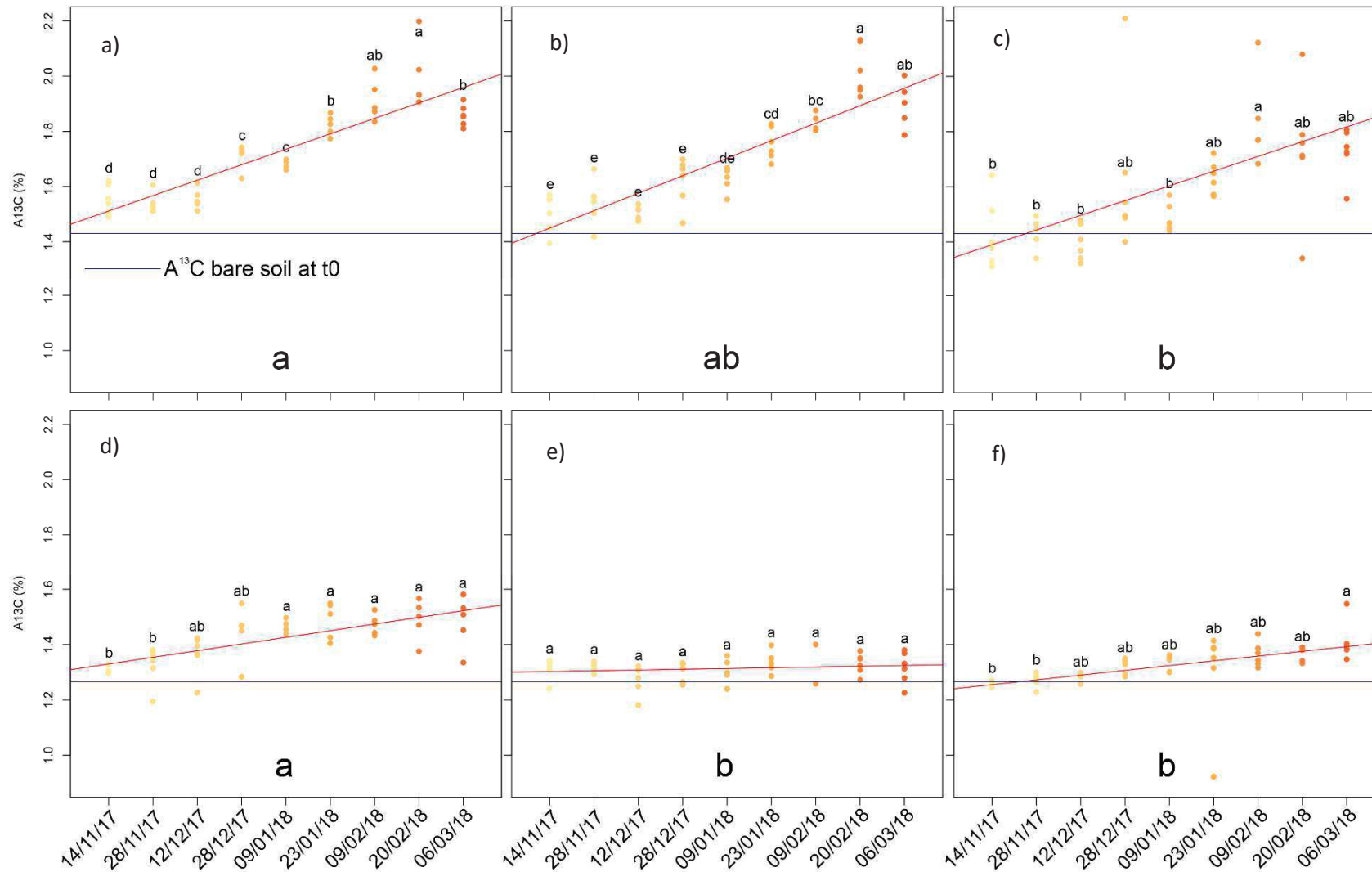
558



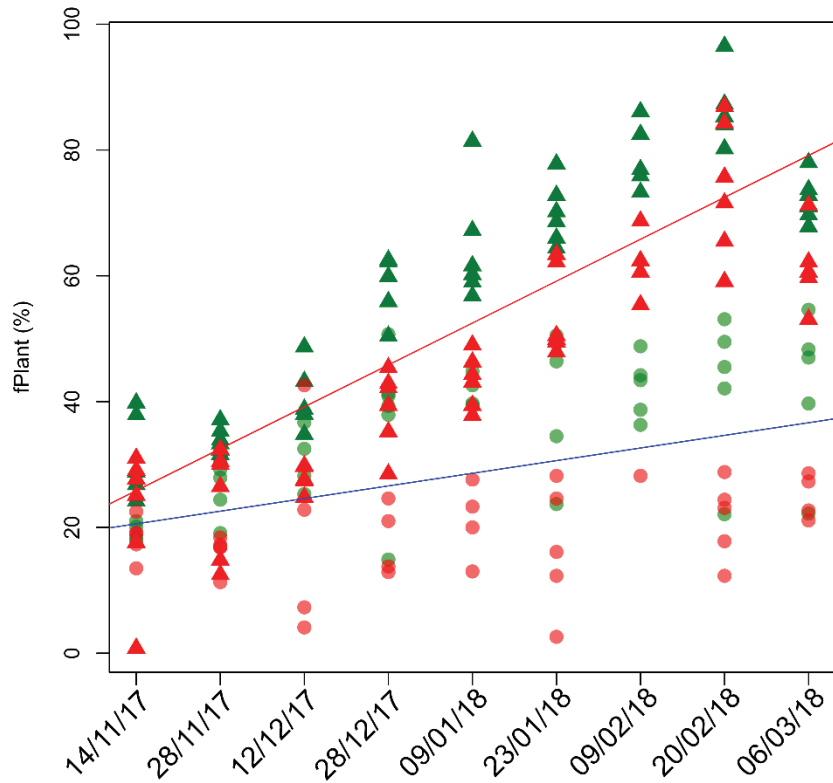
559

560

Figure 2: Comparison of priming effect after 6 months of revegetation between different soils ((a) topsoil and (b) subsoil) for each vegetated treatment (*L. perenne* light yellow, *M. sativa* orange). The data presented shows the priming in the different soil fractions (1.POM, 2.finePOM, 3.silt, 4.silt+clay) the sum of the soil fractions (5.SUM) and the bulk soil data (6.Bulk soil). Negative values means a reduced loss of old C, positive values an increased loss of old C. In each boxplot, the lower edge of the box corresponds to the 25th percentile data point, while the top edge of the box corresponds to the 75th percentile data point. The line within the box represents the median. Different letters above the boxplots indicate statistically significant differences (p < 0.05) among species according to a ANOVA test

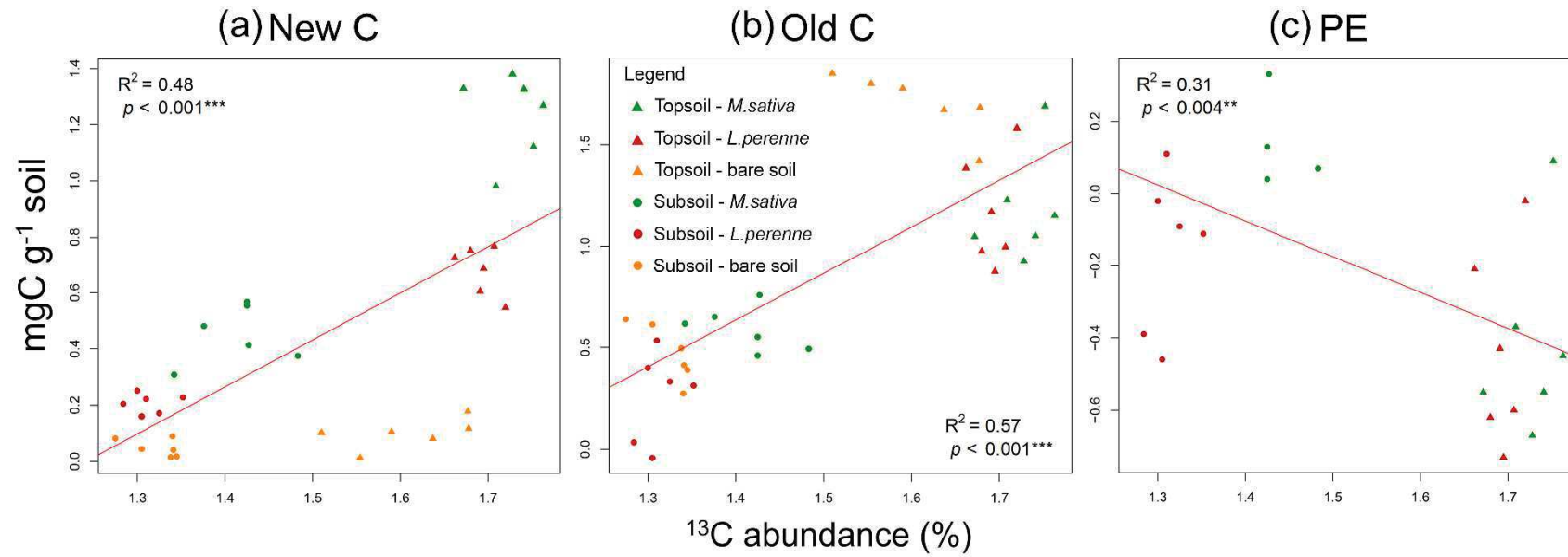


486
Figure 3: Evolution over time of $A^{13}C$, as the percentage of ^{13}C in the respired CO_2 . The results shows the trend for a) topsoil vegetated with *M.sativa*, b) topsoil with *L.perenne* and c) topsoil bare soil control. The second row shows the results for d) subsoil sowed with *M.sativa*, e) subsoil with *L.perenne* and f) subsoil bare soil control. The different dots shows the $A^{13}C$ result for the single subsample of the treatment in shade of yellow/red according to the sampling time. Different letters above the dots indicate statistically significant differences ($p < 0.05$) according to a Tukey HSD test among different sampling dates. Different letters at the bottom of the graph indicate statistically significant differences ($p < 0.05$) according to a Tukey HSD test among different treatments.



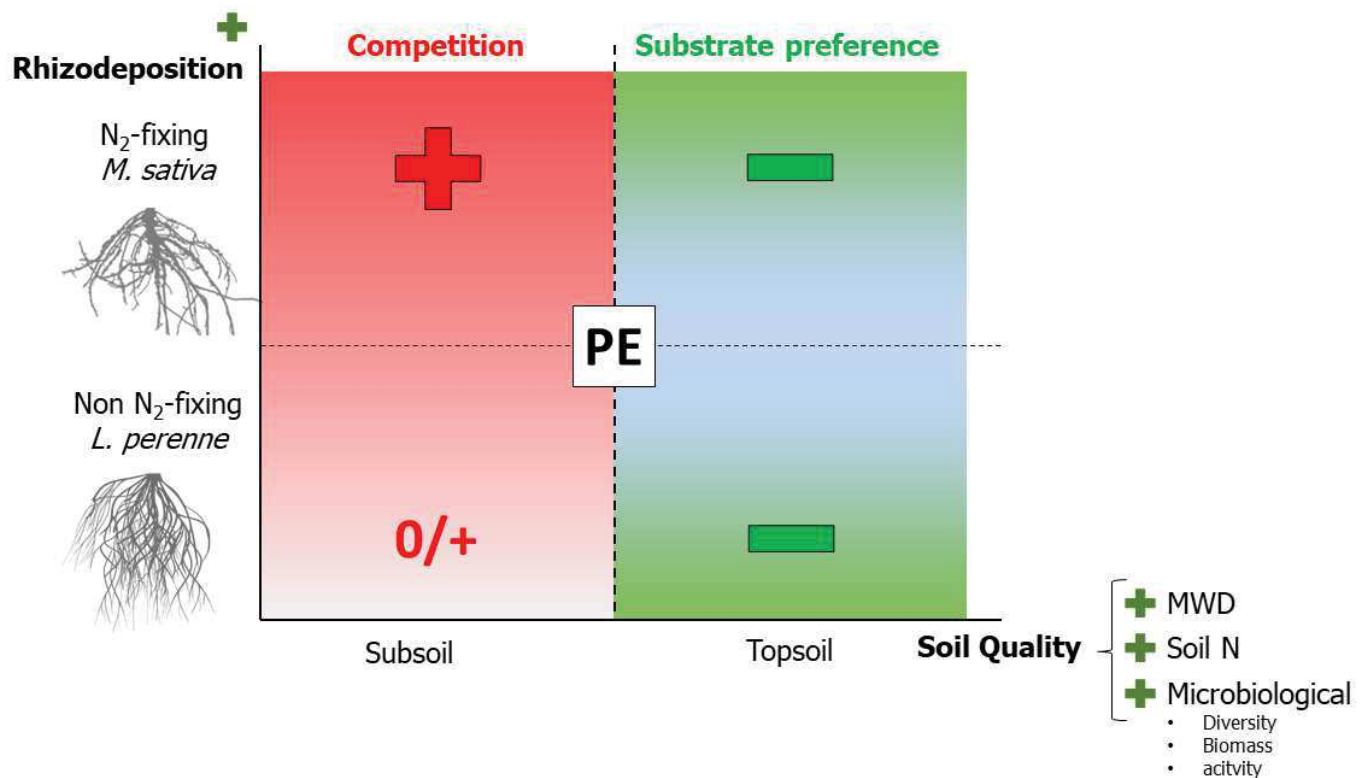
487

488 **Figure 4:** Percentage of C derived from mineralization of plant inputs in soil respired CO₂ (f_{Plant}) over 4 months in the
 489 two vegetated soils. Triangles represent topsoil and dots subsoil. Green represent *M. sativa* and red *L. perenne*,
 490 different saturations have been given to better differentiate the points. The red solid line represent the increase
 491 according to a linear model of the f_{Plant} in topsoil over the 4 months, the blue solid line in subsoil. The slopes of the
 492 linear models are significantly different, $p < 0.001$.



494

495 **Figure 5:** Correlations between a) New carbon inputs in soil, b) old SOC C losses (OldC) and c) priming effect (Priming), with abundance of ^{13}C in respired CO_2 (A^{13}C). Topsoil is
 496 represented by triangles, subsoil by dots, *M.sativa* is green, *L.perenne* red and bare soil control orange. The red line shows the correlation according to a linear model, and the
 497 significance (R^2 , p) is shown in a corner box in every graph.
 498



498

499 **Figure 6:** Reconciliation of Preferential Substrate Utilization hypothesis and competition hypothesis. a) shows the effect
 500 of soil, where the higher input in the fertile soil allow microbial communities to switch preference of substrate and
 501 decrease old C mineralization, while in subsoil, with low fertility and low input of fresh new C, competition drive the
 502 priming effect that is generally higher than topsoil. b) shows the species effect in the two soil conditions. In subsoil low
 503 rhizodeposition from *L. perenne* stimulate and competition for N hinder old C mineralization and result in a slightly
 504 negative priming effect. In topsoil, the N rich rhizodeposition from *M. sativa* increase the soil N content and decrease
 505 competition, allowing microbial communities to mine more efficiently old C and resulting in positive priming effect. In
 506 topsoil, contrary to what expected, we did not find any difference between *L. perenne* and *M. Sativa* in priming effect,
 507 suggesting a lower influence of rhizodeposition when the system is rich and efficiently colonized by roots.

508

509 SUPPLEMENTARY MATERIALS



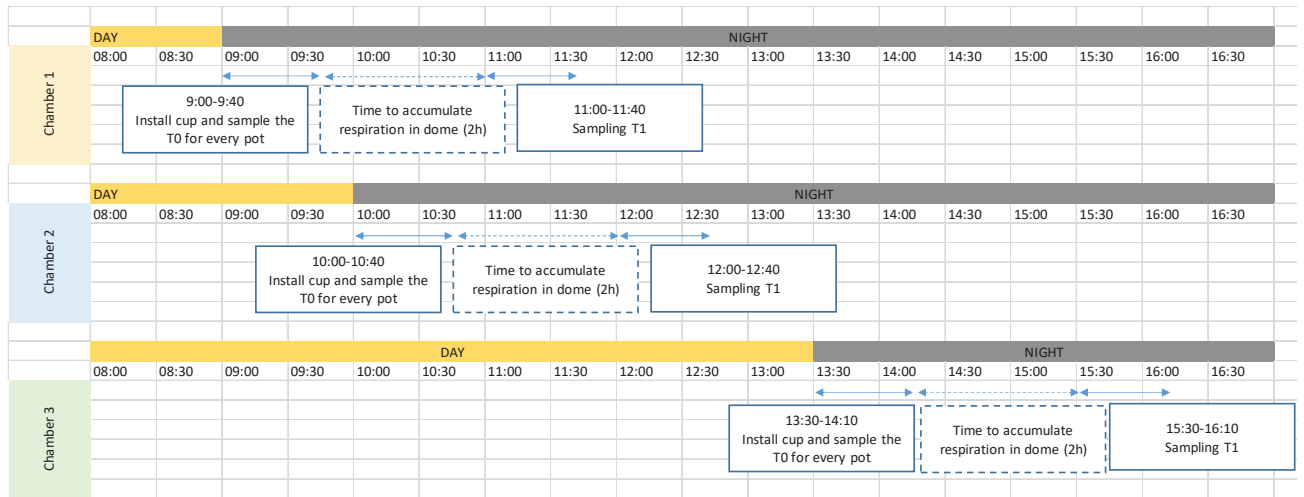
510
511 **Figure S1** : Pot preparation. Starting from left to right : Quartile of soil prior to filling the pots, weighting of the pots while
512 filling and examples of two pots filled with the two different types of soil The soil has been added collecting one scoop
513 of soil from each quartile and keep moving to the next quartile, in the same order, until the desired weight was reached.



514
515 **Figure S2** : From left to right: example of the ring used for soil respiration analysis, ring with the plastic dome in place
516 and ring inside the soil, the red crosses mark the spots were the seeds were planted



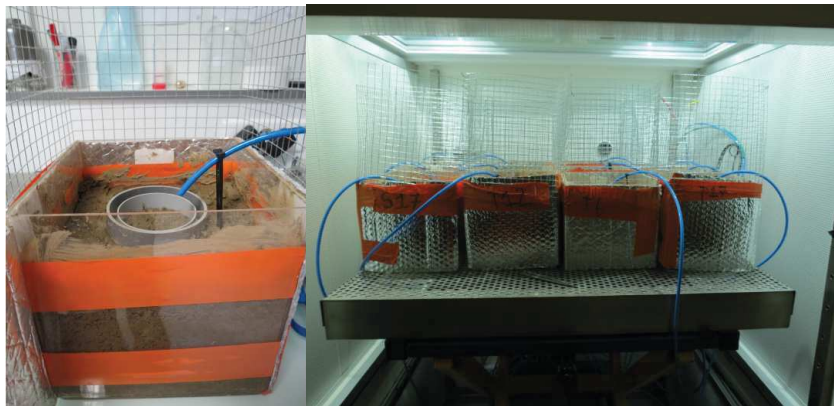
517
518 **Figure S3** : Pots positioned in the growing chamber at a fix distance from lights in the Ecotron facilities



519

520 **Figure S4** : Day and night cycles in the three different grow chambers with timing for air samples collection

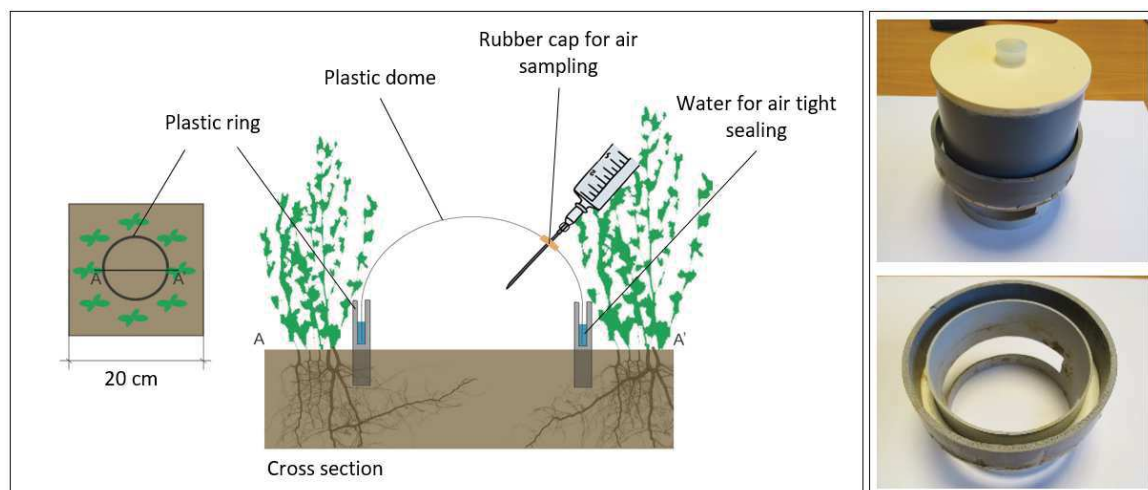
521



522

523 **Figure S5** : plastic tubes used for irrigation, fix on the single pot on the left and positioned in the chamber on the right

524

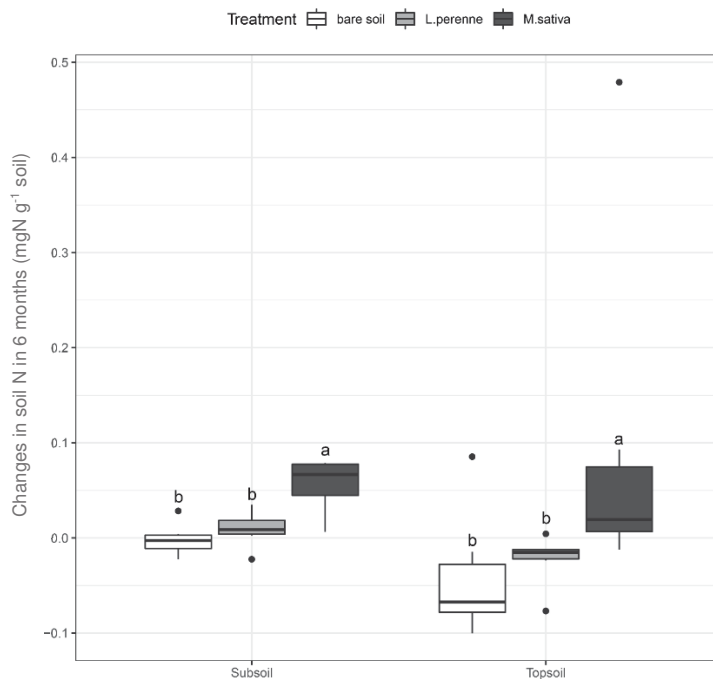


525

526 **Figure S6** : Scheme of the plastic dome used for soil respiration analysis



527
 528 **Figure S7** : Air sampling protocol : a) fill ring with water, b) place the plastic cap on top, c) take a 5ml air samples using
 529 a syringe on the rubber cap and d) transfer the air taken in the airtight exainers



530
 531 **Figure S8**: Comparison of N content in soil between the beginning of the experiment (t0) and the end (t6) in the two
 532 soils (subsoil and topsoil) and the three treatments (*M.satva*, *L.perenne*, and bare soil). No significant differences have
 533 been found between bare soil and *L.perenne*, which show no changes from the initial C content. *M.satva*, instead, is
 534 significantly different compared to the other treatments, showing an increase of soil N. In each boxplot, the lower edge
 535 of the box corresponds to the 25th percentile data point, while the top edge of the box corresponds to the 75th percentile
 536 data point. The line within the box represents the median. Different letters above the boxplots indicate statistically
 537 significant differences ($p < 0.05$) among species and control according to a Tukey HSD test.

Chapter V: General discussion

5.1. Carbon quality matters: coarse particle pool versus fine particle pool

Assessment of C stock of an ecosystem usually considers total soil carbon, not the C in individual fractions. As a result, soil C is presented as a simple number at the plot, catchment, regional or national scale, e.g., the 4P1000 goal, that considers only total C (Minasny et al., 2017). Yet, the soil C pool is a chemically and physically complex system in which C compounds associated with different soil particle fraction sizes may greatly differ in stability and mean residence time. As a result, increasing attention has been paid to the understanding and characterization of soil organic C quality, here defined as the relative amount of fast-turnover particulate organic matter C fractions (C_{POM} , C_{finePOM}) and stable clay and silt associated C fractions (C_{SILT} , $C_{\text{SILT+CLAY}}$) (Balesdent et al., 1998; Cotrufo *et al.*, 2013; Cardinael et al., 2015). A soil with good C quality should be targeted in C sequestration practices, aiming to have a high proportion of stable C in the SILT+CLAY pool.

In both experiments of my thesis, soil particle size fraction related C pools were characterized to assess C quality besides C quantity, and proved to be fundamental in the understanding of the plant-soil system. In Chapter II and III, there was no species effect on the total amount of C stored in soil. However, the quality of C, i.e. its accumulation in different soil fractions, was influenced by the root traits of the different plant species analyzed (Ch. II/III) as well as the chosen soil type (Ch. III), and their effects on microbiological communities. In Chapter IV, applying the concept of 'priming effect' on fraction associated C pools enabled us to highlight that the positive priming in subsoil was mainly due to an increased mineralization of C in the SILT+CLAY pool, while topsoil showed a homogeneous negative priming among pools, allowing us to better disentangle the priming mechanisms in different soil types. All of these findings not only highlight the great importance of looking at C sequestration at the fraction scale, but also challenge the supposed high stability of the SILT+CLAY pool.

5.2. Carbon origin matters: new carbon versus old carbon

The labelling approach to distinguish new C input in soil has been widely applied and is a relatively new frontier in plant-soil studies examining soil C storage (i.e. Dijkstra and Cheng, 2007; Paush et al. 2013;

26 Haddix et al., 2016). In my thesis, the stable labelling approach during 183 days of plants growth allowed
27 to disentangle plant-soil processes connected with soil C storage, and was an efficient way to study soil C
28 storage. We observed how changes in soil C were mainly attributable to the input of new C. Also, in
29 Chapter III we observed a positive synergy with new C input and old C losses, with higher new C input
30 connected with lower old C losses. This result was in accordance with results from De Graaf et al. (2010),
31 and supported the preference substrate utilization theory (Cheng and Kuzyakov, 2005).

32 Considering new C gains and old C changes in different soil fractions allowed us to further unveil
33 mechanisms of soil C storage that would have been hidden without this double approach of isotope
34 labelling and soil fractionation. In Chapter III there was a high response of POM and SILT+CLAY pools to
35 the input of fresh new C from plants, highlighting the double pathway of new C accumulation in soil, from
36 turnover in POM and exudation or microbial mineralization and deposition in the SILT+CLAY pool (Cotrufo
37 et al., 2013). Moreover, the fractionation allowed us to underline how old C is active in tospoil, being
38 mineralized and accumulating from the coarser fraction (especially POM in tospoil) to the fine SILT+CLAY
39 pool. These changes in old C among pools would have been hidden by analysis of total C in bulk soil, and
40 old C would have been wrongfully considered inactive.

41 New C and old C in fractions were only studied in Chapters III and IV, but the lesson learnt from these
42 chapters could make us rethink results in Chapter II, in which new C and old C were not distinguished. If
43 not considering old/new C, in both Chapter II and III, we observed that there was no significant effect of
44 species in C storage in different fractions (ΔC ; Chapter III, Fig. 2, 3). However, considering the new C and
45 old C changes in different fractions, we were able to identify the effect of species on the input of new C
46 (Chapter III, Fig. 4), that in ΔC was masked from the changes of old C and its accumulation in the SILT+CLAY
47 pool. Not only distinguishing between old and new C dynamics helped us to understand the effect of
48 species and the different behaviour of soil pools, but even to shed light on the relationships between
49 factors involved in C-cycling and C storage in different pools. Comparing the correlations in Chapter III

50 Table 3 between microbial/soil and root characteristics and new C, old C and ΔC , underlined how new C
51 accumulation was better predicted compared to ΔC (see also Henneron et al. 2019).

52 We, therefore underline the power of coupling the study of C sources with soil fractionation and related
53 C pools, which helped us greatly to analyse the mechanisms behind soil C storage, as explained in the next
54 sections.

55

56 **5.3. Microbial community matters: priming and entombing**

57 The microbial community is the factor shaping all the processes involved in C cycling. Our main goal was
58 to investigate the influence of species and soil selection on soil C storage in topsoils and exposed subsoils.
59 However, our findings highlight that the role of these two factors always indirectly pass through microbial
60 community biomass and activity via two mechanisms:

61 i) the priming effect (Chapter IV) was the response of microbial communities to revegetation, shaping the
62 losses of C in the system. The productivity of the system (based on soil fertility and plant species
63 performance) will determine the substrate preference of microbial communities and the direction and
64 magnitude of the priming effect (Cheng and Kuzyakov, 2005; De Graaf et al. 2010), as shown in Chapter
65 IV. Moreover, when soil N was low, we found an effect of competition for nitrogen influencing the priming
66 direction and intensity (Cheng and Kuzyakov, 2005). These results support the reconciliation of the
67 Preferential Substrate Utilization Hypothesis with the Competition Hypothesis (Cheng and Kuzyakov
68 2005), and underline the pivotal role of microbial communities in the priming effect.

69 ii) the quality of C stored due to microbial transformations. The common view that microbial communities
70 reduce C sequestration due to increased soil respiration is becoming increasingly redundant. In chapter II
71 and III we found strong links of microbial activity and biomass with C sequestration in the fine SILT and
72 SILT+CLAY fractions. In this regard, two main theoretical framework have been developed in the last years:

- 73 • Microbial Efficiency-Matrix Stabilization (MEMS) from Cotrufo et al. (2013). The main hypothesis
74 behind this framework states that labile C from plant inputs is the main source for microbial
75 exudates and exopolysaccharides, which are the precursors of stable SOM in aggregates and
76 organomineral compounds.
- 77 • Soil microbial carbon pump (MCP) from Liang et al. (2017). Microbial communities are the main
78 factors shaping the sequestration of C by 1) degrading via *ex-vivo* modifications the soil C,
79 consuming labile POM and leaving high recalcitrant and persistent SOM in soil, 2) increasing via
80 *in-vivo* turnover through their metabolism the stability of stored C, as microbial necromass and
81 metabolites, i.e., the 'entombing effect'.

82 Microbial necromass was not measured in this thesis. However, in Chapter IV, I provide evidence of the
83 entombing effect. The increase of soil C is mainly due to accumulation of new C in POM and in SILT+CLAY
84 and mineralization of old C in the SILT+CLAY pool. These C increases were correlated with microbial
85 activity and biomass. As predicted by the MEMS model, the quality of input influences the destination of
86 C: with microbial activity enhanced by labile inputs, while recalcitrant input was stabilized via *ex-vivo*
87 transformations. The transformed labile C by microorganisms as exopolysaccharides was then stabilized
88 in the SILT and SILT +CLAY pools – via *in vivo* turnover that promoted 'matrix stabilization' via
89 organomineral interactions, as part of the 'entombing effect'. We, therefore, argue that the MEMS and
90 MPC theories are complementary (Fig. 1), and the use of fractionation enables us to further expand their
91 understanding by quantifying the effects of the different pathways of stabilization (Fig. 2).

92 This thesis highlights the necessity to jointly consider priming and entombing effects as the two faces of
93 the same 'microbial coin'. The balance between these two processes will affect the final C sequestration
94 efficiency, as stated by Liang et al. (2017). We observed, however, how a higher microbial activity have a
95 positive effect on both i) C entombing via necromass and exopolysaccharides deposition and ii) reducing
96 the priming in fertile soil with high microbial biomass, suggesting an overall positive effect of microbial
97 communities on C sequestration.

99 5.4. Root traits matter: N₂ fixing species (*Fabaceae*) vs non N₂ fixing species 100 (*Poaceae*)

101 Plants are widely recognized as the main factor influencing C input in soil via litter fall, root mortality and
102 exudation (Six *et al.*, 2002; Derrien *et al.*, 2016; Sokol *et al.*, 2019). This thesis focused partly on the
103 comparison between N₂-fixing species (*Fabaceae*) with non N₂-fixing species (*Poaceae*) commonly used
104 for revegetating embankments in the South of France. Coupling isotopes labelling with fractionation
105 techniques, we demonstrate the beneficial effect of N₂-fixing species and the specific root traits that
106 species possessed in this study (low C:N, high hemicellulose and low lignin content, high root elongation
107 rate, low absorptive root diameter, low SRL, and high biomass) on total C sequestration and its
108 accumulation in stable C pools. The once common view that stable C storage is driven by selective
109 preservation of recalcitrant compounds is once again challenged by these results. We found root biomass
110 to be a better predictor of new C gain in every soil pool, more than any other root trait. The reason might
111 be that morpho-physio-phenological (as SRL and C:N, and diameter) can be compensated by the effect of
112 biomass, as performance traits (Violle *et al.*, 2007). In soil planted with *Poaceae* species, C storage in the
113 POM C pool was greater possibly due tissue recalcitrance inhibiting microbiological activity,
114 microbiological biomass and overall mineralization. However, this effect was masked in N₂-fixing species
115 with their higher root biomass and related C input. It is necessary to underline that N₂-fixing species are
116 associated with *Rhizobium* bacteria. This association increases the N content in the root biomass,
117 decreasing the C:N ratio and their recalcitrance. In addition, the symbiosis with *Rhizobium* bacteria
118 increases microbial activity and the deposition of microbiological exopolysaccharides (Garcia *et al.*, 2001).
119 These effects overall increase the new C input in the system, especially in the SILT and SILT+CLAY (Cotrufo
120 *et al.*, 2013). For this reason, is important to consider that the root traits related to high labile C input in
121 this thesis are characterized by an intrinsic high microbiological activity due to symbiosis of N₂ fixing
122 species with *Rhizobium*. When studying Leguminous species and C sequestration, the effect of the
123 symbiosis and the root traits connected with high labile input are therefore synergic in increasing new labile

124 C input, and difficult to disentangle. In general, root biomass and chemical traits (C:N ratio, and
125 lignin/cellulose/hemicellulose ratio) were a better predictor for C storage compared to architectural
126 traits. Recent studies have highlighted correlations between root economic spectrum (RES) and C storage
127 (De Deyn et al. 2008; Roumet et al. 2016; Prieto et al. 2016; Poirier et al. 2018; Henneron et al 2019). The
128 main characterization of RES - as coordinate variation of root respiration rate, decomposability, and
129 morphological and chemical traits related to C economy (Roumet et al., 2016) - is given by the distinction
130 between fast growing, acquisitive species (e.g. Fabaceae) and slow growing, conservative species (e.g.
131 Poaceae) (Chapter II, this thesis). Therefore, our findings are consistent with the bulk of literature that
132 find N₂-fixing Fabaceae in the spectrum of acquisitive species characterized by high input of labile C in the
133 soil, and N₂-fixing species Poaceae representing conservative species with low input of recalcitrant old C
134 (Prieto et al., 2016; Henneron et al., 2019). These results support the correlations between RES and soil C
135 sequestration potential, mediated by root growth strategies and different C economies (Roumet et al.
136 2016; Poirier et al. 2018; Henneron et al 2019). However, when studying RES correlations with C storage
137 is important to differentiate between N₂ fixing and non N₂ fixing species.

138

139 5.5. Soil matters: a major factor in carbon-cycle regulation, but due to indirect 140 effects

141 Soil fractions and the related C pools have shown to be fundamental and understand the C-cycle in soil.
142 The results of this thesis show that soil type has the highest impact on both C storage and priming effect.
143 Reduced root biomass in subsoil due to low fertility decreases the input of new C in every soil C pool and
144 the transfer of C in the SIL+CLAY pool via microbial metabolic transformations (Cotrufo et al., 2013; Vidal
145 et al., 2018). It also has a negative effect on priming, since labile C input are not high enough to allow
146 substrate preferential switch of microbial communities (Cheng and Kuzyakov, 2005; De Graaf et al. 2010).
147 However, when observing the direct effect of soil characteristics on the soil C storage, it is surprising to
148 observe that C saturation has no effect on the increase of protected C in the SILT+CLAY fraction. In our

149 experiment, subsoil had a higher clay percentage and lower initial C content compared to topsoil,
150 decreasing soil C saturation that should positively influence C storage in the SILT+CLAY C pool (Six et al.,
151 2002; Eyles et al., 2015; Shahbaz et al., 2017). Under these premises, we expected a higher rate and
152 amount, or at least relative amount, of C stored in fine SILT+CALY pool. However, topsoil had a higher
153 increase in the SILT+CLAY C pool compared to subsoil in absolute terms, while in relative terms they were
154 comparable. The reasons behind this behavior is attributable to plant biomass and microbial communities
155 in different soils. A lower fertility of subsoil decreases the input of C via plant biomass. The decreased
156 microbial activity and abundance decreased the input of processed C in the SILT+CLAY C pool. Without C
157 input in the SILT+CLAY C pool, increased potential for organomineral interactions did not influence the
158 amount of stored C. With this diagnosis, we could not claim that clay content and C saturation had no
159 effect on potential C storage. However, we can affirm that they were less important to C input by plants
160 and C metabolic transformation by microbial community in respect to soil C storage.

161 Soil N content had a high impact on soil C-cycle, increasing fertility and biomass production and,
162 consequently, new C input. Regarding the priming effect in soil, we confirm that in a poor soil the
163 competition for N reduced the consumption of C from microorganisms and had a positive effect on soil C
164 storage (Cheng and Kuzyakov, 2005). We confirmed that N rich soils positively influenced soil C storage
165 (Dou et al. 2016, Guo et al., 2019).

166 Aggregate stability had a significant effect on C storage due to a double feedback mechanism: new C input
167 in the system participated in creating more stable aggregates that, in turn, protected the encompassed C
168 (Tisdall and Oades 1982; Caesar-Tonthat 2002; Nichols and Wright 2005). The decrease of old C
169 mineralization in SILT+CLAY C pools were the direct result of the higher physical protection of C in stable
170 aggregates (Chevallier et al., 2004). Soil structure, and especially aggregates, seems to be the main direct
171 soil effect that influences C stability, and more studies need to be developed on the subject.

172

173 5.6. Ecological engineering toward a carbon sequestration goal

174 I suggest that we do not only consider soil C storage potential from a point of view of mineralogy or clay
175 content (Hassink 1992, Hassink al. 1997) or C saturation (Six et al. 2002), but we should pay more attention
176 to soil health. More specifically, we need to assess its fertility levels, such as N content, aggregate stability
177 and microbial community development (biomass and/or activity). Microbial diversity could also be an
178 important indicator. These indicators are connected with higher input of C in soil via increased biomass
179 production, transfer to the protected SILT+CLAY pool and negative priming due to the switch of substrate
180 utilization. An overview of the effect of soil and plants on C sequestration can be found in Figure 2.

181 The use of fertile topsoil increases carbon accumulation when compared with poor subsoil and it is
182 therefore desirable for revegetation of geotechnical soils. When revegetating fertile topsoil, fast growing
183 N₂ fixing species with high input of labile C are more efficient to store C in the protected SILT+CLAY pool
184 via higher root input and microbial turnover. Revegetating topsoil also induces a negative priming effect,
185 increasing preexistent C stability.

186 However, the use of topsoil is not always possible. Some particular conditions, eg in quarries and minor
187 road embankments, might require revegetation of subsoil. In this case, I advise to:

188 1) Fertilize soil to increase biomass production and C storage in soil. Fertilization is recognized to
189 increase soil C storage in both unprotected and protected C pools (Dou et al. 2016, Guo et al.,
190 2019). However, to my knowledge, no studies exist on the effect of fertilization on subsoil brought
191 to the surface. Moreover, the C impact of different fertilizer production and transport needs to
192 be compared with the benefits for C storage, or the final result might be detrimental for global C
193 storage.

194 2) Inoculate with microbial communities: we argue that inoculation of bacteria and mycorrhiza
195 (especially *Rhizobium* associated with Leguminous species to increase nodulation, and arbuscular
196 mycorrhiza fungi) would increase the C input in the SILT+CLAY C pool. Li et al. (2016) found a
197 decrease in C loss due to an increase of soil microbial biomass. However they did not consider the

198 different fluxes of C (New C and Old C), so it is not possible to assess if the increase of respiration
199 was detrimental for C balance. Kuimei et al. (2012) observed an increased soil C sequestration
200 with arbuscular mycorrhiza fungi inoculation in a reclaimed mine soil treated with coal gangue,
201 fly ash and sludge.

202 The lower C saturation did not increase protected C storage in subsoil in our experiment, but is still
203 promising for potential C storage if fertility and microbial requirements are met.

204 If neither fertilization nor microbial inoculation are possible, we suggest avoiding the use of N₂ fixing
205 species, since the increase in microbial biomass connected with those species will result in a higher
206 mineralization of old SOC.

207 Figure 3 shows a simple flowchart that provides suggestions for revegetating geotechnical soils and
208 optimize C sequestration. However, it is to be noted that this flowchart is based on results that present a
209 major shortcoming: the short timeframe of experiments. Long-term experiments are now much needed,
210 to explore how the results from this thesis are influenced over time.

211

212 5.7. What research remains to be performed?

213 Countless opportunities for research are possible in the C storage domain. However, this work on C
214 storage in revegetated geotechnical soil sparked some specific questions that I feel should to be tackled
215 to have a more comprehensive view of the system, from both a mechanistic and an applied point of view.

- 216 • It would be vital to extend these studies on fractions and C sources on long term experiments.
217 How subsoil evolves and ‘become topsoil’ is a fundamental aspect to be considered in studies of
218 plant development, microbiological characteristics and soil aggregation etc. However, the cost
219 and experimental setup makes it difficult to implement long-term constant isotope labeling
220 experiment. A solution would be to use C₃ plants grown on soil planted only with C₄ plants (or
221 vice-versa) as they have different isotopic signatures (Hobbie and Werner, 2004; Kuzyakov 2006).

- 222 • While in topsoil, research on aggregate protection and formation are numerous, they have not
223 reached a complete consensus on the processes involved. In subsoil, instead, the role of
224 aggregates in C protection and their formation processes remains still obscure. In Annex I, I
225 present a preliminary work to investigate in depth the influence of soil structure on C protection
226 in topsoil and exposed subsoil.
- 227 • In this thesis, I investigated the influence of microbiological communities on C-cycling and
228 sequestration based on microbiological activity and biomass. However, refined identification of
229 microbiological community structure and diversity would help unveiling key processes and factors
230 in C-cycling. Studying the evolution of microbiological communities on subsoil brought to the
231 surface would be fundamental to better understand its C sequestration potential, the processes
232 behind it, and to have an insight into soil evolution.
- 233 • More studies have to be carried out on inoculation with different strains of fungi and bacteria to
234 understand the mechanisms and influence of inoculation on C-cycling and its role as a 'pump' for
235 complexed C in the protected silt and silt+clay C pools.
- 236 • Microbial communities influence most of the major processes involved in soil C storage, directly
237 or indirectly. More precisely: i) total C input, as microbes are commonly used indicator for soil
238 fertility and health (Waksman, 1922; Waksman and Starkey, 1924; Mader et al., 2002; Suzuki et
239 al., 2005; Schloter et al., 2018), ii) quality of the stored C, determining if the C will accumulate in
240 the unprotected C pool (when microbial abundance and activity is low) or if it will be metabolized
241 and transferred in the protected C pool (when microbial abundance and activity is high) (De Deyn
242 et al, 2008; Cotrufo et al., 2013; Liang et al. 2017), iii) total respired C (increased with increasing
243 microbial activity) and priming effect (decreased when microbial activity is inhibited due to
244 competition or a switch of substrate preference from old C to new C) (Cheng and Kuzyakov., 2005;
245 De Graaf et al., 2010), and iv) increased aggregate formation and stability (Tisdall and Oades 1982;
246 Caesar-Tonthat 2002; Nichols and Wright 2005). Relying on clay abundance or C saturation levels

247 to determine the quantity of protected C might be inaccurate, since they are not an indicator for
248 soil health, and since microbial communities will determine the C input in the silt+clay C pool. For
249 these reasons we state that, given the correlations between microbial activity and many of the
250 key processes involved in C storage, further research should be carried out regarding the use of
251 microbial characteristics as an indicator for potential soil C storage.

252

253 REFERENCES

- 254 Balesdent, J., Besnard, E., Arrouays, D., Chenu, C., 1998. The dynamics of carbon in particle-size fractions
255 of soil in a forest-cultivation sequence. *Plant and Soil* 201, 49-57.
- 256 Caesar-Tonthat, T.C. 2002. Soil binding properties of mucilage produced by a basidiomycete fungus in a
257 model system. *Mycological Research* 106, 930–937.
- 258 Cardinael, R., Chevallier, T., Barthès, B.G., Saby, N.P.A., Parent, T., Dupraz, C., Bernoux, M., Chenu, C.,
259 2015. Geoderma Impact of alley cropping agroforestry on stocks, forms and spatial distribution of
260 soil organic carbon — A case study in a Mediterranean context. *Geoderma* 259–260, 288–299.
- 261 Cheng, W., Kuzyakov, Y., 2005. Root effects on soil organic matter decomposition. In: S. Wright, S., Zobel,
262 R. (Eds.), *Roots and Soil Management: Interactions Between Roots and the Soil*. Agronomy
263 Monograph No. 48, American Society of Agronomy, Madison, Wisconsin, USA 119–143.
- 264 Chevallier, T., Blanchart, E., Albrecht, A., Feller, C., 2004. The physical protection of soil organic carbon in
265 aggregates: A mechanism of carbon storage in a Vertisol under pasture and market gardening
266 (Martinique, West Indies). *Agriculture, Ecosystems and Environment* 103, 375–387.
- 267 Cotrufo, M.F., Soong, J.L., Horton, A.J., Campbell, E.E., Haddix, M.L., Wall, D.H., Parton, W.J., 2015.
268 Formation of soil organic matter via biochemical and physical pathways of litter mass loss. *Nature*
269 *Geoscience* 8, 776–779.
- 270 Cotrufo, M.F., Wallenstein, M.D., Boot, C.M., Deneff, K., Paul, E., 2013. The Microbial Efficiency-Matrix
271 Stabilization (MEMS) framework integrates plant litter decomposition with soil organic matter
272 stabilization: Do labile plant inputs form stable soil organic matter? *Global Change Biology* 19, 988–
273 995.
- 274 De Deyn, G.B., Cornelissen, J.H.C., Bardgett, R.D., 2008. Plant functional traits and soil carbon
275 sequestration in contrasting biomes. *Ecology Letters* 11, 516–531.
- 276 De Graaff, M.A., Classen, A.T., Castro, H.F., Schadt, C.W., 2010. Labile soil carbon inputs mediate the soil
277 microbial community composition and plant residue decomposition rates. *New Phytologist* 188,
278 1055–1064.
- 279 Derrien, D., Barot, S., Chenu, C., Chevallier, T., Freschet, G.T., Garnier, P., Guenet, B., Hedde, M., Klumpp,
280 K., Lashermes, G., Nunan, N., Roumet, C., 2016. Stocker du C dans les sols : Quels mécanismes,
281 quelles pratiques agricoles, quels indicateurs ? *Étude et Gestion des Sols* 23, 193–224.
- 282 Dijkstra, F.A., Cheng, W.X., 2007. Moisture modulates rhizosphere effects on C decomposition in two
283 different soil types. *Soil Biology and Biochemistry* 39, 2264–2274.
- 284 Dou, X., He, P., Cheng, X., Zhou, W., 2016. Long-term fertilization alters chemically-separated soil organic
285 carbon pools: Based on stable C isotope analyses. *Scientific Reports* 6, 1–9. doi:10.1038/srep19061
- 286 Eyles, A., Coghlan, G., Hardie, M., Hovenden, M., Bridle, K., 2015. Soil carbon sequestration in cool-
287 temperate dryland pastures: Mechanisms and management options. *Soil Research* 53, 349–365.

- 288 Garcia, J.A.L., Barbas, C., Probanza, A., Barrientos, M.L., Manero, F.J.G. 2001. Low molecular weight
289 organic acids and fatty acids in root exudates of two *Lupinus* cultivars at flowering and fruiting
290 stages. *Phytochem Analysis* 12: 305–311.
- 291 Guo, Z., Zhang, Z., Zhou, H., Wang, D., Peng, X., 2019. The effect of 34-year continuous fertilization on the
292 SOC physical fractions and its chemical composition in a Vertisol. *Scientific Reports* 9, 1–10.
- 293 Haddix, M.L., Paul, E.A., Cotrufo, M.F., 2016. Dual, differential isotope labeling shows the preferential
294 movement of labile plant constituents into mineral-bonded soil organic matter. *Global Change*
295 *Biology* 22, 2301–2312.
- 296 Hassink, J., 1992. Effects of soil texture and structure on carbon and nitrogen mineralization in grassland
297 soils 126–134.
- 298 Hassink, J., Whitmore, A.P., Kubat, J., 1997. Size and density fractionation of soil organic matter and the
299 physical capacity of soils to protect organic matter. *European Journal of Agronomy* 7 (1–3), 189–
300 199.
- 301 Henneron, L., Cros, C., Picon-cochard, C., Rahimian, V., Fontaine, F., 2019. Plant economic strategies of
302 grassland species control soil carbon dynamics through rhizodeposition. *Journal of Ecology*
- 303 Hobbie, E.A., Werner, R.A., 2004. Review and Synthesis bulk carbon isotope patterns in C3 and C4 plants:
304 a review and synthesis. *New Phytologist* 161, 371–385.
- 305 Kuimei, Q., Liping, W., Ningning, Y., 2012. Effects of AMF on soil enzyme activity and carbon sequestration
306 capacity in reclaimed mine soil. *International Journal of Mining Science and Technology*, 22, 553-
307 557
- 308 Kuzyakov, Y., 2006. Sources of CO₂ efflux from soil and review of partitioning methods. *Soil Biology and*
309 *Biochemistry* 38, 425–448.
- 310 Li, J.H., Zhang, J.i., Li, W.J., Xu, D.H., Knops, M.H.J., Du, G.Z., 2016. Plant functional groups, grasses versus
311 forbs, differ in their impact on soil carbon dynamics with nitrogen fertilization. *European Journal of*
312 *Soil Biology* 75, 79-87
- 313 Liang, C., Schimel, J.P., Jastrow, J.D., 2017. The importance of anabolism in microbial control over soil
314 carbon storage. *Nature Microbiology* 2, 1–6. doi:10.1038/nmicrobiol.2017.105
- 315 Mader P, Fliessbach A, Dubois D, Gunts L, Fried P, Niggli U, 2002. Soil fertility and biodiversity in organic
316 farming. *Science* 296, 1694-1697
- 317 Minasny, B., Malone, B.P., McBratney, A.B., Angers, D.A., Arrouays, D., Chambers, A., Chaplot, V., Chen,
318 Z.S., Cheng, K., Das, B.S., Field, D.J., Gimona, A., Hedley, C.B., Hong, S.Y., Mandal, B., Marchant, B.P.,
319 Martin, M., McConkey, B.G., Mulder, V.L., O'Rourke, S., Richer-de-Forges, A.C., Odeh, I., Padarian,
320 J., Paustian, K., Pan, G., Poggio, L., Savin, I., Stolbovoy, V., Stockmann, U., Sulaeman, Y., Tsui, C.C.,
321 Vågen, T.G., van Wesemael, B., Winowiecki, L., 2017.. Soil carbon 4 per mille. *Geoderma* 292, 59–
322 86.
- 323 Nichols, K.A., Wright, S.F., 2005. Comparison of glomalin and humic acid in eight native U.S. soils. *Soil*
324 *Science* 170, 985–997.

- 325 Pausch, J., Tian, J., Riederer, M., Kuzyakov, Y., 2013. Estimation of rhizodeposition at field scale: Upscaling
326 of a ¹⁴C labeling study. *Plant and Soil* 364, 273–285.
- 327 Poirier, V., Roumet, C., Munson, A.D., 2018. The root of the matter: Linking root traits and soil organic
328 matter stabilization processes. *Soil Biology and Biochemistry* 120, 246–259.
- 329 Prieto, I., Stokes, A., Roumet, C., 2016. Root functional parameters predict fine root decomposability at
330 the community level. *Journal of Ecology* 104, 725–733.
- 331 Roumet, C., Birouste, M., Picon-Cochard, C., Ghestem, M., Osman, N., Vrignon-Brenas, S., Cao, K. fang,
332 Stokes, A., 2016. Root structure-function relationships in 74 species: Evidence of a root economics
333 spectrum related to carbon economy. *New Phytologist* 210, 815–826.
- 334 Schloter, M., Nannipieri, P., Sørensen, S.J., van Elsas, J.D., 2018. Microbial indicators for soil quality.
335 *Biology and Fertility of Soils* 54, 1–10.
- 336 Shahbaz, M., Kuzyakov, Y., Sanaullah, M., Heitkamp, F., Zelenev, V., Kumar, A., Blagodatskaya, E., 2017.
337 Microbial decomposition of soil organic matter is mediated by quality and quantity of crop residues:
338 mechanisms and thresholds. *Biology and Fertility of Soils* 53, 287–301.
- 339 Six, J., Conant, R.T., Paul, E.A., Paustian, K., 2002. Stabilization mechanisms of soil organic matter :
340 Implications for C-saturation of soils 155–176.
- 341 Sokol, N.W., Kuebbing, S.E., Karlsen-ayala, E., Bradford, M.A., 2019. Evidence for the primacy of living root
342 inputs , not root or shoot litter , in forming soil organic carbon 233–246.
- 343 Suzuki, C., Kunito, T., Aono, T., Liu, C.T., Oyaizu, H., 2005. Microbial indices of soil fertility. *Journal of*
344 *Applied Microbiology* 98, 1062–1074.
- 345 Tisdall, J.M., Oades, J.M., 1982. Organic matter and waterstable aggregates in soils. *Journal of Soil Science*
346 33, 141±163.
- 347 Vidal, A., Hirte, J., Bender, S.F., Mayer, J., Gattinger, A., Höschel, C., Schädler, S., Iqbal, T.M., Mueller,
348 C.W., 2018. Linking 3D Soil Structure and Plant-Microbe-Soil Carbon Transfer in the Rhizosphere.
349 *Frontiers in Environmental Science* 6, 1–14.
- 350 Violle, C., Navas, M.L., Vile, D., Kazakou, E., Fortunel, C., Hummel, I. et al. (2007). Let the concept of trait
351 be functional!. *Oikos*, 116, 882–892.
- 352 Waksman, S. A. and Starkey, R. L., 1924. Microbiological analysis of soil as an index of soil fertility: VII.
353 Carbon dioxide evolution. *Soil Science* 17, 141-161.
- 354 Waksman, S. A., 1922. Microbiological analysis of soil as an index of soil fertility: III. Influence of
355 fertilization upon numbers of microorganisms in the soil. *Soil Science* 14, 321-346.

FIGURES AND TABLES

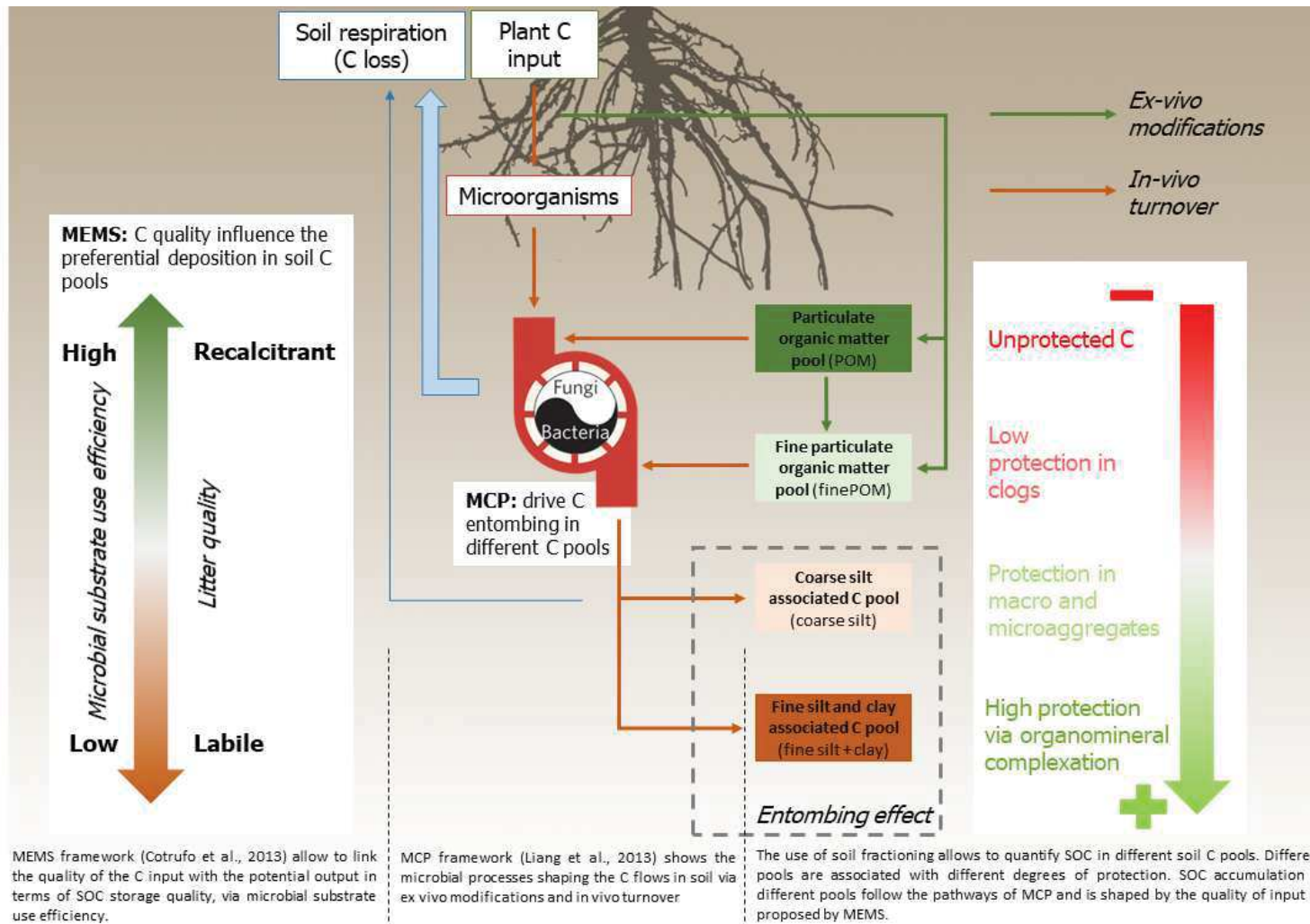


Figure 2: Conceptual framework illustrating complementarity between MEMS and MCP models, enriched by including the soil C pools. Primary plant's carbon inputs quality influence the final stabilization of stored C (MEMS, Cotrufo et al. 2013). The microbial carbon pump determine the entombing of C in the soil system, via ex-vivo modifications (green arrows) and in-vivo transformation (brown arrows) (MCP, Liang et al. 2017). Finally, the quality of C input will determine the C distribution in different soil C pools associated to soil fractions, through the microbial carbon pump. Labile C input will favor in-vivo turnover, increasing C in the silt and silt+clay fractions, protected in microaggregates and via organomineral interactions with fine silt and clay minerals. Recalcitrant C decrease in vivo turnover, and C accumulate mainly in unprotected POM and finePOM fractions via ex-vivo modifications.

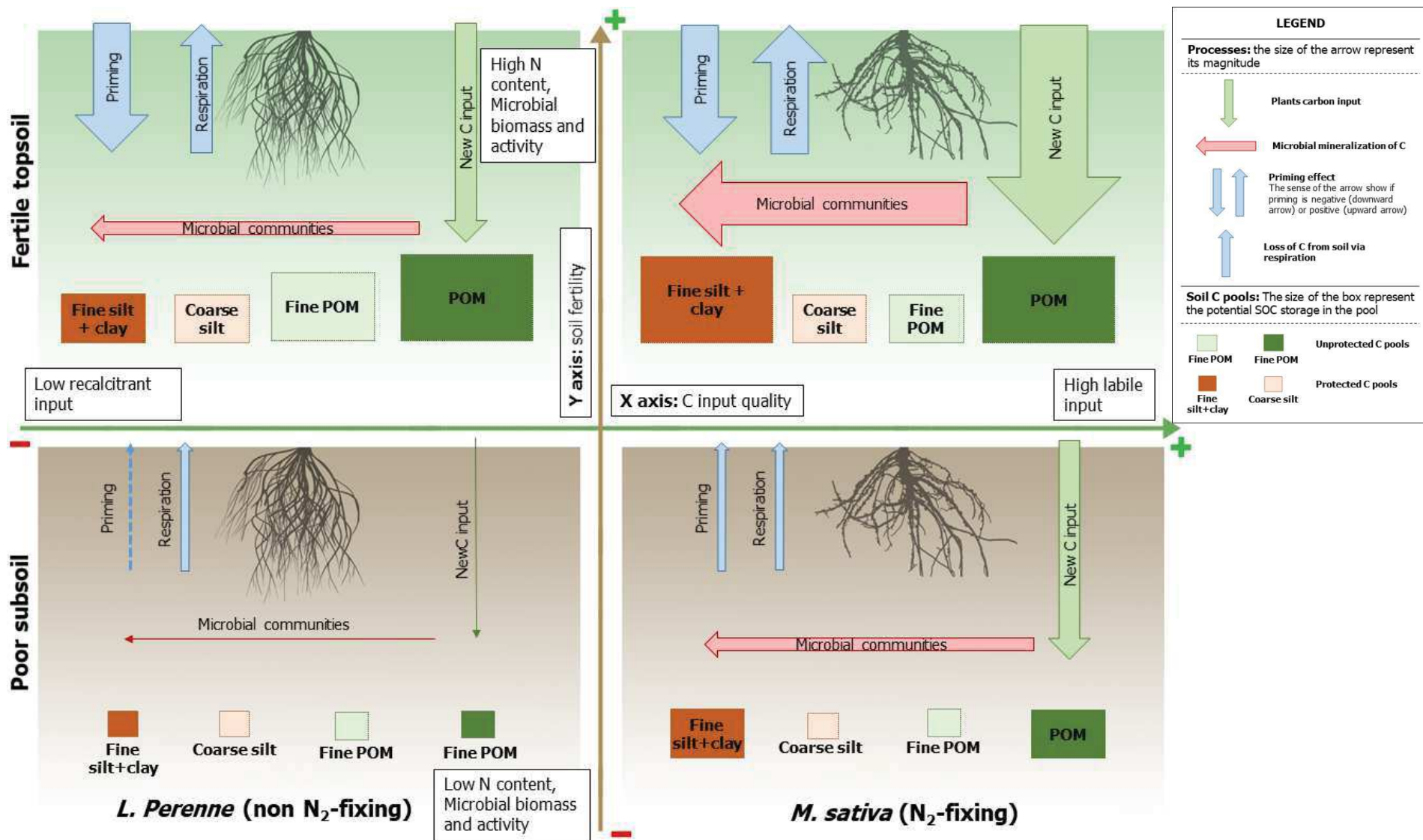


Figure 3: Scheme illustrating the changes in the C storage mechanisms along two main axes: x – Soil fertility and y – C input quality. Top right has the higher C storage potential, with high fertility soil revegetated with N₂-fixing species, that have high labile C input, positively influencing POM and, most importantly, fine silt+clay fraction accumulation through high microbial activity. Top left corner shows the potential soil C storage of fertile soil revegetated with non N₂-fixing species. The lower input of recalitrant C decrease microbial biomass and activity, and increase POM and finePOM accumulation via decreased mineralization. In fertile topsoil priming effect is high and negative. Bottom right corner shows the effect of revegetating poor subsoil with N₂-fixing species: decreased C input due to fertility decreases the accumulation in the POM fraction, and decreased microbial biomass/activity its complexation in the protected silt+clay fraction. Priming effect is lower in intensity but positive; increasing the loss of preexistent SOC. Bottom left corner shows the effects of revegetation of poor subsoil with non N₂-fixing species. Decreased input and microbial activity decrease the C accumulation in every soil fraction, however priming effect almost absent due to plant-microbes competition for nitrogen. 195

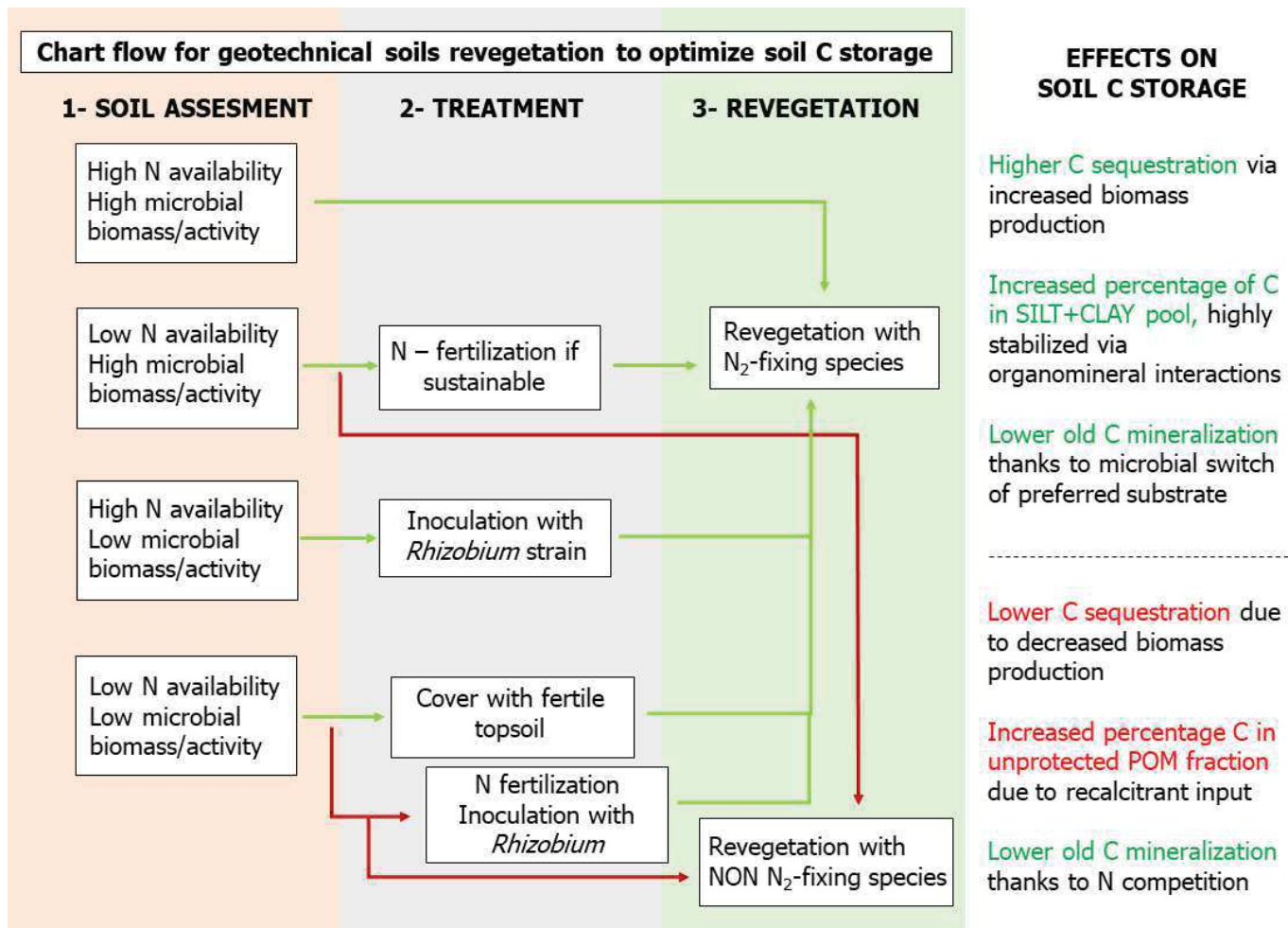


Figure 4: flowchart for soil revegetation to increase C sequestration in geotechnical embankments. First step is soil assessment in regard to N content and microbial biomass and activity. The second step shows the treatments to implement if N content is low (fertilization) or microbial communities are underdeveloped (inoculation). The fourth step shows the suitable species for revegetation given the soil conditions. The last ox the effects on C sequestration given the soil, the treatments and the plant species selected. Green arrow shows the suggested pathway to take, red arrow the alternative unadvised pathway if the first is not possible. This flowchart, however, is based on a short term experiment. Long term experiment should be implemented to improve it.

Annex I: Perspectives: the influence of vegetation on soil microstructure and its implications on soil carbon sequestration: a geotechnical approach

1 INTRODUCTION

2 A particular interest in sustainability has been voiced in both environmental and geotechnical disciplines,
3 given the global climate change challenge that requires immediate action in multiple sectors. However, the
4 research on sustainability remains largely confined in the peculiarity of each discipline, which has its specific
5 assumptions and methodology characterizing the sustainability. We argue that a higher multidisciplinary
6 approach is needed to hybridize research and find transdisciplinary methodologies and points of view on
7 sustainability in every discipline. In this part of the research, we aim to bridge C storage research from a
8 plant/soil science point with geotechnical engineering research. Soil microstructure have proven to be a good
9 common ground between the two fields, since it is largely studied both with regards to C sequestration and
10 in the geotechnical engineering field for characterization of the soil structural properties.

11 Soil structure has been proven to be central with regards to C sequestration, especially regarding the role of
12 aggregates. Aggregates forms through binding of soil particles by fine roots and fungal hyphae (Tisdall and
13 Oades 1982). Glycoproteins, polysaccharides, and mucilage, from plants cement their structure and influence
14 their stability (Tisdall and Oades 1982; Caesar-Tonthat 2002; Nichols and Wright 2005). Aggregates occlude
15 C in their structure, physically impairing the accessibility of microbes (O'Brien & Jastrow, 2013). The efficiency
16 of aggregates C protection will depend on their stability and the amount of C stored inside their structure.
17 Aggregates is a dynamics process, and the higher is their stability the higher they will resist to disaggregation
18 (Eyles et al., 2015). In soil sciences most of studies refers to three main classes: microaggregates (0.02-
19 0.2mm), macroaggregates (0.2-3mm) and clots (3-5mm). Aggregation in soil will deeply influence the void
20 ratio, a common indicator used in geotechnical research to define soil structural characteristics. Aggregates
21 structure gives a double porosity behavior to soil, with micropores characteristic of intra-aggregates
22 structure, and macropores formed by the interaction between different aggregates (Koliji et al., 2008). In
23 geotechnical studies, a common method used to investigate soil porosity and deriving void ratio is mercury
24 intrusion porosimetry (MIP). MIP allow characterizing the cumulative and relative abundance of voids of
25 different pore classes (Russo et al., 2016). The aggregation process and characteristics are expected to be

26 correlated with void ratio in different pore classes. Soil porosity and connectivity also influence the possibility
27 of microbes to be in contact with substrates and their consumption (McCarthy et al., 2008; Lugato et al.,
28 2009). Vegetation can influence soil porosity in different classes due to i) root channels, ii) hyphae
29 development, iii) wet and dry cycles, iv) cementation and clogging of micropores due to rhizodeposition and
30 v) aggregation and disaggregation processes favored by plants influence (McCarthy et al., 2008; Lugato et al.,
31 2009). Extensive studies have been implemented on aggregate formation and C protection. However, most
32 of the studies see aggregates as 'building blocks of soil' (Malamoud et al., 2009) and overlook the more
33 complicated structure deriving by their interactions. Moreover, studies on aggregate formation and C
34 protection have seldom been implemented on subsoil, where the aggregate formation processes are still
35 debated. Soil microstructure has great potential to shape C sequestration in soil, and we aim to assess
36 evolution of aggregate characteristics due to revegetation in topsoil and subsoil brought to the surface.
37 Moreover, we aim to assess pore ratio in soil and the influence of vegetation using MIP, and correlate it to
38 aggregate characteristics, to better understand how aggregates shape soil structure. The use of MIP together
39 with aggregate stability and C analysis will allow comparing methods characteristics of different disciplines
40 and exploring possible exchanges and overlapping between these fields.

41

42 OBJECTIVES AND HYPOTHESIS

43 Our first objective is to investigate the influence of vegetation on microstructure using the MIP methodology.
44 For this, we assessed bulk void ratio at time 0 and after 6 months of two soils showing contrasting
45 characteristics (topsoil 0-30 cm depth and subsoil 110-140 cm depth) vegetated with *M. sativa* and *L.*
46 *perenne*, plus bare soil controls. Comparing void ratio in bare soil control after 6 months of experiment (time
47 6) with the initial soil (time 0) will allow us to assess the effect of wet and dry cycles on microstructure (since
48 soil was kept at 45% of water holding capacity with irrigation to compensate evaporation) and compare it
49 with the effect of revegetation. Void ratio will be cumulated in different classes relative to different

50 aggregates and processes as a proxy for: microaggregates porosity, macroaggregates porosity deriving from
51 microaggregates interaction and clots porosity deriving from macroaggregates interactions.

52 Our second objective is to characterize aggregates and their characteristics for bare soil control and
53 vegetated treatment with *M. sativa* and *L. perenne*. For this, we measured aggregate stability, quantity of C
54 protected inside of aggregates, quantity of fresh new C inputted in different aggregates classes in 6 months,
55 thanks to the constant CO₂ enrichment with ¹³C.

56 Our final objective is to investigate the relationship between aggregate stability and void ratio in different
57 pore classes, ii) between C protected in different aggregate classes and void ratio in different pore classes
58 and iii) if new C input in different aggregate size influence macro- and microporosity.

59 We hypothesize that plants will increase macroaggregates and clots porosity due to channeling of roots and
60 aggregates formation. However, vegetation might clots micropores due to rhizodeposition (McCarthy et al.,
61 2008). In this case, aggregate stability will increase with increased void in macroaggregates and clots (due to
62 aggregate formation and inter-aggregate porosity) while it will be negatively correlated with porosity in
63 microaggregates, due to bioclogging from microbial activity that cement and increase aggregate stability
64 (Ivanov and Chu, 2008). However, wet and dry cycle will probably drive the formation of soil structure.

65 Another hypothesis is that the protection of C will increase when decreasing the porosity (and void ratio) in
66 macro and microaggregates, since the microbes will not have access to the occluded C. Finally, we expect
67 that new C input is positively correlated with porosity in macroaggregates and clots (due to the role that
68 fresh C input plays in aggregate formation, and root channeling connected with new C deposition) but
69 negatively correlated with porosity in microaggregates, due to the clogging from rhizodeposition and
70 microbiological exudation and exopolysaccharides. The analysis will be conducted using pearson's
71 correlations between C protection and new C input in microaggregates, macroaggregates and clots, and the
72 void ratio (as proxy for porosity) in three different pore classes.

73

74 **STATE OF THE WORK**

75 Analyses on aggregate stability, C protection in aggregates and new C input in different aggregates classes
76 have been performed. A first MIP analysis campaign has been carried out to design the work. A second
77 campaign to acquire MIP replicates is in progress and expected to finish by the end of October 2019. After,
78 correlations with aggregate properties will be investigated to study the relations between vegetation, soil
79 structure in terms of aggregation and porosity, and C protection. Methodology and preliminary results are
80 presented in the following sections.

81

82 METHODOLOGY

83

84 *Mercury intrusion porosimetry (MIP) curves and cumulative porosity for different pore classes*

85 MIP test allow to characterize the porosity of the sample in an entrance pore diameter that ranges between
86 0.001 to 300 μm . Abundance of pores of different diameters define the microstructure of the soil. Once
87 grouped in different pore size classes, we believe to find correlations between pores and aggregate
88 characteristics in soil.

89 **Methodology:**

- 90 1. 1-2 g of sample are dehydrated according to the freeze-drying method (Delage et al. 1984).
- 91 2. MIP test is performed in a double chamber Micromeritics Autopore III apparatus.
- 92 3. Place the sample in the filling low-pressure apparatus (dilatometer).
- 93 4. The samples is outgassed and under vacuum, and after filled by mercury. The chamber is at ambient
94 absolute pressure.
- 95 5. Pressure is then rise up to 200 kPa using of compressed air
- 96 6. Chamber is depressurized and the samples were transferred to the high-pressure unit,
- 97 7. The pressure is then raised to 205 MPa following a previously set intrusion program. At any intrusion
98 step a time sufficient to observe a quasi-static penetration of mercury was allowed.
- 99 8. A blank test is performed to corrections the results and prevent errors deriving from the
100 compressibility of the intrusion system.
- 101 9. Finally, SEM analyses were performed on dehydrated samples in order to highlight their fabric.

102 Output: Intruded void ratio and pore size density function for different pore classes rangion from 0.001 to
103 300 μm

104 *Aggregate stability*

105 Aggregates provide physical protection to carbon. However, the degree of protection of carbon depends on
106 their stability. The more stable are the aggregates, the more resilient will be to changes in environmental
107 condition, decreasing their disaggregation and ensuring stable physical protection to the carbon occluded.
108 Mean weight diameter is a standard indicator for aggregate stability, as the mean diameter of aggregates that,
109 starting from a 5-3mm diameter, have undergone a disaggregation process via wet and drying. The higher
110 the MWD, the lower the disaggregation.

111 **Methodology according to le Bissonais et al. (2006):**

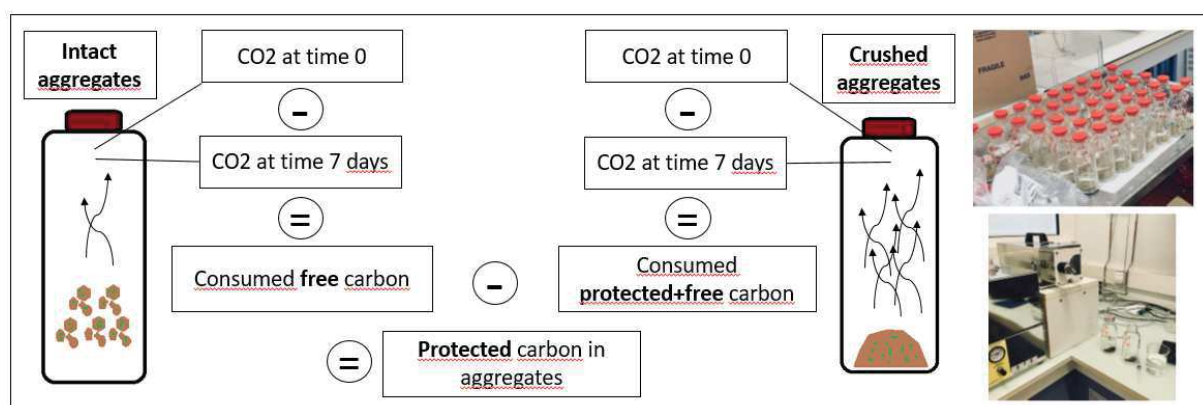
- 112 1. 20 g of soil collected and air dried
- 113 2. The sample is sieved first at 5mm and after at 3mm, to isolate the 3-5mm fraction
- 114 3. Aggregates are put in the oven for 24h so they are at the same matrix potential
- 115 4. 5g of 3-5mm fraction are weighted and gently immerse in a 250 cm³ beaker filled with 50 cm³ of
116 ethanol for 10 minutes
- 117 5. Ethanol is sucked off with a pipette
- 118 6. Sample transferred in a 250cm³ Erlenmeyer flask containing 50cm³ of deionized water and brought
119 to 200cm³
- 120 7. Flask is agitated 20 times and left 30 minutes for sedimentation of coarse particles
- 121 8. Water sucked off with a pipette
- 122 9. Mixture of soil and water transferred to a 50µm sieve previously immersed in ethanol
- 123 10. Sieve gently moved 5 times to separate <50 µm from those >50 µm, use of ethanol for the wet sieving
124 to reduce additional breakdown
- 125 11. >50 µm fraction is collected from the 50-µmsieve, oven-dried and gently dry-sieved by hand on a
126 column of six sieves: 2000, 1000, 500, 200, 100 and 50 µm
- 127 12. Mass percentage of the different fraction is calculated, and for subtraction even the <50µm fraction
- 128 13. MWD is calculated as the sum of the mass fraction of soil remaining on each sieve after sieving
129 multiplied by the mean aperture of the adjacent mesh

130 Output: MWD for different soils and treatments

131

132 *Protected carbon: aggregate mineralization*

133 Aggregates provide physical protection to carbon. However, not all the carbon is automatically protected
134 inside the aggregates. The protection will depend on the porosity of the aggregates and the amount of
135 microbial biomass enclosed in the aggregates itself. This will ultimately influence the capacity of microbes to
136 get in contact with the C substrate and mineralize it. We aim to assess the degree of C protection in different
137 aggregates sizes of the two different soils (topsoil vs subsoil) and three different treatments (*M. sativa*, *L.*
138 *perenne*, bare soil). The soil nature will influence pore size, microorganisms' abundance and aggregate
139 stability. First, to assess the unprotected C in aggregates we measure the amount of CO₂ released when
140 incubating undisturbed aggregates of different classes. After, to assess the amount of total C (unprotected
141 and protected) we finely grind aggregates the aggregates (to remove their physical protection on carbon)
142 and assess the CO₂ respired during incubation. The different between these two values (CO₂ deriving from
143 protected C and CO₂ deriving from total C) will allow us to assess the amount of soil derived CO₂ that is
144 protected in different aggregates classes (3-5 mm, 0.2-3 mm, 0.02-0.2 mm) for different soils (topsoil and
145 subsoil) and species (*M.sativa*, *L.perenne* and bare soil) (Figure A1).



146 **Figure**

147 **A1:** : scheme of the microcatalometer methodology

148 **Methodology:**

- 149 1. Manually crush the soil and push it through a 5000 μm sieve (aggregates 3000-5000 μm fraction)
- 150 2. Sieve at 3mm and 0.2mm (aggregates < 200 μm fraction and 3 mm to 200 μm).
- 151 3. Collect the different fractions and separate them in half
- 152 4. Crush half one half of each fraction to obtain two subsamples: uncrushed aggregates and crushed
- 153 aggregates (20g of aggregates for each sample)
- 154 5. Bring them to 75% of water holding capacity
- 155 6. Samples placed in 125 ml jars with parafilm allowing the interchange of gases (but not water) and
- 156 incubated at 28 °C for 7 days.
- 157 7. Each sample was adjusted for soil moisture and, just after, the bottles were air tightly closed and
- 158 measurements of respiration made. After 6 hours of incubation (without any gas interchange)
- 159 measurements were made.
- 160 8. The differences of CO₂ between these two measurements gave the amount of respired CO₂ in 6h
- 161 per treatment, soil and aggregate class.

162 Output: amount of respired CO₂ for crushed and uncrushed aggregates. The difference between these

163 measurements represent the aggregates protected carbon in potential respiration. These results were

164 available for 3-5mm, 0.2-3mm and 0.02-0.2mm aggregate classes.

165

166 *Plant derived fresh carbon (new C) stored inside aggregate structures*

167 It is well known how aggregates provides protection for C, however the aggregate formation processes are

168 still debated. Especially in subsoil were little is known about aggregate structures and formation. C deriving

169 from plants, often processed by microbes, is recognized as one of the main actors in aggregate formation.

170 The input of C as plants' exudates and microbiological exudates and exopolysaccharides cement the mineral

171 structure of the aggregate that will provide protection from microbial mineralization. We aim to investigate

172 the pathways of C input in different aggregate classes to acquire information on aggregate formation and C

173 protection in the two different soils.

174 **Methodology:**

175 1. A subsample from the aggregate abundance samples was taken, representative of the following
176 aggregate classes:

177 1) aggregates 2000-5000 μm (2-5 mm)

178 2) aggregates 200-3000 μm (0.2-3 mm)

179 3) micro-aggregates 20-200 μm (<0.2mm)

180 2. The subsample is finely ground with an agate mortar and stored

181 3. The sample were analyzed to asses SOC and ^{13}C with an elemental analyzer Isoprime100 coupled
182 with an Elementar Varo Isotope Cube at INRA Nancy.

183 4. To calculate the proportion of NewC in aggregates, an isotope mixing model according to the work
184 of Balesdent and Mariotti (1996) was used:

$$185 \quad \%C_{new} = \frac{\delta(t1) - \delta(t0)}{\delta B - \delta(t0)} \quad [1]$$

186 Where %Cnew is the percentage of new carbon in the measured SOC of a specific aggregate fraction,
187 $\delta(t1)$ is the $\delta^{13}\text{C}$ signature of the SOC measured in a specific aggregate fraction at the end of the
188 experiment (t1), $\delta(t0)$ is the $\delta^{13}\text{C}$ signature of the SOC before the experiment (t0), δB is the $\delta^{13}\text{C}$
189 signature of the new C input in the system, in our case the signature of the root biomass (as the
190 average of adsorptive and transport roots signature).

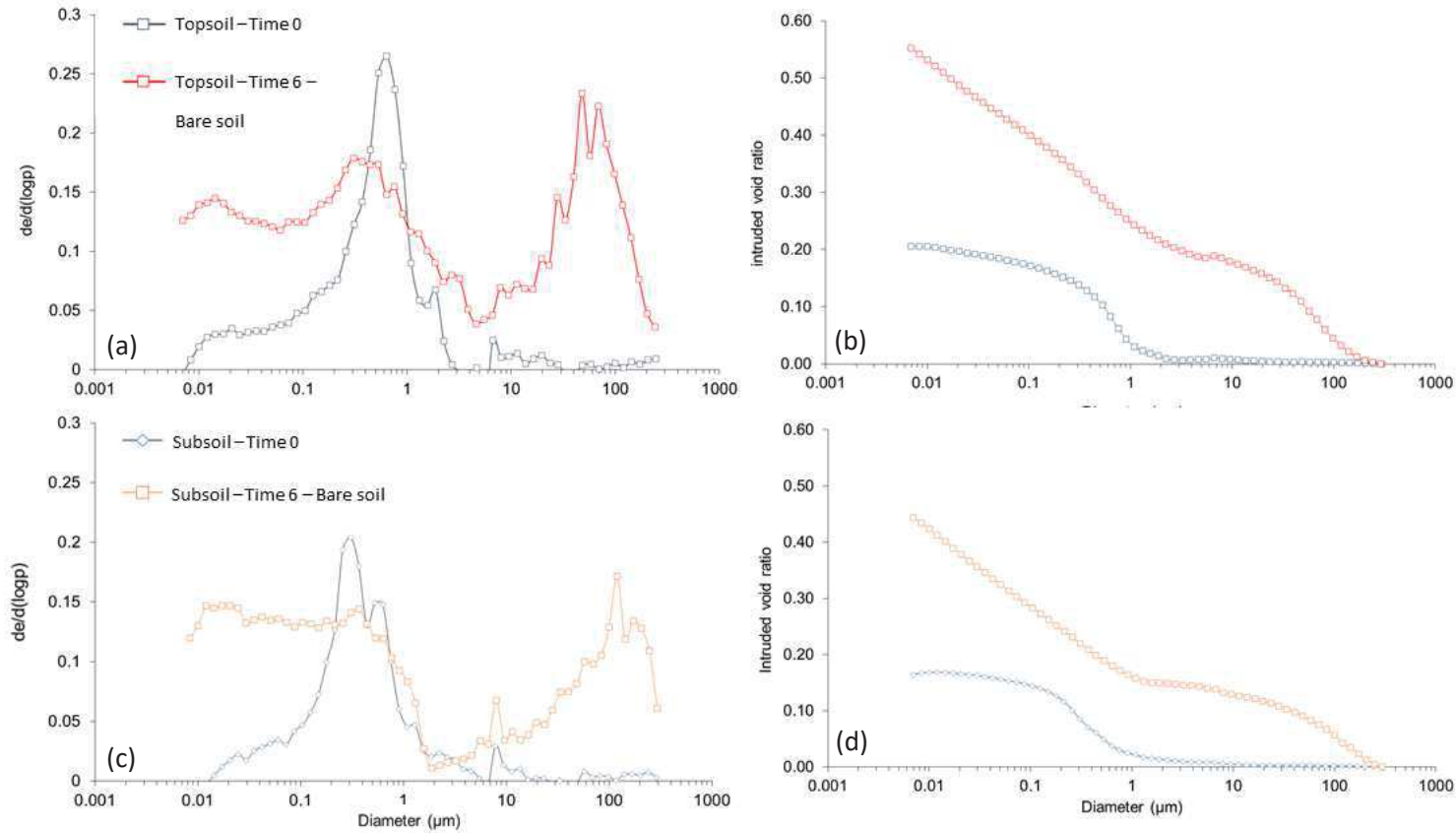
191 5. Multiply the total SOC for the %Cnew provides the amount of NewC in mgC g^{-1} soil.

192 Output: Amount of total SOC and NewC in the different classes (3-5 mm, 0.2-3 mm, 0.02-0.2 mm) for different
193 soils (topsoil and subsoil) and species (*M.sativa*, *L.perenne* and bare soil).

199 PRELIMINARY RESULTS AND MAIN DISCUSSION POINTS

200 *Mercury intrusion porosimetry (MIP) curves and cumulative porosity for different pore classes*

201 **Bare soil condition: Effect of wet and dry cycles**

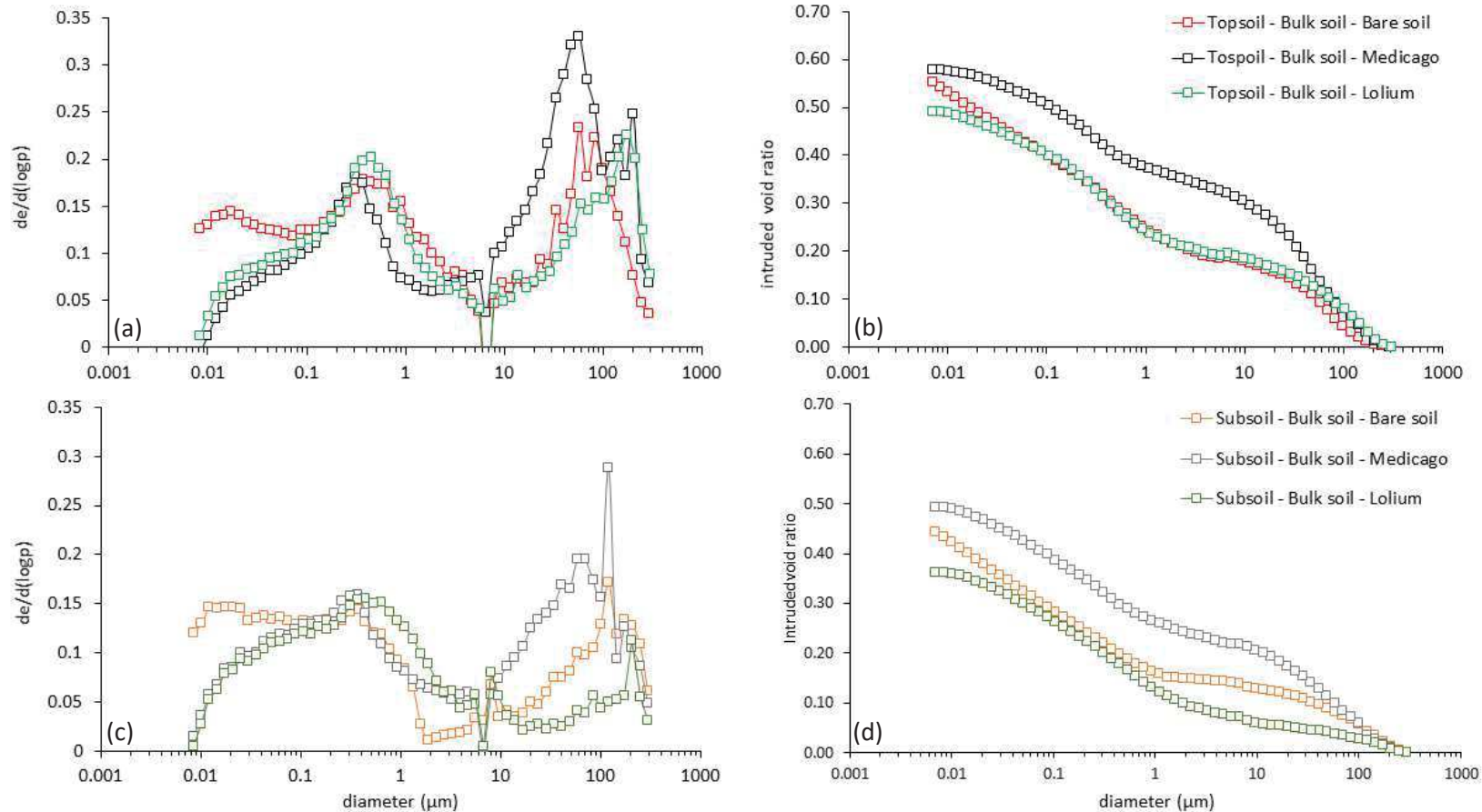


202

203 **Figure A2:** Evolution of microstructural voids in 6 months of wet and dry cycles, with no vegetation sowed. Figure (a) shows the pore size density function of topsoil at time 0 (blue
204 boxes) and time 6 (red boxes) without vegetation. (b) shows the total intruded void ratio for different diameter classes in topsoil. (c) shows the pore size density function of subsoil at
205 time 0 (blue boxes) and time 6 (orange boxes) without vegetation (d) the total intruded void ratio for different diameter classes in subsoil.

- 206
- Wet and dry cycles have a high effect on soil structures: soil structure pass from a mono-modal curve structure to a bi-modal curve structure in both soils.
- 207
- Void ratio highly increase in the micropores ($<0.1 \mu\text{m}$) and macropores ($>10 \mu\text{m}$) classes due to wet and dry cycles. Mesopores ($0.1-10 \mu\text{m}$) decrease during
- 208
- the 6 months experiment.
- The wet and dry cycles proved to influence both aggregates formation and stabilization processes (Shiel et al. 1988; Deneff et al. 2001). We hypothesize
- 209
- that, after the soil preparation (that included crushing and sieving) the soil lost its primary microstructure. Wet and dry cycles increase aggregate formation
- 210
- and, consequently, the microporosity deriving from intra-aggregates structure and the macroporosity deriving from inter-aggregates interactions.
- 211
- 212

213 **Vegetated treatment compared to bare soil after 6 months of growth**



214

215 **Figure A3:** Evolution of microstructural voids in 6 months of soil vegetated with *M.sativa* and *L.perenne* compared to bare soil control. Figure (a) shows the pore size density function
 216 of topsoil in bare soil control (red boxes), *M.sativa* (black boxes), and *L.perenne* (green box) after 6 months of growth. (b) shows the total intruded void ratio for different diameter
 217 classes in topsoil. (c) shows the pore size density function of subsoil in bare soil control (orange boxes), *M.sativa* (grey boxes), and *L.perenne* (dark green boxes) after 6 months of
 218 growth. (d) shows the total intruded void ratio for different diameter classes in subsoil.

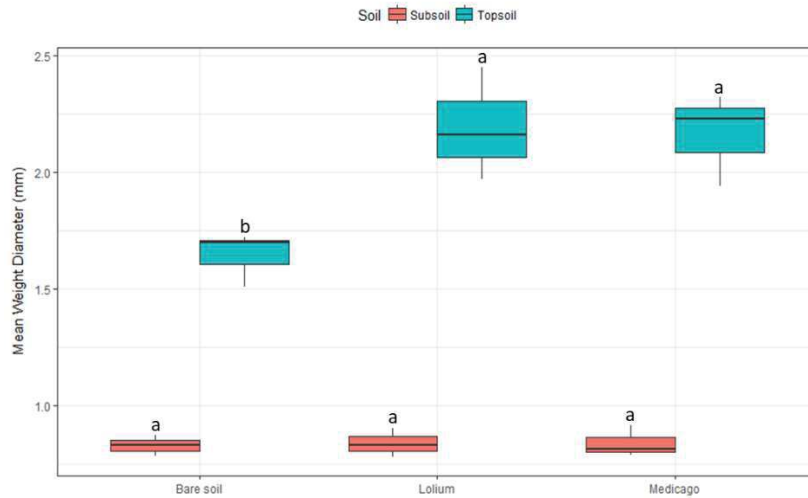
219

- *M. sativa* show an increase in total porosity in both subsoil and topsoil, while *L.perenne* decrease the total porosity (Figure A3b,d).

- 220
- *M.sativa* increase the macroporosity in both soils (> 10 μm), while *L.perenne* show a decrease in macroporosity in bare soil (Figure A3a,c).
- 221
- Both *M. sativa* and *L. perenne* decrease the microporosity of the system (<0.1 μm) (Figure A3a,c).
- 222
- The increase in macroporosity due to *M.sativa* might be correlated with increased aggregate formation and interactions, and root channeling effect. The
- 223
- decrease of microporosity is imputable to exudates from microbial activity and plants that clog the micropores in aggregates. However, replicates are
- 224
- needed to verify these hypothesis.

225

226 *Aggregate stability: Mean weight diameter (MWD)*

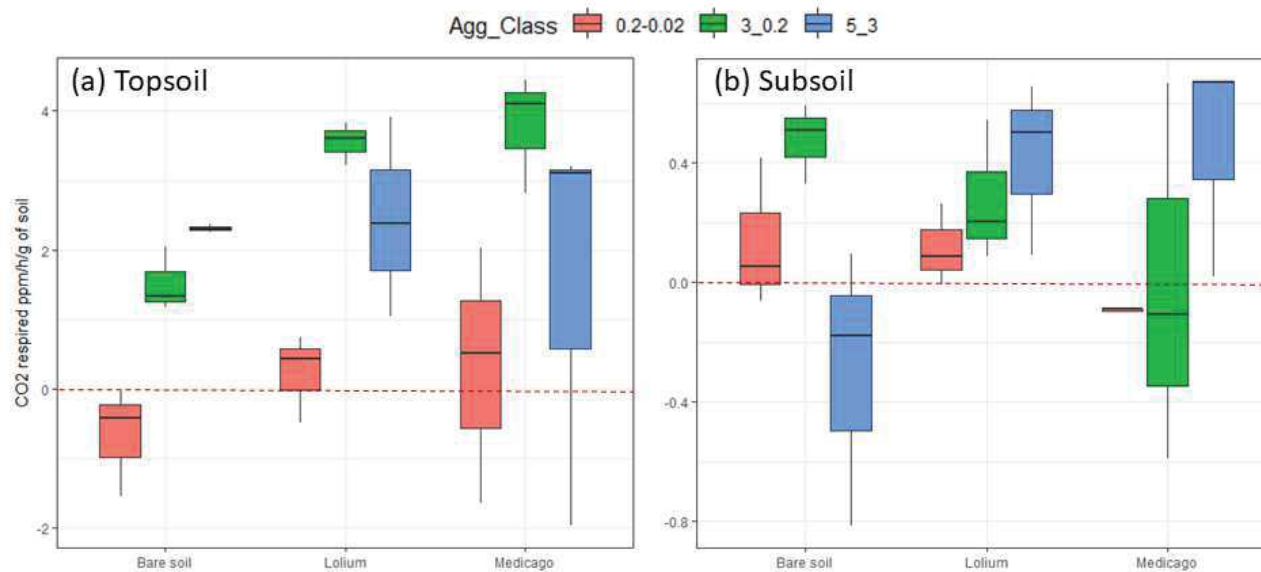


227

228 **Figure A4:** Mean weight diameter (MWD) in topsoil (blue boxplot) and subsoil (red boxplot) for the three different treatments (*M.sativa*, *L.perenne* and bare soil control) after 6 months
229 of revegetation. In each boxplot, the lower edge of the box corresponds to the 25th percentile data point, while the top edge of the box corresponds to the 75th percentile data point.
230 The line within the box represents the median and black dots indicate outliers. Different letters above the boxplots indicate statistically significant differences ($p < 0.05$) between families
231 and controls according to Tukey HSD test.

- 232
- Subsoil and topsoil have a significant different MWD after 6 months of revegetation, with a higher aggregate stability in topsoil.
- 233
- No significant effect of vegetation in subsoil.
- 234
- In topsoil vegetated treatment have a significantly higher stability compared to bare soil control. However, we didn't observe any effect of different
- 235
- vegetation.

236



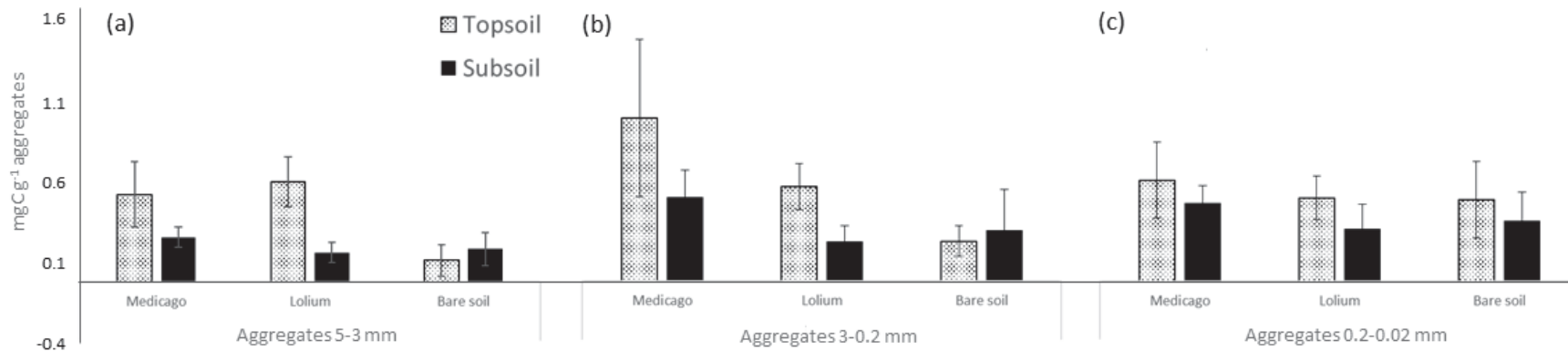
238

239 **Figure A5:** amount of CO₂ (respired ppm h⁻¹ g⁻¹ of soil) protected inside different aggregate classes (5-3 mm clogs in blue, 3-0.2 mm macroaggregates in green, 0.2-0.02 mm
 240 microaggregates in red) in (a) topsoil and (b) subsoil. The protected C is calculated as the difference between the respired CO₂ deriving from incubation of undisturbed aggregates (CO₂
 241 deriving from unprotected C) and CO₂ deriving from incubation of crushed aggregates (CO₂ deriving from consumption of protected and unprotected C). In each boxplot, the lower edge
 242 of the box corresponds to the 25th percentile data point, while the top edge of the box corresponds to the 75th percentile data point. The line within the box represents the median and
 243 black dots indicate outliers. The red dotted line is the 0 line, meaning no protection of C in aggregates.

- 244
- In topsoil the higher C protection is found in the macroaggregates, with vegetation that increase the amount of protected C underlining the reactivity of
- 245 this aggregate class to revegetation. In topsoil clogs no effect of vegetation can be found, with increased standard variation in vegetated treatment but no
- 246 differences with bare soil.
- In subsoil we observe a very different trend, with vegetation decreasing the C protection in the 3-0.2mm macroaggregates, while increasing the amount of
- 247 protected C in the 5-3 clogs, that did not presented any protection in bare soil control.
- 248

- In both topsoil and subsoil, microaggregates do not have any role in C protection, since no changes are observed when crushing them. However, since the crushing was done by hand in an agate mortar it is not sure that the structures were efficiently disaggregated, leaving a possible bias in the methodology.

251 *Plant derived NewC input in aggregates*



253 **Figure A6:** newC (mg new C g⁻¹ aggregates) deriving from plant input in aggregates for gram of aggregates of different classes for the three analyzed treatment (*M.sativa*, *L.perenne*,
 254 and bare soil control) after 6 months in topsoil (light dotted bars) and subsoil (solid black bars). (a) Show the C concentration in the clogs (5-3mm diameter), (b) in the macroaggregates
 255 (3-0.2 mm), and (c) in the microaggregates (0.2-0.02mm). Bars represent the standard deviation.

- In clots (Figure 5A,a), vegetated treatment store more new C compared to bare soil, while in subsoil no significant differences seems to occur.
- The higher increase in C seem to be in macroaggregates (Figure 5A,b), higher in *M.sativa* compared to *L.perenne* and bare soil.
- In microaggregates, no effect of vegetation seem to influence the quantity of new C moved (Figure 5A,c).
- Bare soil control shows increase in NewC, probably due to mosses colonization that mineralized enriched CO₂. The analysis of deeper layer of soil is needed to avoid the contamination.

267 FUTURE WORK

- 268 1. Replication of MIP results to confirm the trends.
- 269 2. MIP results will be separated in different pore classes to have cumulative data for void ratio in
270 different pore classes relative to different aggregate sizes.
- 271 3. Implement principal component analysis and Pearson's correlations between i) aggregate stability
272 MWD, ii) amount of C protected in different aggregates classes in CO₂ equivalent, iii) new C input in
273 different aggregate classes, and iv) void ratio in different pore classes representing microaggregates,
274 macroaggregates and clots, in the two soils and for the different species.
- 275 4. Discussion on the effect of vegetation on soil structure and relationship between aggregate
276 characteristics and soil structure in terms of void ratio. Use of the data to link the C input in
277 aggregates with the soil structure formation, and the feedback between the structure and the C
278 protection.
- 279 5. Results will help to understand the differences in C fluxes in aggregates in topsoil and subsoil brought
280 to the surface and test the aggregate hierarchy theory of Tisdall and Oades (1982), widely accepted
281 for topsoil, on subsoil brought to the surface. Preliminary results suggest that subsoil brought to the
282 surface might not share the same aggregation processes than topsoil.

283

284 REFERENCES

- 285 Balesdent, J. & Mariotti, A. 1996. Measurement of soil organic matter turnover using $\delta^{13}\text{C}$ natural abundances.
286 In: *Mass Spectrometry of Soils* (eds T.W. Boutton & S. Yamasaki), pp. 83-111. Marcel Dekker Inc., New
287 York.
- 288 Caesar-Tonthat, T.C. 2002. Soil binding properties of mucilage produced by a basidiomycete fungus in a
289 model system. *Mycological Research* 106, 930–937.
- 290 Delage, P., Pellerin, F.M., (1984). Influence de la lyophilisation sur la structure d'une argile sensible du
291 Québec. *Clay minerals* 19 : 151-160
- 292 Denef, K., Six, J., Bossuyt, H., Frey, S.D., Elliott, E.T., Merckx, R., Paustian, K., 2001. 1-s2.0-
293 S0038071701000761-main.pdf 33, 1599–1611.
- 294 Eyles, A., Coghlan, G., Hardie, M., Hovenden, M., Bridle, K., 2015. Soil carbon sequestration in cool-temperate
295 dryland pastures: Mechanisms and management options. *Soil Research* 53, 349–365.
- 296 Ivanov, V., Chu, J., 2008. Applications of microorganisms to geotechnical engineering for bioclogging and
297 biocementation of soil in situ. *Reviews in Environmental Science and Biotechnology* 7, 139–153.
- 298 Koliji, A., Vulliet, L., Laloui, L., 2008. New basis for the constitutive modelling of aggregated soils. *Acta*
299 *Geotechnica* 3, 61–69.
- 300 Le Bissonnais, Y., 2016. Aggregate stability and assessment of soil crustability and erodibility: I. Theory and
301 methodology. *European Journal of Soil Science* 67, 11–21.
- 302 Lugato, E., Morari, F., Nardi, S., Berti, A., Giardini, L., 2009. Relationship between aggregate pore size
303 distribution and organic-humic carbon in contrasting soils. *Soil and Tillage Research* 103, 153–157.
- 304 Malamoud, K., McBratney, A.B., Minasny, B., Field, D.J., 2009. Modelling how carbon affects soil structure.
305 *Geoderma* 149, 19–26.
- 306 McCarthy, J.F., Ilavsky, J., Jastrow, J.D., Mayer, L.M., Perfect, E., Zhuang, J., 2008. Protection of organic carbon
307 in soil microaggregates via restructuring of aggregate porosity and filling of pores with accumulating
308 organic matter. *Geochimica et Cosmochimica Acta* 72, 4725–4744.
- 309 Nichols, K.A., Wright S.F., 2005. Comparison of glomalin and humic acid in eight native U.S. soils. *Soil Science*
310 170, 985–997.
- 311 O'Brien, S.L., Jastrow, J.D., 2013. Physical and chemical protection in hierarchical soil aggregates regulates
312 soil carbon and nitrogen recovery in restored perennial grasslands. *Soil Biology and Biochemistry* 61,
313 1–13.
- 314 Russo ,G., Rezza, A., Mancuso, C., Oliviero, V., D'Onza, F., Gallipoli, D., Wheeler, S., 2016. Microstructure
315 analysis of laboratory and in-situ compacted silts. *E3S Web of Conferences* 9, 06003
- 316 Shiel, R.S., Adey, M.A., Lodder, M., 1988. The effect of successive wet/dry cycles on aggregate size
317 distribution in a clay texture soil. *Journal of Soil Science* 39, 71–80.

318 Tisdall, J. M., & Oades, J. M. (1982). Organic matter and water-stable aggregates in soils. *Journal of Soil*
319 *Science*, 33, 141–163.

320

321

Résumé exhaustif: Objectifs, résultats, conclusions générales

267 OBJECTIFS GENERAUX ET HYPOTHESES

268 Les objectifs généraux appliqués de la thèse sont :

- 269 i. Comprendre l'effet des caractéristiques des plantes et du sol sur la séquestration du carbone dans
270 le sol en termes de quantité et de qualité (objectif fondamental)
- 271 ii. Identifier les pratiques possibles en matière de plantes et de sols qui peuvent être mises en œuvre
272 pour augmenter le stockage du carbone dans les remblais des routes et ferroviaires et,
273 éventuellement, dans les sols gris des travaux géotechniques (objectif appliqué)

274 Différentes questions spécifiques concernant les mécanismes fondamentaux du cycle C ont été abordés
275 dans chaque chapitre de la thèse.

276

277 *Chapitre II : Voie de la persistance : les caractéristiques des racines des plantes modifient*
278 *l'accumulation de C dans différents réservoirs de carbone du sol par médiation microbienne*

- 279 i. Objectif 1 : Comprendre les relations entre les caractéristiques des racines et l'accumulation de C dans
280 différents bassins de carbone du sol pour 12 espèces herbacées différentes couramment utilisées dans
281 la revégétalisation des talus.

282 Hypothèse 1 : Les caractéristiques liées à l'apport de C labile (taux d'allongement des racines, teneur en
283 hémicellulose, biomasse racinaire) favorisent l'accumulation de C dans les bassins protégés de limon
284 grossier et de limon fin + argile par activité microbienne. Les caractères racinaires liés à la récalcitrance
285 (teneur élevée en lignine et en cellulose, rapport C:N élevé) favorisent l'accumulation de C dans le mélange
286 de matière organique en particules (POM) grossier non protégé.

- 287 ii. Objectif 2 : Quel est l'effet de la sélection des espèces sur la séquestration du carbone dans différents
288 bassins de carbone du sol ?

289 Hypothèse. 2 : Les espèces fixatrices de diazote (N₂) favorisent l'accumulation de C dans les bassins protégés
290 de limon fin+argile car elles ont des caractéristiques plus liées à l'apport de C labile, tandis que les espèces
291 non fixatrices de N₂ favorisent l'accumulation de C dans la fraction POM.

292

293 *Chapitre III : Les destins du carbone du sol nouveau et ancien diffèrent dans le sol superficiel et le sous-*
294 *sol nouvellement exposé et s'expliquent par les traits racinaires, des microbes et des particules du sol.*

295 i. Objectif 1 : Quantifier les flux de nouveau C introduit par les plantes et de vieux C préexistant dans
296 différents bassins de sol;

297 Hypothèse 1 : les fractions granulométriques du pétrole associées aux fractions de taille des particules du
298 pétrole peuvent réguler les destins de l'ancien C et du nouveau C dans le processus de séquestration du C

299 ii. Objectif 2 : Rechercher l'effet synergique de la nouvelle entrée C et des changements de l'ancienne
300 entrée C dans les différents bassins de carbone.

301 Hypothèse 2 : Le sort du nouveau C et de l'ancien C montrera des modèles indépendants.

302 iii. Objectif 3 : Étudier si les différents acteurs impliqués dans le stockage du carbone et l'influence que la
303 plante et le sol ont sur eux peuvent expliquer les schémas des nouveaux flux de carbone et des anciens
304 flux de carbone dans différents bassins de carbone du sol.

305 Hypothèse 3 : Nous faisons l'hypothèse que les traits racinaires liés à la composition chimique et à la
306 récalcitrance entraîneront une nouvelle accumulation de C dans la POM, tandis que les traits liés à un
307 apport élevé en C entraîneront le stockage dans des fractions protégées par consommation et dépôt
308 microbiologiques. Je m'attends à ce que la stabilité des agrégats soit corrélée positivement avec la nouvelle
309 accumulation de C total et dans le POM fin et les fractions grossières de limon en raison de la protection
310 physique des agrégats. Nous nous attendons à ce que la teneur en N du sol soit positivement corrélée avec
311 la nouvelle teneur en C. Nous pensons que la fraction fine dans le sol est corrélée positivement avec le
312 nouveau stockage du carbone dans la fraction de limon fin + argile en raison des interactions

313 organominérales, et que le nouveau stockage du carbone dans le limon fin + argile est plus élevé dans le
314 sous-sol que dans le sol superficiel en raison des niveaux inférieurs de saturation en carbone du sol. Enfin,
315 je m'attends à ce que l'activité, la diversité et l'abondance microbiennes soient fortement liées à la quantité
316 de nouveau C déposé dans les fractions de limon grossier et de limon + argile protégées, et à la
317 consommation et à la transformation du nouveau C dans les fractions grossières et fines non protégées du
318 POM et du POM fin en raison des minéralisations des communautés microbiennes.

319

320 *Chapitre IV : La qualité du sol détermine le 'priming effect' et les espèces végétales l'affinent : le rôle*
321 *de la préférence du substrat et de la concurrence dans le sol superficiel et le sous-sol*

322 i. Objectif 1 : Quantifier les changements dans le C et l'apport de nouveau C dans le sol pour
323 déterminer les pertes de l'ancien C dans le sol superficiel et le sous-sol remontés à la surface
324 et revégétalisé et le 'priming effect' de la revégétalisation avec des espèces fixant N₂
325 (*Medicago sativa*) et une espèce non fixant N₂ (*Lolium perenne*)

326 Hypothèse 1 : Notre hypothèse est que le sol superficiel aura des pertes plus élevées de vieux C en raison
327 de la biomasse et de l'activité microbienne plus élevées. Cependant, en raison de la plus grande protection
328 du vieux C dans le sous-sol et des changements des conditions environnementales dus à la revégétalisation,
329 nous émettons l'hypothèse que le sous-sol aura des pertes de vieux C plus élevées que le sol nu, ce qui
330 signifie un 'priming effect' positif plus élevé que le sol de surface.

331 ii. Objectif 2 : Quantifier le 'priming effect' dans différents bassins C liés aux fractions
332 granulométriques du sol.

333 Hypothèse 2 : Étant donné la protection plus élevée de C dans la fraction plus fine du sol (fractions limon
334 et limon + argile), nous supposons que le 'priming effect' se produira dans les fractions de matière
335 organique particulaire non protégée (POM et POM fin).

336 iii. Objectif 3 : Étudier l'évolution dans le temps des sources de C respiré dans le système (représentées
337 par l'abondance du ^{13}C) et ses corrélations avec les nouvelles pertes de C, les nouvelles entrées de C
338 et le priming effect.

339 Hypothèse 3 : La source de respiration dans le système sol-plante se tournera davantage vers les intrants
340 végétaux marqués au fil du temps, avec le développement des plantes. Les nouveaux apports de C seront
341 positivement corrélés avec l'abondance du ^{13}C dans le CO_2 respiré (A13C). Cependant, je m'attends à des
342 comportements différents dans les deux sols en ce qui concerne les pertes de nouveau C. Dans le sol
343 superficiel , je suggère que l'A13C sera corrélé négativement avec les pertes de nouveau C, en raison d'un
344 apport élevé de nouveau C dans le système et de l'utilisation accrue de nouveau C comme substrat pour la
345 croissance microbienne (reflétée par un A13C supérieur). Dans le sous-sol, je fais l'hypothèse d'une
346 corrélation positive entre l'A13C et les pertes de nouveau C, puisqu'un faible apport de nouveau C
347 augmentera l'activité microbienne qui, ne pouvant satisfaire leurs besoins énergétiques principalement à
348 partir de ces sources labiles, exploitera le nouveau C plus efficacement. De la même façon, le 'priming
349 effect' sera corrélé négativement à A13C dans le sol arable, tout en étant corrélé positivement dans le sous-
350 sol.

351

352 APPROCHE ET CONCEPTION EXPERIMENTALE

353 Pour atteindre ces objectifs, deux expériences ont été conçues et réalisées dans le cadre de ce projet de
354 recherche.

355 Dans la première expérience, 12 espèces herbacées différentes ont été cultivées en monoculture dans 72
356 boîtes de culture (six répétitions par espèce). Sur ces six répétitions, la moitié a été utilisée pour
357 l'échantillonnage du sol, tandis que l'autre moitié a été cultivée dans des boîtes munies de fenêtres en PVC
358 utilisées pour observer la croissance des racines. Toutes les deux semaines, chaque fenêtre de racines a été
359 photographiée pour évaluer le taux d'allongement des racines et les caractéristiques des racines. Après 10

360 mois, des carottes de sol ont été prélevées pour évaluer 1) les caractéristiques architecturales des racines,
361 2) la composition chimique des racines, 3) le carbone du sol dans quatre fractions de sol différentes (POM
362 <200 µm ; POM fin 50-200 µm, limon 20-50 µm, limon + argile <20 µm), 4) la respiration microbienne induite
363 (SIR) du substrat comme indicateur d'activité microbiologique.

364 Dans la deuxième expérience, deux des 12 espèces présentant des tendances aux extrémités opposées du
365 spectre économique racinaire (*Lolium perenne* et *Medicago sativa*) ont été sélectionnées et cultivées en
366 monoculture en pots. Les pots ont été cultivés dans des microcosmes avec des conditions
367 environnementales constantes et du CO₂ atmosphérique constamment enrichi en ¹³C pendant 183 jours
368 sur deux types de sol. Les deux types de sol, soit le sol superficiel (0-30 cm) et le sous-sol (110-140 cm), ont
369 été extraits du même profil de sol à Pisciotta (SA), en Italie. Les sols étaient argileux et présentaient des
370 caractéristiques contrastées (teneur en azote, stabilité des agrégats, biomasse et activité microbienne). De
371 plus, dans le sol superficiel, la teneur en argile était légèrement inférieure à celle du sous-sol (-8 %) et la
372 teneur en C nettement supérieure (sol superficiel 12 mgC g⁻¹ sol ; sous-sol 6 mgC g⁻¹ sol), ce qui entraîne un
373 niveau de saturation en C supérieur. Les plantes et les sols ont été croisés et six pots répliqués ont été
374 semés. Par ailleurs, six pots témoins nus (non semés) ont été mis en place pour chaque sol. Toutes les deux
375 semaines, la respiration du sol était échantillonnée pour évaluer ¹³C% de CO₂ respiré et le CO₂ dérivé de la
376 plante, et après six mois, les pots étaient collectés et le sol échantillonné pour une gamme de différentes
377 caractéristiques du sol, des racines et des caractéristiques microbiologiques.

378 PRINCIPAUX RESULTATS

379 Au chapitre II, nous n'avons observé aucun effet significatif des espèces sur l'accumulation de C dans les
380 différents gisements de C associés aux fractions du sol. Cependant, lorsque nous avons observé l'effet de
381 la famille, les espèces de Fabaceae fixatrices de N₂ ont accumulé plus de C dans la fraction de limon fin
382 protégée, tandis que les espèces de Poaceae non fixatrices de N₂ dans la fraction POM. Les caractéristiques
383 des racines différaient significativement entre les deux familles, les Poaceae ayant des tissus plus
384 récalcitrants (lignine et cellulose élevées, et rapport C:N élevé), une biomasse racinaire plus faible et un

385 taux d'allongement des racines plus faible. Les espèces de Fabaceae présentaient des tissus plus labiles
386 (hémicellulose élevée et faible rapport C:N), une biomasse plus élevée et un taux d'élongation des racines
387 plus élevé. Les espèces de Fabaceae ont également augmenté l'activité microbienne. Grâce à l'analyse en
388 composantes principales et aux corrélations de Pearson, nous avons montré l'effet d'un apport élevé de C
389 labile (typique des espèces acquiescentes à croissance rapide) entraînant une accumulation plus élevée dans
390 la fraction de limon protégée. Les espèces conservatrices à croissance lente, à l'autre extrémité du spectre
391 économique racinaire, augmentent l'accumulation de C dans la POM non protégée. Cette différence dans
392 les stratégies d'accumulation de C a confirmé la corrélation entre le spectre économique racinaire et le
393 stockage de C dans différents bassin de C. Cette différence était due à l'effet de l'espèce sur l'activité
394 microbienne. Une activité microbienne élevée chez les espèces de Fabaceae a favorisé la minéralisation de
395 l'intrant C et son entombage dans la fraction limoneuse, tandis que l'activité microbienne plus faible chez
396 les espèces de Poaceae a diminué la décomposition et la minéralisation du C introduit par rotation des
397 racines et augmenté sa stabilité et son accumulation dans la fraction POM.

398 Dans le chapitre III, nous avons montré comment l'apport de C dérivé de nouvelles plantes et les pertes de
399 C préexistant étaient en synergie, avec un apport plus élevé de nouveau C diminuant les pertes d'ancien C.
400 Les espèces plantées en surface ont considérablement augmenté l'apport de nouveau C dans le sol et
401 diminué le rendement du C ancien. En particulier, *M. sativa* avait un apport plus élevé et des pertes plus
402 faibles que *L. perenne*. L'apport de nouveau C s'est principalement fait au niveau des fractions POM et
403 limons fins+argile dans les sols. Dans le sol superficiel, l'ancien C a diminué dans tous les gisements sauf
404 dans la fraction limons fins+argile, où il s'est accumulé. Dans le sous-sol, l'ancien C a diminué dans tous les
405 gisements sauf dans le POM, où la diminution n'a pas été significative. Les différentes caractéristiques des
406 racines, des microbes et du sol étaient mieux corrélées avec l'apport de nouveau C dans les fractions que
407 les changements de l'ancien C. Les anciennes pertes de C semblaient plus liées au choix du sol et "
408 intrinsèques " au système du sol. Cette entrée de nouveau C était principalement corrélée positivement
409 avec la production de biomasse racinaire, tandis que le rapport C:N était corrélé négativement avec la

410 nouvelle entrée de C dans les fractions POM et limons fins+argile. Les caractères racinaires sont mal corrélés
411 aux variations de quantité de l'ancien C. Les caractéristiques microbiologiques ont été le principal facteur
412 à l'origine des nouveaux apports de C, corrélés positivement à l'augmentation du nouveau C dans chaque
413 fraction. Ils étaient aussi positivement corrélés avec l'ancienne accumulation de C dans la fraction limons
414 fins+argile. En ce qui concerne les caractéristiques du sol, la stabilité des agrégats et la teneur en N étaient
415 en synergie et en corrélation positive avec les nouveaux apports de C dans le système et l'accumulation des
416 anciens C dans la fraction limons fins+argile. La fraction fine du sol (<20µm) a été corrélée négativement
417 avec la nouvelle entrée de C et, étonnamment, l'ancienne accumulation de C dans la fraction limons
418 fins+argile. Ces résultats ont clairement montré comment le type de sol constitue le facteur principal influant
419 sur le stockage et le cycle du carbone dans le sol car la fertilité et l'activité microbienne du sol constituent
420 le moteur de la séquestration du carbone. Les espèces végétales ont un effet secondaire sur le stockage et
421 le cycle du carbone dans le sol. *M. sativa* est l'espèce la plus influente parmi les 12 étudiées et agit en
422 augmentant l'apport de nouveau C grâce à une production plus élevée de tissus labiles et une activité
423 microbienne accrue. Une faible saturation en C du sol ne semble pas avoir d'influence positive sur le
424 stockage du C dans la fraction limons fins+argile. Cependant, lorsque l'apport de nouveau C dans la fraction
425 limons fins+argile est normalisé par la biomasse racinaire (pour estimer l'apport de nouveau C par g de
426 racine), le sous-sol a un rendement de stockage C supérieur à celui de la terre végétale, et *L. perenne* a un
427 apport supérieur par g de biomasse produite. Une saturation plus faible en C pourrait donc avoir un effet
428 positif sur le stockage du C dans le sol, mais cet effet est atténué par la fertilité du sol (qui détermine la
429 production de biomasse et l'apport de C dans le système) et l'activité microbienne (qui transforme l'apport
430 de C et le transfère dans la fraction limons fins+argile par métabolisme microbien). Dans ce chapitre, nous
431 montrons clairement la puissance du couplage des techniques de marquage isotopique avec le
432 fractionnement du sol pour décrire efficacement les changements de C dans le sol et étudier leurs
433 corrélations avec les différents acteurs impliqués.

434 Enfin, dans le Chapitre IV, nous montrons une fois de plus comment le sol est l'élément principal qui façonne
435 le 'priming effect', avec des pertes de carbone plus élevées dans le sol superficiel que dans le sous-sol en
436 raison de la biomasse et de l'activité microbienne accrues, mais un 'priming effect' négatif dans le sol
437 superficiel et positif dans le sous-sol. L'augmentation de l'apport de nouveau C dans le sol favorise le
438 passage de la préférence pour le substrat des plantes de l'ancien C préexistant à l'apport de nouveau C.
439 Ceci peut être observé dans les résultats de respiration du sol : dans le sol superficiel, l'augmentation de la
440 signature du ^{13}C au cours des six mois est supérieure à celle de le sol superficiel, atteignant une quantité
441 plus élevée de CO_2 provenant de la minéralisation du nouveau C introduit par rapport à l'ancien C
442 préexistant dans le sol. La quantité totale d'ancien C consommée dans un sol végétalisé diminue par
443 rapport à un sol nu, ce qui entraîne un 'priming effect' négatif. Dans le sous-sol, l'apport de nouveau C n'est
444 pas assez élevé pour permettre le changement de préférence du substrat, et les communautés
445 microbiennes continuent d'utiliser l'ancien C préexistant pour l'acquisition des nutriments. Dans le sous-
446 sol, nous pouvons observer un effet significatif des espèces, *M. sativa* ayant un 'priming effect' positif plus
447 élevé que *L. perenne*. Ceci peut s'expliquer par la concurrence entre les communautés microbiennes et les
448 plantes pour l'acquisition d'azote. L'absorption racinaire par *L. perenne* concurrence les communautés
449 microbiennes pour l'acquisition d'azote et réduit leur activité, ce qui réduit globalement leur efficacité à
450 consommer l'ancien C et entraîne un faible 'priming effect' (pas significativement différent du sol nu). *M.*
451 *sativa* étant une espèce fixatrice de N_2 , elle ne concurrence pas les microorganismes pour le N.
452 L'augmentation de l'intrant de C labile augmente en fait la biomasse et l'activité microbiennes et l'extraction
453 de l'ancien C pour l'exploitation des ressources. Pour cette raison, *M. sativa* a un 'priming effect' positif
454 plus élevé. Dans ce chapitre, nous réconcilions les théories de la préférence pour le substrat et celles de la
455 concurrence, qui déterminent le 'priming effect' et dépendent de la fertilité du sol et, ensuite, des espèces
456 végétales. Le 'priming effect' de la fertilité du sol se manifeste par la préférence du substrat, le sol fertile
457 permettant aux communautés microbiennes de changer de substrat et ayant pour résultat un 'priming
458 effect' négatif. Les sols pauvres ne permettent pas le changement de substrat et donnent lieu à un 'priming

459 effect' positif, dont l'ampleur est déterminée par l'absence de concurrence microbienne pour l'azote par
460 les plantes. Nous avons également observé que le 'priming effect' dans le sous-sol était plus élevé dans les
461 fractions limon et limon fin + argile, remettant en question la stabilité effective de ces fractions.

462

463 CONCLUSION ET APPLICATION PRATIQUE

464 Avec cette recherche, nous avons mis en évidence comment les espèces fixant N₂ sont plus efficaces pour
465 la séquestration du C grâce à un apport plus élevé de C labile qui augmente le stockage total du C, plus
466 particulièrement dans les bassins de C stables limon et limon + argile. L'apport plus élevé dans les bassins
467 protégés limon et limon + argile est lié aux caractéristiques racinaires liées à la labilité (en particulier les
468 caractéristiques chimiques des racines) qui augmentent l'activité microbologique. Dans cette perspective,
469 l'étude du spectre économique racinaire est un outil prometteur pour établir un lien entre les traits
470 racinaires et la séquestration du carbone. La symbiose avec la bactérie *Rhizobium* joue également un rôle
471 important en augmentant la production et le dépôt d'exopolysaccharides dans les fractions fines du sol.

472 Le sol est le principal facteur qui influe sur le stockage du C, et l'analyse des bassins de carbone liés aux
473 fractions du sol couplé à l'expérience de l'étiquetage isotopique est une méthodologie puissante pour
474 démêler les mécanismes du cycle C. Le sol superficiel a un apport plus élevé en C en raison d'une fertilité
475 plus élevée et d'une activité microbienne plus élevée, ce qui augmente le dépôt de C dans la fraction
476 protégée de limon et de limon + argile. Le sol superficiel a également moins de pertes de carbone ancien
477 grâce au passage de la consommation préférentielle de substrat de l'ancien C vers le nouveau C des
478 communautés microbiologiques. Globalement, l'effet de la saturation en C sur le stockage du C dans la
479 fraction limon + argile semble être soumis à la qualité du sol en termes de teneur en N et d'activité
480 microbologique. Cependant, lorsque ces exigences sont satisfaites, il peut stocker C plus efficacement,
481 comme le suggère la quantité plus élevée de C déplacée dans les fractions de limon + argile par g de racine
482 dans le sous-sol (faible saturation en C) par rapport à la terre végétale (saturation en C élevée).

483 Le sol est également le principal moteur de le 'priming effect', le sol superficiel présentant un 'priming
484 effect' négatif en raison du passage des communautés microbiologiques de l'ancien C au nouveau C. Dans
485 le sous-sol, le 'priming effect' est positif et la concurrence détermine son ampleur : *L. perenne* diminue le
486 'priming effect' positif (presque aucun 'priming effect') grâce à la compétition pour l'azote qui inhibe

487 l'activité microbiologique. *M. sativa*, d'autre part, augmente l'azote du sol grâce à sa capacité de fixation de
488 l'azote et augmente l'activité microbiologique, ce qui augmente globalement le 'priming effect' positif.

489 Une de nos principales indications pratiques est de ne pas considérer le potentiel de stockage du C du sol
490 uniquement du point de vue de la minéralogie, de la teneur en argile ou de la saturation en C, mais de faire
491 attention à la santé du sol. Plus spécifiquement, pour évaluer ses niveaux de fertilité (teneur en N), la
492 stabilité des agrégats (MWD) et le développement des communautés microbiennes (évaluation de leur
493 biomasse et/ou activité). La diversité microbienne pourrait également être un indicateur important. Ces
494 indicateurs sont liés à un apport plus élevé de C dans le sol par le biais d'une production accrue de biomasse,
495 d'un transfert vers un bassin limons fins+argile protégé et d'un 'priming effect' négatif dû à un changement
496 d'utilisation du substrat.

497 L'utilisation de le sol superficiel fertile augmente l'accumulation de carbone par rapport à un sous-sol
498 pauvre et il est donc souhaitable pour la revégétalisation des sols géotechniques. Lors de la revégétalisation
499 de le sol superficiel fertile, les espèces à croissance rapide qui fixent l'azote (c.-à-d. les légumineuses) avec
500 un apport élevé de C labile sont plus efficaces pour stocker le C dans un bassin protégé de limons et de
501 limons fins+argile par un apport racinaire et un renouvellement microbien *in vivo* plus élevés. De plus, la
502 revégétalisation de le sol superficiel a un 'priming effect' négatif, ce qui augmente la stabilité du C
503 préexistant.

504 Cependant, l'utilisation de terre végétale n'est pas toujours possible. Certaines conditions particulières
505 peuvent nécessiter la revégétalisation du sous-sol ; par exemple, en cas d'indisponibilité de le sol superficiel
506 fertile, l'impact écologique de l'enlèvement de le sol superficiel fertile d'une zone différente, ou en raison
507 de vastes zones excavées qui seraient trop coûteuses économiquement et écologiquement pour être
508 couvertes de terre végétale fertile (comme de vastes carrières). Dans ce cas, nous conseillons de:

509 1) Fertiliser le sol pour augmenter la production de biomasse et le stockage du C.

510 2) Ensemencer avec des communautés microbiennes.

511 De plus, la saturation en C basse n'augmente pas le stockage du C protégé dans le sous-sol dans notre
512 expérience, mais elle est encore prometteuse pour le stockage potentiel du C si la fertilité et les exigences
513 microbiennes sont respectées. Si la fertilisation et l'inoculation microbienne sont impossibles, nous
514 suggérons d'éviter l'utilisation d'espèces fixant l'azote, car l'augmentation de la biomasse microbienne liée
515 à ces espèces entraînerait une minéralisation plus importante de l'ancien C.

516